FLOW CHARACTERISTICS AND BED DEFORMATION AROUND A BOX GROYNE IN OPEN CHANNEL

by

Feng CAI

Dissertation Supervisor: Prof. Akihiro TOMINAGA

Nagoya Institute of Technology
Nagoya, Japan
June 2013

Abstract

In the modern river ecological project, groyne is able to support an abundant habitat for aquatic life except for the functions of navigation and riverbank protection, which is available for minimizing the river degradation and benefits the river restoration. A box groyne is composed of various types of single groyne to satisfy the different river ecological requirements. In contrast to the widely applications of the box groyne in river engineering, less information about the box groyne with special shaped groyne in river is available. The present study mainly aimed at the box groyne with longitudinal block composed by straight and L-shape groyne. In order to create an appropriate watery and sedimentary environment for aquatic life in the groyne zone, the investigation of the flow characteristics and bed deformation around the box groyne both under the emerged and submerged condition is necessary.

The effects of different configurations of longitudinal block are discussed by measurement of three-dimensional flow field in the fixed bed both under emerged and submerged condition. The longitudinal block is configured in the upstream side and downstream side of the lateral entrance with different block lengths, and the spacing of box groyne is also the important consideration. The calculation methods of exchange coefficient obtained by Particle Image Velocimetry (PIV) and Dye Concentration Measurement (DCM) experiment are both modified to adapt the emerged box groyne in this study. The sediment experiment and velocity measurement in the movable bed are conducted in a box groyne with different block lengths and positions. The flow characteristics obtained by the experiment of fixed bed is helping to investigate the formation mechanism of bed deformation with the measured flow field after bed deformation in the movable bed.

Flow characteristics change greatly when varying the position and length of longitudinal block in the emerged box groyne under fixed bed. The longitudinal block placed in the upstream side causes weaker driving gyre, smaller mean velocity in the inner zone and stronger velocity fluctuation with longer length and enhances the turbulence motion at the entrance. Setting the longitudinal block in the downstream side greatly promotes the development of secondary gyre when the block becomes long, and it reduces mean velocity and

turbulence inside the box groyne. The upstream setting of longitudinal block essentially promotes the development of vortex structure by reducing the energy diffusion with the fluid from the inner zone of box groyne in the upstream of mixing layer, and benefit the mass and momentum exchange around the entrance by increasing the turbulent flow in the downstream side of entrance.

The different configurations of longitudinal block in length and position also largely affects the flow structure around submerged box groyne in the fixed bed. The vertical mixing layer (VML) on the lateral side is sensitive to the longitudinal block set in the lateral entrance, bringing different behaviors to the horizontal flow pattern in the inner zone. The longitudinal block also has an indirect effect on the horizontal mixing process due to the changed flow pattern inside the submerged box groyne. The setting of longitudinal block clearly improves the three-dimensionality of flow and diversifies the circulation flow in the submerged groyne zone. The mean velocity in the inner zone of most cases with a downstream longitudinal block increases, while it of cases with an upstream longitudinal block decreases. The relatively low mean velocity in the groyne zone for cases with an upstream longitudinal block is able to provide a good shelter for the aquatic animal during the flooding season. Under the submerged condition, the vertical mixing layer moves toward the box groyne, and the arc shape of it has larger curvature than it under emerged condition. The exchange process is promoted by the upstream longitudinal block and downstream longitudinal block with moderate length.

Narrow or widen the spacing of box groyne also lead to the change of flow structure and mass exchange between the box groyne and main channel. When the box groyne is emerged, the mean velocity in the inner zone increases as adding the spacing of box groyne. Lowering the spacing of box groyne makes the vortex structure develop insufficiently when it gets the downstream of entrance, and less vortex structure enters in the inner zone. But when the spacing is long, although sufficiently developed large coherent structure delivers the amount of water to the inner zone from the downstream side of entrance, the intensity of vortex structure is reducing by the energy diffusion in long mixing layer. When the box groyne becomes submerged, the mean velocity in the inner zone and the three-dimensionality generally reduces as adding the spacing of submerged box groyne. In general, the setting of longitudinal block has the similar effect on the flow pattern in the

cases with different spacing.

Scour hole around the first groyne is concerned in this study due to its threat to the safety of groyne structure. The setting of longitudinal block has an efficient effect on the reduction of the scour hole, mainly caused by the restrictions on development of horseshoe vortex. The maximum scour depth generally decreases as the length of downstream longitudinal block increases when the box groyne is emerged. And the longitudinal block set in the upstream side has a great effect on reducing the maximum scour depth. But when box groyne becomes submerged, the long longitudinal block has no superiority on scour reduction and the effect of upstream longitudinal block is weakened. The scour hole in front of the second groyne is observed in the most emerged cases with an upstream longitudinal block, which is induced by the strong vortex structure inputting to the inner zone. Under the submerged condition, there also has a scour hole induced by horseshoe vortex in front of the second groyne for the cases with an upstream longitudinal block. The sediment deposited in the inner zone is largely reduced by setting the long longitudinal block in the upstream side, whereas it increases when the length of downstream longitudinal block is equal or less than 0.5S under the submerged condition.

The setting of longitudinal block in the lateral side of box groyne creates a rich environment with a diversified gyre system and strong three-dimensional flow, and the dead water zone behind the longitudinal block is a good shelter area for aquatic animal and a deposition placement for growth of aquatic plant. And its restrictive effect on scour process around first groyne is also an important advantage for groyne protection. In general, the setting of longitudinal block in the lateral side of box groyne is able to provide a suitable habitat for aquatic life.

Keywords: box groyne, PIV, emerged, submerged, L-shape groyne, 3D flow structure, local scour, sediment experiment

Table of Contents

Chapter 1 Introduction **1**

1.1 Background and motivation 1

1.2 Previous researches: a brief overview 3

1.2.1 Hydrodynamics of the flow around groynes 3

1.2.2 Bed deformation around the groyne 5

1.2.3 Different shapes of groyne 7

1.3 Research objectives 10

1.4 Dissertation Overview 11

Chapter 2 Experimental Arrangement **13**

2.1 Introduction 13

2.2 Laboratory flume 13

2.2.1 The flume with fixed bed 13

2.2.2 The flume with movable bed 14

2.3 Model of groyne 15

2.4 Instrument of Particle Image Velocimetry (PIV) in the fixed bed 17

2.4.1 Brief overview of Particle Image Velocimetry (PIV) 17

2.4.2 Application of PIV in this study 18

2.5 Dye concentration measurement (DCM) instrument in the fixed bed 20

2.6 Sediment material and measurement techniques in the movable bed 21

2.6.1 Properties of sediment material 21

2.6.2 Measurement techniques of bed morphology 22

2.6.3 Measurement techniques of flow velocity 23

2.7 Flow conditions 24

2.8 Summary 24

Chapter 3 Flow Characteristics of Emerged Box Groyne in the Fixed Bed . 25

3.1 Introduction 25

3.2 Effects of the position and length of longitudinal block 26

3.2.1 Mean velocity in the inner zone of box groyne 26

3.2.2 Flow structures 27

3.2.3 Turbulent characteristic 39

3.2.4 Exchange processes 46

3.2.5 Bed shear stress 52

3.3 Effects of the spacing of box groyne 55

3.3.1 Mean velocity in the inner zone of box groyne 55

3.3.2 Flow structures 55

3.3.3 Turbulent characteristic 61

3.3.4 Exchange processes 65

3.4 The box groyne with piles group in front of the first groyne 65

3.5 Summary 66

Chapter 4 Flow Characteristics of Submerged Box Groyne in the Fixed Bed 71

4.1 Introduction 71

4.2 Effects of the position and length of longitudinal block 72

4.2.1 Mean velocity in the inner zone of box groyne 72

4.2.2 Flow structures 74

4.2.3 Turbulent characteristic 91

4.2.4 Exchange processes 98

4.2.5 Bed shear stress 100

4.3 Effects of the spacing of box groyne 102
4.3.1 Mean velocity in the inner zone of box groyne 102
4.3.2 Flow structures 103
4.3.3 Turbulent characteristic 111
4.3.4 Exchange processes 115

4.4 Summary 116

Chapter 5 Bed Deformation and Flow Characteristics of Box Groyne in the Movable Bed 119

5.1 Introduction 119

5.2 Bed deformations and flow characteristics around the emerged box groyne . 120
5.2.1 The sketch of bed deformation in the case without the longitudinal block (CASE RE1) 120
5.2.2 The sketch of bed deformation in the case with an upstream longitudinal block (Group RE2) 122
5.2.3 The sketch of bed deformation in the case with a downstream longitudinal block (Group RE3) 126
5.2.4 Maximum scour depth and profile of bed deformation 128
5.2.5 Flow structures in the groyne field 131

5.3 Bed deformations and flow characteristics around the submerged box groyne 132
5.3.1 The sketch of bed deformation in the case without the longitudinal block (CASE RS1) 132
5.3.2 The sketch of bed deformation in the case with an upstream longitudinal block (Group RS2) 134
5.3.3 The sketch of bed deformation in the case with a downstream longitudinal block (Group RS3) 137
5.3.4 Maximum scour depth and profile of bed deformation 140
5.3.5 Flow structures in the groyne field 147

5.4 Summary 147

Chapter 6 Conclusions and Recommendations 151

6.1 Conclusions 151

6.2 Recommendations 157

References 159

Chapter 1

Introduction

1.1 Background and motivation

Groyne is an effective hydraulic structure widely used in coastal engineering or river engineering to interrupts flow field and training the sediment movement. The river with groyne generally behave a different status on flow structure and river morphology, to operate a sophisticated process of achieving relative balance from a series of dynamical actions as working of vortex structure, flow acceleration in main stream and diving force of the water. In the modern river engineering, river training as bank protection and navigation is the common application of groyne, while the river restoration also is its important advantages and attracts more and more attention nowadays. Groyne with appropriate configuration is able to support an abundant habitat for aquatic life, which is available for minimizing the river degradation and benefits for the river restoration. Single groyne has various types classified by their shape, as straight groyne, L-shape groyne, T-shape groyne, J-hook groyne etc. (as shown in Fig. 1.1 (a)). A box groyne is composed of these various types of single groyne to satisfy the different river ecological requirements (as shown in Fig. 1.1 (b).). The box groyne is as an individual groyne combination and different with the groyne group. But when it constitutes a group, it likes the groyne group. The "box" is original by its appearance. The typical box groyne is shown in Fig. 1.2. The (a) of Fig. 1.2 shows the traditional one while Fig. 1.2 (b) shows the box groyne with a longitudinal block in the lateral entrance.

The benefit of groyne on river restoration is clear due to promoted deposition for supporting vegetation and increased pool for gain of fish biomass, more large fish and diverse fish community (Shield et al. 1995, Schlosser 1987). The inner zone of box groyne provides a suitable habitat for fish, especially in flood season. The impact of groyne on fish biomass shown in Table 1.1 presents its great benefit for increasing fish populations. The traditional box groyne has a monotonic flow pattern and high velocity inside the groyne

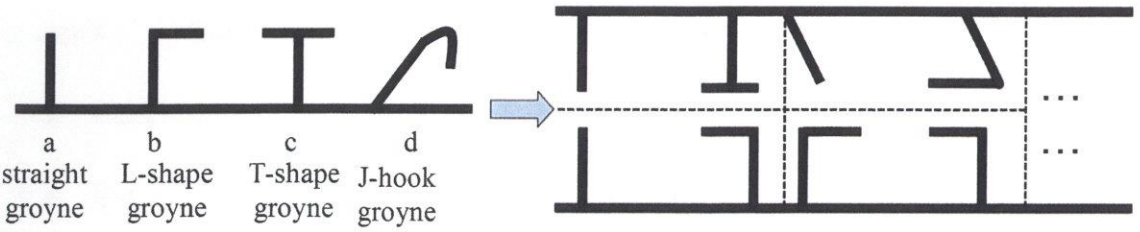

(a) (b)

Figure 1.1: Sketch of single and box groyne

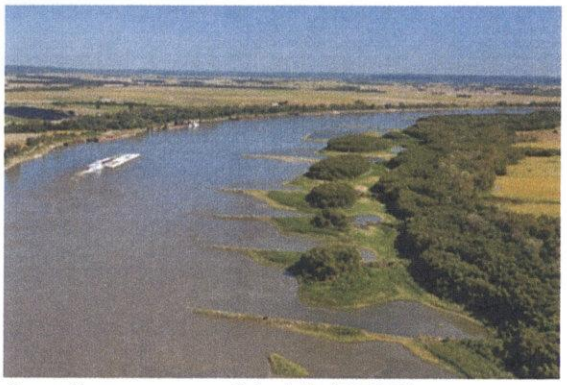

http://www.army.mil/article/70627/

(a)

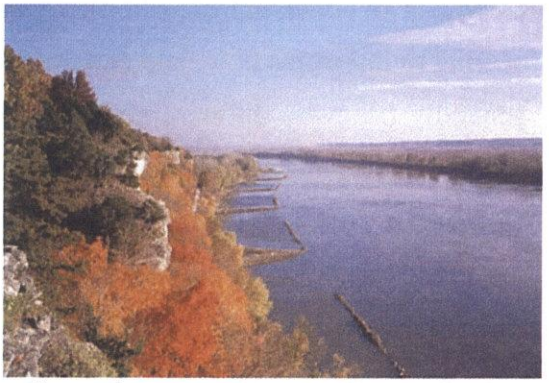

http://www.dnr.mo.gov/water-trail/riversafety.htm

(b)

Figure 1.2: The box groyne in upper Upper Mississippi River

zone, and thus it can not provide a good ecological environment for the aquatic life. Although the optimization by changing the ratio of groyne length and spacing is able to create much abundant circulation flow system in the inner zone (Weitbrecht et al., 2008), its effect is limited and not economic. Furthermore, an enlarged scour hole around the traditional box groyne jeopardizes the groyne structure. The river restoration for aquatic-habitat objectives may be addressed within orthodox incised channel-erosion control projects with little additional cost (Shields et al., 1995), and thus the traditional box groyne is not suitable to satisfy the modern river ecological demanding. Setting a longitudinal block in the lateral entrance of traditional box groyne (as shown in Fig. 1.2 (b)) is a good option to solve this problem with little price. It has an ability to create a rich gyre system and strong three-dimensional flow, and the dead water zone behind the longitudinal block is a good place for some aquatic life. Furthermore, its flexible configurations are able to accommodate

to various fields of river engineering, especially for river ecological engineering. But the longitudinal block in the lateral entrance must be affecting the mass and energy exchange of box groyne with the main stream. Physical-habitat restoration should not be attempted unless water quality is adequate to support aquatic life (Kern 1992). The configurations of box groyne need to ensure that it has enough ability to maintain a healthy, vigorous and sustainable environment for aquatic life.

Table 1.1: Reported effects on fish biomass of adding groynes or extending groynes in Eroded, Warmwater Streams. (Obtained from Kuhnle et al. 1999)

Condition	Impact of groynes on fish biomass	Biomass measured	Reference
Reaches with groynes compared with reaches with continuous stone toe protection running parallel to bank	Increased 5.7 times	Catch per unit of effort of electrofishing	Knight and Cooper (1991)
Very short groyne extended~4 times original length at angle of about 45°. Maximum scour hole depth increased from 32 to 72 cm	Increased 15 times	Catch per unit of effort of electrofishing	Shield et al. (1995b)
Reaches with groynes compared with reaches with continuous stone toe protection running parallel to bank	Increased 1.6 times	Catch per unit of effort of electrofishing	Shields et al., unpublished data (n.d.)
Reaches with groynes added to stone toe protection compared with continuous stone toe protection running parallel to bank	Increased 1.2 times	Rotenone collections	Shields et al., unpublished data (n.d.)

1.2 Previous researches: a brief overview

1.2.1 Hydrodynamics of the flow around groynes

There are numerous studies investigating the flow hydrodynamics around the single and multiple groynes in experimental channel or river. The model experiment in laboratory flume is an efficient method to explore some basic flow phenomena especially when it is greatly developed by modern measurement technology, such as Laser Visualization Techniques, Particle Image Velocimetry (PIV), Particle Tracking Velocimetry (PTV), Acoustic Doppler Velocimeters (ADV) and so on (Tominaga et al. 2000, Weitbrecht et al. 2002, Kuhnle et al. 2008, Kadota et al. 2010). The much accuracy flow field obtained from these measurement technologies provides visual and meticulous understanding on flow hydrodynamics around the groyne. In addition to laboratory experiment, many models are built in the numerical study to investigate the flow characteristics in two-dimensional and three-dimensional flow as Reynolds-averaged Navier-Stokes (RANS) with K-E turbulence

model and Large Eddy Simulations (LES) (Liu et al. 1994, Ouillon et al. 1997, McCoy 2006, Kuhnle et al. 2008)

The flow characteristics of single emerged groyne are examined by the experiment of Rajaratnam et al. (1983) on separating stream line, mixing layer and bed shear stress in smooth fixed bed. Kuhnle et al. (2008) used an ADV to examine the three-dimensional flow fields around a submerged groyne with sloped sides, and found the length of the mixing layer is about 1.6 times the length of groyne and 4 times the height of groyne. In order to capture the coherent structures around a single groyne, Kadota et al. (2009) applied proper orthogonal decomposition (POD) analysis the instantaneous velocity obtained by PTV both under the emerged and submerged condition, which is able to clearly highlight the typical fluctuating flow pattern and large-scale motion relating to the instantaneous shear stress and energy transport. Ouillon et al. (1997) developed a steady three-dimensional RANS solver with the k-model to study the flow around a groyne with the evolution of the free surface.

Spacing is a sensitive factor affecting the flow pattern and sediment transportation. The ratio of spacing and groyne length greatly affect the flow pattern, as show in Fig. 1.3. Weitbrecht et al. (2002) also described the generation of the gyre system in the groyne field with different aspect ratio W/L, as shown in Fig. 1.4. It presents that the two side-by-side gyres is generated when the aspect ratios is low ($W/L < 0.7$), and the single gyre system appears when aspect ratio increases ($W/L < 0.7$) and keeps stable for $W/L = 1.5$, finally the further increased aspect ratio forms the two-gyre system. The study of Sobhan et al. (1999) considers the spacing of 4.5 to 5 times the groyne length is able to effectively protect the river bank while 2 to 2.5 times is widely used in practice. Due to its relationship with the dynamical motion of mixing layer in the upper water, the submergence height is an important factor for submerged box groyne, and be discussed in many studies (Tominaga et al. 2001, Uijttewaal 2005, Thiemann et al. 2005). Tominaga et al. (2001) studies the effect of submergence in the three-dimensional flow field with two straight groynes by the PIV measurement in both horizontal and vertical planes in open channel. The results present the submerged condition greatly affects the flow structure around box groyne, while submerged box groyne strengthens the vortex structure and the mass exchange compared with the non-submerged spur dikes in a spur-dike zone. Deflection of mixing layer in the horizontal plane becomes large as the relative height of groyne increased. The study of McCoy (2006) based

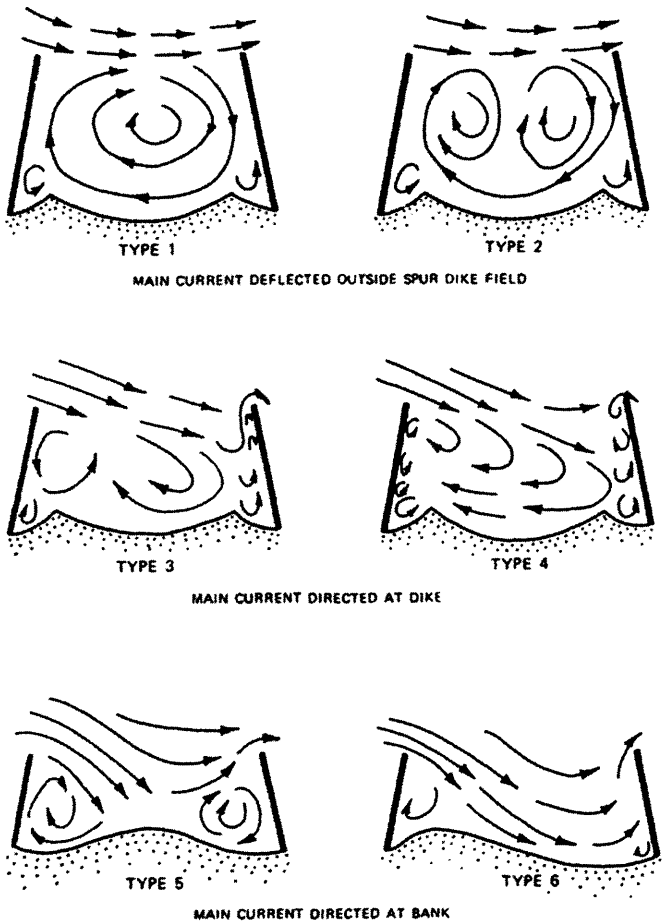

Figure 1.3: Effect of groyne spacing on flow pattern in the box groyne(obtained from Copeland 1983)

on LES simulation examines the three-dimensional flow of a single box groyne and a series of box groyne and aims at the visual and analysis of vortex structure.

1.2.2 Bed deformation around the groyne

Bed deformation around the groyne is greatly related to the groyne protection and the creation of diverse river morphology. In particular, Local scour around groyne is most concerned about due to its threat to structural safety. Fig. 1.5 presents a typical flow and scour pattern around a circular pier, which pointing out that the horseshoe vortex formed in the upstream side of structure plays main role in carrying the scour process. In order to predict the maximum scour hole around the groyne in equilibrium, some empirical or semi-empirical equations are developed by Inglis (1949), Ahmad (1953) Melville (1997).

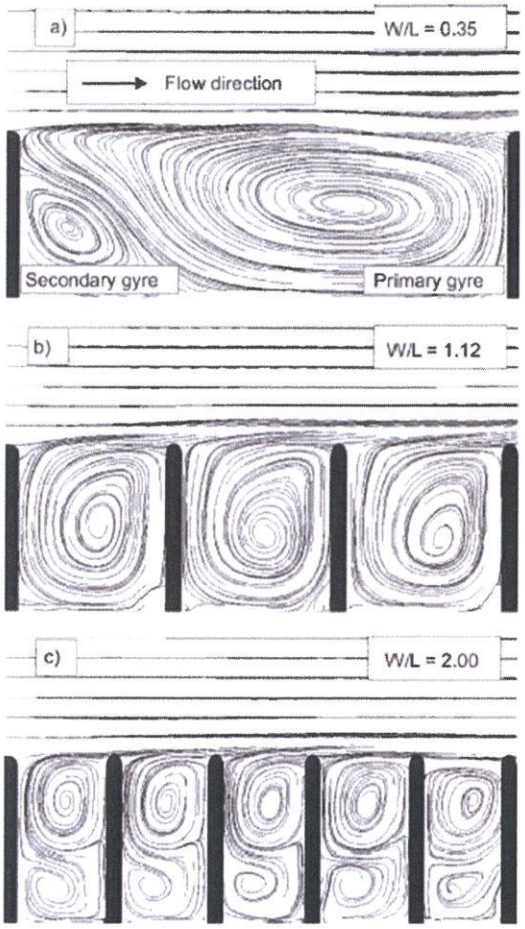

Figure 1.4: Gyre system with different aspect ratio W/L (W:groyen length, L:Spacing) (obtained from Weitbrecht et al. 2008)

And the value of maximum scour hole is depend on factors as properties of fluid, flow condition, material of bed sediment, geometry of channel and structure of groyne and so on (Zhang et al. 2008). Coleman et al. (2003) proposed a revised definition of the relationship between dimensionless time and equilibrium of scour development in a flat bed, which expressed as a function of relative flow intensity and relative abutment length. Kuhnle et al. (1997, 1999 and 2002) conducted a series of sediment experiment on emerged and submerged groyne, to investigate the geometry of the scour hole affected by length, angle and the submergence ratio of groyne. And the effects of submergence, groyne length, water depth and opening ratio (ratio of the groyne area to the cross-section area of stream) on the development and pattern of the scour hole with vertical groyne were widely discussed by Elwady et al. (2001). For most sediment experiments concerning on bed load, the flow and

bed deformation of a group groyne with the impermeable and permeable condition were investigated from the experiment of the total sediment load including bed load and suspended load by Zhang (2005), while the numerical model with three-dimensional turbulent module and total sediment module were developed to simulate bed evolution.

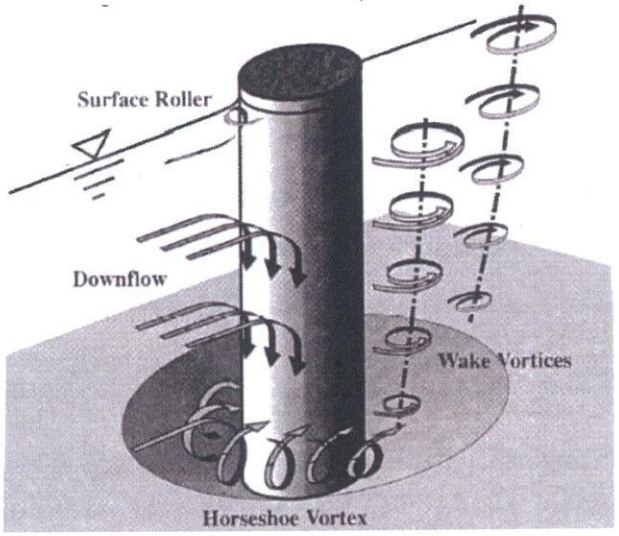

Figure 1.5: Flow and scour pattern at a circular pier (obtained from Melville and Coleman 2000)

1.2.3 Different shapes of groyne

As mentioned above, there are various types of single groyne classified by their shape. The former researches about the flow hydrodynamics and local scour around the straight groyne or the skew straight groyne is widely and in detail, while the investigation of other shapes of single groyne is less in contrast to their widely used in river engineering practices. Due to the importance of the head shape, the transformed head of groyne redistributes the flow structure around the tip of groyne, and then affects the dispersion both in longitudinal and transverse direction and the dynamic mechanism of sediment transportation (Walter et al. 1964, Zhang et al. 2008, Cheng et al. 1994, Ying and Jiao 2004, Ahmad et al. 2009). In order to reduce the adverse cause and effects of groyne, Walter et al. (1964) designed a new structure called an "L-head" groyne and conducts a series laboratory experiment in movable bed to investigate its design parameter. The report informs that this kind of groyne is able to form the bigger sand bars in the main channel, which performs against the

navigation. The effectiveness of the L-head is able to work when the closed ratio is between 45% and 65%, and a certain water of about 32.96% of groyne height could be allowed to overtop the structures without affecting the efficiency of the extension of L-head under the submerged condition. In particular, the scour hole around the groyne is reduced with the decrease of the entrance width.

The study of L-shape groyne was also carried out by Cheng et al. (1994) on the measurement of flow velocity in the fixing bed and bed deformation in the movable bed. They call L-shape groyne as "Hooked groyne", and the hooked part is the longitudinal block in this study. It shows that the flow pattern varies with the different combinations of hooked lengths and hooked angles according to the submerged and non-submerged conditions. The flow velocity in upstream and downstream of groyne both are significantly reduced for the groyne hook. The implementation of hook decreases the vortex induced by the flow detach in groyne tip, so as to reduce the energy loss behind the groyne. And under the same hook length, different hook angles have different influence on the velocity distribution on the upstream and downstream of groyne head. According to the results of sediment experiment, the scour is reduced as the increase of ratio of hooked-length to groyne length (D/L) due to the weaker vortex intensity near the groyne. And the range of scour-deposition varies with D/L=0.33~0.55 is a threshold zone, for their best behaviors to the change of straight groyne.

Kadota et al. (2010) studied the coherent flow structures and bed deformation around T-shaped and L-shaped groynes in straight open channel. The experimental results present that coherent patterns change greatly with the groyne type (as shown in Fig. 1.6), especially for L-shaped groyne, and the largely distributed coherent structures are related with formation of sand waves in the downstream of groyne. The L-shaped groyne directing to upstream (LU- shaped groyne) has less velocity difference between the main stream and dead water zone significantly and it is more suitable for stabilizing the flow and bed deformation. And the larger Reynolds stress distribution between the main stream and dead water zone shown is related to the stronger mixing process in the T- shaped and LU- shaped groyne.

The scouring profile with bed and suspended load along the channel with a series of L-shaped groynes was investigated by Ahmad et al. (2009) experimentally. Be different with most of previous studies on scour at groyne concerning with the equilibrium status,

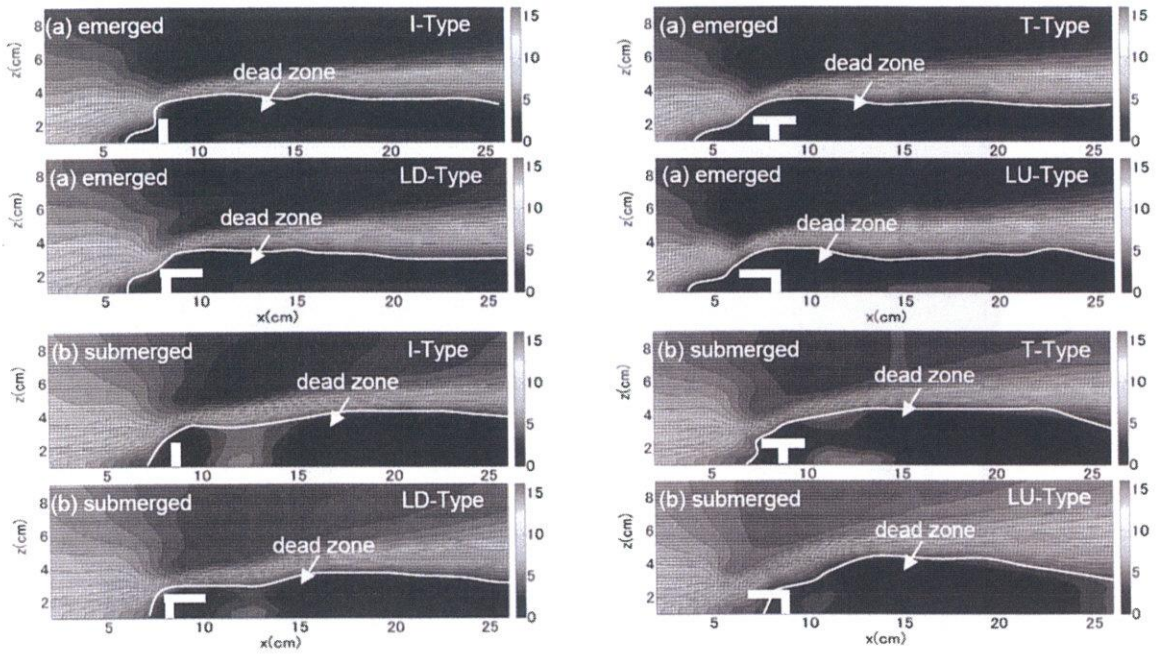

Figure 1.6: Magnitude of the mean velocity field around several types of groynes under the emerged and submerged conditions(obtained from Kadota 2010)

they aims on the temporal evolution of the longitudinal bed profile as shown in Fig. 1.7. It is observed that the scour appear around the first groyne at firstly, and then extents to the downstream. The sediment deposits increasingly between the first groyne and second groyne firstly, but then it deposits less even becomes erosion as time going on. They put forward an equation of estimating the maximum scour depth around a series of L-shaped groynes with parallel wall in the downstream direction under equilibrium condition.

In addition to the mentioned above, the investigations of T-shaped groyne are developed by laboratory experiment and numerical simulation. Ghodsian and Vaghefi (2009) found some valuable conclusions about influencing parameters on the maximum scour depth around the T-shaped groyne in 90 degree channel bend by adopting model experiment. According to the experimental results, Vaghefi et al. (2012) introduced the equations for calculating the scour hole induced by T-shaped groyne. A fully complex three-dimensional flow of two T-shaped groynes is clarified by the Mansoori et al. (2012) using numerical model of SSIIM.

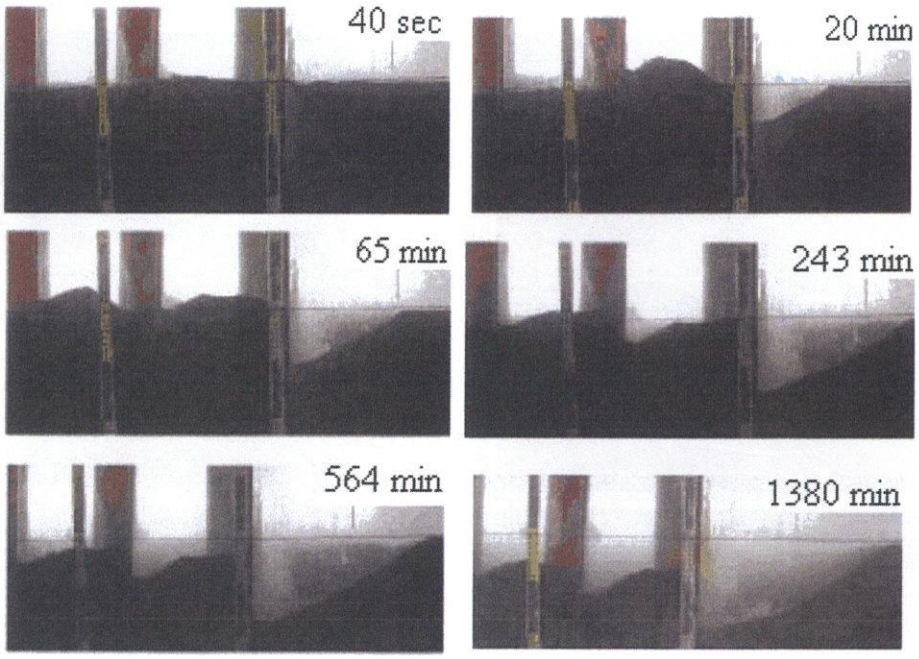

Figure 1.7: Temporal bed deformation of a series of L-shape groyne (obtained from Ahmad et al. 2009)

1.3 Research objectives

In the inner zone of groyne field, the different configurations of box groyne diversify the circulating flow in number, scale and strength. Such abundant flow structure makes the box groyne area to be a miniature aquatic system, which carries out the exchange of mass, sediment and energy with the main stream by reformed entrance. The flexible configurations of box groyne are able to accommodate to various fields of river engineering, especially for river ecological engineering.

In contrast to the widely applications of box groyne in river engineering, less information about the box groyne with special shaped groyne in river is available. The present study mainly aimed at the box groyne with longitudinal block composed by straight and L-shape groyne, as shown in Fig. 1.8. In order to create an appropriate watery and sedimentary environment for aquatic life in the groyne zone, the investigation of the flow characteristics and local scour around the box groyne both under the emerged and submerged condition is necessary. The schematic research subject showed in Fig. 1.9 gives a clear clarification about the research of box groyne with different configuration in this study.

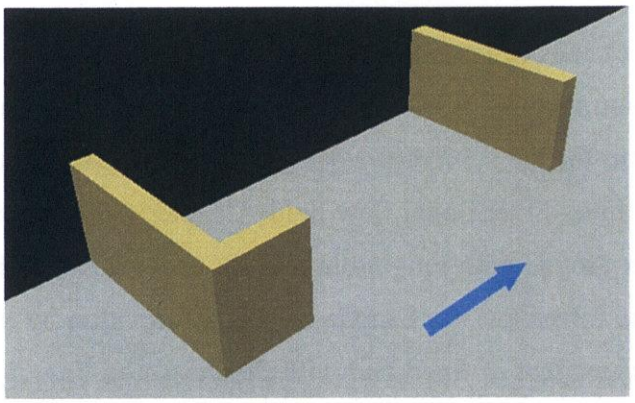

Figure 1.8: Sketch of adopted model

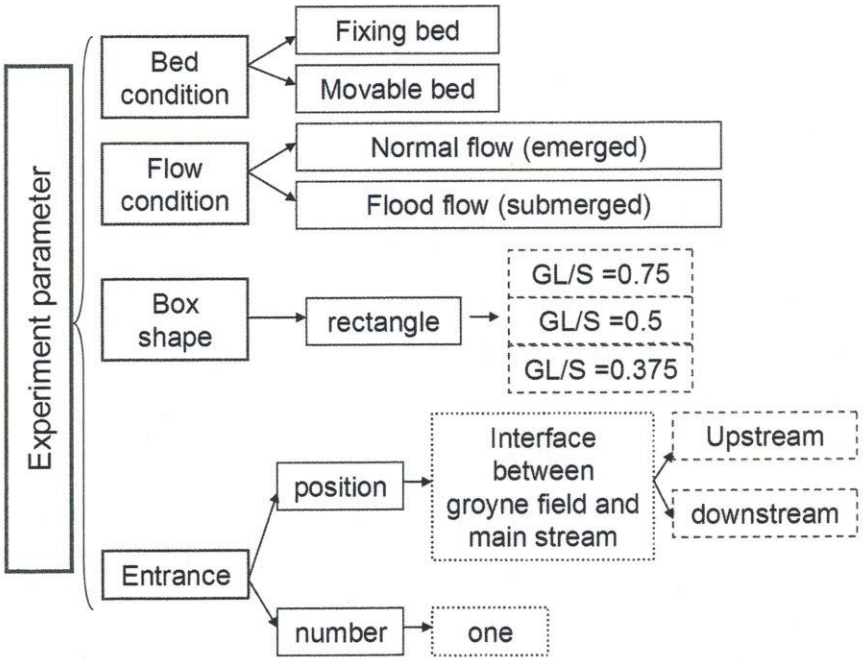

Figure 1.9: Schematic research subject of this study

1.4 Dissertation Overview

The present dissertation is organized in 6 chapters as follows:

In this chapter, the research background with motivation and previous research, research objectives and main contents of each chapter are acquired a brief introduction. Chapter 2 describes the arrangement of laboratory experiments in the fixed bed and movable bed. Chapter 3 discusses the experiment results of emerged box groyne with longitudinal block

under different block length, position and spacing of box groyne in the fixed bed, and analyzes the calculation method of exchange coefficient in detail. While Chapter 4 presents a similar exploration for the submerged box groyne in the fixed bed and emphasis on the description of the three-dimensional flow field. Chapter 6 discusses the sediment experiment results of box groyne with longitudinal block under different block length, position, and investigates the formation mechanism of bed deformation by the flow characteristics obtained by the experiment of fixed bed with the measured flow field after bed deformation in the movable bed. Chapter 6 summarizes the main findings of this study and offers recommendations for river engineering practice.

Chapter 2

Experimental Arrangement

2.1 Introduction

A description of laboratory experiments operated in this study is presented in this chapter. Overviews of flume geometry, arrangement of groyne model, adopted measurement techniques, sediment materials and flow conditions are described.

2.2 Laboratory flume

2.2.1 The flume with fixed bed

For the experiments of Particle Image Velocimetry (PIV) and dye concentration measurement (DCM), the laboratory flume with transparent sidewall made of glass materials was used, as shown in Fig. 2.1. The straight rectangular flume was 0.3m in width, 0.4m in height and 7.5m in length with an adjustable bottom slope. The slope of the flume i was set at 1/2000 for the present experiment. The measurement section was located in 4.4~4.6m downstream from the water entrance. The initial flow conditions were controlled by adjustable pump and downstream weir.

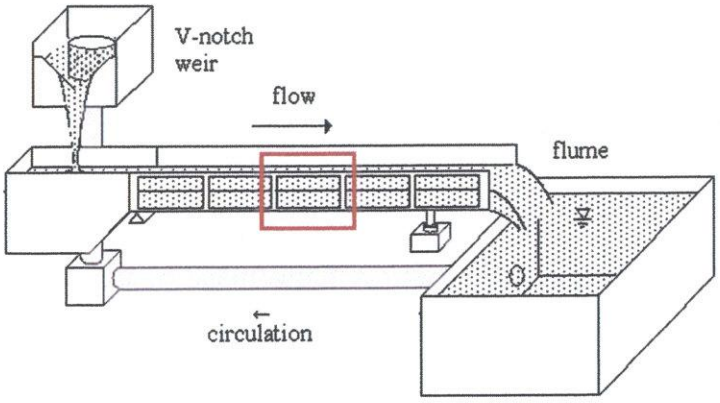

Figure 2.1: Sketch of the flume with fixed bed

In order to keep the same hydraulic condition, there are procedures to be taken more carefully as follows:

a) The depth of the water in the lower main tank should be in the same water level

b) The discharge was checked by comparing the measured results obtained by two methods. The first one is measured by the triangular weir in the upper tank. The sketch (Fig. 2.2) and equation of triangular weir is shown bellow. The second way is done by measuring the rate of mass of the flowing water.

$$Q = CHt^{5/2} \tag{2.1}$$

$$C = 1.354 + 0.004/Ht + (0.14 + 0.2/\sqrt{W})(Ht/B - 0.09)^2 \tag{2.2}$$

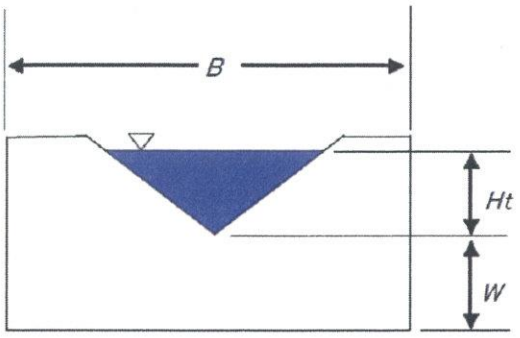

Figure 2.2: Sketch of the triangular weir (V-notch weir)

c) The depth of the water in the main channel was the last parameter that should be checked and kept on the same level in each case under same flow condition.

2.2.2 The flume with movable bed

For the sediment experiment, the laboratory flume made by transparent acrylic materials was used, as shown in Fig. 2.3. The straight rectangular flume was 0.3m in width, 0.19m in height and 6m in length with a slope of 1/2000. The flume was divided into the fixed section and movable section, as shown in Fig. 2.4. The section of x=0.3~2.3m and x=3.8~5.8m was the fixed section lifted by the C type of structural steel. The movable section was 1.5m length with 6.5cm sand depth.

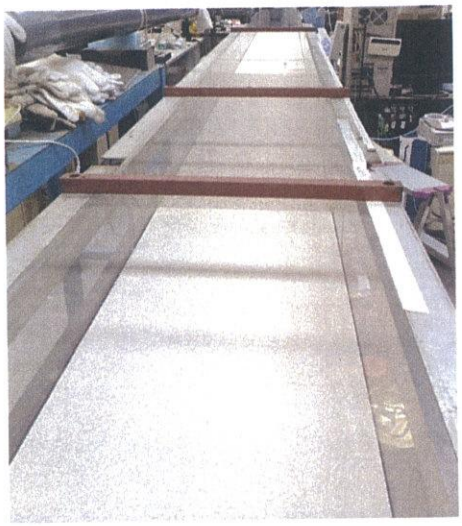

Figure 2.3: Photo of the flume with movable bed

2.3 Model of groyne

As shown in Fig. 2.5, the experimental box groyne was consisted of straight groyne and L-shaped groyne with the head directing to upstream or downstream. The groyne model was made of transparent acrylic acid resin, as shown in Fig. 2.6. The thickness of acrylic plate (groyne width) was 1cm. The height was 4.5cm for experiment in the fixed bed and 10cm for experiment in the movable bed. All the cases are divided into 3 groups as R1, R2 and R3 according to the different block position. For the normal case, the spacing of box groyne was 18cm. Besides the normal cases, the box groynes with different spacing (12cm and 24cm) or types also were considered in the study. The parameters of the box groyne model are shown in Table 2.1 and Table 2.2. The 3cm interval is able to ensure that more details among different cases are acquired and enough vectors could be obtained at the narrowest entrance.

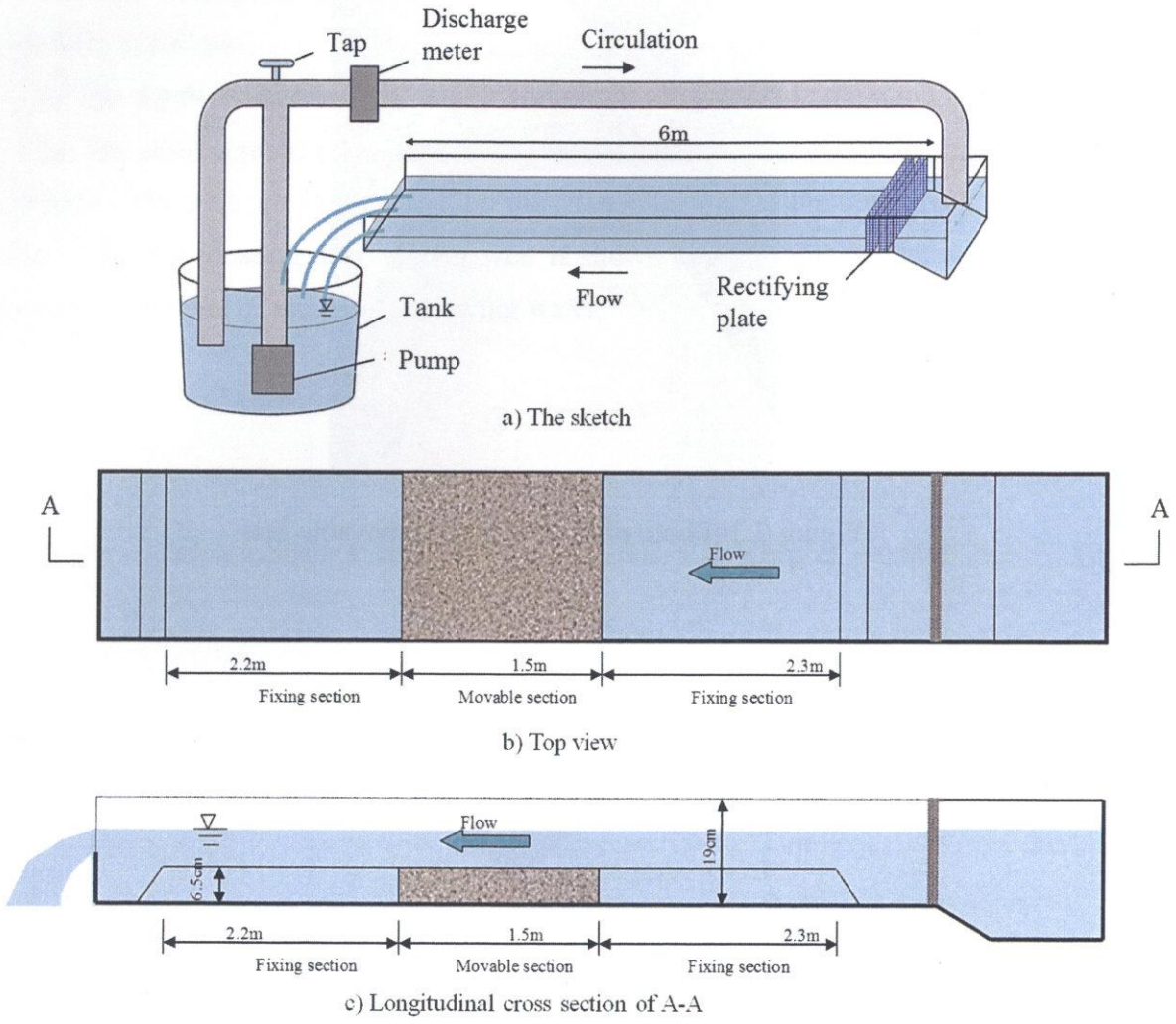

Figure 2.4: The flume with movable bed

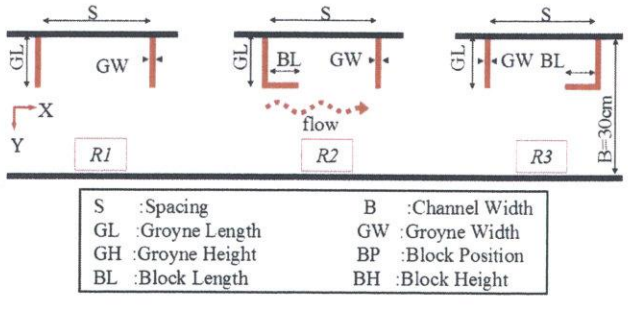

Figure 2.5: Arrangement of box groyne model

Figure 2.6: The photo of model

Table 2.1: The model parameters of different groyne spacing

Name	R1			R2			R3		
S/cm	12	18	24	12	18	24	12	18	24
GL/cm	9								
GW/cm	1								
BP	none			upstream			downstream		
BL/cm	none			6	9	12	6	9	12

Table 2.2: The model parameters of groyne with 18cm spacing

Name	R1	R2					R3				
		1	2	3	4	5	1	2	3	4	5
GL/cm	9										
GW/cm	1										
S/cm	18										
BP	none	upstream					downstream				
BL/cm	none	3	6	9	12	15	3	6	9	12	15

2.4 Instrument of Particle Image Velocimetry (PIV) in the fixed bed

2.4.1 Brief overview of Particle Image Velocimetry (PIV)

As the purpose of the visualization of flow around box groyne, Particle Image Velocimetry (PIV) technique was used to measure velocity distributions. Particle Image Velocimetry (PIV) is an efficient measurement technique for measuring the instantaneous velocity filed in a cross section without disturbing the flow field. PIV is a whole-flow-field technique which records images of flow fields in a cross-section for a variety of applications in gaseous and liquid media, and to extract instantaneous velocity information out of these images (Raffel et al. 2007).

A typical setup for PIV technique in a wind tunnel is briefly sketched in Fig. 2.7.Small tracer particles are added to the flow. A plane (laser sheet) within the flow is captured twice by means of a laser (the time delay between pulses depending on the mean flow velocity and the magnification at imaging). It is assumed that the tracer particles move with local flow velocity between the two captures. The light scattered by the tracer particles is recorded via a high quality lens either on a single frame (e.g. on a high-resolution digital or film

camera) or on two separate frames on special cross-correlation digital cameras. The output of the digital sensor is transferred to the memory of a computer directly. The displacement of the particle images between the light pulses has to be determined through evaluation of the PIV recordings. In order to be able to handle the great amount of data which can be collected employing the PIV technique, sophisticated post-processing is required. For evaluation the digital PIV recording is divided in small subareas called "interrogation areas". The local displacement vector for the images of the tracer particles of the first and second capture is determined for each interrogation area by means of statistical methods (auto- and cross-correlation). It is assumed that all particles within one interrogation area have moved homogeneously between the two captures. The projection of the vector of the local flow velocity into the plane of the light sheet (two-component velocity vector) is calculated taking into account the time delay between the two captures and the magnification at imaging.

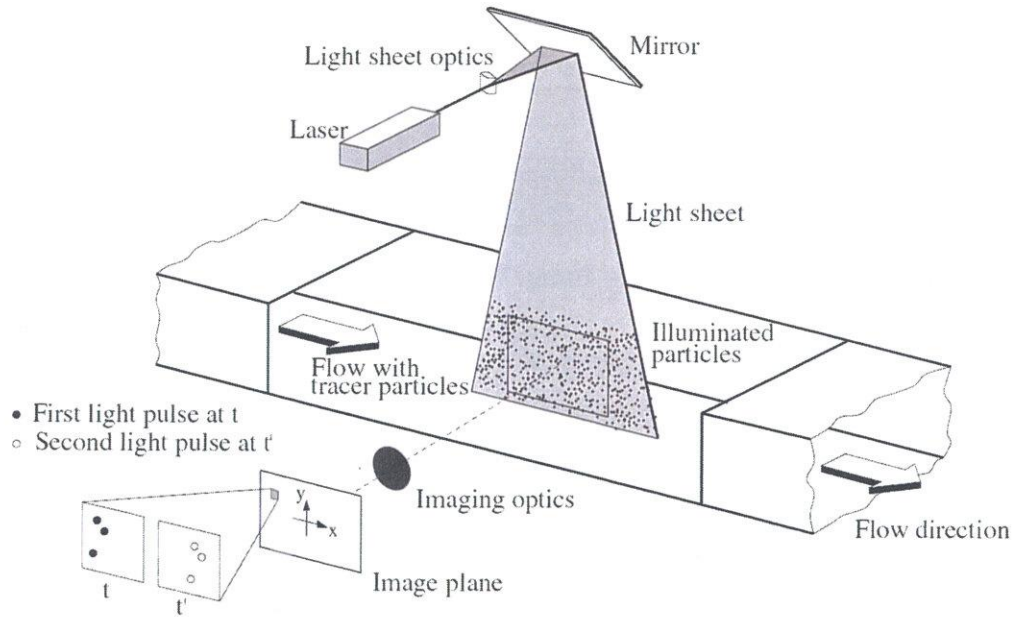

Figure 2.7: Typical setup for PIV technique in a wind tunnel

2.4.2 Application of PIV in this study

In this study, PIV was used to measure velocity distributions on two planes to explore the three-dimensional characteristics (as shown in Fig. 2.8 and 2.9). In order to capture clearer move tracer, nylon resin particle with 80 micron in diameter and 1.02 in specific weight

was used. The argon laser light sheet with about 2~3mm thickness was projected on the plane. In the horizontal plane, 8 horizontal (x-y) planes with 4mm interval were measured from the layer of 4mm from the bottom for the emerged condition, while 13 horizontal (x-y) planes with 5mm interval were measured from the layer of 5mm from the bottom for the submerged condition. In the vertical plane, 15 vertical (x-z) planes with 10mm or 15mm interval were measured from the layer of 5mm from the left side of channel wall, as shown in Fig. 2.10.

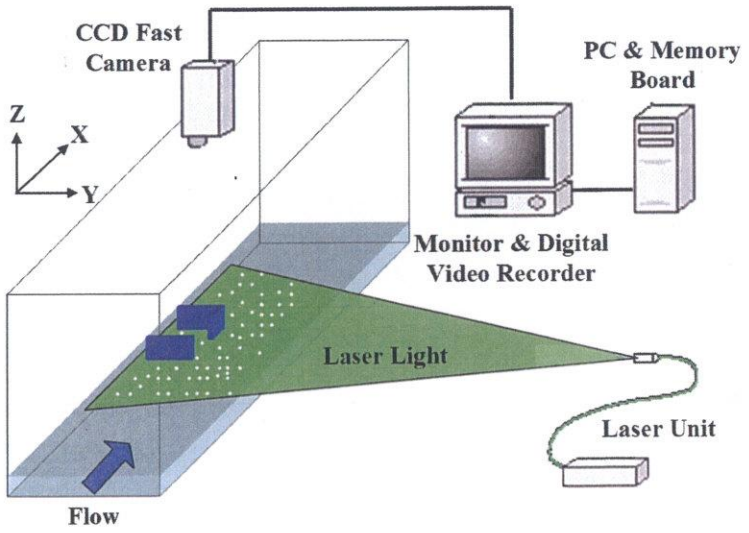

Figure 2.8: Arrangement of PIV on the horizontal plane $(x - y)$

The visual images were taken by high-speed video camera and recorded as "BMP" files with 640x480 pixels on the horizontal plane and 640x160 pixels on the vertical plane. The spatial resolution was about 0.465~0.667 mm/pixel. The velocity vectors were calculated by using commercial PIV software (VISIFLOW by AEA Technology). The post-processing of data was operated by the FORTRAN programming. The resolution of the image analysis was 32x32 pixels with overlap 75%. In the present analysis, the time-averaged flow velocity vectors were obtained by processing 1600 successive images in 16s with an interval of 1/100s for the horizontal plane and 3200 successive images in 16s with an interval of 1/200s for the vertical plane.

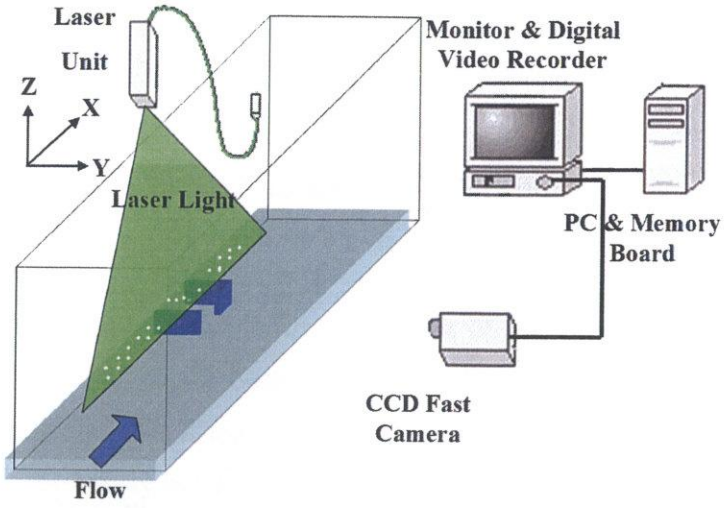

Figure 2.9: Arrangement of PIV on the vertical plane $(x - z)$

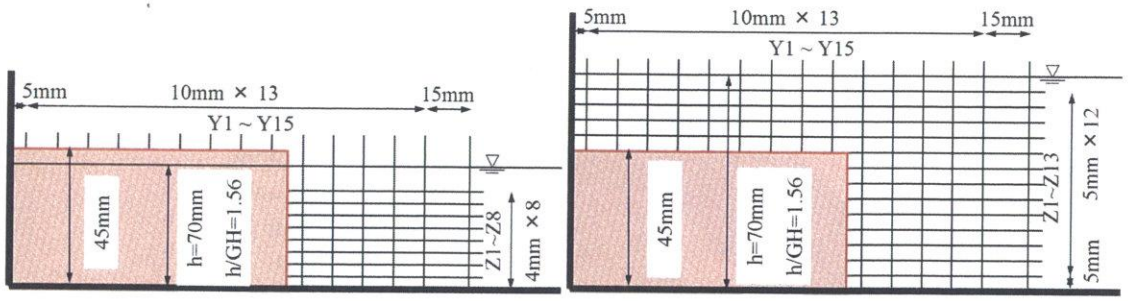

(a) Emerged condition (b) Submerged condition

Figure 2.10: Projection of the laser sheet

2.5 Dye concentration measurement (DCM) instrument in the fixed bed

With the purpose of performing the water exchange process, the dye concentration measurement (DCM) was conducted using blue dye ($KMnO_4$) as a tracer. Dye concentration measurement is an efficient approach for flow visualization and examination of exchange and diffusion process (Babarutsi et al. 1991, Uijttewaal et al. 2001, Tominaga et al. 2008). Fig. 2.11 presents the procedure of DCM. A thin plate was blocked at the entrance of box groyne to create a stationary flow condition, in that case, the tracer with small volume was distributed homogeneously over the entire inner zone and till be a constant concentration. Then the plate was removed slowly to begin the water exchange process. The concentration of dye was measured by a video image analysis. The process of dye diffusion was

taken by a video camera and still images were picked up. To obtain local depth-integrated dye concentration, the groyne zone was subdivided into 10×10 rectangular domains, and the average density of grayscale in the groyne zone was measured by image analysis. The grayscale level is calibrated against known dye concentrations. The grayscale level is related to the concentration linearly when the grayscale level is below 180 in 256 gradation scale. Therefore, the grayscale level is used as a measure of dye concentration in the range below 180. When flow is coming into the inner zone of box groyne from the transparent main stream, the dye concentration is diffused and the color becomes bright. Dark parts in pictures are places where a dye is not diffused or it is accumulated by the flow. The average grayscale level is calculated in the inner zone of box groyne at a certain time-interval by using image analysis and then it is normalized by the initial grayscale level.

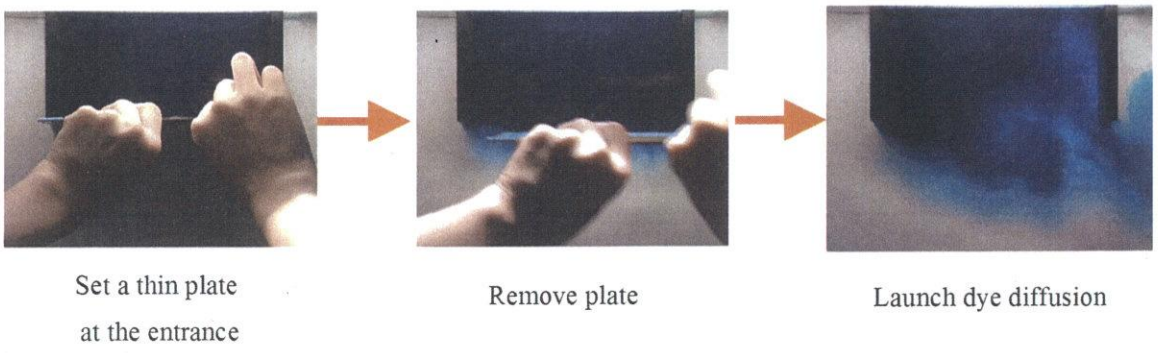

Figure 2.11: The procedure of dye concentration measurement (DCM)

2.6 Sediment material and measurement techniques in the movable bed

2.6.1 Properties of sediment material

The sediment used for the bed evolution experiment in the movable bed had a mean diameter dm of $591\mu m$, a median diameter d_{50} of $571\mu m$ and a geometric standard deviation d_{75}/d_{25} of 1.225, as the sieve analysis results shown in Fig. 2.12. The sediment density was 2.65 g/cm^3, and the critical shear velocity was 1.77 cm/s by using the Iwagaki Formula (1956).

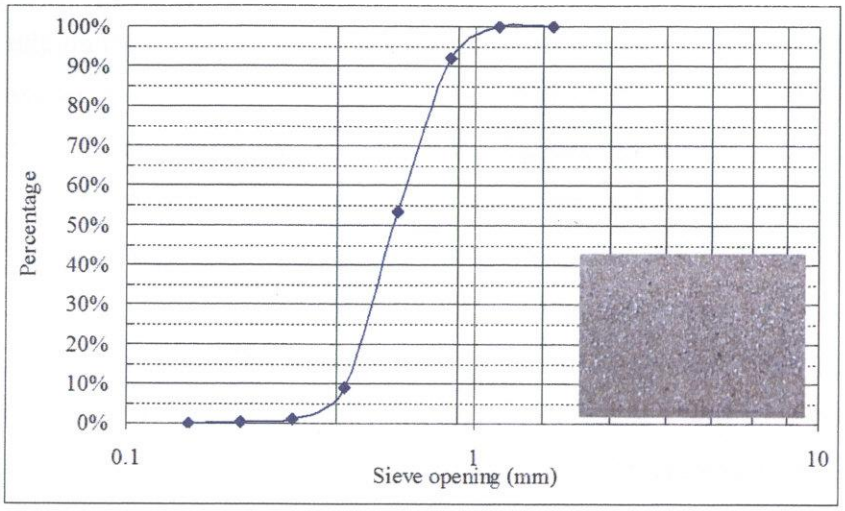

Figure 2.12: Cumulative semi-logarithmic probability size-frequency graph

2.6.2 Measurement techniques of bed morphology

The measurement of bed deformation was adopted after 120min water time. A laser-distance meter (CMOS multi-function Analog Laser Sensor IL-600 (KEYENCE), as shown in Fig. 2.13) was used to determine the bed deformation when the measured section of flume was completely drained out. The laser-distance meter has a measurement range of about 200~1000mm, a spot diameter of about $1.6(\pm 0.5\%)$, and a sampling rate of 0.33/1/2/5ms. All these measurement devices were mounted on an instrument carriage running on the rails over the channel.

(a) Laser sensor (b) Instrument

Figure 2.13: Arrangement of devices measuring bed deformation

2.6.3 Measurement techniques of flow velocity

The measurement of flow velocity under the movable bed was adopted after 120min water time, and finished in 180min without large development of bed deformation. Electromagnetic current meter (as shown in Fig. 2.14) was used to measure two-dimensional flow velocity around the box groyne field under movable bed condition. The experiment apparatus is shown in Fig. 2.15. The electromagnetic current meter (I-type) has a sampling rate of 50 Hz, and 32s were taken at each point. The measured depth was about 2~3cm below the water surface under the emerged condition and 3~4cm below the water surface under the submerged condition. The different measured height was because of the high deposition in the inner zone of box groyne. All these measurement devices were mounted on an instrument carriage running on the rails over the channel.

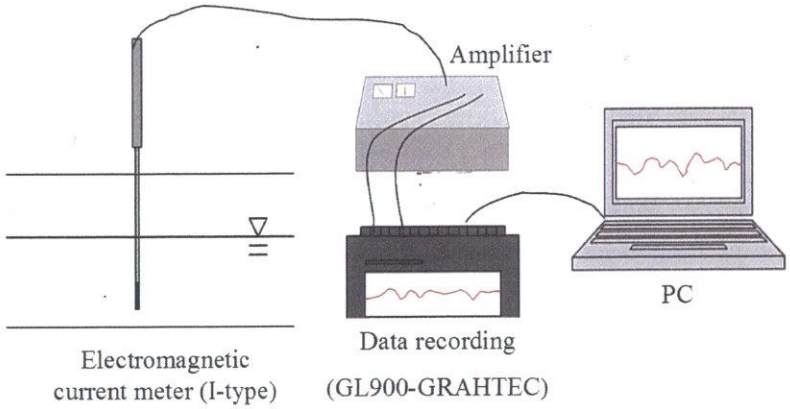

Figure 2.14: Arrangement sketch of Electromagnetic Current Meter (EMV)

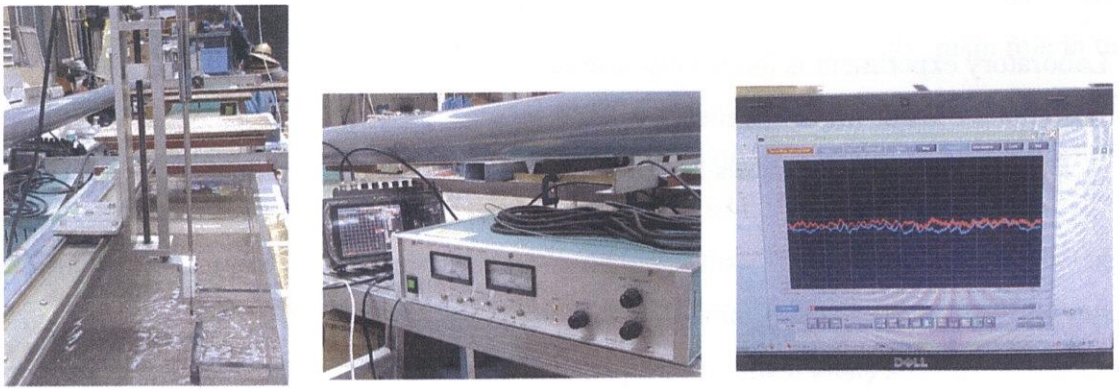

Figure 2.15: Apparatus of Electromagnetic Current Meter (EMV)

2.7 Flow conditions

The emerged and submerged conditions were both taken into consideration in this study. All the flow conditions are shown in Table 2.3 and Table 2.4. In the fixed bed, only two flow conditions were considerate. In the movable bed, high discharges were used to explore the effect of discharge on the bed deformation.

Table 2.3: The flow conditions in the fixed bed

Type	Slope	Depth (h) /m	h/GH	Q/ m^3/s	Mean Velocity/m/s	Fr	Re	t/°
Emerged	1/2000	0.04	0.89	0.00179	0.149	0.238	4694	20.55
Submerged	1/2000	0.07	1.56	0.00317	0.151	0.182	6399	19.73

Table 2.4: The flow conditions in the movable bed

Type	Slope	Depth (h) /m	h/GH	Q/ m^3/s	Mean Velocity/m/s	Fr	Re	t/°
Emerged	1/2000	0.04	0.89	0.00178	0.148	0.236	4707	20.62
Emerged-h	1/2000	0.04	0.89	0.00298	0.248	0.397	7859	20.97
Submerged	1/2000	0.06	1.33	0.00331	0.184	0.240	7503	18.52

2.8 Summary

Laboratory experiment is the mainly research method adopted in this study. The important information about flume geometry, arrangement of groyne model, adopted measurement techniques, sediment materials and flow conditions are introduced in this chapter.

Chapter 3

Flow Characteristics of Emerged Box Groyne in the Fixed Bed

3.1 Introduction

In this chapter, the laboratory experiments are used to investigate the flow field with instantaneous and time-averaged velocity around the emerged box groyne, and the mass exchange processes between the inner zone of the emerged box groyne and the main stream. The measurement technology of Particle Image Velocimetry (PIV) is used to explore the flow field and mass exchange process by analyzing the flow vectors. The Dye Concentration Measurement (DCM) provides a distinct and visual method to present the development of vortex structure in the mixing layer and its effects on the mass exchange between the inner zone of the emerging box groyne and the main stream.

In the emerged box groyne, the vertical mixing layer on the lateral side dominates the flow pattern in the inner zone; hence, the longitudinal block set in the lateral entrance brings large change to the flow field in the inner zone. Under the same hydraulic condition, when the ratio of groyne length and flume width (GL/B) is fixed, the scale and strength of the initial vortex structure detached from the tip of first groyne is similar. Then, the development of vortex structure is largely affected by the placement and length of the set longitudinal block, the length of second groyne, the spacing of box groyne and so on. In this section, the effects of the placement and length of the longitudinal block and the spacing of box groyne on flow field are studied. For the groyne, the strong horseshoe vortex (HV) system generated and developed around the tip of first groyne is the main role in the formation of the scour hole around the first groyne. This study presents the arrangement of pile group on the front of the first groyne, which is able to control the development of scour around the first groyne by reducing the generation of HV.

The time-averaged flow velocity indicates different flow types in the box groyne area along with the placement and the length of a longitudinal block. To explore the inner characteristics of flow structures around a box groyne, statistical analysis, such as autocorrelation, Weiss function and turbulence intensity are applied. Beside that, mass exchange

coefficient reveals characteristic of the water exchange process between the inner zone of the box groyne and the main stream. In particular, a detailed description of the bed shear stress distribution in the groyne field region is conducted.

3.2 Effects of the position and length of longitudinal block

In this section, the spacing of box groyne is set as S/GL=2 (S=18cm), which is able to present single gyre to two gyres in the inner zone of box groyne according to the study of V. Weitbrecht (2008). The arrangement of longitudinal block is shown in Table 2.2.

3.2.1 Mean velocity in the inner zone of box groyne

The longitudinal block prevents the main stream delivering energy to the inner zone of box groyne, so as to induce the large difference in velocity distribution. Fig. 3.1 shows the characteristic of mean velocity in the inner zone of box groyne U_{ig}, which is obtained by averaging the all time-averaged velocity in the inner zone of box groyne. Compared with the case without the longitudinal block (CASE RE1), only the CASE RE21 (BL/S=0.17) presents a little bit higher mean velocity. It means the existence of the long longitudinal block in the lateral entrance of box groyne obstruct the mass exchange between the inner zone and main stream, then reduces the global vitality of water in the inner zone of box groyne. For the reason why the short longitudinal block set in upstream side of entrance increases the mean velocity in the inner zone, the next section will give an explanation. For those two groups RE2 and RE3, the mean velocity inside the groyne area both tends to diminish as the increasing longitudinal block length, while the decreasing tendency in group RE2 is greater than that in group RE3. The mean velocity in group RE3 is almost 50% less than that in group RE2. There is relatively small mean velocity in the CASE RE25 (BL/S=0.83), RE34 (BL/S=0.67), RE35 (BL/S=0.83) especially, being likely to be a dead water zone in the most inner region.

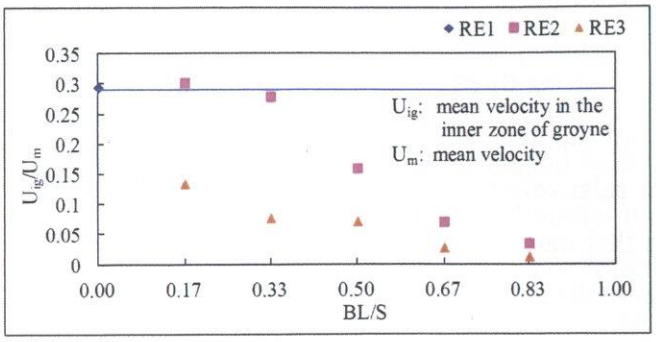

Figure 3.1: Comparison of mean velocity in the inner zone of emerged box groyne for all layers

3.2.2 Flow structures

Flow pattern around the groyne area

Due to the longitudinal block directs to the inside of box groyne, the difference between each case in the upstream and downstream regions of groyne is inconspicuous compared to that in the box groyne field. As a result, this study focuses on the finite section with about 5 cm of upstream and downstream from the groyne. The horizontal time-averaged velocity vectors at the middle height of water depth (laser height z=20mm, z/GH=0.44) are used as representative patterns, although the velocity vectors have a small difference in pattern among the different heights. The time-averaged velocity vectors and contours on the horizontal plane are shown in Fig. 3.2~3.4 respectively, revealing the flow features around box groynes, such as different types of circulating flow.

a) CASE RE1 The vector graphs of Case RE1 in Fig. 3.2 show a typical flow pattern for the traditional box groyne with straight groyne. In the upstream and downstream regions of groyne, a small circulating gyre is generated by the shear flow respectively. In the groyne field, a circulating flow called driving gyre with anticlockwise direction occupies the inner zone, also drives the secondary gyre (or driven flow) with clockwise direction, and it creates a two-gyre system. The secondary gyre in CASE RE1 is mainly located in the inner corner of upstream side with small size, and it is also located as a pair in the upstream and downstream sides when the plane is close to the channel bottom. The stream from upstream dissipates and transports the energy through the mixing effect with the inflow from the inner zone of box groyne, to form the mixing layer with arc shape, where the

mixing process is dominated by large coherent structure (LCS). In particular, the water particle mingles with strong three dimensional characters at the tip of first groyne. Due to the expelling effect of the first groyne, the main streamline deflects to the opposite side of groyne, causing the relatively small velocity in the downstream direction around the tip of second groyne. In that case, the stream (back flow in CASE RE1 of Fig. 3.2) from the recirculating region in the downstream may flow into the inner zone of box groyne under a certain condition. In this study, only CASE RE1 has significant phenomenon of back flow, because its main streamline is expelled farthest without the flow diversion effect of block.

b) GROUP R2 Setting the longitudinal block at the upstream side of entrance weakens the driving gyre in the groyne field and enlarges the secondary gyre. In addition, the scale of driving gyre diminishes with increasing block length, while the scale of secondary gyre enlarges and even occupies almost 2/5 of the inner zone in CASE RE25. Due to the shielding effect of longitudinal block, a shielding area is generated in the outer area of longitudinal block, as shown in Fig. 3.2 In the shielding area of group RE2, the stream flows toward the upstream along the block and rejoins the main stream, to form a single circulating flow. This stream is constituted by the flow from the inner zone of groyne and the vortex structure delivered from mixing layer. From the time-averaged velocity vectors in Fig. 3.2 and the contours of dimensionless time-averaged velocity in the longitudinal direction in Fig. 3.3, it can be easily found that the shielding area of group RE2 enlarges in strength and length scale with longer longitudinal block. As shown in the contours of dimensionless time-averaged velocity in the transverse direction for CASE RE21, RE22, and RE23 (shown in Fig. 3.4), nearby area around the longitudinal block tip presents higher transverse velocity than that of the first groyne tip in CASE RE1. That means the longitudinal block placed in the upstream side promotes the interchange mechanism by narrowing the entrance, especially when the entrance has enough space to launch exchange process and develop the vortex. It also explains that the mean velocity of CASE RE21 is higher than that of CASE RE1. The reduction of negative transverse velocity in the inner side of the second groyne shows that the longer block weakens the development of vortex structure. Nevertheless, the gyres in the upstream and downstream regions of box groyne are in small difference among each case, which is also the same in group RE3.

c) GROUP R3 Comparing the time-averaged velocity between CASE RE21 and RE31 in Fig. 3.2, it reveals that just moving the short longitudinal block from upstream to downstream of entrance radically causes a great difference in the flow pattern. The center of driving gyre moves toward the outside with reduced dominated area while the secondary gyre expands its territory. Therefore, the placement of longitudinal block plays an important role in the distribution of flow of the box groyne field. The longitudinal block in the downstream side prevents the vortex structure to enter the inner area of groyne, so as to deflect the direction of flow to the upstream around longitudinal block. Hence, the active area of driving gyre is restricted near the entrance, which causes that the high area of negative velocity in longitudinal direction moves to the entrance in group RE3 while that is close to the inner side in group RE2 (as shown in Fig. 3.3). It is noticed that the driving gyre migrates to the main stream side with decreasing scale and strength with the increase of the longitudinal block length till it stays almost the outer side of the block (as shown in Fig. 3.2~3.4). It means that because the entrance becomes narrower, vortex structure develops less when it reaches the upstream of block. Furthermore, the longer longitudinal block increases the difficulty for vortex to enter the inner zone of groyne. Meanwhile, the number of gyre inside the box groyne adds up to three when the ratio of block length to groyne spacing BL/S is equal or greater than 50%. In the shielding area of group RE3, the partial stream also shows the characteristic flowing toward the downstream along the block to be a part of driving gyre. X_c shown in Fig. 3.2 is the distance from the start point of reverse flow to the outer wall of the second groyne, and it differs from each block length and reaches maximum in CASE RE33 (as shown in Fig. 3.5). This shows that when entrance is large enough for the activity and development of vortex structure, the vortex structure would show the tendency of entering the inner zone to promote the water exchange. In that case, the vortex structure along the block with the short distance from the entrance is prone to flow upstream to enter the inner zone. As the longitudinal block length is growing, vortex structure with weak development trends to move downstream along the block instead of flowing into the inner zone of groyne area, because its weak development can not provide enough support of reversing to the entrance. As a result, the narrow entrance, the shorter reverse flow induced by vortex with less development in the shielding area. However, when the entrance is too narrow to be hard for entering, the vortex structure prefers to move in the shielding area with the weaker development along the block, to generate the circulating

flow in the outer area of box groyne.

Among the different horizontal measured layers, the time-averaged flow increases in the flow intensity as the increasing measured height with similar circulating flow pattern. For the emerged condition, the flow inside the groyne area hardly presents obviously three-dimensional characteristics, but it appears three-dimensional flow around the tip of first groyne and in front of the longitudinal block in the area of main stream.

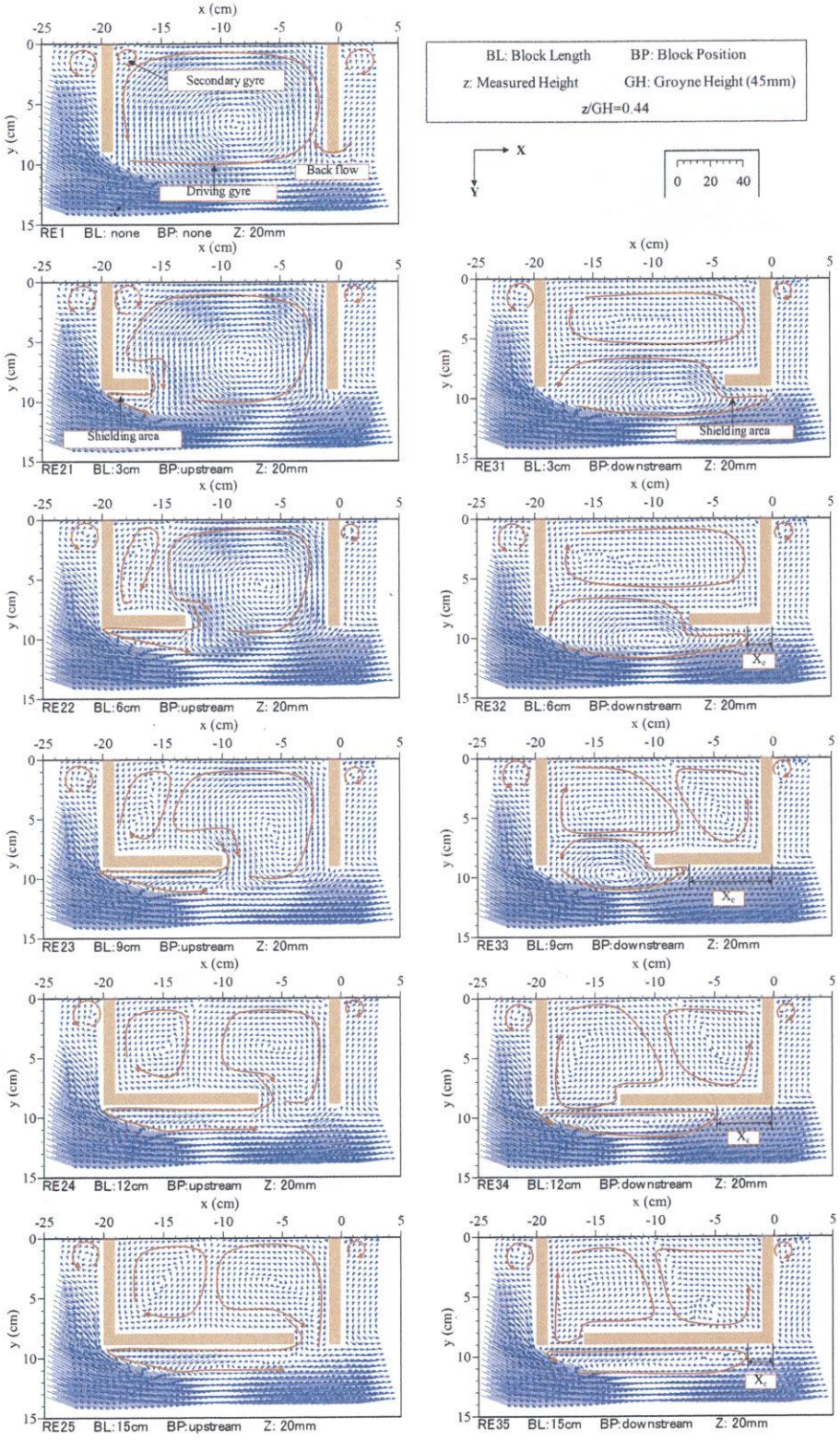

Figure 3.2: Time-averaged velocity vectors on the horizontal plane (x-y) near the middle of water depth (z/GH=0.44)under emerged condition

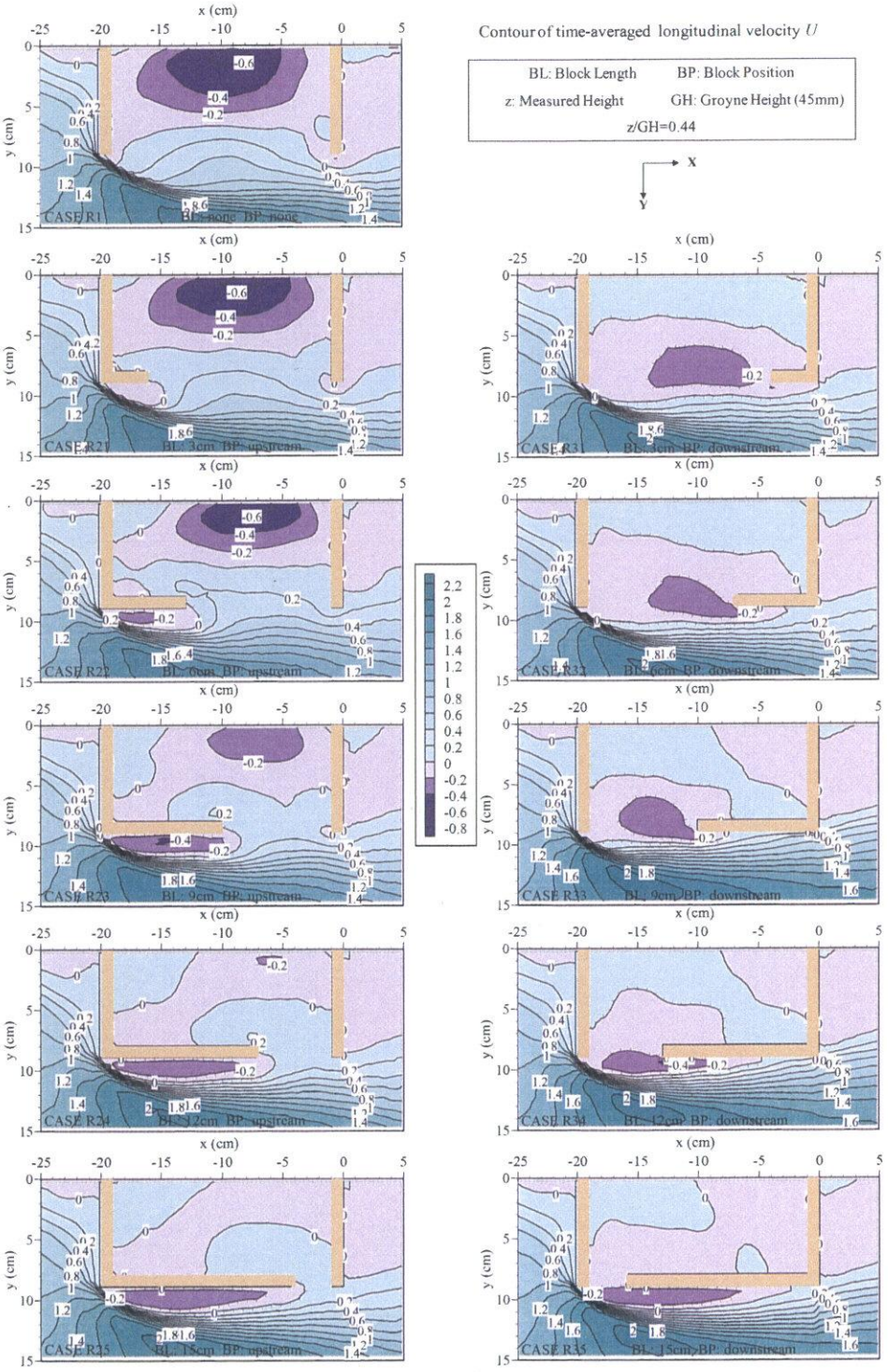

Figure 3.3: Contours of dimensionless time-averaged velocity in the longitudinal direction (U) on the horizontal plane (x-y) near the middle of water depth (z/GH=0.44)under emerged condition

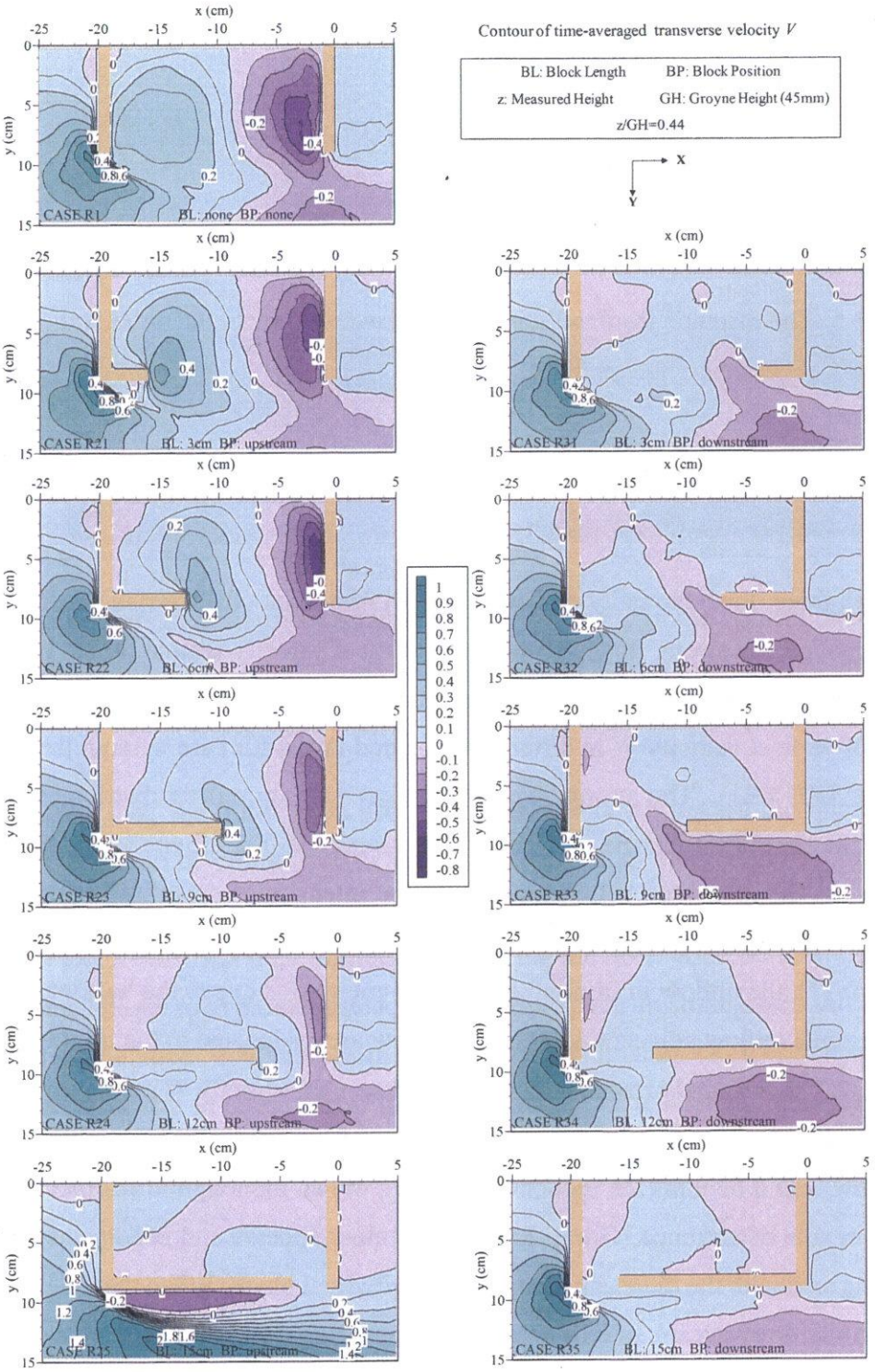

Figure 3.4: Contours of dimensionless time-averaged velocity in the transverse direction (V) on the horizontal plane (x-y) near the middle of water depth (z/GH=0.44)under emerged condition

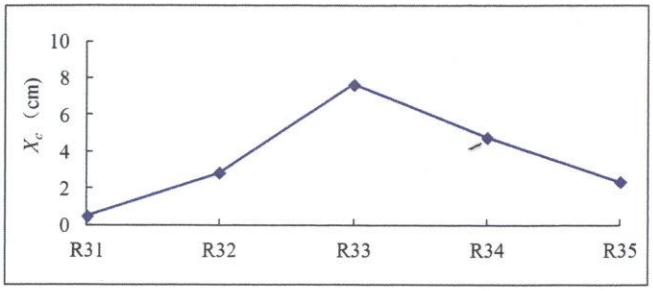

Figure 3.5: The distance from the start point of reverse flow to the outer wall of the second groyne X_c under emerged condition

The distribution of vertical velocity W

Although three dimensionality of flow is not an important characteristic in the inner zone of box groyne, the strong flow with negative vertical velocity around the tip of first groyne can not be ignored, which is relative to the local scour. Fig. 3.6 shows the horizontal distribution of vertical velocity W in different measured layers for case without the longitudinal block (CASE RE1). The strong negative vertical velocity mostly distributes in the areas around the tip of first groyne and from the upstream of first groyne to the middle of box groyne. As the measured height increasing, the intensity of downflow is stronger, and it causes a large gradient of the water table around the first groyne. On the plane of z=32mm (z/GH=0.71), the upflow in front of the first groyne wall is due to the backwater of groyne, and the zonal upflow adjacent with the downflow area is located in the mixing layer.

Fig. 3.7 shows the horizontal distribution of vertical velocity W on the plane of z=8mm (z/GH=0.18) for all cases. In general, the setting of longitudinal block reduces the area of downflow, and it benefits the reduction of scour. When the longitudinal block is set in the upstream side of entrance (Group RE2), the upflow appears and becomes stronger in the shielding area with the increasing length of longitudinal block. When the longitudinal block is set in the downstream side of entrance (Group RE3), the flow around the longitudinal block becomes complex, The cases with short longitudinal block (CASE RE32, RE33) present the upflow around the longitudinal block, while the cases with long longitudinal block (CASE RE34, RE35) present the downflow. The vertical distribution of velocity on the plane y=95mm (y/GL=1.06) for Group RE3 demonstrates a clearer flow pattern in front of the entrance, as shown in Fig. 3.8. For most cases with or without longitudinal block,

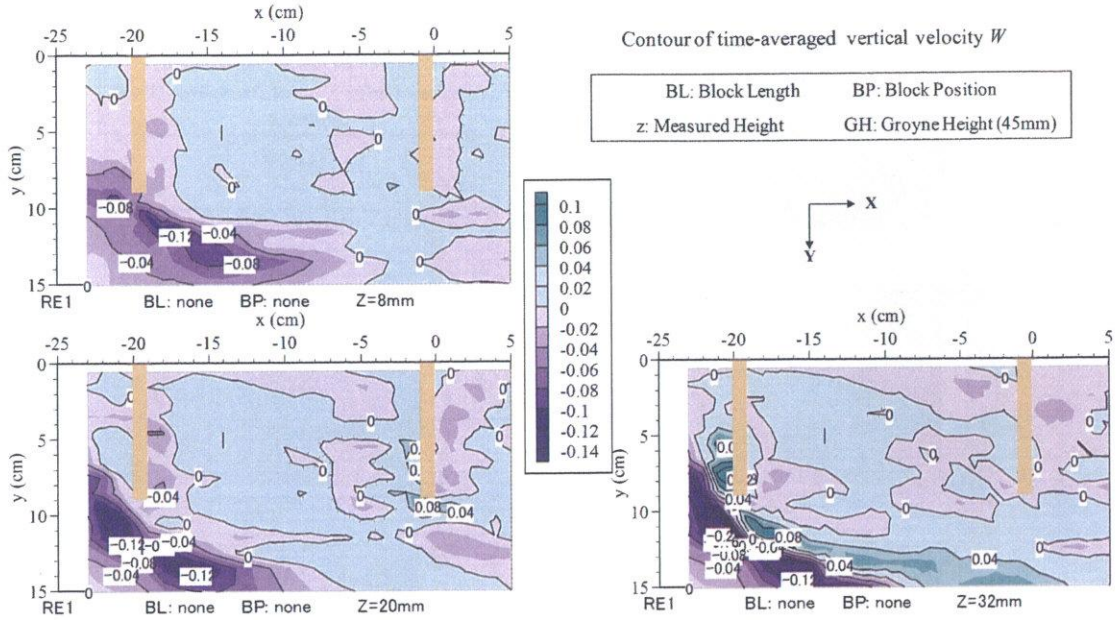

Figure 3.6: Contours of dimensionless time-averaged velocity in the vertical direction (W) on the horizontal plane (x-y) in different measured layers for case without the longitudinal block (CASE RE1)

the flow path is that, the fluids from upstream side flow down toward the flume bottom, and then some turn to be upflow due to adverse pressure from the bottom. A part of them flow toward the inner zone of box groyne because of the mixing effect, but the existence of longitudinal block obstructs their normal path entering the inner zone, so they climb along the longitudinal block to bypass it instead of the normal path. In some cases, this condition change. When the upper flow reaches the front of longitudinal block, it accompanies with strong vortex structure in some cases, like CASE RE33. The adverse pressure from the longitudinal block divides the flow as shown in CASE RE33 in Fig. 3.8.

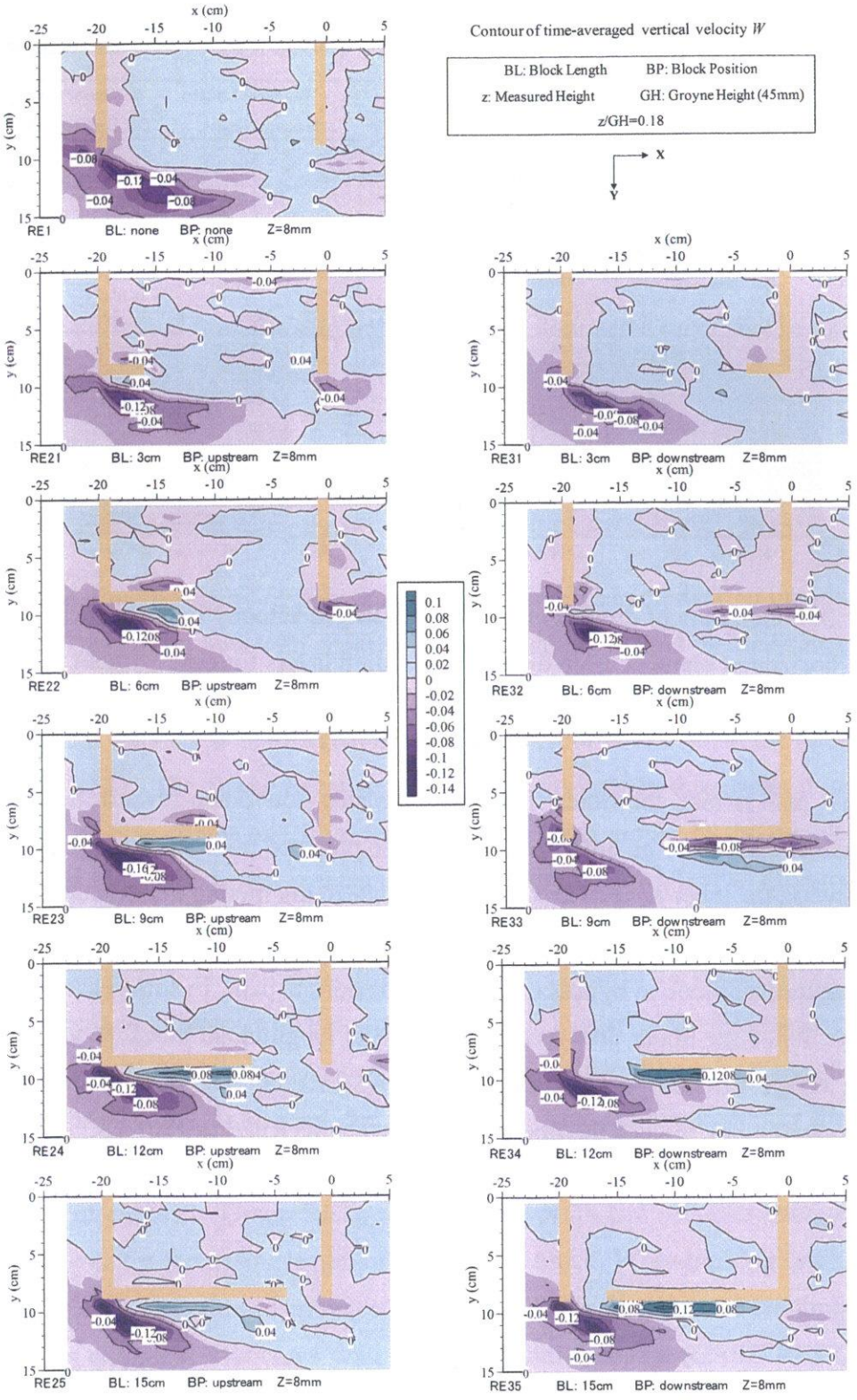

Figure 3.7: Contours of dimensionless time-averaged velocity in the vertical direction (W) on the horizontal plane (x-y) near the bottom of the channel (z/GH=0.18)under emerged condition

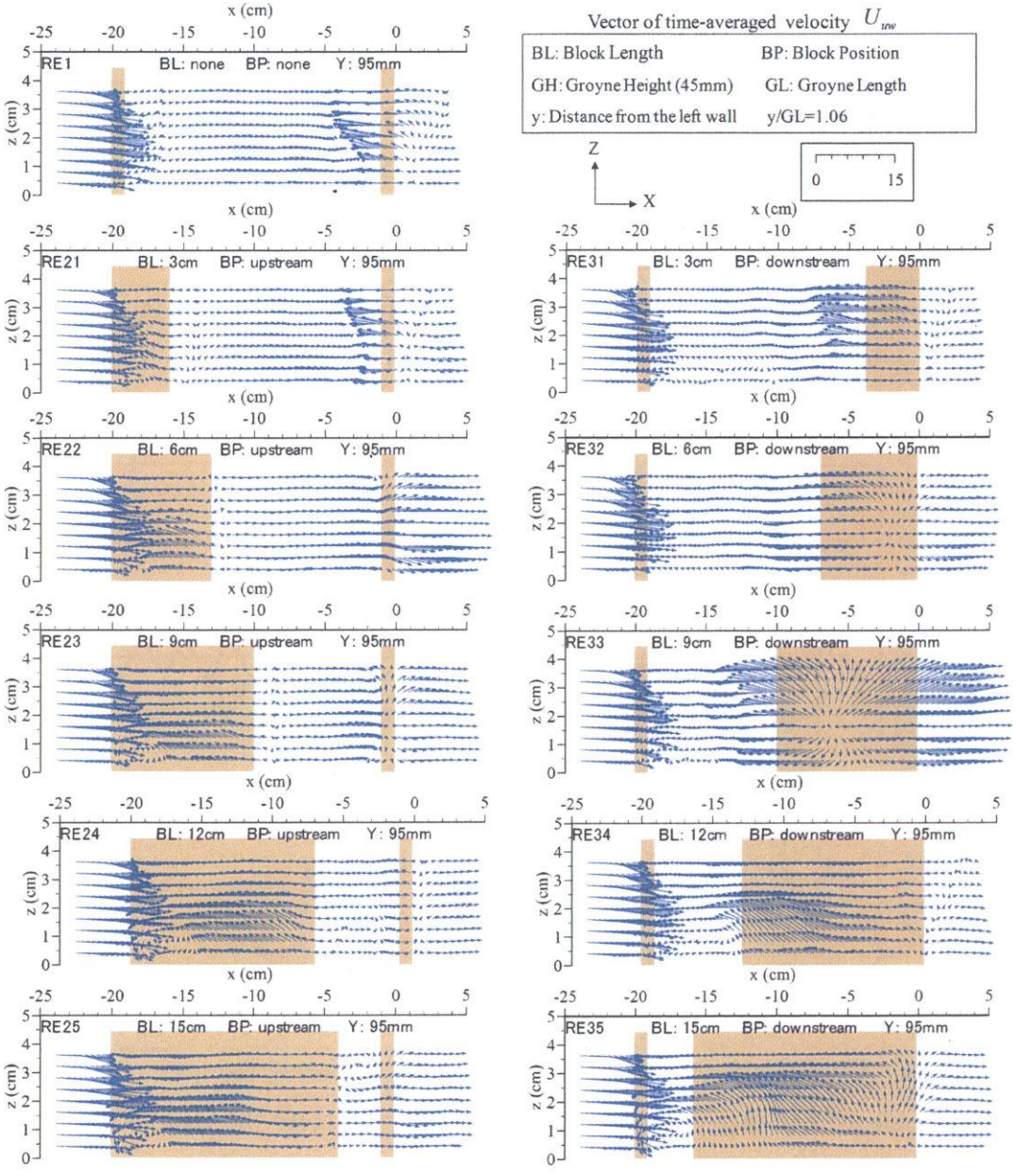

Figure 3.8: Time-averaged velocity vectors on the vertical plane (x-z) y=95mm (y/GL=1.06) under emerged condition

Velocity fluctuation in the groyne area

The Autocorrelation analysis is adopted to explore the periodicity of the velocity fluctuation for each case. The velocity fluctuation in the downstream side of entrance hardly presents clearly a periodicity characteristic because it is easily affected by the complex turbulence. The instantaneous transverse velocity in the upstream side of entrance is recognized for its representative periodic motion. The autocorrelation coefficient of transverse components R_{vv} and period T are shown in Fig. 3.9. In group RE2, the longer longitudinal block, the larger amplitude appears. In group RE3, CASE RE33 has maximum amplitude. It's because that the large area of activity increases the energy diffusion in the inner zone. Comparing the period in CASE RE23 with RE33 and CASE RE24 with RE34, it is clearly that the longitudinal block setting in upstream extends the period of velocity fluctuation

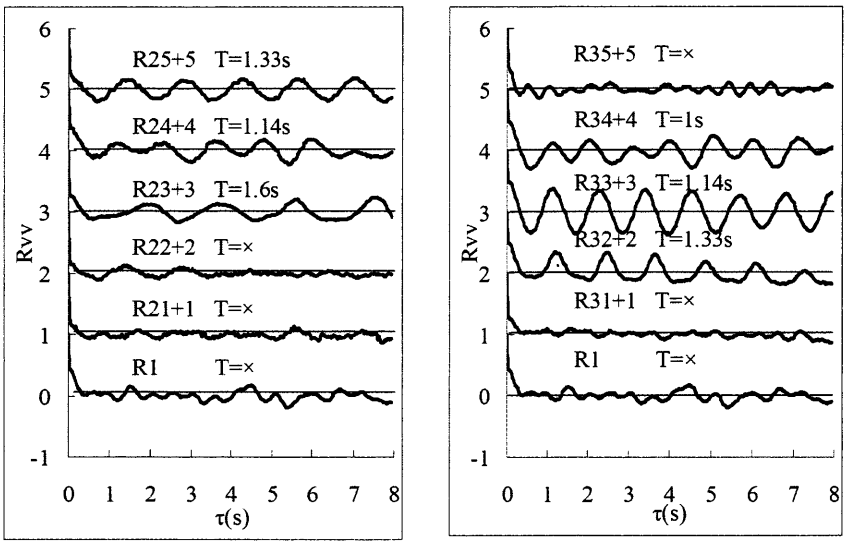

(a) (b)

Figure 3.9: Autocorrelation results for velocity fluctuation in the transverse direction at the upstream of entrance on the horizontal plane (x-y) near the middle of the channel (z/GH=0.44)under emerged condition

Velocity distribution in the main stream

In the main stream, the longitudinal block still has a large impact on the flow structure. Fig. 3.10 shows the vertical distribution of longitudinal velocity on the plane y=125mm (y/GL=1.39) and the plane in the middle of flume y=150mm (y/GL=1.67) for the CASE

RE1, RE23 and RE33. On the plane y=125mm (y/GL=1.39), the longitudinal velocity in the cases with the longitudinal block is higher than that in the case without the longitudinal block. In particular, the case with downstream longitudinal block (CASE RE33) presents highest value. On the plane y=150mm (y/GL=1.67), the longitudinal velocity in the cases with the longitudinal block is smaller than that in the case without the longitudinal block. It means that, the setting of the longitudinal block makes the area of high longitudinal velocity in the main stream to move closer to the groyne zone comparing with that in the case without the longitudinal block.

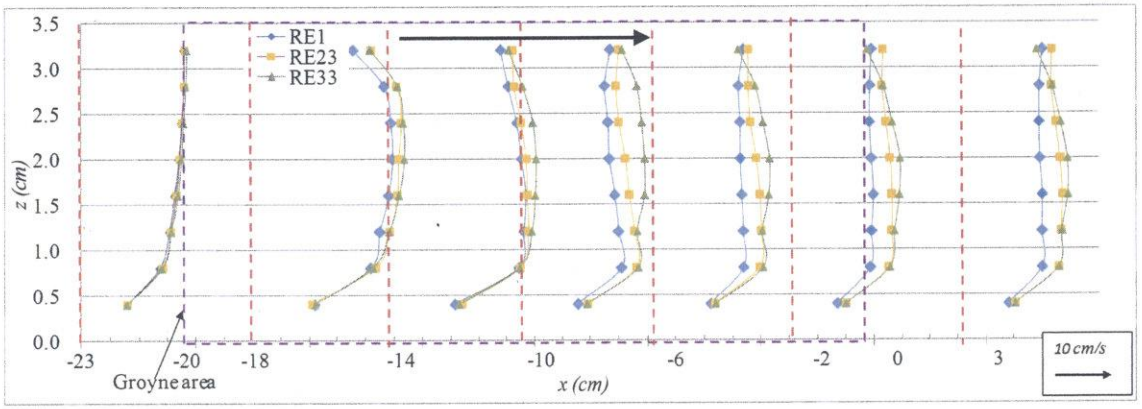

(a) y=125mm (y/GL=1.39)

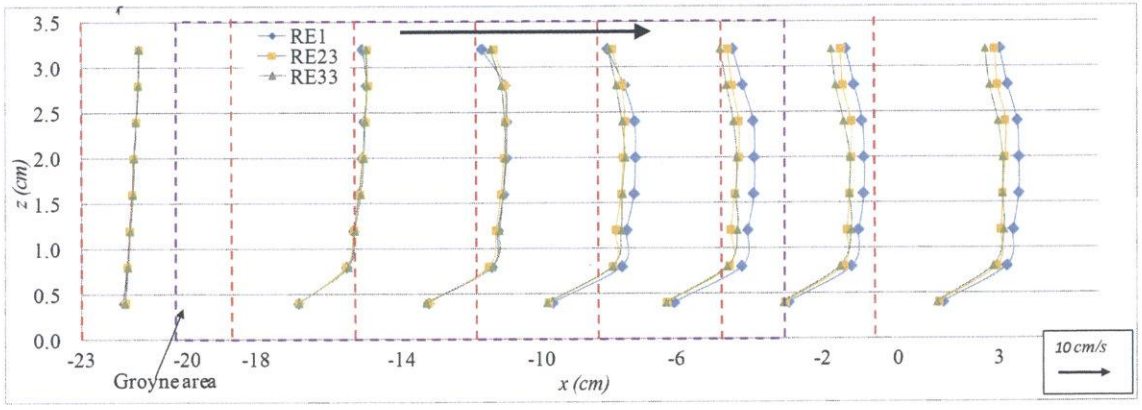

(b) y=150mm (y/GL=1.67)

Figure 3.10: Vertical distribution of longitudinal velocity (U) on the vertical plane (x-z)under emerged condition

3.2.3 Turbulent characteristic

The first groyne of box groyne converge the flow to enhance the turbulence motion caused by velocity differences, while the longitudinal block affects the turbulence distribution. In

the mixing layer, active interaction produces large velocity fluctuation to induce high turbulence; hence, the effects of the longitudinal block on the mixing process directly causes the distribution differences of turbulence. The turbulence distribution is related to the generation and dissipation of vortex structure. Turbulence characteristics in transverse direction at the entrance between the inner box groyne area and main stream present the exchange ability of box groyne with the external environment.

Turbulence intensity

The time-averaged turbulence intensity is denoted by in longitudinal component u' and transverse component v'. The contour of dimensionless time-averaged turbulence intensity is shown in Fig. 3.11 and Fig. 3.12. In all cases, an area containing strong turbulence is formed, indicating the general location of mixing layer. This area conducts vigorous interaction between the main flow and the flow from the inner zone of box groyne.

a) GROUP RE1 The tip of the two groynes centralizes the amount energy of turbulence both in two directions, especially, the vortex with high energy shed from the first groyne enhances the turbulence intensity in the longitudinal direction. Due to the Kelvin-Helmhotz instability, the strongest turbulence is placed in the upstream side between the two groynes. Along with the movement to the downstream, the shedding vortex has the deflection of motion trace and the energy diffusion caused by mixing effect. In that case, in the mixing layer, the turbulence intensity decreases in the longitudinal direction between the two groynes, but the area of strong turbulence becomes widen as going downstream. The vortex structure moves into the inner groyne area along the wall of the second groyne, inducing the high turbulence in transverse direction around the nearly wall area of second groyne.

b) GROUP R2 Due to obstruction of the longitudinal block, the flow from the inner area of box groyne is hardly conveyed to the some sections of mixing layer directly, but via the link of shielding area. Hence, the vortex structure would be well developed with less resistance from the outflow of box groyne, which makes higher value in turbulent intensity both in two directions. As shown in Fig. 3.12, the tip of longitudinal block centralizes high turbulence value in transverse direction corresponding to the velocity distribution shown in Fig. 3.4. As the length of longitudinal block increases from 3cm (CASE RE21) to 6cm

(CASE RE22), the area with high turbulence in main stream enlargers (as shown in Fig. 3.11 and 3.12), but turbulent motion inside the box groyne weakens. When the length keeps increasing, the area with high turbulence in main stream reduces but is still larger than the area in the case without the longitudinal block.

c) GROUP R3 Compared to CASE RE1, there is not obvious difference in the turbulence intensity around the tip of first groyne for group RE3. However, larger turbulence is centralized near the tip of longitudinal block due to the generation of vortex. Compared to group RE2, the area with large turbulence is clearly smaller in group RE3, which due to the less development of large coherent structure. The diverse lengths of longitudinal block produce various distributions of turbulent intensity, especially, the turbulence intensity decreases along with the increasing block length. For group RE3, the CASE RE33 shows highest turbulence value around the entrance, which means strong exchange capacity.

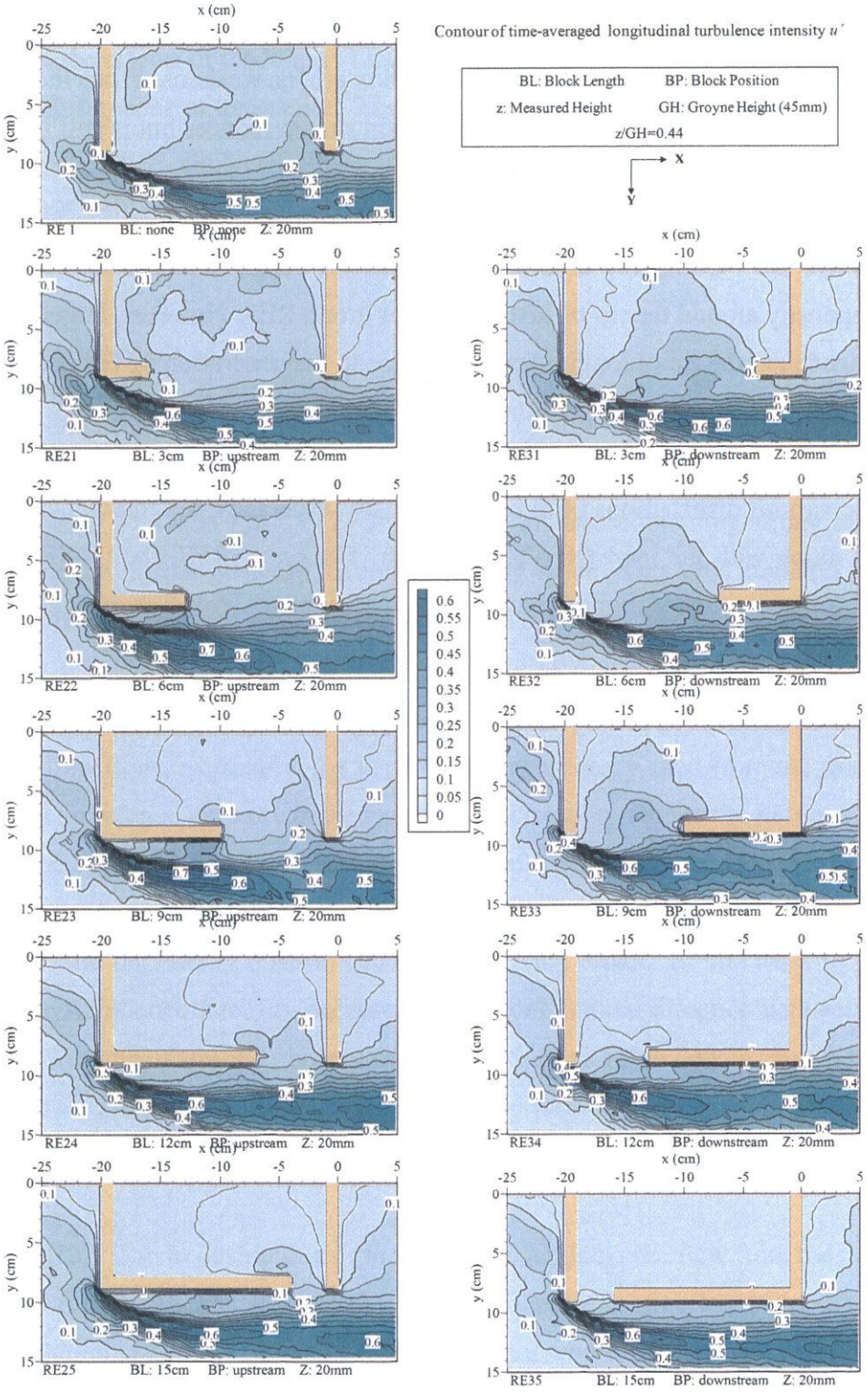

Figure 3.11: Contours of dimensionless time-averaged turbulence intensity in the lon gitudinal direction (u') on the horizontal plane (x-y) near the middle of water deptl (z/GH=0.44)under emerged condition

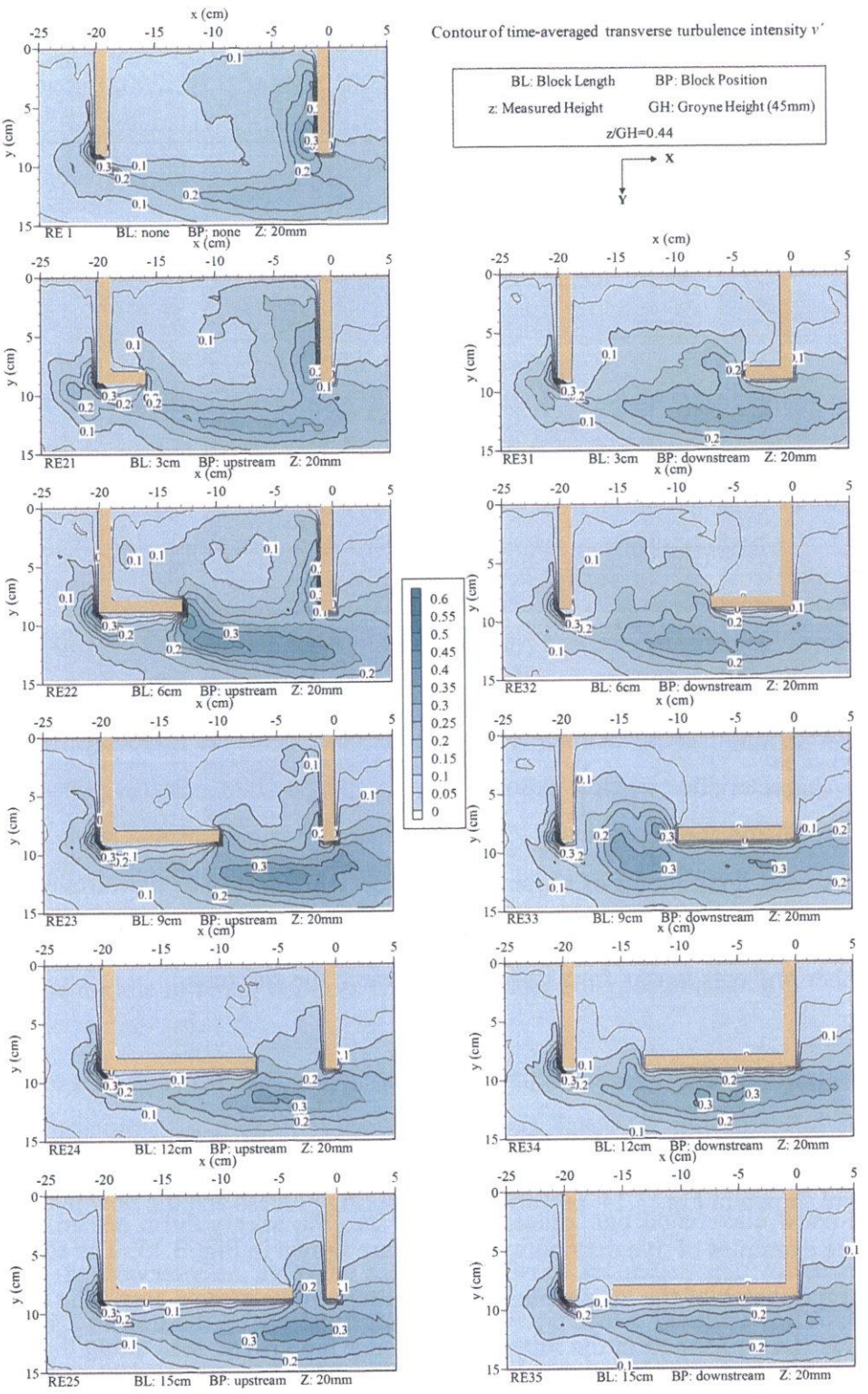

Figure 3.12: Contours of dimensionless time-averaged turbulence intensity in the transverse direction (v') on the horizontal plane (x-y) near the middle of water depth (z/GH=0.44)under emerged condition

Okubo-Weiss parameter

The Okubo-Weiss (OW) parameter (Weiss, J.,1991; Weiss, J.B., 2002) is adopted to describe the instantaneous turbulence flow field in two dimensional hydrodynamics, which shows the relative dominance of strain and turbulence vorticity. The OW parameter is defined as:

$$OW = S^2 - \omega^2 \tag{3.1}$$

where $S^2 = (u_x - v_y)^2 + (v_x + u_y)^2$ presents the component of strain and $\omega^2 = (v_x - u_y)^2$ means the components of flow vorticity. The positive and negative values of OW parameter demonstrate the dominance the shear and rotational motions respectively. The vortex structure is able to be characterized by strongly negative value of OW parameter. From the distribution of instantaneous OW parameter (as shown in Fig. 3.13), the district clarification is acquired about the advection of vortex and its pathway to the inner zone of box groyne. The shear force and rotation are alternatively distributed, and the advection of them to the inner zone mainly passes by the downstream of entrance. Compared to the inflow around the downstream of entrance, the flow shows relatively weak shear and rotation characteristics when it exports from the upstream of entrance, due to the energy dissipation inside the box groyne. The strong advection also brings in active turbulence motion, so the distribution of shear and rotation corresponds to the turbulence intensity distribution. The longer longitudinal block reduces the quantity of input vortex and inflow, and further prevents vortex from developing around the entrance.

Large coherent structures (LCS)

The dye images for the box groyne without a longitudinal block (CASE RE1) at several stages are shown in Fig. 3.14, performing the mixing process and the flow inside the goryne area. The examples of dye distribution images are shown in Fig. 3.15. The showing arrows indicate the sketch of the instantaneous flow pattern in the groyne area. The large coherent structures (LCS) formed in the mixing layer enter the groyne area along the groyne wall, and then the powerful energy makes them penetrate further to be the driving gyre. As a result, the intensity of large coherent structure reaches the entrance dominates the scale and strength of driving gyre, and further affects the secondary gyre. The scale of large coherent structures is greatly developed in the mixing layer and crosses the entrance with

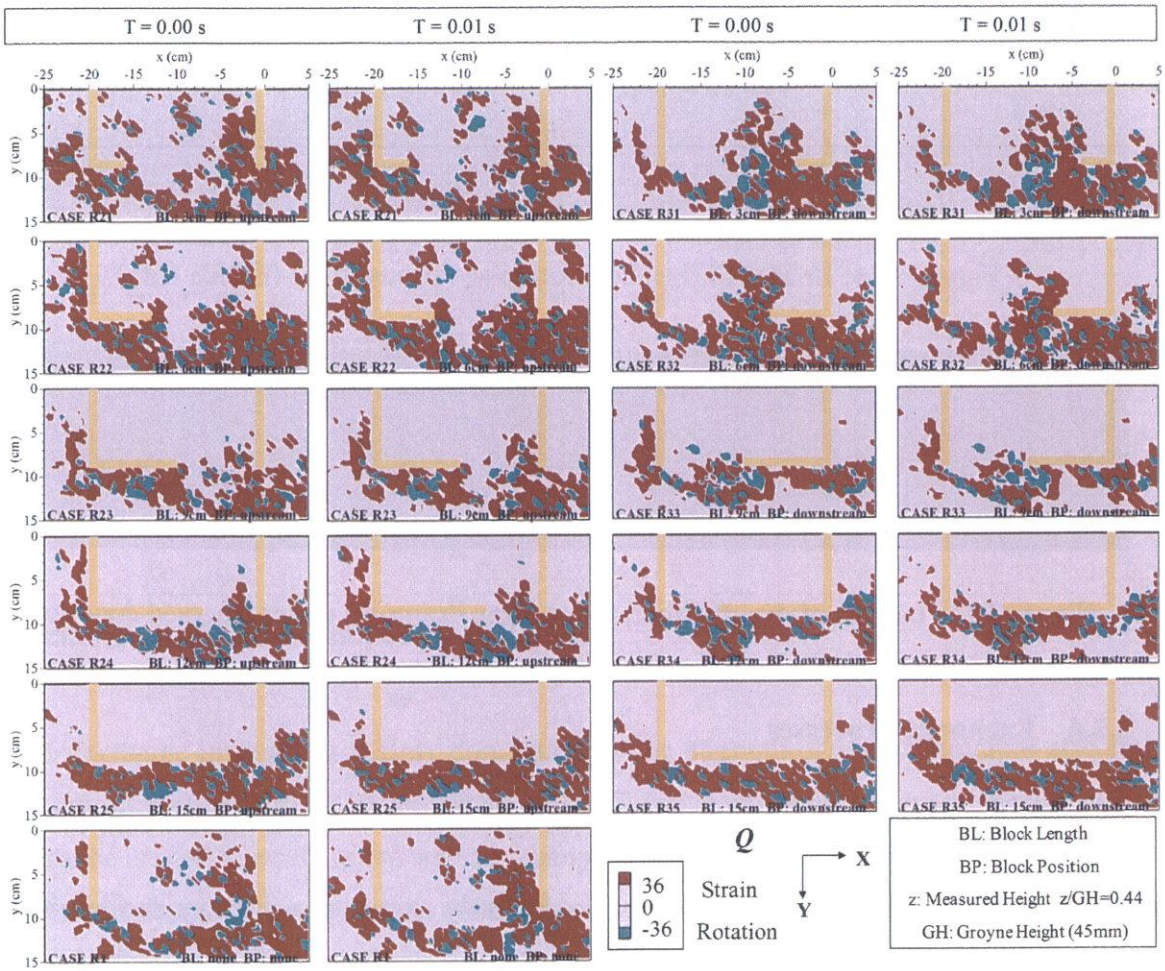

Figure 3.13: Contours of instantaneous Okubo-weiss parameter on the horizontal plane (x-y) near the middle of water depth (z/GH=0.44)under emerged condition

large size; in that case, the box groyne with long longitudinal block acquires less energy from large structures, as it can not provide sufficient space for movement of structures, as the images shown in Fig. 3.15. Regard to the same block condition, the secondary gyre driven by the driving gyre presents higher intensity and lager scale when the block is settled in the downstream, as to the interface between secondary gyre and driving gyre occurs in the position where the large structures just penetrate the driving gyre to deliver high propelling energy. As to the shielding effect of block, the blue water from the inner groyne area flows toward upstream along the block causing the mixing layer with high dye concentration.

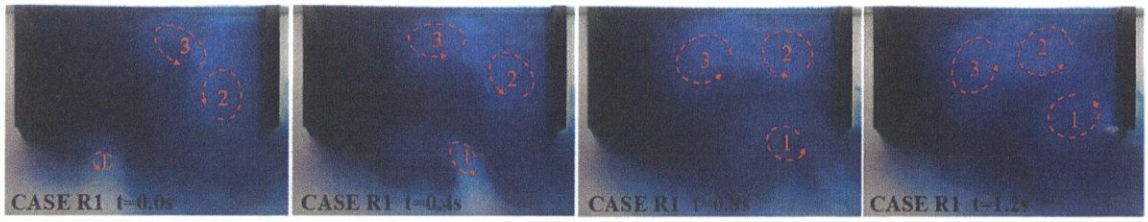

Figure 3.14: Images of dye distribution at various times (CASE RE1)

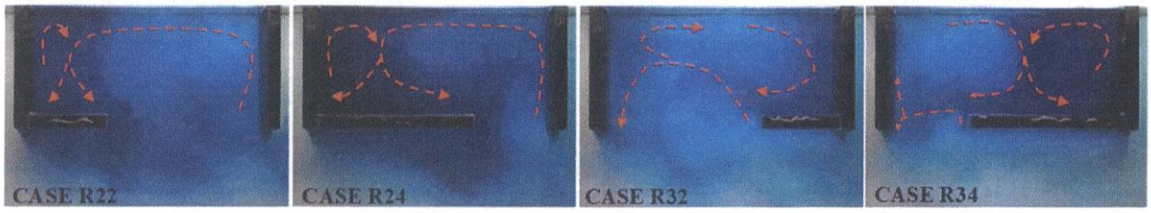

Figure 3.15: Images of dye distribution for some examples under emerged condition

3.2.4 Exchange processes

Distribution of transverse velocity at the entrance

Based on the time-averaged transverse velocity, mass exchange was examined on the entrance of the box groyne zone. Fig. 3.16 shows the longitudinal distribution of the vertical-averaged transverse velocity along the lateral boundary Y9 (y/GL=0.94, shown in Fig. 2.7) of the box groyne. The minus value means the inflow of box groyne, while the plus value means the outflow of box groyne. For most cases, the inflow almost occurs in the downstream part of entrance while the outflow occurs in the upstream part of entrance, and the turning point moves to the downstream and upstream with the increasing length of the longitudinal block in Group RE2 and Group RE3 respectively. The cases with short upstream longitudinal block (CASE RE21, 22, 23) show higher value in the velocity gradient and maximum velocity of outflow than the case without longitudinal block (CASE RE1). The cases with a downstream longitudinal block (Group RE3) show weaker outflow than the case without longitudinal block (CASE RE1). It is noticed that, the area under the inflow curve is smaller than the area under the outflow curve. The reason is that, the inflow inputs to the inner zone as the form of rotating large coherent structure (as shown in section 3.2.2.4). And it easily mistakes the time-averaged results when it is only analyzed by the data from one vertical plane at the entrance.

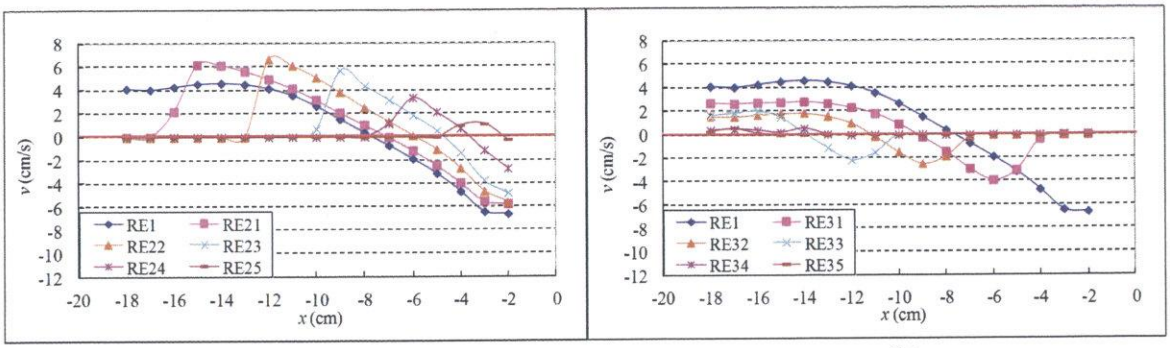

(a) (b)

Figure 3.16: Longitudinal distributions of time-averaged transverse velocity along the interface under emerged condition

Exchange coefficient obtained by PIV data

The exchange intensity is mainly dominated by the strength of vortex structure affecting the entrance of box groyne. Mass exchange coefficient contributed by transverse velocity in entrance is used to evaluate the water exchange feature at the entrance between box groyne and main stream. Weibrecht et al. (2008) introduced a calculating method to determine the mass exchange coefficient k by instantaneous data of PIV, as follows:

$$k = \overline{E'}/U = \overline{\frac{1}{2L}\int_0^L |v|dx}/U \tag{3.2}$$

where E' is the instantaneous exchange velocity, while U is the time-averaged velocity in main stream and L is the length of entrance.

The results are shown in Fig. 3.17. Compared to CASE RE1, the exchange coefficient of the group RE2 with the stronger vortex flow around the entrance is higher while that of group RE3 is lower. It is noticed that CASE RE23 and CASE RE33 have the highest mass exchange coefficient between their own groups respectively, to benefit the water exchange of box groyne with main stream. In particular, CASE RE25 shows a high exchange ability for inputting sediment with low mean velocity in the inner zone, which benefits the sediment deposit inside the box groyne.

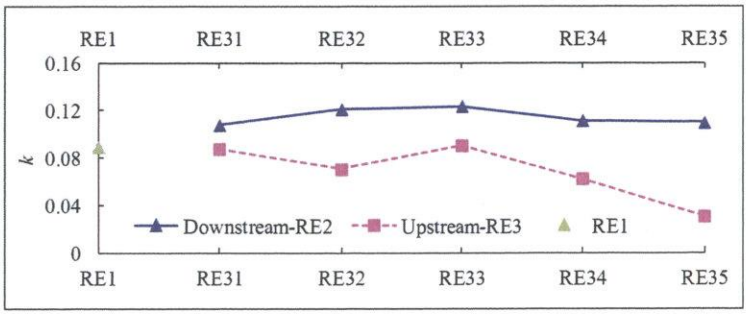

Figure 3.17: Exchange coefficient obtained by PIV data under emerged condition

Exchange coefficient obtained by DCM

From the variation images of the dye distribution shown in Fig. 3.14, the water exchange process is seen to be extremely affected by the large coherent structures (LCS). The classical theory considers exchange between the groyne area and the main stream as a liner reduction process (Uijttewaal et al. (2001), Weitbrecht et al. (2008) and Tominaga et al. (2008)). The variation of dye concentration in a groyne region is read as:

$$\frac{dC_g}{dt} = -\frac{1}{T_r}(C_g - C_s) \tag{3.3}$$

where C_g and C_s are the concentrations in the groyne region and main stream respectively, and T_r is the residence time. For the box groyne, the T_r is equal to $A/(kU_S L$. In here, A is the area of inner zone; k is the exchange coefficient; U_s is the time-average velocity in the main stream; L is the width of entrance and equal to $(S - BL)$. The exchange coefficient obtained by the DCM can be read as:

$$k_{DCM} = \frac{A}{T_r U_s L} \tag{3.4}$$

Under the transparent main stream $C_s = 0$, $1/T_r$ is acquired from the slope S of the liner approximation curve, which is determined by the regression analysis to the variation of the dye concentration.

The comparison of water exchange coefficients judged by DCM and PIV method is shown in Fig. 3.18. According to the comparison of Weitbrecht et al. (2008), the exchange coefficients under the case without longitudinal block (CASE RE1) can be obtained with similar values by these two methods. However, the results showed in Fig. 3.18 present the great differences between these two methods. The previous DCM study is based on that the mixing layer almost places at the entrance area, thus the zero value of Cs is appropriate.

But due to the strong intensity and the arc shape of mixing layer in the cases of this study, the water at the entrance is mixed with the dye water inside the mixing layer instead of mixing with the transparent main stream directly. The powerful LCS input the dye water exiting from the inner zone to the groyne zone again at the downstream of entrance (as shown in Fig. 3.14). Hence as the actual situation in this study, the concentrations of main stream considered in the equation (1) is not transparent ($C_s > 0$), causing the exchange coefficient obtained by DCM to be smaller than the actual value. To achieve closer value with actual value, a simple modification is adopted to the equation in DCM.

Assuming the $C_s = \alpha C_g$, then substituting it into the equation 3.2 and equation 3.3:

$$k_{m(DCM)} = \frac{AS}{U_s L(1-\alpha)} \tag{3.5}$$

The residence time T_r is equal to $(1-\alpha)/S$; the α is considered as a constant, and equal to 0.585 derived by the proportion between the original exchange coefficients of DCM and PIV from the case without longitudinal block (CASE RE1). The modified exchange coefficients for DCM are shown in Fig. 3.19. However, the values of DCM and PIV are not fitting well enough when the block is long. The PIV method just judges the exchange ability of entrance by considering the transverse velocity at the entrance, being suitable for the situation with single gyre or two gyres but with a fairly small secondary gyre in the inner zone of groyne, as CASE RE1 and RE21. But for the box groyne with strong secondary gyre, the PIV method ignores the interchange effect of interface between the two gyres in the inner zone of box goryne, causing the exchange coefficient in PIV to be larger than the actual value. Hence, the modification to the PIV equation is necessary, in this study, it is assumed that exchange coefficient is proportional to the ratio of the $L(GL)/A$. The following method is adopted:

$$k_{m(PIV)} = R_i R_{gi} \frac{L(GL)}{A} k_{PIV} \tag{3.6}$$

where the R_i is the improved coefficient associated with the promotion effect of upstream longitudinal block to the driving gyre, the $R_i L(GL)/A$ is the ratio of affecting area by driving gyre, which need be area calculation when it is used in other type case, and the value of R_i is 1.23 for the case with an upstream longitudinal block and 1 for the case without longitudinal block or with a downstream longitudinal block in this study; the R_{gi} is the reduction coefficient associated with the gyre number j in the inner zone, and the

value is 1 for the case with two or less gyres and 0.69 for the case (as CASE RE33) with three gyres in the inner zone in this study. The value of 0.69 is determined by the ratio of the area of two main gyres to the area of inner zone. It's noticed that the gyre number in the inner zone is different from the gyre number in the groyne field for several cases as CASE RE34 and CASE RE35 due to their driving gyre is located in the outside area of groyne. According to the modification, the comparisons of exchange coefficient are presented on the Fig. 3.20, and the correlation coefficient between the values of DCM and PIV is 0.99 for the group RE2 and 0.97 for the group RE3, showing the compatibility of the equation (4) to the cases in this study. Fig. 3.21 shows the temporal variation of dye concentration and the resident time T_r. Generally, the exchange process becomes slower with increased block length. Under the same longitudinal block length condition, the cases with a downstream longitudinal block display lower exchange ability. When the longitudinal block is placed in the upstream, the resident time in the cases with short block length (CASE RE21, RE22) is close to it in the case without longitudinal block (CASE RE1). For the exchange coefficient shown in Fig. 3.20, the cases with short longitudinal block (CASE RE21, RE22) in the upstream present higher exchange ability than the case without longitudinal block, to further clarify the effect of short longitudinal block placed in the upstream on the enhancement of interchange mechanism.

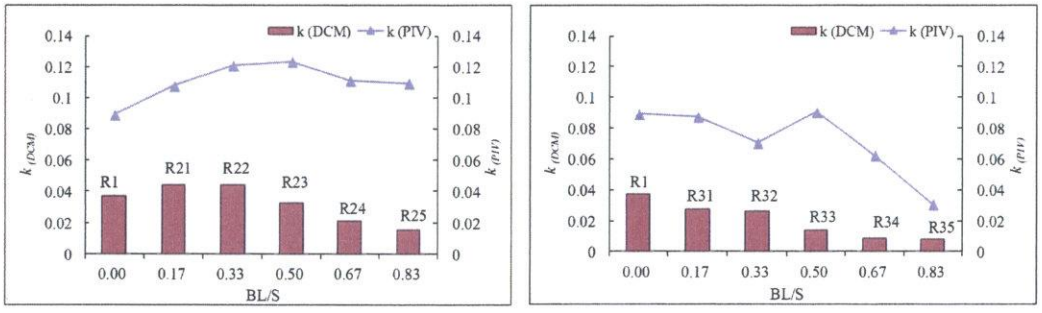

(a) (b)

Figure 3.18: Exchange coefficient obtained by DCM and PIV method under emerged condition(a: effects of the length of upstream longitudinal block; b: effects of the length of longitudinal downstream block)

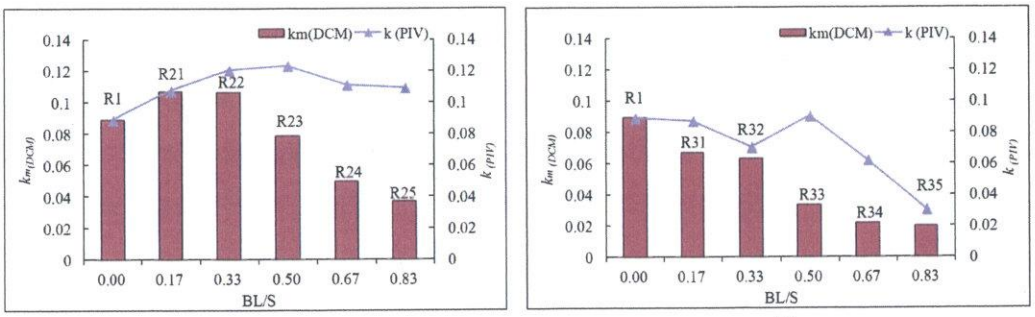

(a) (b)

Figure 3.19: Exchange coefficient obtained by modified DCM and PIV method under emerged condition(a: effects of the length of upstream longitudinal block; b: effects of the length of longitudinal downstream block)

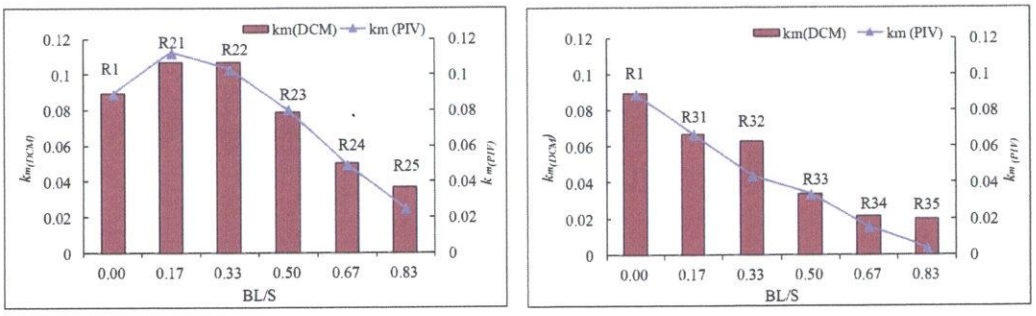

(a) (b)

Figure 3.20: Exchange coefficient obtained by modified DCM and modified PIV method under emerged condition(a: effects of the length of upstream longitudinal block; b: effects of the length of longitudinal downstream block)

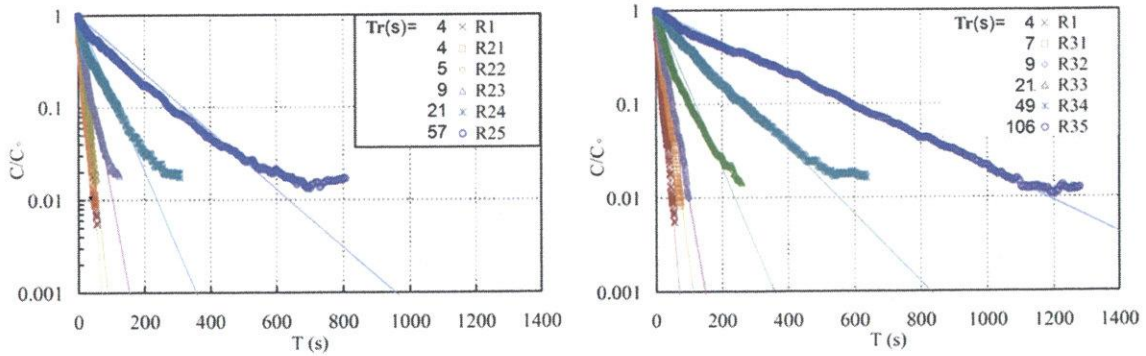

(a) (b)

Figure 3.21: Temporal variation of dye concentration under emerged condition(a: effects of the length of upstream longitudinal block; b: effects of the length of longitudinal downstream block)

3.2.5 Bed shear stress

From the available information in previous researches, the distribution of bed shear stress affected by the HV system determines the formation and evolution of scour around the box groyne. The following equation is conducted to calculate the bed shear stress in the open channel:

$$\tau_b = \rho C_f (u_b^2 + v_b^2) \tag{3.7}$$

$$\tau_{bx} = \rho C_f u_b \sqrt{u_b^2 + v_b^2} \tag{3.8}$$

$$\tau_{by} = \rho C_f v_b \sqrt{u_b^2 + v_b^2} \tag{3.9}$$

where C_f is generalized Darcy-Weisbach friction factor, which is equal to the Darcy-Weisbach friction factor f divided by 8. The dimensionless bed shear stress τ_b/τ_0 is introduced to illustrate the distribution of bed shear stress here. The τ_0 is the bed shear stress in the coming flow, which is calculated by the mean bulk velocity u_m and the mean generalized Darcy-Weisbach friction factor C_{fm}:

$$\tau_0 = \rho C_{fm} u_m \tag{3.10}$$

hence,

$$\frac{\tau_b}{\tau_0} = \frac{C_f}{C_{fm}} \cdot \frac{u_b^2 + v_b^2}{u_m^2} \tag{3.11}$$

$$\frac{\tau_{bx}}{\tau_0} = \frac{C_f}{C_{fm}} \cdot \frac{u_b \sqrt{u_b^2 + v_b^2}}{u_m^2} \tag{3.12}$$

$$\frac{\tau_{by}}{\tau_0} = \frac{C_f}{C_{fm}} \cdot \frac{v_b \sqrt{u_b^2 + v_b^2}}{u_m^2} \tag{3.13}$$

In the far upstream of groyne area, $v_b = 0$ and $\tau_{bx} = \tau_0$, then

$$\alpha = \frac{C_f m}{C_f} = (\frac{u_b}{u_m})^2 \tag{3.14}$$

The U_b/U_m is roughly evaluated from the log law distribution for smooth bed:

$$\frac{u_b}{u_m} = \frac{\frac{1}{k} \ln \frac{z_b u_*}{\nu} + 5.5}{\frac{1}{k} \ln \frac{h u_*}{\nu} - \frac{1}{k} + 5.5} \tag{3.15}$$

where z_b is the measured height. The α is obtained as 0.781 for emerged condition. Fig. 3.22 shows the contours of dimensionless time-averaged bed shear stress. The bed shear stress increases steeply from the tip of spur dike and reach the maximum value between

the two groynes in the main channel. Due to the measurement limitation, the description showing the effect of the HV system on the bed shear stress is lacking in the results, which leads the lower value of bed shear stress around the tip of groyne. When the longitudinal block is set, the maximum value zone moves to the groyne side with the smaller value. In some cases without longitudinal block or with short longitudinal block (CASE RE1, RE21, RE22, RE23, RE31, RE32, RE33), there is the high bed shear stress related to strong input vortex structure in the front area of the second groyne (CASE RE1 and Group RE2) or the tip of the longitudinal block (Croup RE3). It supports the sediment entering the groyne zone at the bed even the scouring in this position. The shape of this zone with high value skews to the upstream side for CASE RE1, RE31, RE32 and RE33, while it distributes along the wall of second groyne for CASE RE21, RE22 and RE23. These phenomena determine the sediment distribution in the inner zone of box groyne, which will be detailed described in the section about the experimental results of movable bed.

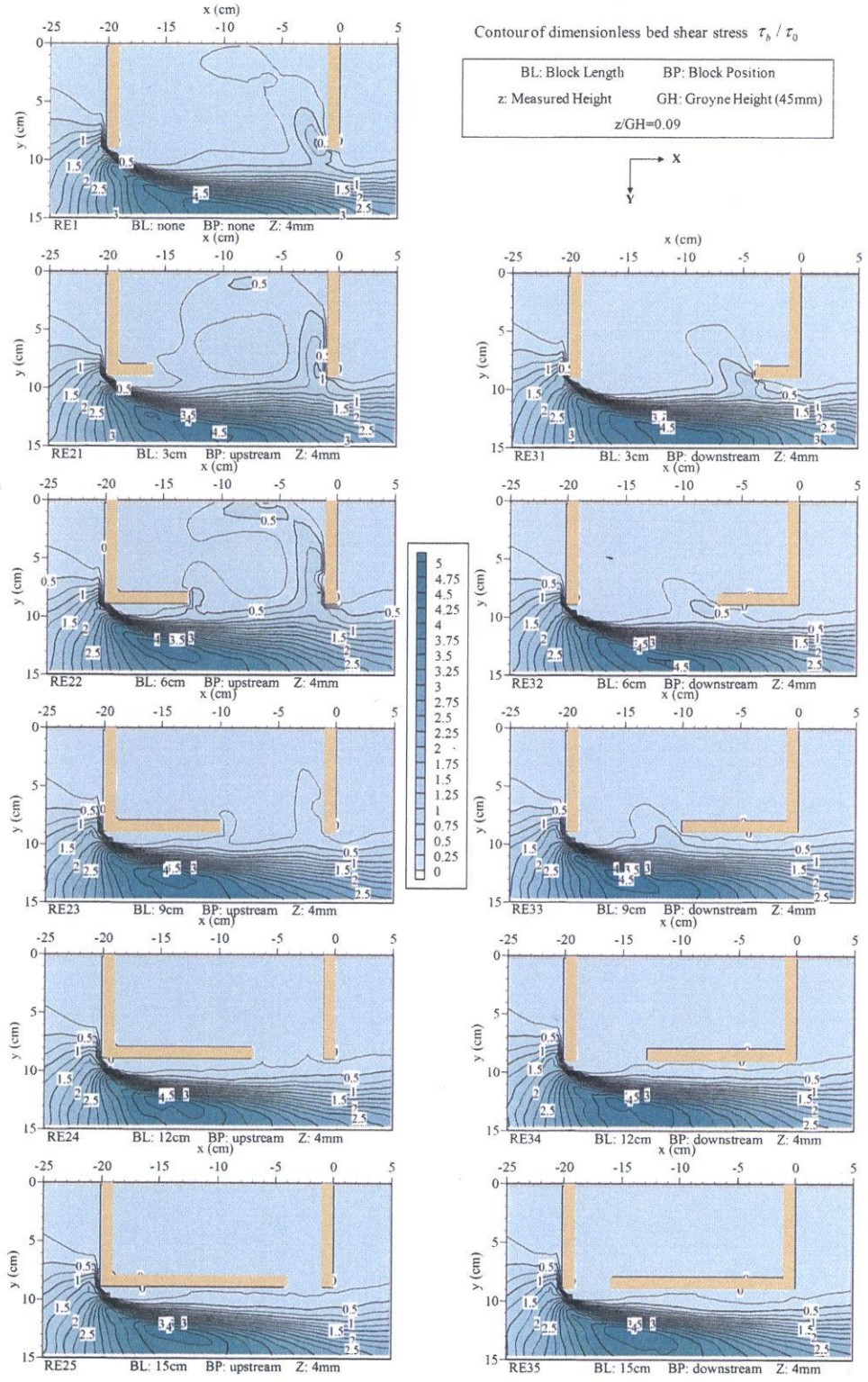

Figure 3.22: Contours of dimensionless time-averaged bed shear stress(τ_b/τ_0)under emerged condition

3.3 Effects of the spacing of box groyne

Beside the spacing 18cm (S/GL=2), the other two kinds of spacing as 12cm (S/GL=1.33) and 24cm (S/GL=2.67) are introduced to explore the effect of different spacing of groyne on the flow field around the box groyne. The length of longitudinal block taken as 0.5 ratio of spacing is 6cm and 12 cm for 12cm spacing and 24 cm spacing respectively. The following table gives the case name:

Table 3.1: The name of the case with other spacings under emerged condition

Spacing (cm)	Block Position		
	none	upstream	downstream
12	RE1-12	RE23-12	RE33-12
24	RE1-24	RE23-24	RE33-24

3.3.1 Mean velocity in the inner zone of box groyne

Fig. 3.23(a) shows the comparisons of mean velocity in the inner zone of box groyne U_{ig} under different spacing ratio. As adding the spacing of box groyne, the mean velocity in the inner zone increases with decreasing slope whether there is longitudinal block or not. The effect of longitudinal block on the mean velocity in the inner zone for different spacing is shown in Fig. 3.23(b). With the spacing increasing, the reduction becomes larger when the longitudinal block is set in the upstream side of entrance, while it becomes smaller when the longitudinal block is set in the downstream side of entrance. It is induced by the energy diffusion in the mixing layer as going downstream.

3.3.2 Flow structures

Flow pattern around the groyne area

Fig. 3.24 shows the time-averaged velocity vectors for the cases with 12cm and 24cm spacing on the horizontal plane. Fig. 3.25 and Fig. 3.26 show the time-averaged velocity contour for the cases with 12cm (S/GL=1.33), 18cm (S/GL=2) and 24cm (S/GL=2.67) spacing on the horizontal plane of z/GH=0.09. Compared with the time-averaged velocity

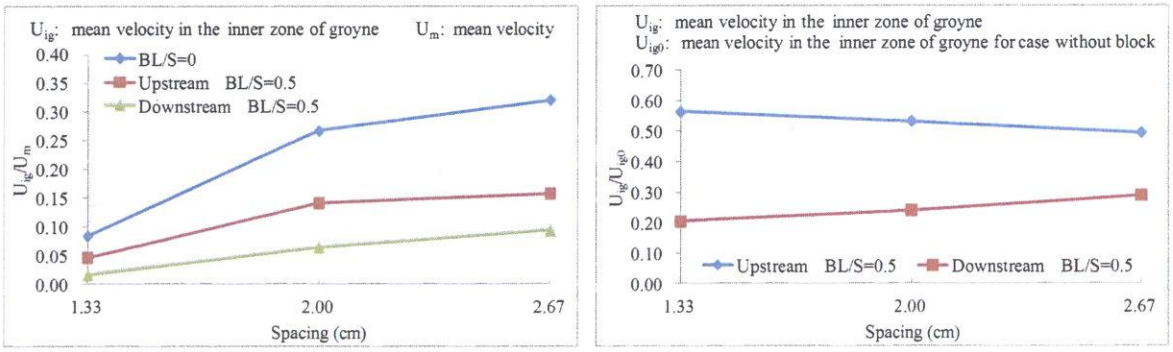

Figure 3.23: Comparisons of mean velocity in the inner zone of emerged box groyne U_{ig} under different spacing ratio

for the case with 18cm spacing, it is clear that the gyre system and in the groyne field is largely changed by the different spacing of box groyne.

a) Spacing=12cm For the case without the longitudinal block (CASE RE1-12), two-parallel-gyre system is generated like the driving gyre is expelled to the entrance area along with the enlarged secondary gyre, and the center of driving gyre locates in the outside of box groyne. Lowering the spacing of box groyne makes the vortex structure develop insufficiently when it gets the downstream of entrance. Less vortex structure enters in the inner zone when the second groyne places around the top of the arc curve of mixing layer. These two reasons make the smaller value of velocity in the downstream of entrance. When the longitudinal block is set in the upstream side of entrance (CASE RE23-12), the large coherent structure directly generates a gyre at the entrance, meanwhile pushes part of energy to the inside along the wall of second groyne to be other gyres in the inner zone, and it creates two gyres with the same direction of rotation. When the longitudinal block is set in the downstream side of entrance (CASE RE33-12), the driving gyre locates outside areas as the case with long longitudinal block under the condition of 18cm spacing. The setting of the longitudinal block makes the area of the highest longitudinal velocity move to the opposite of the box groyne, which is different with the case with 18cm spacing.

b) Spacing=24cm For the case without the longitudinal block (CASE RE1-24), the two-gyre system like in CASE RE1-18 still exists but with a larger secondary gyre. When the longitudinal block is set in the upstream side of entrance (CASE RE23-24), the secondary

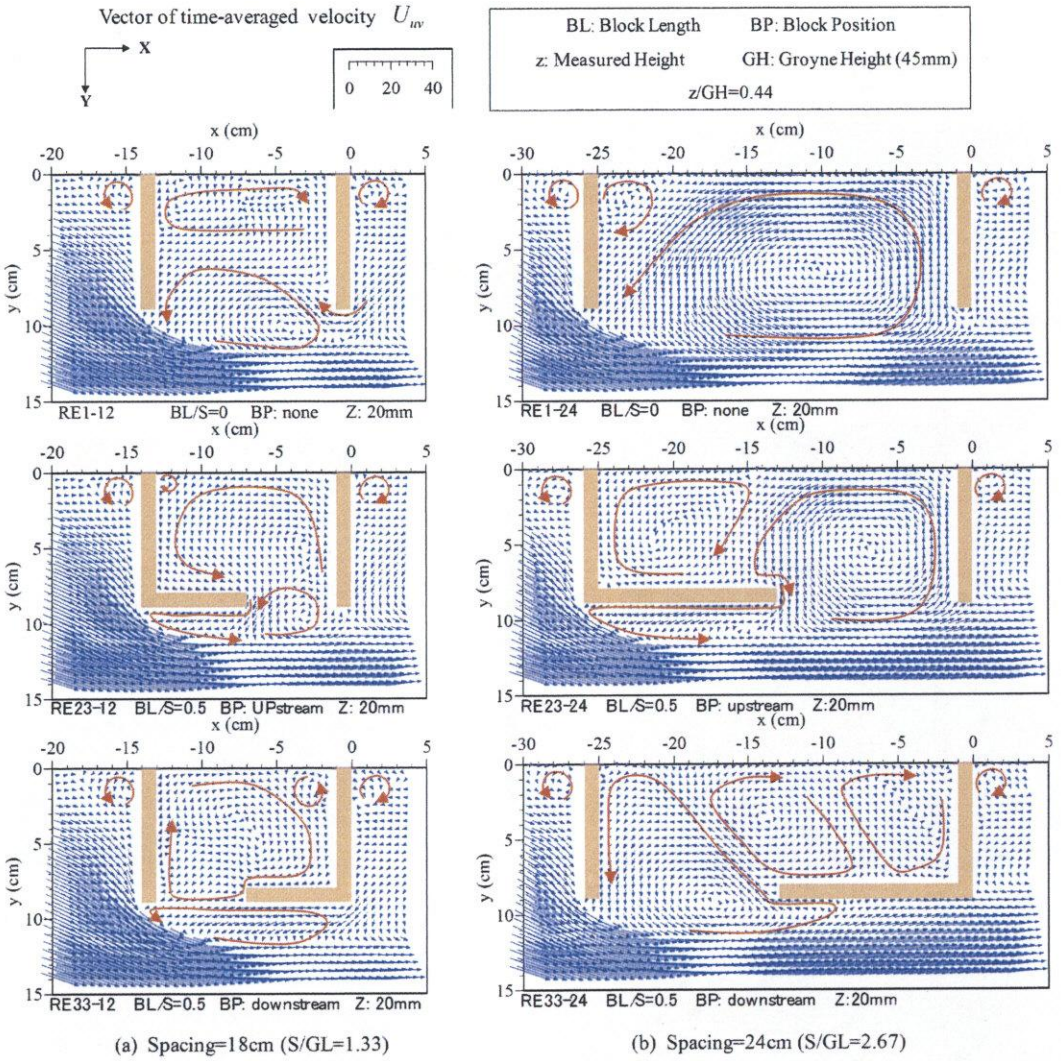

Figure 3.24: Time-averaged velocity vectors on the horizontal plane (x-y) near the middle of water depth (z/GH=0.44) for the cases with different spacings under emerged condition

gyre enlarges. When the longitudinal block is set in the downstream side of entrance (CASE RE33-24), the three-gyre system generates. The longer mixing layer between two groynes promotes more mass exchanges between the inner zone and the main channel, and then increases the mean velocity in the inner zone. The vortex structure with sufficient development gives much water with high energy to the inner zone from the downstream of entrance, causing the higher velocity distribution in the transverse direction than the cases with 18cm spacing, as shown in Fig. 3.26(b) (c). The setting of the longitudinal block makes the area of the highest longitudinal velocity move to the box groyne, which is the same as the case with 18cm spacing. It is noticed that, there are many similarities between the emerged case

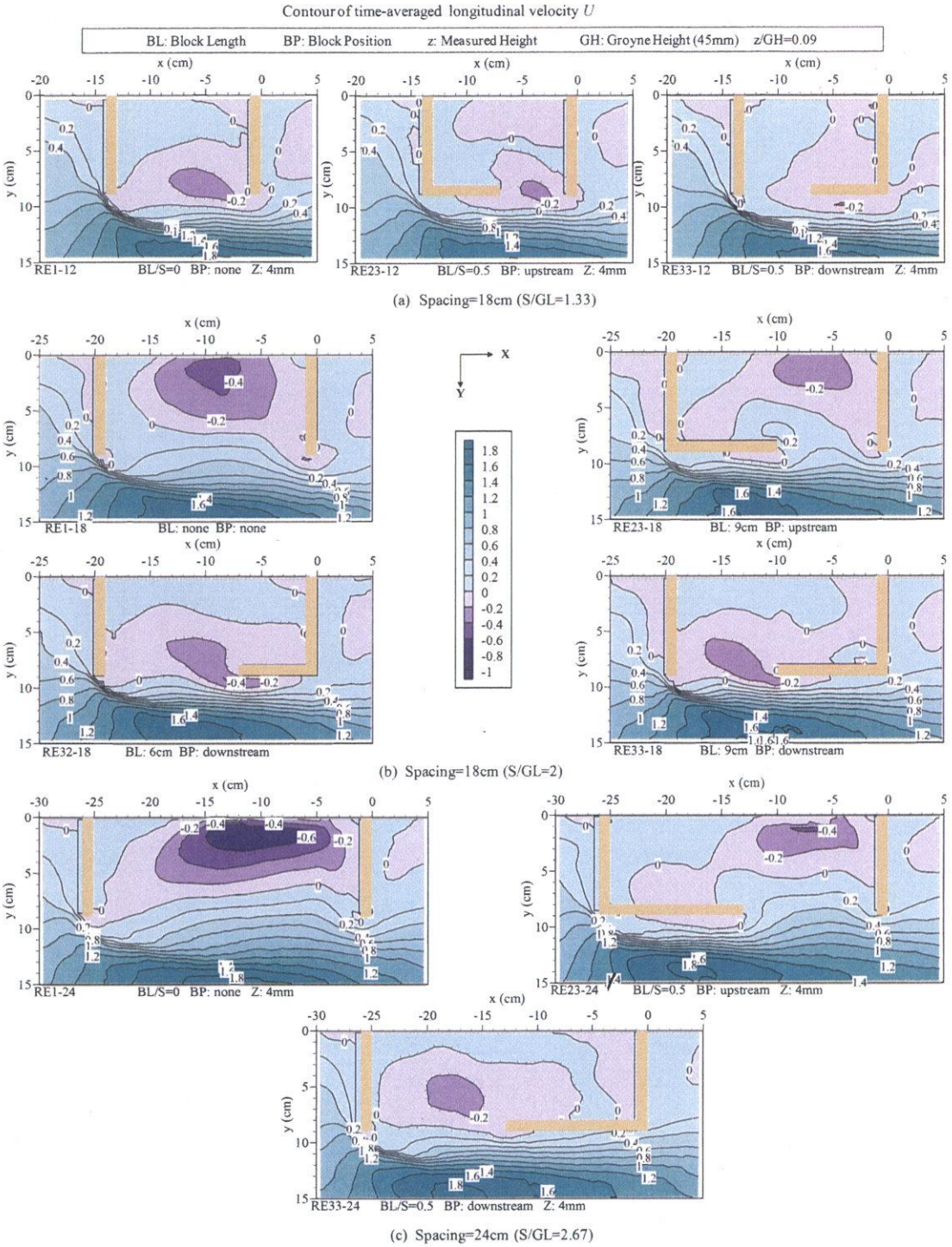

Figure 3.25: Contours of dimensionless time-averaged velocity in the longitudinal direction (U) on the horizontal plane (x-y)(z/GH=0.09) for the cases with different spacings under emerged condition

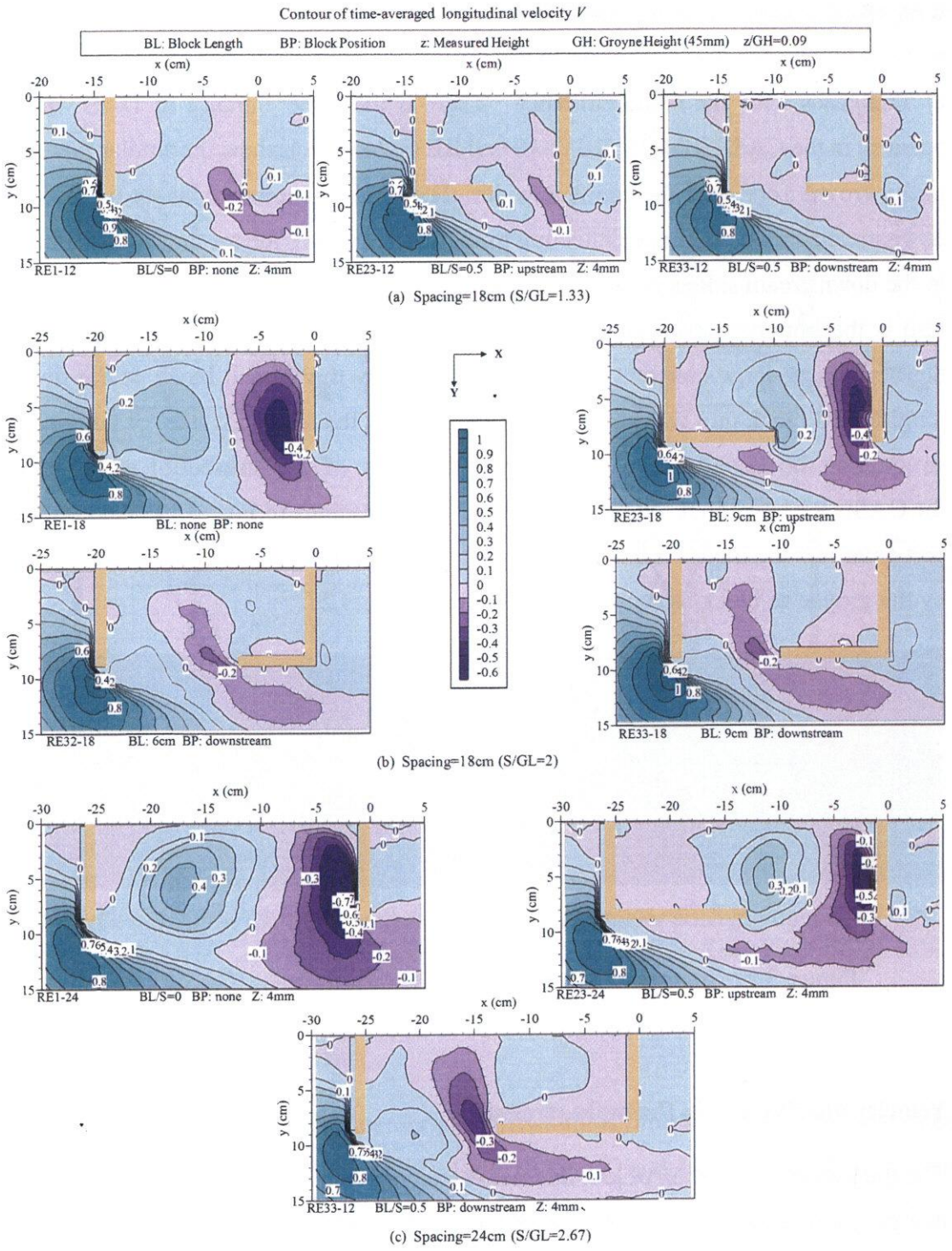

Figure 3.26: Contours of dimensionless time-averaged velocity in the transverse direction (V) on the horizontal plane (x-y)(z/GH=0.09) for the cases with different spacings under emerged condition

with 18cm spacing (S/GL=2) and 24cm spacing (S/GL=2.67).

c) The cases with the same entrance There is the same entrance in 12cm width and position in the CASE RE1-12, RE32-18 and RE33-24, which show the similar flow pattern in the groyne zone with the entrance width. The same phenomenon about the flow in the downstream side of entrance deflecting to the upstream side means the longitudinal block in the downstream side is not the only reason for this phenomenon, and the entrance width also is the important even key parameter affecting the flow direction. It is because that the developing large coherent structure is divided by the second block or the tip of the longitudinal block into two parts when it develops as the shape like the of large coherent structure in the second image (t=0.4s) from the image of dye distribution at various times for CASE RE1 (without longitudinal block, 18cm spacing) in Fig. 3.14. And only small part enter into the inner zone with relatively small size and be easily deflected the direction by the groyne or block as shown in the images of Fig. 3.27.

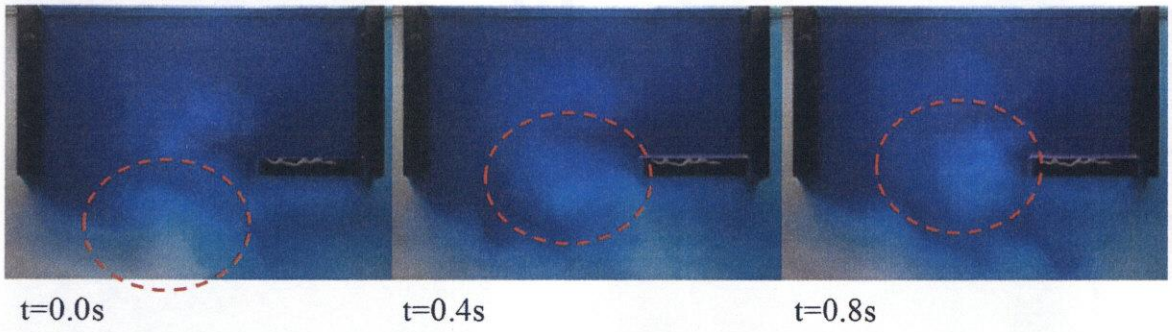

Figure 3.27: Images of dye distribution at various times (CASE RE32-18)

Velocity distribution in the main stream

The transverse distribution of longitudinal velocity in the sections of first groyne, middle of box groyne and second groyne is shown in Fig. 3.28. In the section of first groyne, different spacing and the arrangement of longitudinal velocity hardly affect the longitudinal velocity near the middle of main stream. In the section of middle of box groyne with 18cm and 24cm spacing, the setting of longitudinal block makes the area of high longitudinal velocity move close to the box groyne as mentioned in the above section. While the longitudinal block makes the area of high longitudinal velocity move to the opposite of the box groyne with

12cm spacing. The sharp fall in the mass transport to the inner zone of box groyne for the case with 12cm spacing causes the higher velocity of main stream in the section of second groyne.

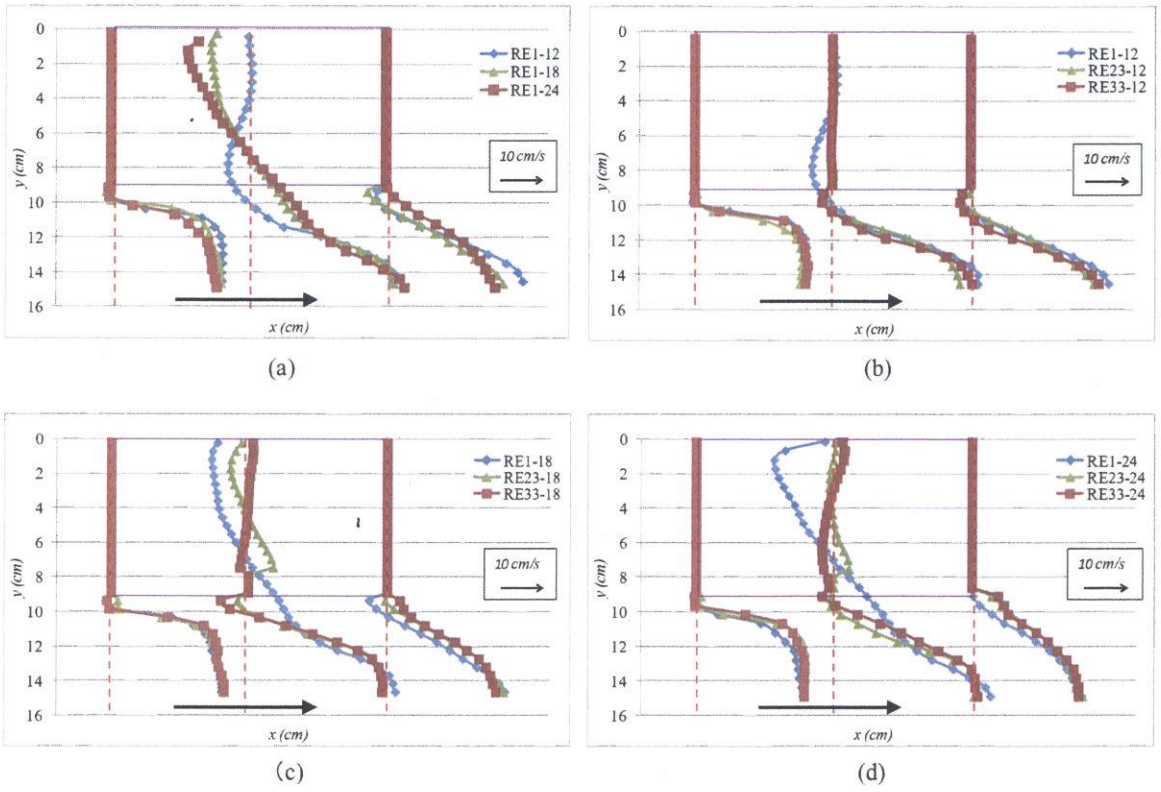

Figure 3.28: Transverse distribution of longitudinal velocity (U) on the horizontal plane (x-y) of z/GH=0.09 for the cases with different spacings under emerged condition

3.3.3 Turbulent characteristic

Fig. 3.29 and Fig. 3.30 show the contour of dimensionless time-averaged turbulence intensity for the cases with 12cm (S/GL=1.33), 18cm (S/GL=2) and 24cm (S/GL=2.67) spacing on the horizontal plane of z/GH=0.09. Regardless of the different spacing, the downstream longitudinal block has the effect of reducing the turbulence on the area around the tip of first groyne. As shown in Fig. 3.30, the distribution of turbulence intensity in the transverse direction shows the transverse turbulence is summoned by the tip of longitudinal block, and it benefits the mass exchange in the interface of box groyne.

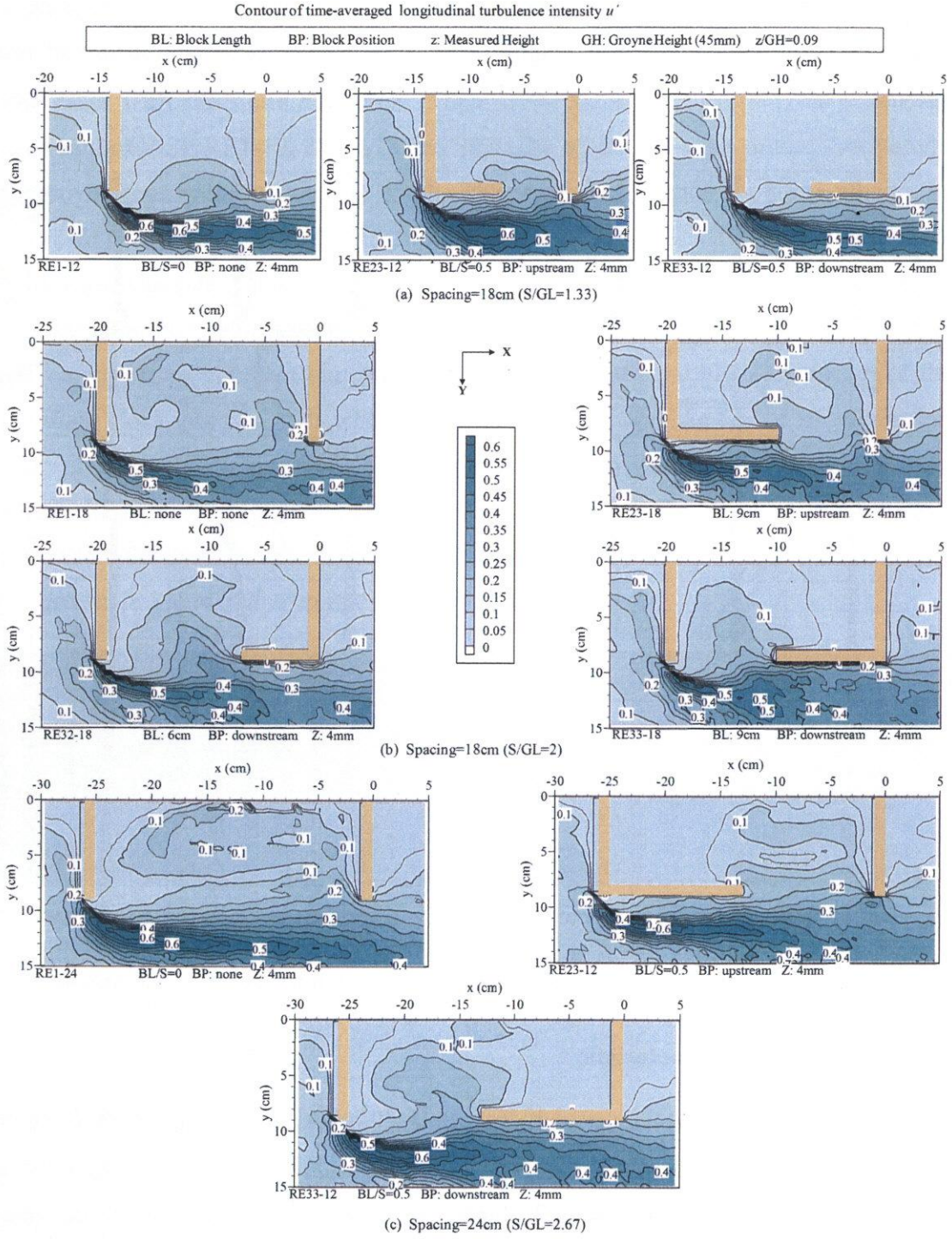

Figure 3.29: Contours of dimensionless time-averaged turbulence intensity in the longitudinal direction (u') on the horizontal plane (x-y)(z/GH=0.09) for the cases with different spacings under emerged condition

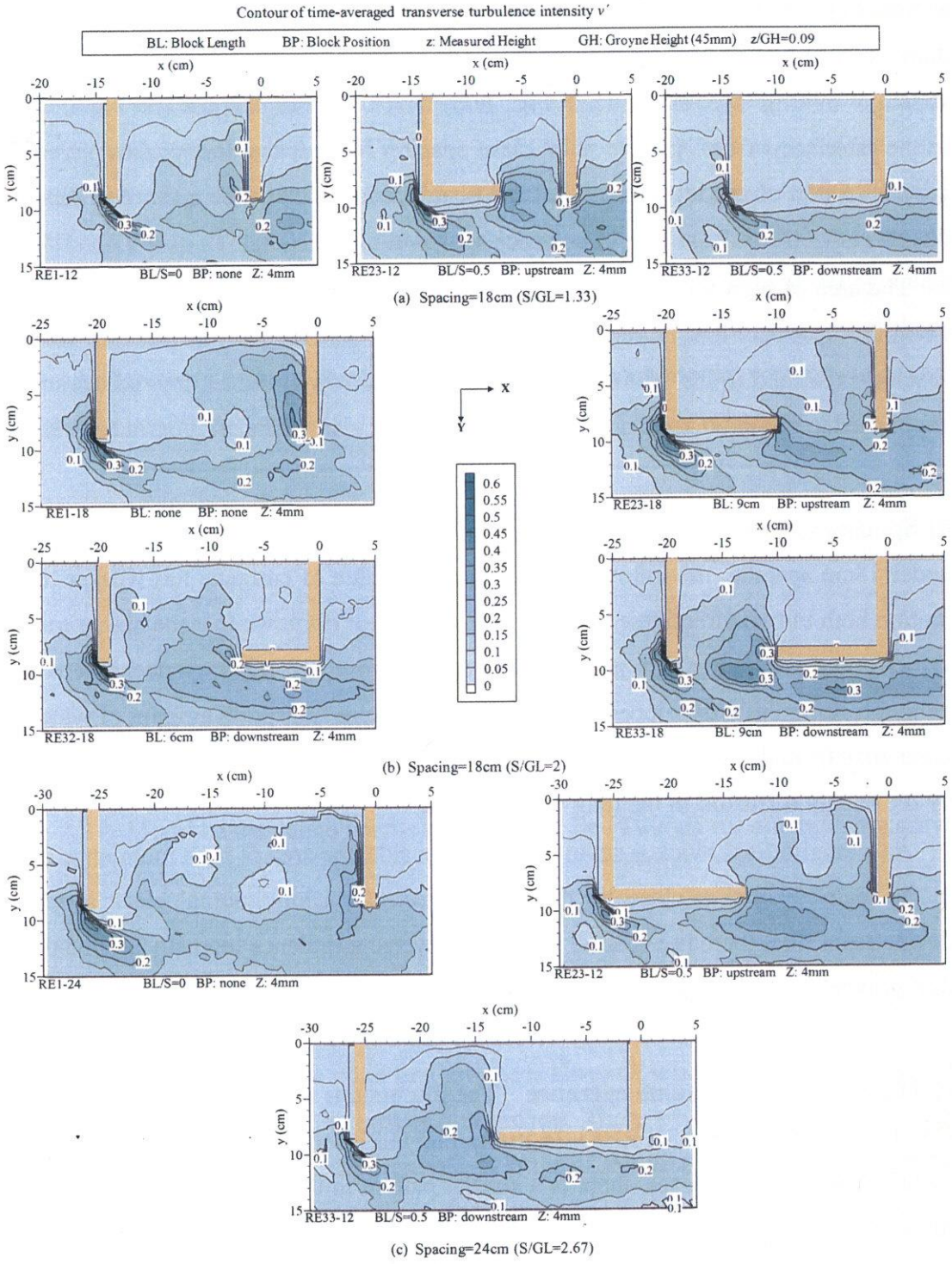

Figure 3.30: Contours of dimensionless time-averaged turbulence intensity in the transverse direction (v') on the horizontal plane (x-y)(z/GH=0.09) for the cases with different spacings under emerged condition

a) Spacing=12cm Compared with other cases with the same ratio of longitudinal block, there is still higher turbulence intensity in longitudinal direction distributed in the downstream of mixing layer as shown in Fig. 3.29, which presents that the less mass exchange in the interface of box groyne with 12cm spacing reduces the energy dissipation in the groyne section of mixing layer. Weaker turbulence intensity in the transverse direction is distributed in the downstream of entrance shown in Fig. 3.30.

The area of high turbulence intensity in the main stream becomes wider and stronger when the upstream longitudinal block is set, as the phenomenon in the case with 18cm spacing explained in the section 3.2.2. Due to the narrow entrance, few vortex structures are pushed to the inner zone under the condition of the downstream longitudinal block.

b) Spacing=24cm Compared with the cases with the same ratio of longitudinal block under 18cm spacing, the inflow in the downstream side of entrance has weaker turbulent motion both in two directions. In the section of 3.3.1, it is known that the higher transverse velocity is presented in this place. What causes these two contrary phenomena is that, although sufficiently developed large coherent structure transports amount of water to the inner zone from the downstream side of entrance, the intensity of vortex structure is reduced by the energy diffusion in the long mixing layer.

As a longitudinal block is set in the upstream side, the area of high turbulence intensity in the main channel is closer to the box groyne. As a longitudinal block is set in the downstream side, there is a smaller area of transverse turbulence intensity around the tip of first groyne.

c) The cases with the same entrance The discussions are between the CASE RE1-12, CASE RE32-18 and CASE RE33-24 in the Fig. 3.29 and Fig. 3.30. As the similar flow pattern between these cases, there is a similar pattern in the distribution of time-averaged turbulence intensity supporting the descriptions about the case with the same entrance in the section 3.3.1. But the intensity of the CASE RE32-18 and CASE RE33-24 is stronger and larger distributes in the inner zone than the condition in CASE RE1-12, which is induced by the effect of the longitudinal block. The smaller longitudinal turbulence around the tip of first groyne is presented in the CASE RE32-18 because of its larger adverse longitudinal velocity here as shown in Fig. 3.25.

3.3.4 Exchange processes

The modified method described in the section 3.2.3 is conducted to modify the original exchange coefficient obtained by PIV in the cases with different spacing, and the results are shown in the Fig. 3.31.In particular, the determination of driving gyre for CASE RE23-12 is difficult due to its special gyre system described in the section 3.3.1.2, hence, the ratio of affecting area by driving gyre is picked as the two times of the ratio of affecting area by the first driving gyre. The case without the longitudinal block has the strongest exchange ability, while the case with the downstream longitudinal block has the weakest. In general, the exchange coefficient in the case with 18cm spacing (S/GL=2) is highest.

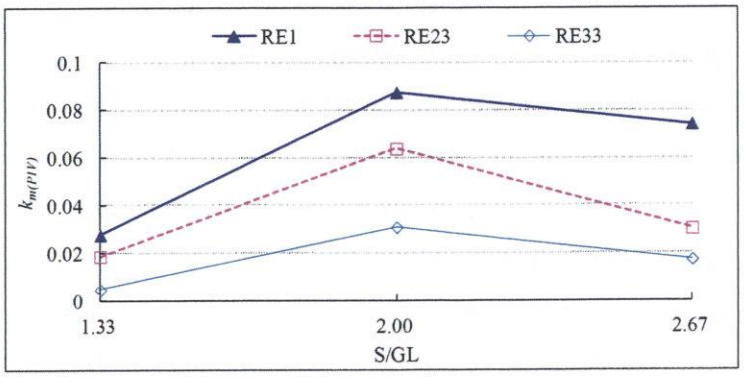

Figure 3.31: Modified exchange coefficient obtained by PIV data for emerged boxgroyne under different spacings

3.4 The box groyne with piles group in front of the first groyne

The large scour hole around the tip of first groyne is always a serious problem in the groyne engineering for its damage to the root of first groyne. There are many efforts on avoiding this problem. Setting the diversion groyne in front of the first groyne is able to reduce the velocity of coming flow to control the formation of HV system and transverse velocity around the tip of first groyne. Modifying the structural style of groyne to benefit its safety also makes a good effect in the practice. This study introduces the pile into the protection of groyne. The pile group is arranged in front of first groyne, as shown in Fig. 3.32.

The time-averaged velocity vectors and contours on horizontal plane are shown in Fig. 3.33. The piles redistribute the flow field in front of the first groyne and uniform the outflow. The velocity gradient around the tip of first groyne slows down obviously. The lower

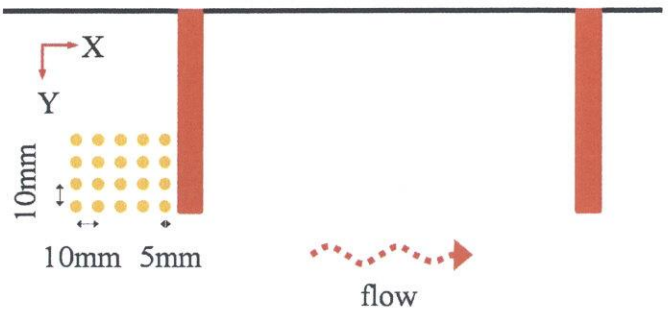

Figure 3.32: Arrangement of pile group in front of first groyne

turbulence intensity around the tip of first groyne showed in the Fig. 3.34, presents that the formation of HV structure and shedding vortex structure are controlled successfully, which benefits the reduction of the scour hole around the tip of first groyne. And wide mixing layer around the pile group and the tip of first groyne means more dissipation of energy conducted here. These two phenomena bring the smaller value of turbulence intensity to the downstream of mixing layer, which is related to the energy transport to the inner zone of box groyne. Hence, as the observation from the Fig. 3.33, the gyre structure in the inner zone of groyne shows the similar shape with the case without the pile group, but weaker intensity as reducing about 60% mean velocity in the inner zone of groyne. The weak vortex structure has not the ability of deep entering the inner zone makes the area of maximum longitudinal velocity away from the inside wall. The value of exchange coefficient obtained by PIV is about 0.035, almost 40% of the value in the case without the pile group. In the experiment of bed load, the maximum scour depth is largely reduced compared with the case without the pile group. In general, the arrangement of pile group in front of the first groyne has great advantages in the protection of groyne and providing the suitable environment for aquatic life.

3.5 Summary

The results of the characteristics of flow structure, turbulence and mass exchange around the emerged box groyne studied by laboratory experiment are presented in this chapter. They emerged box groynes with various spacing and different longitudinal blocks in length and position are compared and analyzed about their effects on the flow characteristics under the same flow condition. The setting of longitudinal block is able to lower the velocity in

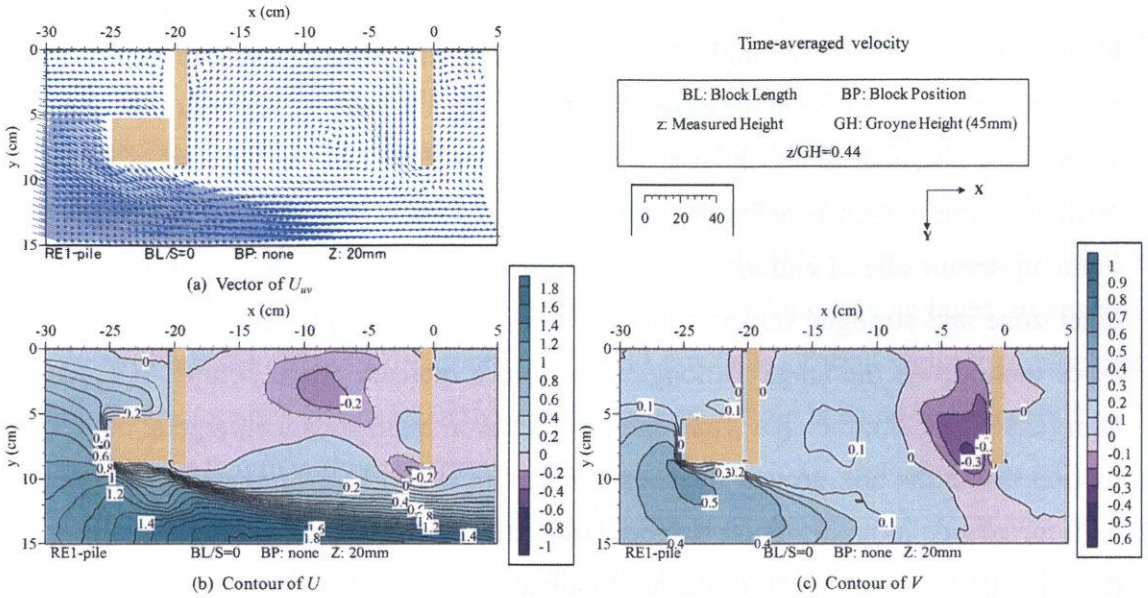

Figure 3.33: Time-averaged velocity on the horizontal plane (x-y) near the middle of water depth (z/GH=0.44) for the case with piles group in front of the first groyne under emerged condition

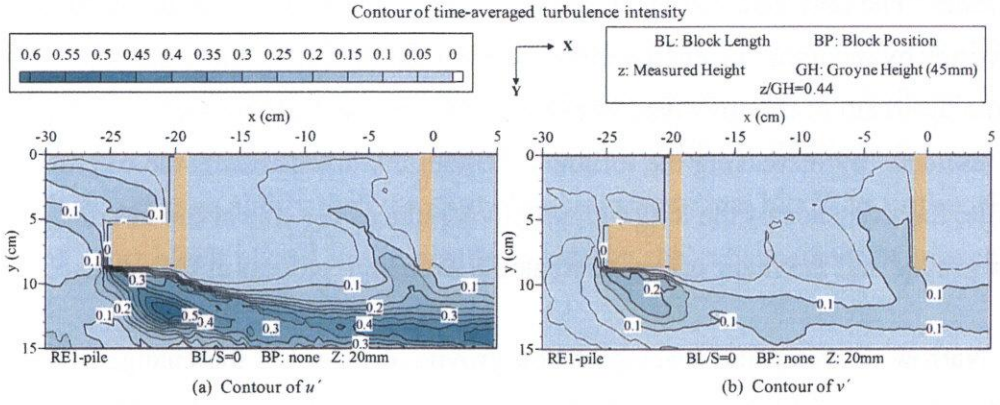

Figure 3.34: Time-averaged turbulence intensity on the horizontal plane (x-y) near the middle of water depth (z/GH=0.44) for the case with piles group in front of the first groyne under emerged condition

the inner zone and create a dead water zone, and also benefit the reduction of scour around the tip of first groyne. The abundant configuration of emerged box groyne is able to realize the application for different demanding in river restoration.

Flow pattern changes greatly when varying the placement and length of longitudinal

block. The setting of the longitudinal block makes the area of high longitudinal velocity in the main stream to move closer to the groyne zone comparing with that in the case without the longitudinal block. It also reduces the area of vertical velocity around the tip of first groyne, which benefits the reduction of scouring. The longitudinal block placed in the upstream side of entrance causes weaker driving gyre, smaller mean velocity in the inner zone and stronger velocity fluctuation with longer length and enhances the turbulence motion. As the length of longitudinal block increases from 3cm (CACE RE21) to 6cm (CASE RE22), the area with high turbulence in main stream enlargers, but turbulent motion inside the box groyne weakens. When the length keeps increasing, the area with high turbulence in main stream reduces but is still larger than the area in the case without the longitudinal block. Setting the longitudinal block in the downstream side of entrance promotes the development of secondary gyre greatly, meanwhile, the driving gyre moves toward the outside with reduced dominated area when the block turns longer, and it reduces mean velocity and turbulence inside the box groyne. Generally, the setting of longitudinal block has the effect of enhancing the velocity intensity at the entrance by narrowing the entrance. The upstream setting of longitudinal block essentially promotes the development of vortex by reducing the energy diffusion with the fluid from the inner zone of box groyne in the upstream of mixing layer, so as to benefit the mass and momentum exchange around the entrance by increasing the turbulent flow in the downstream side of entrance. Meanwhile, the existence of the longitudinal block reduces the size of the interface between the box groyne and the main stream to weak the exchange process at the entrance.

Narrow or widen the spacing of box groyne also lead to the change of flow structure and mass transport between the box groyne and main channel. As adding the spacing of box groyne, the mean velocity in the inner zone increases with decreasing slope whether there is longitudinal block or not. With the spacing increasing, the reduction becomes larger when the longitudinal block is set in the upstream side of entrance, while it becomes smaller when the longitudinal block is set in the downstream side of entrance. The case without the longitudinal block has the strongest exchange ability, while the case with the downstream longitudinal block has the weakest. And the he exchange coefficient in the case with 18cm spacing (S/GL=2) is highest. In particular, for the case without the longitudinal block under 12cm spacing (S/GL=1.33) (CASE RE1-12), two-parallel-gyre system is generated like the driving gyre locates the entrance area along with the parallel secondary

gyre. Lowering the spacing of box groyne makes the vortex structure develop insufficiently when it gets the downstream of entrance. Hence, less vortex structures enter in the inner zone when the second groyne places around the top of the arc curve of mixing layer. But when the spacing is long, although sufficiently developed large coherent structure delivers the amount of water to the inner zone from the downstream side of entrance, the intensity of vortex structure is reduced by the energy diffusion in the long mixing layer. In general, the theory about the effect of different lengths and positions of the longitudinal block on the flow characteristics works when the spacing of box groyne is equal to or larger than 2 times of groyne length without oversize.

There are two useful methods evaluating the exchange ability of box groyne, which are based on PIV and DCM respectively. But they still have some weaknesses to make an overall evaluation for the box groyne in this study. Hence the estimation equations of water exchange coefficient obtained by PIV and DCM methods are modified to suitable for the box groyne with a several gyres system and arc shape of mixing layer respectively, and has fairly good applicability. According to the results obtained by modified method, it can get some findings about the exchange ability of the whole box groyne. Generally, with block length increasing, the exchange process becomes slower. Under the same longitudinal block length condition, the cases with downstream longitudinal block display lower exchange ability. The cases with short longitudinal block (RE21, RE22) in the upstream present higher exchange ability than the case without longitudinal block, to further clarify the effect of short block placed in the upstream side on the enhancement of interchange mechanism.

Chapter 4

Flow Characteristics of Submerged Box Groyne in the Fixed Bed

4.1 Introduction

The occurrence of flooding usually causes the box groyne to become submerged. The mass and momentum exchanged with the overtopping flow make a significant change to the circulation flow pattern and the mechanism of water entrainment from the main stream in the groyne zone. In this chapter, the laboratory experiments are used to investigate the three-dimensional flow field with instantaneous and time-averaged velocity around the submerged box groyne, and the mass exchange processes between the inner zone of the submerged box groyne and the main stream. The measurement technology of Particle Image Velocimetry (PIV) is used to explore the three-dimensional flow field and mass exchange process by analyzing the flow vectors.

The flow structures inside the submerged box groyne are associated with two mixing layers. One is the vertical mixing layer (VML) on the lateral plane of box groyne as emerged condition, and the other is the horizontal mixing layer (HML) on the roof plane of box groyne. The combined actions of these two mixing effects contribute to generate complicate three-dimensional flow structure around the groyne area, which is totally different from the flow field under the emerged condition. On the horizontal plane, the vertical mixing layer (VML) on the lateral side is sensitive to the longitudinal block set in the lateral entrance, which brings large change to the horizontal flow pattern in the inner zone. The effects of longitudinal block on the vertical mixing layer (VML) under the emerged condition are presented in the last chapter. Will these effects be enhanced, weakened or completely changed under the submerged condition? Some new effects even may be found. How about the horizontal mixing layer (HML) on the roof plane, is it also easily affected by the placement and length of the setting longitudinal block? This chapter will give the answers to these questions. In this chapter, the effects of the placement and length of the longitudinal block and the spacing of box groyne on the three-dimensional flow field of submerged box groyne are studied.

The Time-averaged flow velocity indicates different flow types in the box groyne area along with the placement and the length of a longitudinal block. To explore the inner characteristics of flow structures around a box groyne, the turbulence intensity is applied. Beside that, the mass exchange coefficient reveals characteristic of the water exchange process between the inner zone of the box groyne and the main stream. In particular, local scour around the box groyne is always the important research topic in the river engineering, hence, a detailed description of the bed shear stress distribution in the groyne field region is conducted.

4.2 Effects of the position and length of longitudinal block

In this section, the spacing of box groyne is set as S/GL=2 (S=18cm), and the arrangement of longitudinal block is shown in Table 2.2.

4.2.1 Mean velocity in the inner zone of box groyne

The longitudinal block prevents the main stream delivering energy to the inner zone of box groyne in the lateral interface, so as to induce the large difference in velocity distribution. Fig. 4.1 shows the comparison of the mean velocity in the inner zone U_{ig}, which is obtained by averaging the all time-averaged velocity in the inner zone of box groyne. And the mean velocity in the inner zone of emerged box groyne is also presented for comparison.

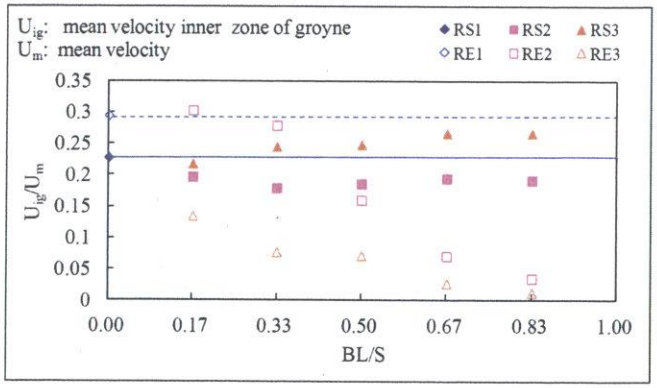

Figure 4.1: Comparison of mean velocity in the inner zone of box groyne for all layers

In the lateral interface, because the longitudinal block prevents the main stream delivering energy to the inner zone of box groyne, there are existing large differences of velocity

intensity in the groyne zone for the emerged cases with various block length, as the description in section 3.2.1. For the submerged cases, the longitudinal block still obstructs the mass exchange via the lateral interface, but a great quantity of water delivered by horizontal mixing layer (HML) injects into the groyne zone to activate its mean velocity. The mean velocity in the cases with an upstream longitudinal block (Group RS2) is lower than the case without the longitudinal block (CASE RS1), and minimum value appears in the case with the 0.33S block length (CASE RS22). The most cases with a downstream longitudinal block (Group RS3) show higher velocity intensity than CASE RS1, and the value of mean velocity increases with the longer block length. Compared with the cases under the emerged condition, the cases without the longitudinal block or with a short length of the upstream longitudinal block (CASE RS1, RS21 and RS22) show weaker vitality of water inside the box groyne, and it means the effect of the vertical mixing layer (VML) becomes weak when the box groyne is submerged. Under the submerged condition, the mean velocity in the cases with longitudinal block is approaching the value of the case without longitudinal block. These two phenomena reveal the fact that the horizontal mixing effect contributes more extensively to the water inputs under the submerged condition.

Three-dimensional characteristic is the notable feature for the submerged box groyne, and it provides the fluid particle various paths to enter and exit the groyne zone. In this study, the coefficient F_t in the following is introduced to describe the three-dimensionality of flow by estimating the impact of vertical velocity on the total velocity:

$$F_t = \frac{U_{UVW} - U_{UV}}{U_{UVW}} = \frac{\sqrt{U^2 + V^2 + W^2} - \sqrt{U^2 + V^2}}{\sqrt{U^2 + V^2 + W^2}} \tag{4.1}$$

where U is the time-averaged longitudinal velocity; V is the time-averaged transverse velocity; W is the time-averaged vertical velocity. The characteristics in the three-dimensionali shown in Fig. 4.2 present the arrangement of longitudinal block improves the degree of three-dimensionality. Furthermore, the three-dimensional flow is definitely enhanced by the longer block when the length of block is not longer than 0.5S. When the block excesses 0.5S, the increase of block length is almost not helpful to the further enhancement in the cases with an upstream longitudinal block (Group RS2), and lowers the three-dimensionality in the cases with a downstream longitudinal block (Group RS3). Due to the high three- dimensionality among their group, the cases with 0.5S length of block (RS23 and RS33) are selected as typical cases for some discussions in the following.

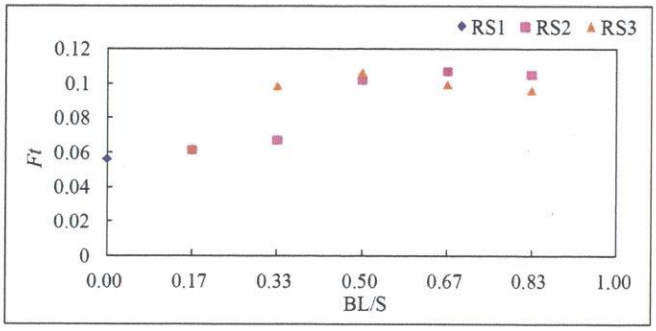

Figure 4.2: Comparison of three-dimensionality in the inner zone of submerged box groyne

4.2.2 Flow structures

Due to the longitudinal block directs to the inside of box groyne, the difference between each case in the upstream and downstream regions of groyne is inconspicuous compared to that in the box groyne field. As a result, this study focuses on the finite section with about 5 cm of upstream and downstream from the groyne.

The effect of position of longitudinal block

The three-dimensional streamlines and time-averaged velocity vectors U_{uv} and U_{uw} on the horizontal (x-y) and vertical (x-z) plane respectively are shown in Fig. 4.3~4.7, serving to describe the three-dimensional flow around the box groynes with longitudinal block set in different position. The cases with 0.5S length of block (RS23 and RS33) are selected as typical cases in this discussion.

In the upstream of first groyne, the incoming fluid reached the groyne wall is divided into three parts because of the adverse pressure gradients induced by the first groyne, as shown in Fig. 4.3 and the velocity vectors on the transverse section (y-z) of Fig. 4.6(a). The incoming fluid between the left wall and the vertical plane of $y/GL \approx 0.44$ flows toward the left wall and most of it flows over the crest of first groyne. The incoming flow between the vertical planes of $y/GL \approx 0.44$ and y/GL=1 is split into the upflow and downflow from the line of $z/GH \approx 0.70$. On the plane close to the bottom (z=5mm, z/GH=0.11) and the plane close to the left wall (y=5mm, y/GL=0.06), the fluid in the upstream of first groyne flows back to the upstream, to generate the secondary gyre at the corner near the junction between the groyne and the bottom (as shown in y=45mm of Fig. 4.3 (b)) and the left wall (as shown in z=20mm of Fig. 4.3 (a)) respectively. Because the head of longitudinal

block directs to the inside of box groyne, the flow structures in the upstream side are similar among the different cases.

The vortex structures detached from the top and side of the first groyne wall predominate the two mixing layer (HML and VML) respectively. They enter the box groyne zone from various entrances, and the mergence or collision of these two kinds of vortex structure from different sources complicate the three-dimensional flow in the groyne zone. Fig. 4.3(b) shows that the amount of fluids fed by the horizontal mixing layer (HML) enter in front of the second groyne and generate the large recirculation flow in the groyne zone. A weak gyre is observed at the corner between the first groyne and the bottom inside the box groyne. As shown in Fig. 4.3(a), on the x-y plane close to the bottom (z=5mm, z/GH=0.11), the fluid velocity is highly accelerated by the shrink of channel accompanied with the intense mixing effect, to feed great of momentum and mass to the groyne zone. When the plane level is elevated to the middle (z=20mm, z/GH=0.44) and the top (z/GH=1) of the groyne height, the acceleration is reduced to induce the shape deformation of the vertical mixing layer (VML) and the weakening of the vortex development. With the elevation of plane level, the arc-shape of the vertical mixing layer (VML) becomes flat and close to the lateral entrance; meanwhile the inflow of the lateral entrance is weakened even to be zero on the top plane of the box groyne. From the three-dimensional streamlines and velocity vectors of the case without the longitudinal block (CASE RS1), the circulation flow pattern inside the box groyne without the block is visualized. The water in the vertical mixing layer (VML) flows down as going downstream and it's prone to enter into the inner zone from the low level of the downstream side of entrance. When it reaches the left wall of channel, small part of it climbs along the wall and flows out due to the adverse pressure of wall. Most of it generates the horizontal gyre with the water from the horizontal mixing layer (HML) on the roof of box groyne. The gyre spirals upward toward the roof by combined with the vertical gyre. Its core changes from being parallel to being perpendicular with the bottom as the height grows. The original water from the vertical mixing layer (VML) flows out the box groyne from the lateral and roof boundary finally.

Because the upstream longitudinal block definitely promotes the development of vortex structure in the vertical mixing layer (VML) as described in the last chapter, the negative transverse velocity (inflow) at the lateral entrance is gained in the case with upstream longitudinal block (CASE RS23). And the shear flow with large longitudinal velocity is

observed instead of the recirculation flow at the lateral entrance for CASE RS23. The right groyne zone shielded by the downstream longitudinal block in the CASE RS33 once was the dead water zone in the emerged case, but shows the high reverse velocity in longitudinal direction now, as shown in Fig. 4.5. It indicates that the high velocity distribution near the bottom plane in the groyne zone is also largely contributed by the inflow from the roof entrance associated with the horizontal mixing layer (HML). This phenomenon also is the maximum difference from the emerged case on the plane near the bottom. The patterns of the velocity distribution of the case without longitudinal block (CASE RS1) and case with downstream longitudinal block (CASE RS33) are similar on the z/GH=1 plane. It presents the fact that the effect of the downstream longitudinal block on the upper flow is limited.

As described above, for the cases without longitudinal block (CASE RS1) and case with upstream longitudinal block (CASE RS23), some intense fluids fed by the vertical mixing layer (VML) enter the groyne zone along the junction between the bottom and the upstream wall of second groyne. Then it causes the strong upflow and even outflow when they reach the left wall of channel, and this phenomenon is particularly enhanced in the case with an upstream longitudinal block (as shown in Fig. 4.4 (b)). On the x-z plane near the tip of groyne, shown in Fig. 4.4 (b), the positive vertical velocity along the upstream wall of second groyne is obviously observed in the CASE RS23. This is because the shear flow with large longitudinal velocity around the lateral entrance (shown in Fig. 4.4 (a)) forms the upflow along the wall when it reaches the second groyne. It also can explain the phenomenon about the relatively small negative vertical velocity along the second groyne in the middle section in the CASE RS23. The high value of vertical velocity in the case with downstream longitudinal block (CASE R33) shows the prominent ability of attracting the inflow from the roof interface and promoting the water vitality in the groyne zone (as shown in Fig. 4.5(b) and 4.7(b)).

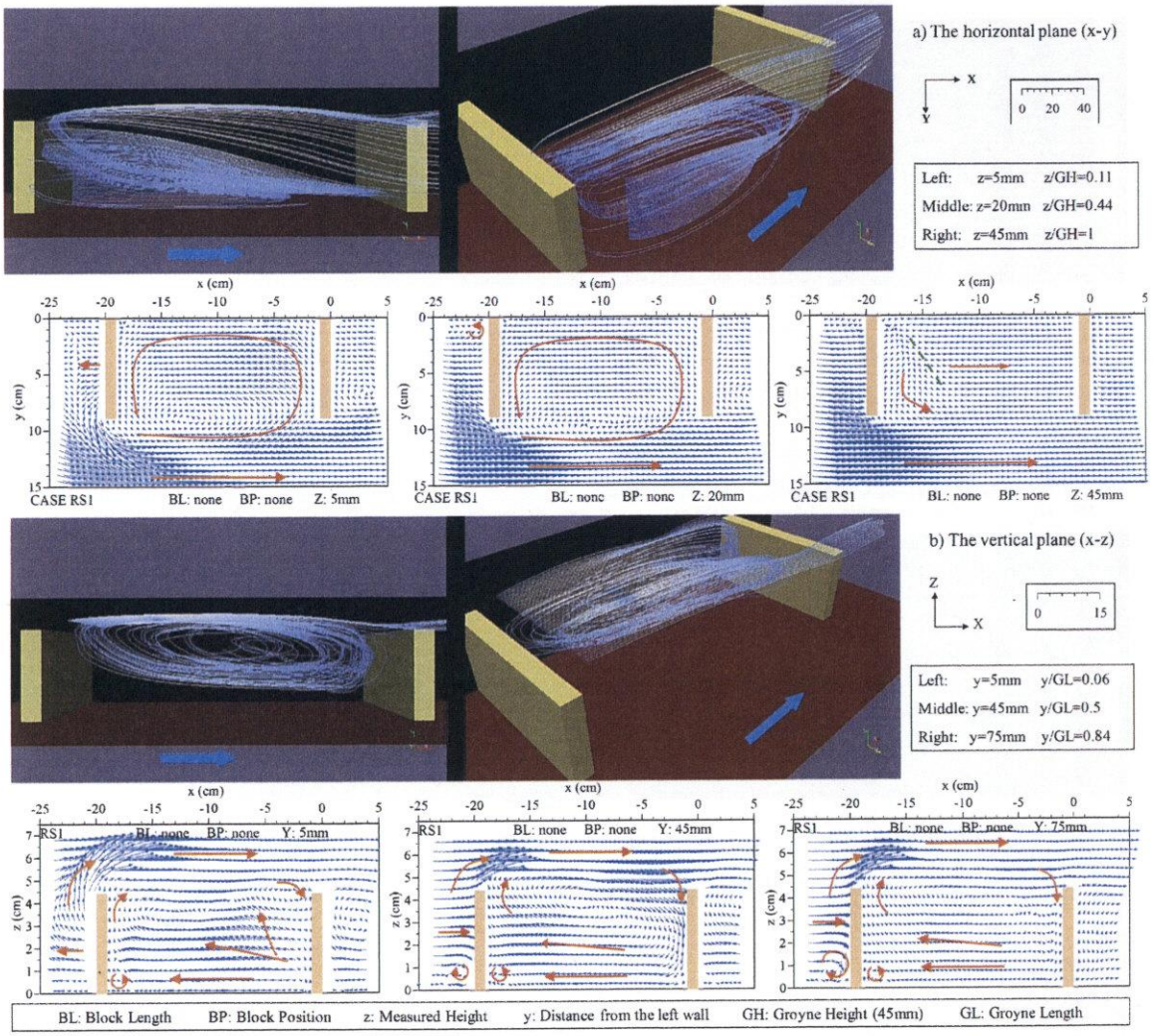

Figure 4.3: Three-dimensional streamlines and time-averaged velocity vectors on the horizontal plane (x-y and vertical (x-z) plane for the case without longitudinal block (CASE RS1)

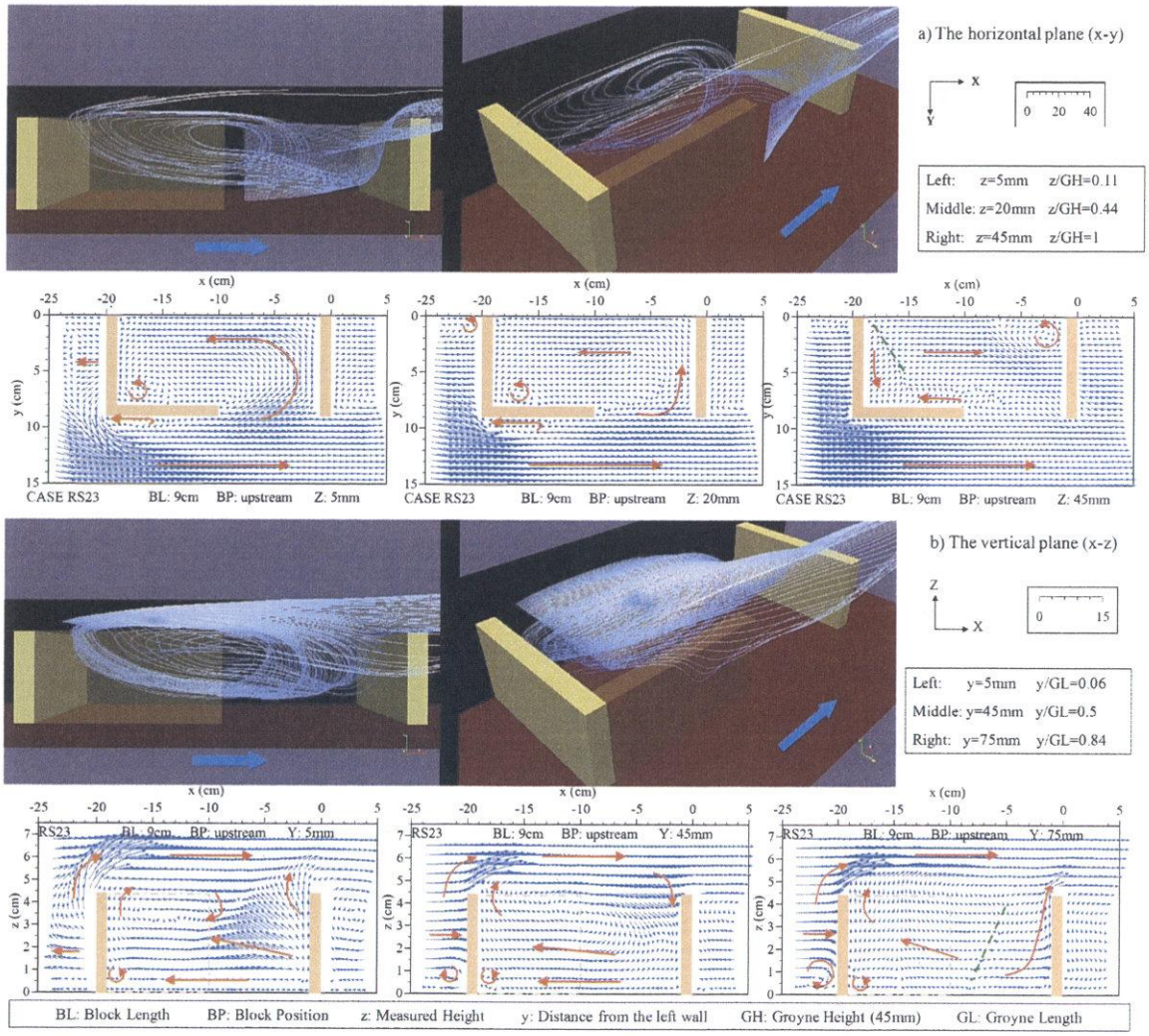

Figure 4.4: Three-dimensional streamlines and time-averaged velocity vectors on the horizontal plane (x-y) and vertical (x-z) plane for the case with an upstream longitudinal block (BL/S=0.5 CASE RS23)

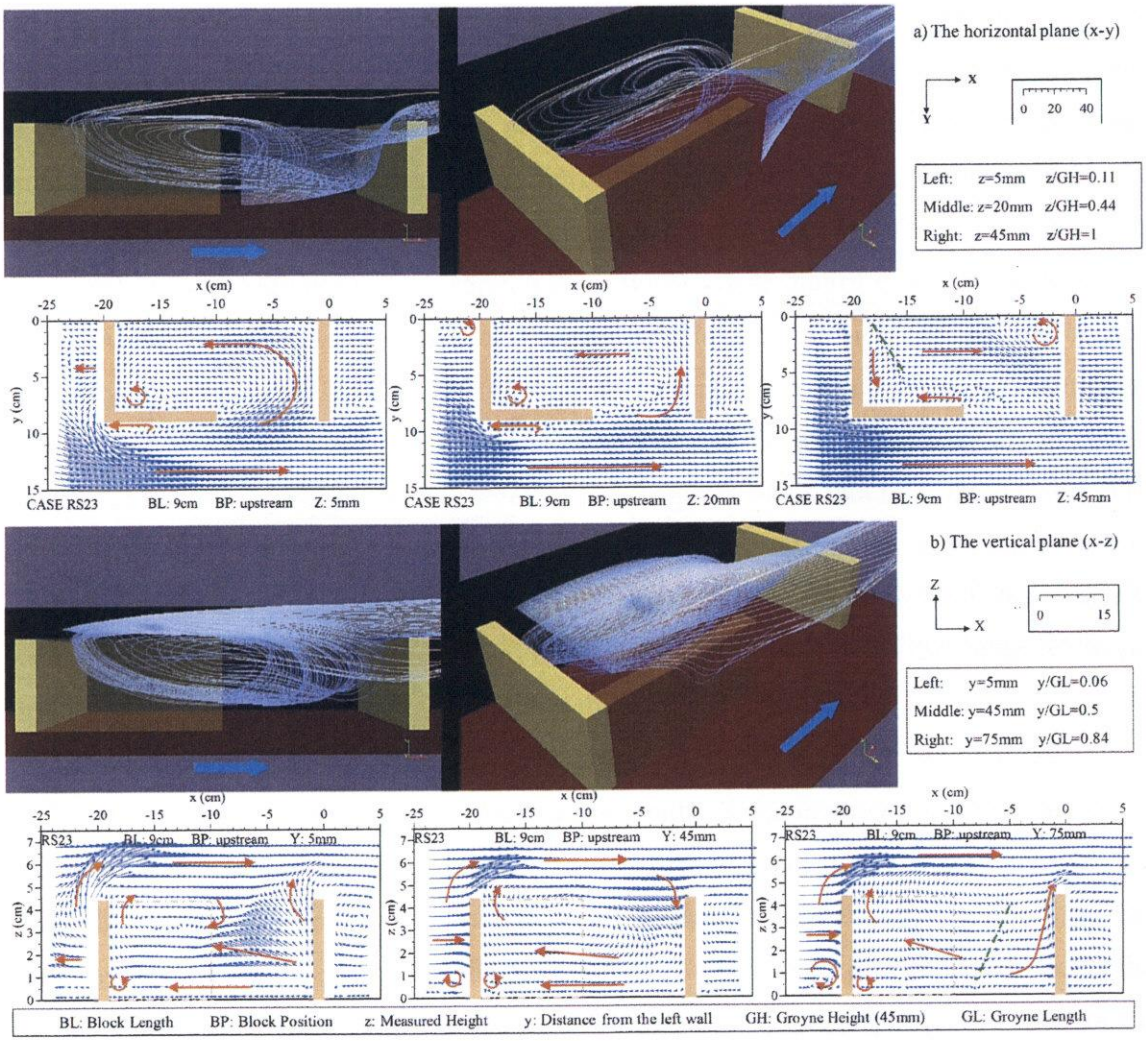

Figure 4.5: Three-dimensional streamlines and time-averaged velocity vectors on the horizontal plane (x-y) and vertical (x-z) plane for the case with a downstream longitudinal block (BL/S=0.5 CASE RS33)

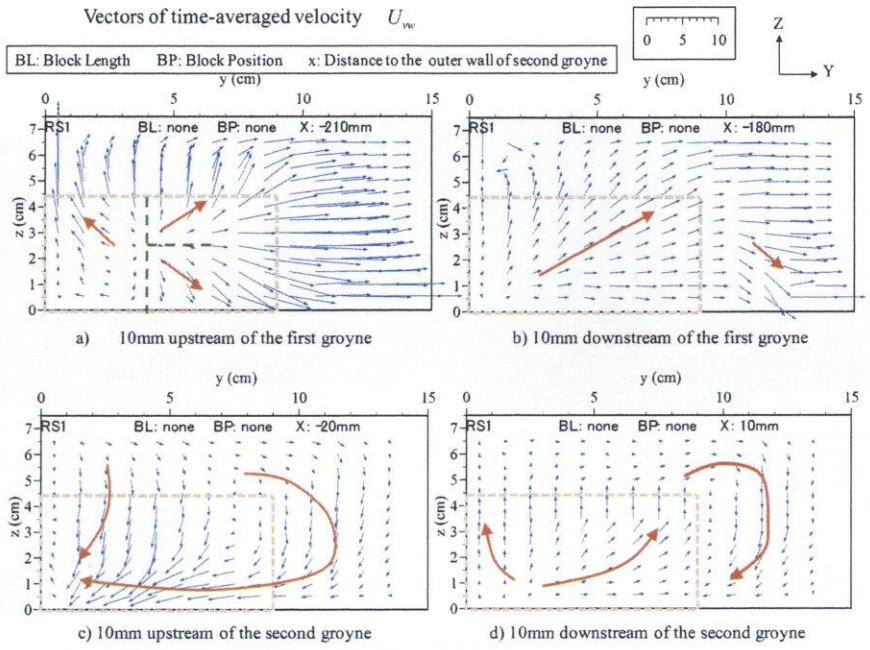

Figure 4.6: Time-averaged velocity vectors on the various transverse plane (y-z) for the case without longitudinal block (CASE RS1)

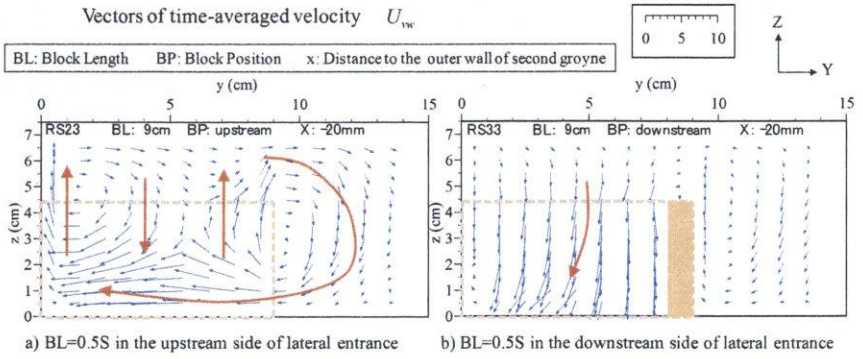

Figure 4.7: Time-averaged velocity vectors on the transverse plane (y-z)(x=-20mm) for the case with longitudinal block (CASE RS23 and RS33)

The effect of length of longitudinal block

Fig. 4.8~4.16 shows the contour of time-averaged velocity on the horizontal plane (x-y) of z/GH=0.44 and the vertical plane (x-z) of y/GL=0.5.

(a)GROUP RS2 As shown in Fig. 4.9~4.12, the longer length of the upstream longitudinal block causes the change of flow pattern around the box groyne. On the horizontal plane of z/GH=0.4, the area with high value of longitudinal velocity in the inner zone becomes smaller as the longitudinal block getting longer, and it is as same as the emerged condition. But this area still keeps high value of longitudinal velocity with large range when the length of longitudinal block is 15cm (GL/S=0.83), while that of emerged cases is very small. And it provides more evidence about the conclusion that the flow near the bottom is largely contributed by the inflow from the roof entrance. The range of the shielding area with back flow enlarges with the increasing longitudinal block under the emerged condition, but it keeps range and intensity whether the length of block changes in the submerged cases. In front of the second groyne, the area and intensity of the negative transverse velocity are enhanced with increasing length of block, which is relative to the promotion of vortex structure induced by the upstream longitudinal block. But when the entrance is very small (CASE RS25), the value of it steeply falls.

On the vertical plane of y/GL=0.5, the area with high value of longitudinal velocity in the inner zone locates in low level. And as the length of the upstream longitudinal block increased, its range and intensity is reduced at firstly and enhanced when the length is very long, but it is still weaker than the case without the longitudinal block (CASE RS1). The characteristic of negative vertical velocity in front of the second groyne also presents the similar situation as the longitudinal velocity. The difference is that the weakest case for the distribution of longitudinal velocity is CASE RS23 (BL/S=0.5), while if for the distribution of vertical velocity is CASE RS22 (BL/S=0. 33).

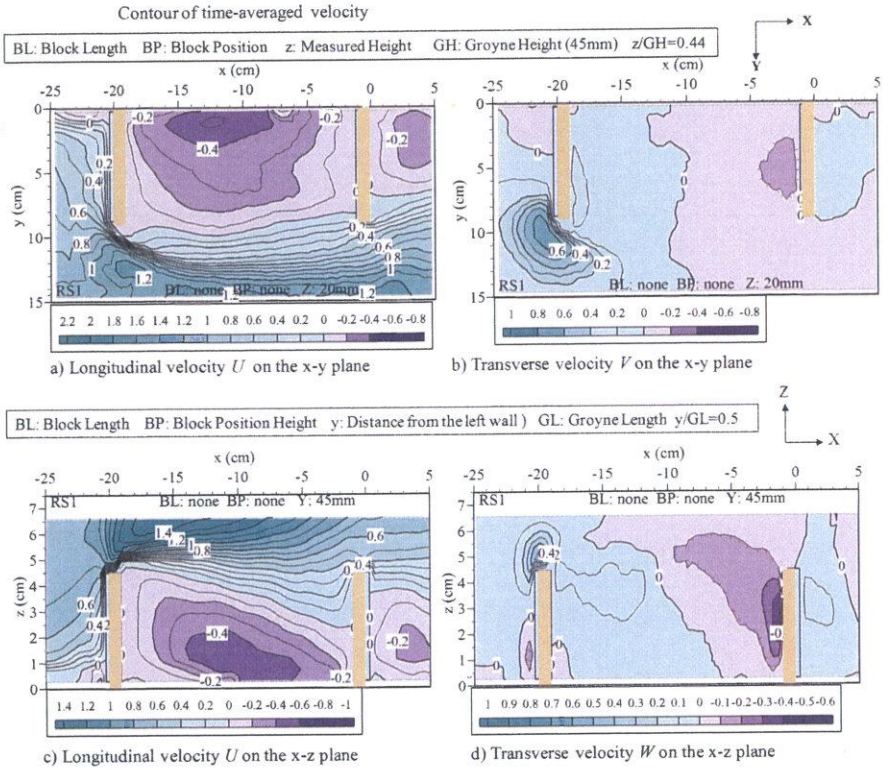

Figure 4.8: Contours of dimensionless time-averaged velocity on the horizontal plane (x-y)of z/GH=0.44 and vertical plane (x-z)of y/GL=0.5 for the case without longitudinal block (CASE RS1)

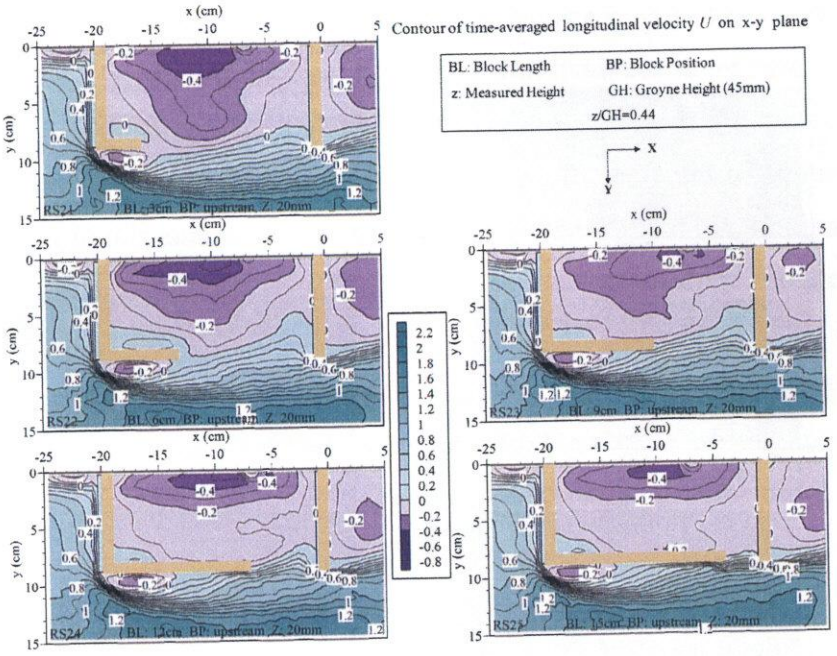

Figure 4.9: Contours of dimensionless time-averaged longitudinal velocity U on the horizontal plane(x-y)of z/GH=0.44 for the group with upstream longitudinal block (Group RS2)

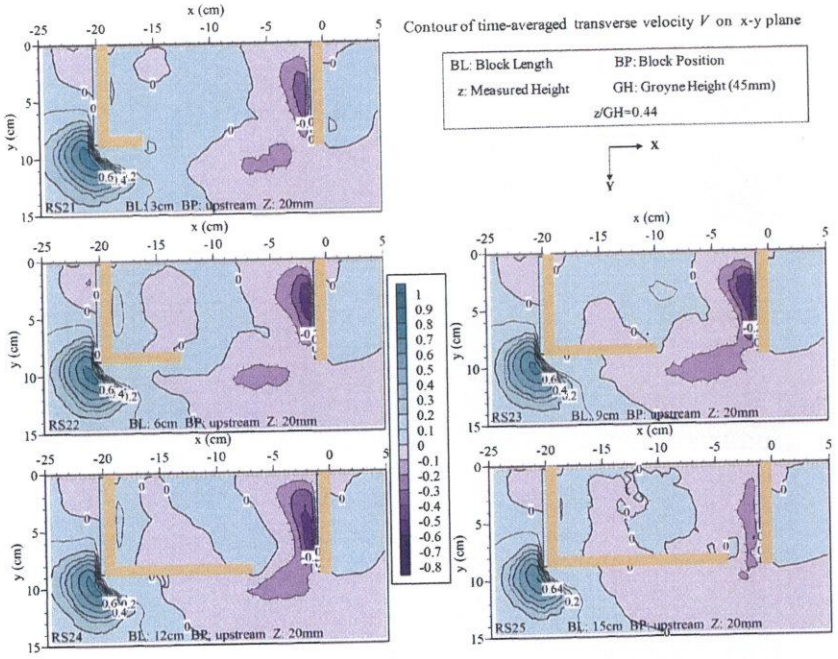

Figure 4.10: Contours of dimensionless time-averaged transverse velocity V on the horizontal plane (x-y)of z/GH=0.44 for the group with upstream longitudinal block (Group RS2)

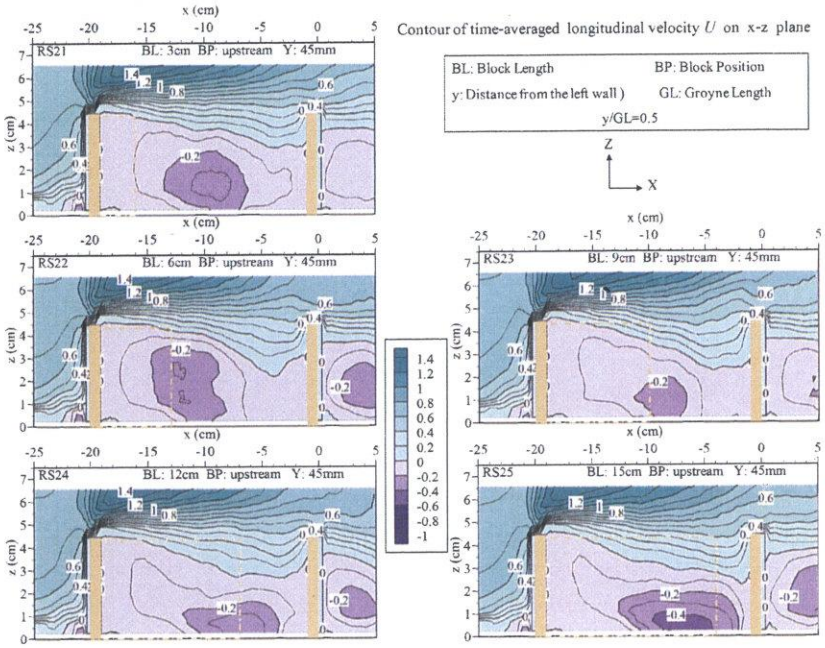

Figure 4.11: Contours of dimensionless time-averaged longitudinal velocity U on the vertical plane (x-z)of y/GL=0.5 for the group with upstream longitudinal block (Group RS2)

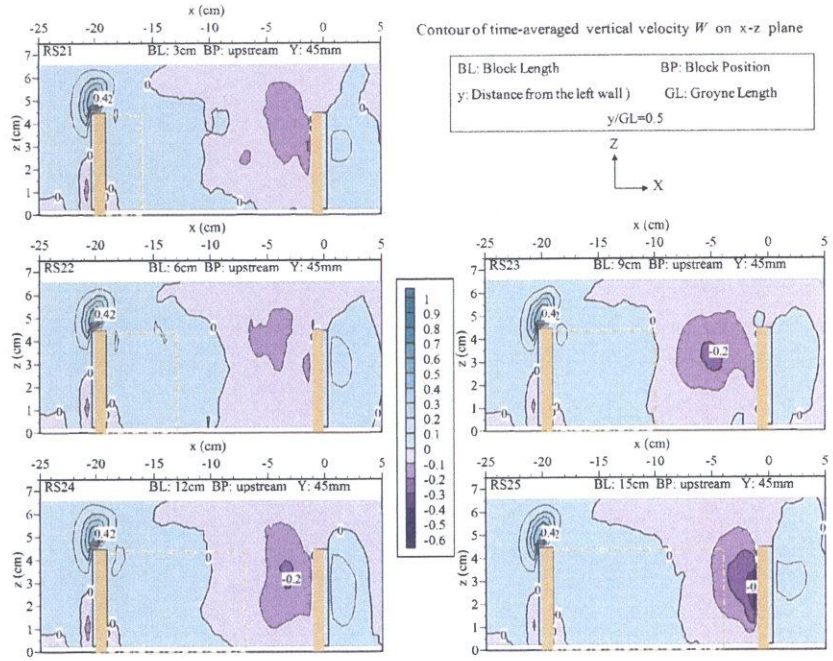

Figure 4.12: Contours of dimensionless time-averaged vertical velocity W on the vertical plane (x-z)of y/GL=0.5 for the group with upstream longitudinal block (Group RS2)

(b)GROUP RS3 As shown in Fig. 4.13~4.16, the longer length of the downstream longitudinal block also brings the different flow pattern to the box groyne. On the horizontal plane of z/GH=0.4, the area with high value of longitudinal velocity in the inner zone locates near the inside wall of box groyne, showing totally different distribution with the emerged cases. And it is enhanced compared with the case without longitudinal block. The distribution of high longitudinal velocity in the inner zone moves close the second groyne. As the length of longitudinal block increased, the transverse velocity in the entrance become weak also means the reduction of mass exchange in the lateral boundary.

On the vertical plane of y/GL=0.5, the area with high value of longitudinal velocity in the inner zone enlarges when the longitudinal block is long. But the distribution of longitudinal velocity is not as sensitive to the change of block length as the cases with upstream longitudinal. The distribution of negative vertical velocity in front of the second groyne is enhanced with the increasing length of longitudinal block, and the rate of improvement is slight when the block is long. It is noticed that, there is the similar distribution of time-averaged velocity on the vertical plane of y/GL=0.5 between the cases with 15cm longitudinal block (CASE RS25 and RS35).

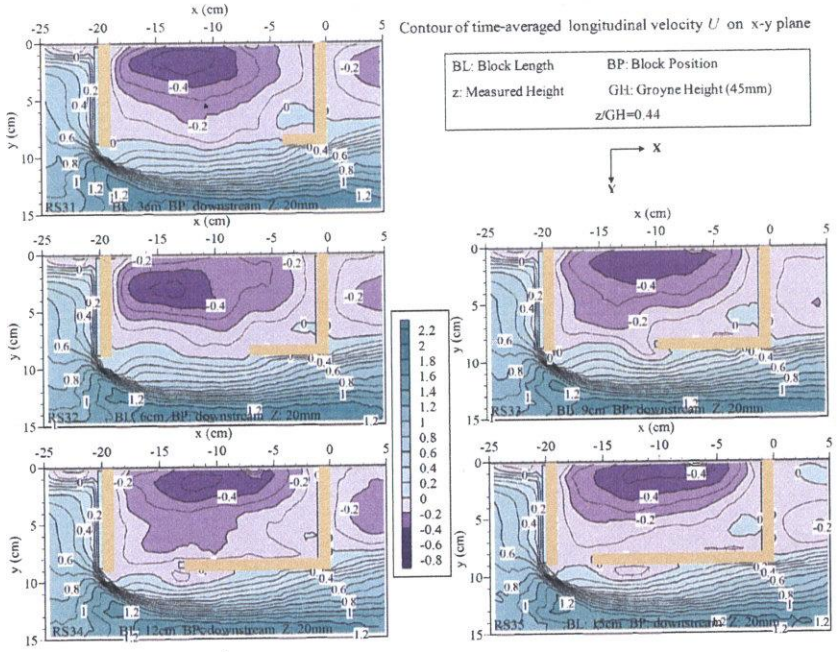

Figure 4.13: Contours of dimensionless time-averaged longitudinal velocity U on the horizontal plane (x-y)of z/GH=0.44 for the group with downstream longitudinal block (Group RS3)

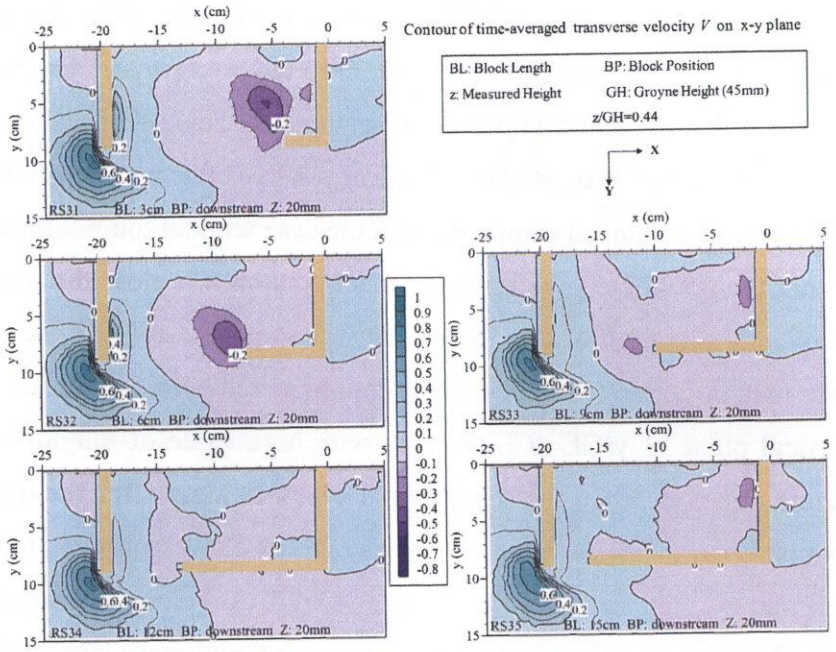

Figure 4.14: Contours of dimensionless time-averaged transverse velocity V on the horizontal plane (x-y)of z/GH=0.44 for the group with downstream longitudinal block (Group RS3)

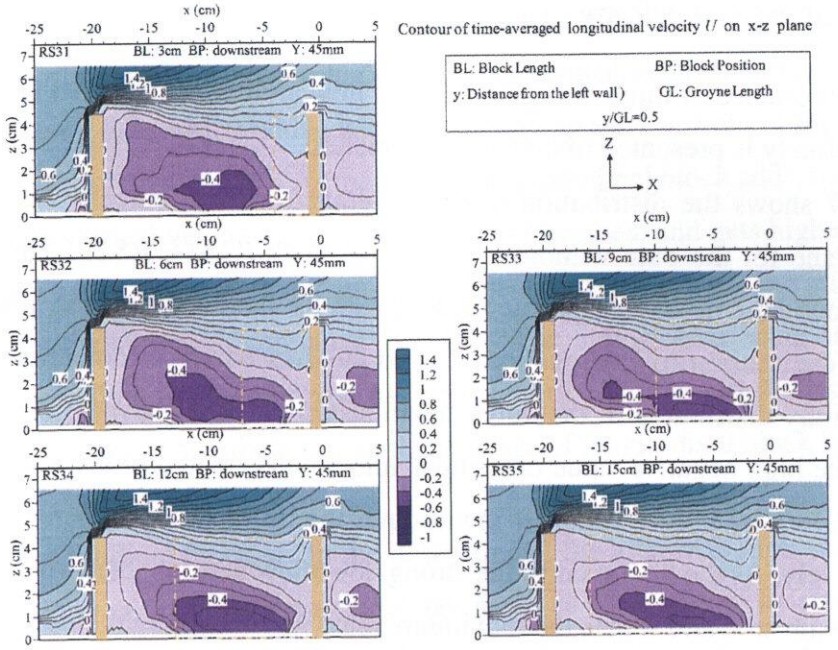

Figure 4.15: Contours of dimensionless time-averaged longitudinal velocity U on the vertical plane (x-z)of y/GL=0.5 for the group with downstream longitudinal block (Group RS3)

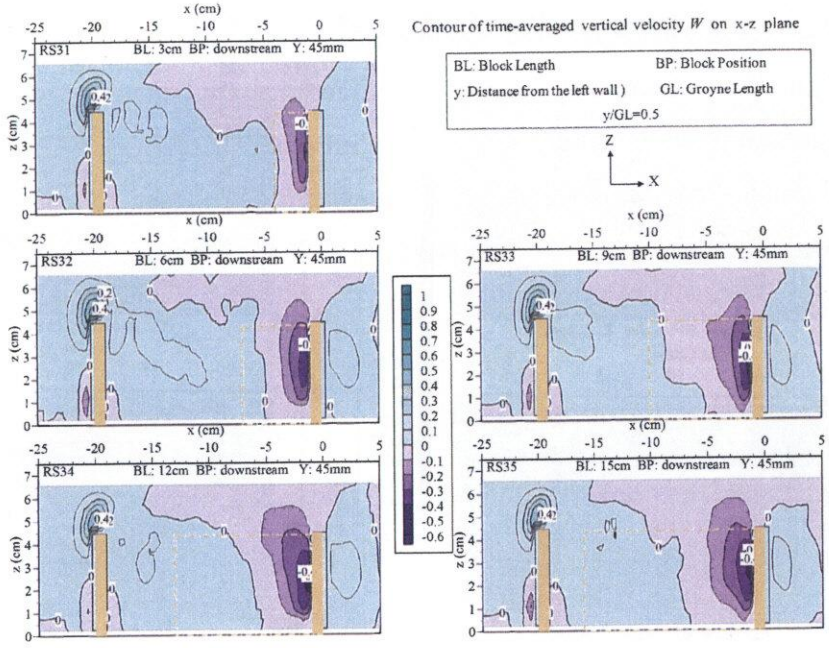

Figure 4.16: Contours of dimensionless time-averaged vertical velocity W on the vertical plane (x-z)of y/GL=0.5 for the group with downstream longitudinal block (Group RS3)

Distribution of vertical velocity

Due to the importance of three dimensionality of flow around box groyne, the distribution of vertical velocity is presented in detail in this section.

Fig. 4.17 shows the distribution of time-averaged vertical velocity on the different horizontal plane for the case without longitudinal block (CASE RS1). The intensity of downflow around the tip of first groyne reduces with the increasing height, which is different with the distribution of emerged cases. And the distribution of downflow in the main stream is mainly distributed in the downstream section of box groyne. So there are two zones with the high negative value of vertical velocity distributed in the main zone on the plane of z/GH=0.44, induced by the flow around the tip of first groyne and overtopping flow respectively. As the height adds, the strong downflow between the two groynes moves toward upstream side and it gets the maximum value when the height closes to the middle of groyne height. Inside the box groyne, the upflow between the tow groynes increases in value and reduces in range as the height adds.

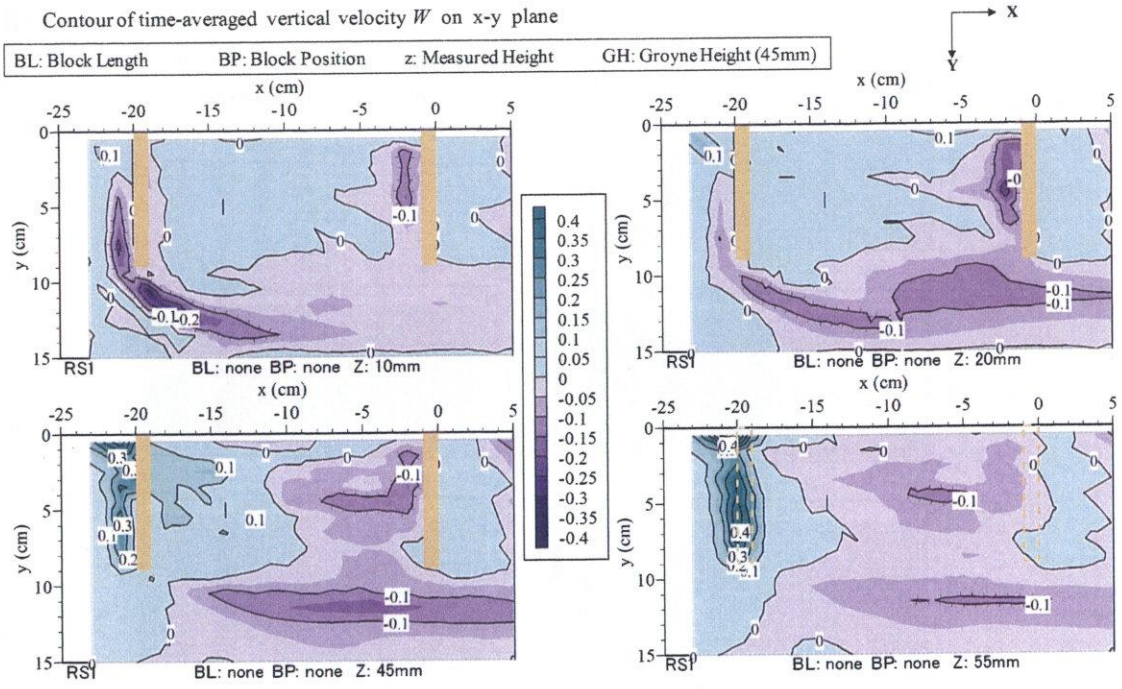

Figure 4.17: Contours of dimensionless time-averaged vertical velocity W on the various horizontal plane (x-y) for the case without longitudinal block (CASE RS1)

Fig. 4.18 shows the distribution of time-averaged vertical velocity on the horizontal

plane of z/GL=0.44 for the cases with longitudinal block. When the longitudinal block set in the upstream, the area with high value of negative vertical velocity in the main stream enlarges, and strong flow with positive vertical velocity appears in front of the long longitudinal block (CASE RS24, RS25). As the length of longitudinal block adds, the maximum value of negative vertical velocity in the main stream increases, and gets highest when the length of block is 6cm (BL/S=0.33), then still keeps high value around the middle of box groyne when the block length continues increase. The upflow distributed at the corner between the left wall and second groyne has been described in the last section, and it becomes stronger and larger distribution with the increase of longitudinal block length beside the 15cm length (GL/S=0.83).

When the longitudinal block set in the downstream, the area with high value of negative vertical velocity in the main stream becomes small as the length of longitudinal block grows. And strong flow with positive vertical velocity also appears in front of the longitudinal block. The distribution of high value of negative vertical velocity in front of the second groyne enlarges and increases in value when the length of longitudinal block is added. And it means the ability of attracting inflow from the roof boundary is enhanced by the longer block. It is noticed again that, there is the similar distribution of vertical velocity in the inner zone on the horizontal plane of z/GL=0.4 between the cases with 15cm longitudinal block (CASE RS25 and RS35). The similarity of flow pattern in the inner zone is because the flow inside the box groyne is almost contributed by the horizontal mixing layer (HML) when the length of longitudinal block is long enough.

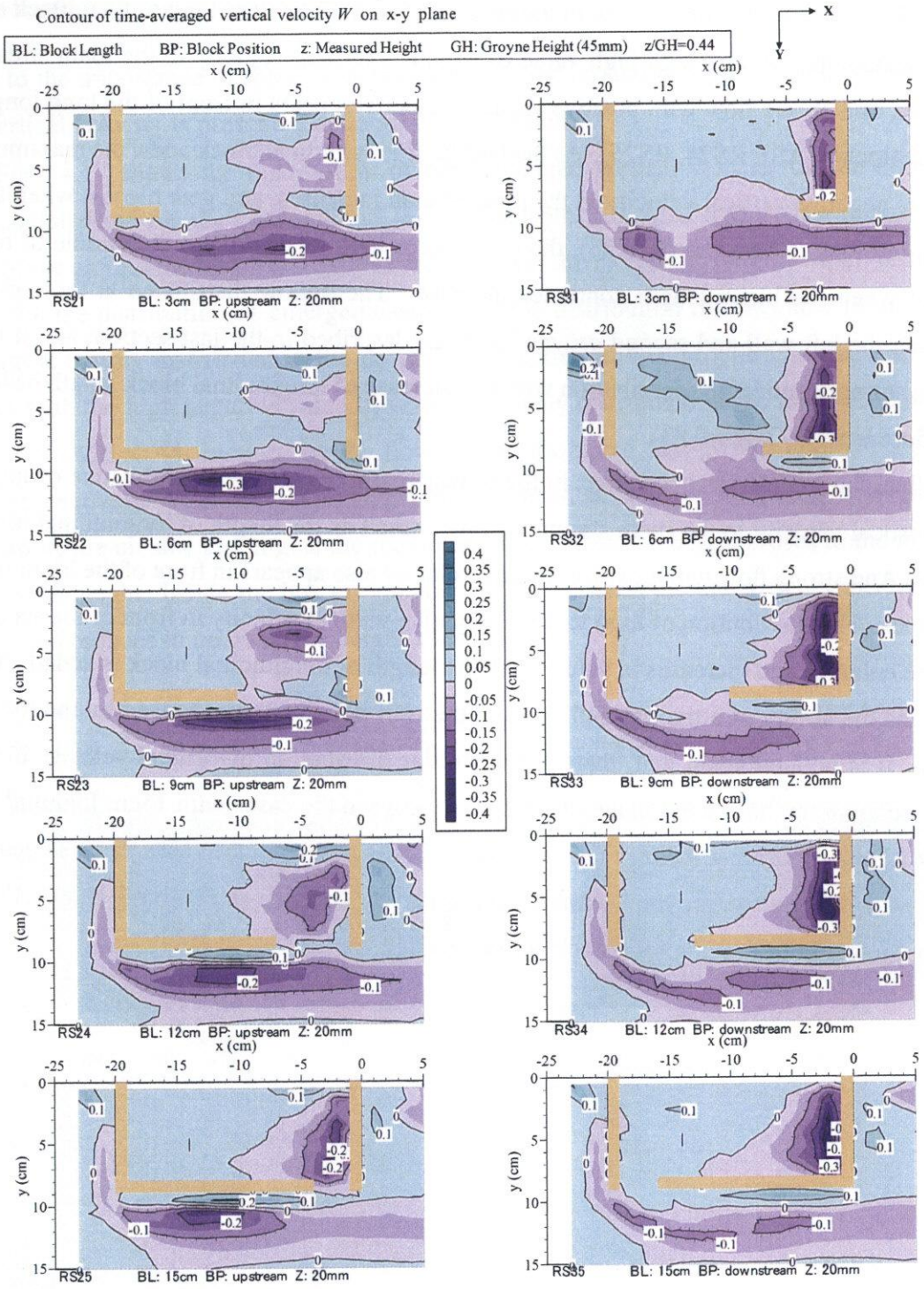

Figure 4.18: Contours of dimensionless time-averaged vertical velocity W on the horizontal plane (x-y) of z/GH=0.5 for the cases with longitudinal block (Group RS2 and Group RS3)

Distribution of velocity in the main stream

In the main stream, the longitudinal block still has a large impact on the flow structure. The velocity in the low level of main stream is related to the sediment transport in the main channel. The profiles of time-averaged longitudinal velocity distribution (U) on the horizontal plane of z/GH=1.22 in Fig. 4.19 and on the vertical plane of y/GL=1.17 in Fig. 4.20 are used to clarify the effect of the arrangement of longitudinal block on the main stream.

In the upstream of box groyne, the presence of block hardly affects the distribution of longitudinal velocity. The effect of upstream longitudinal block on the main stream is obvious. On the plane of z/GH=1.22, the reduction of the longitudinal velocity induced by the upstream longitudinal block is observed. The reduction is delivered to the center of main stream as going downstream, and the velocity deflection reaches maximum at the tip of block for the cases with short longitudinal block. The maximum of velocity deflect for the case with 15cm block length (CASE RS25) places in the upstream side of longitudinal block. On the plane of y/GL=1.17, the acceleration and the deceleration of the longitudinal velocity is observed in different position respectively. The acceleration moves from the groyne height level to the bottom plane as going downstream. Meanwhile the range of the deceleration is enlarged in the upper plane as going downstream. And these effects are enhanced with the longer length of longitudinal block. From the above phenomena, it can be found that the upstream longitudinal block makes more water in the upper level beyond the box groyne flow transported to the low level of the main stream as going downstream. The effect of the downstream longitudinal block on the distribution of longitudinal velocity on the z/GH=1.22 plane is weak. But Fig. 4.20(b) clearly shows the case with a short length of longitudinal block (CASE RS31) has the effect on the acceleration of flow from the low level to the high level as going downstream.

4.2.3 Turbulent characteristic

In the mixing layer, active interaction produces large velocity fluctuation to induce high turbulence; hence, the effects of the longitudinal block on the vertical mixing process directly causes the distribution differences of turbulence. But the change of flow structure inside the box groyne affects the horizontal mixing layer; hence, the longitudinal block also has an indirect effect on the horizontal mixing process. The turbulence distribution is related to

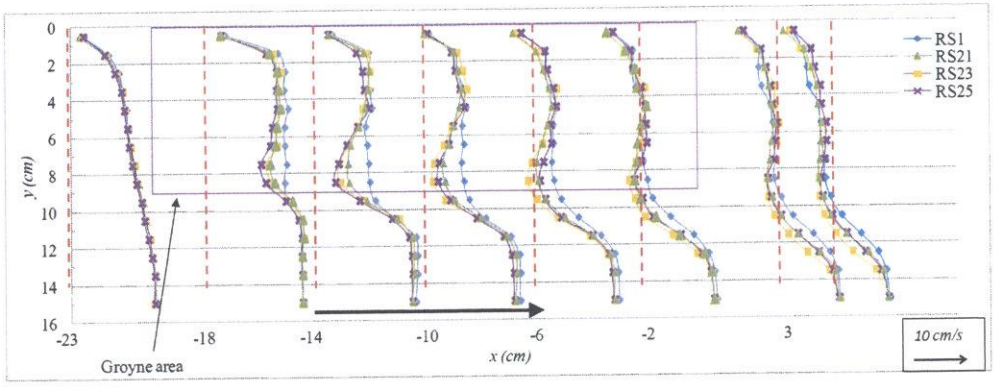

a) Longitudinal block in the upstream side of lateral entrance

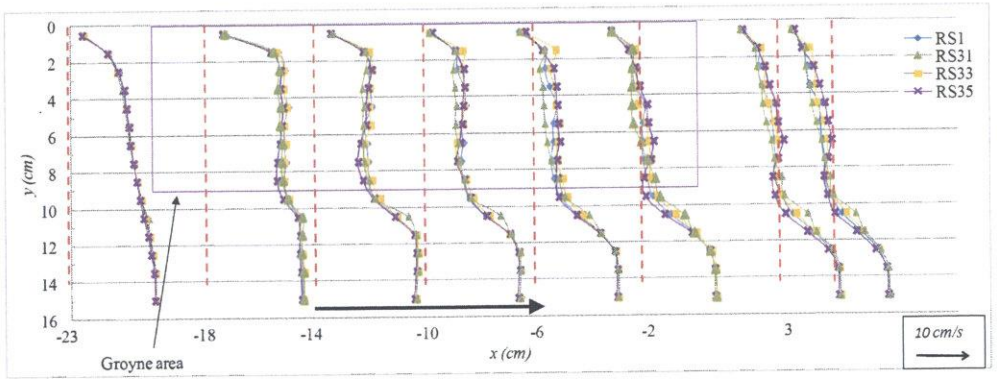

b)) Longitudinal block in the downstream side of lateral entrance

Figure 4.19: Transverse distribution of time-averaged longitudinal velocity (U) on the horizontal plane of z/GH=1.22 under the submerged condition

the generation and dissipation of vortex structure. Turbulence characteristics in transverse direction at the entrance between the inner box groyne area and main stream present the exchange ability of box groyne with the external environment.

The time-averaged turbulence intensity is denoted by in the longitudinal component u', the transverse component v' and the vertical component w'. The contours of dimensionless time-averaged turbulence intensity on the horizontal plane (x-y) of z/GH=0.44 and the vertical plane (x-z) of y/GL=0.5 are shown in Fig. 4.21~4.23. For all cases, an area containing strong turbulence is formed, indicating the general location of mixing layer. This area conducts vigorous interaction between the main flow and the flow from the inner zone of box groyne. Compared with the distribution of longitudinal turbulence on the horizontal plane in emerged case, the area with high value of longitudinal turbulence in the main stream related to the mixing layer moves toward the box groyne, and the arc shape of area has larger

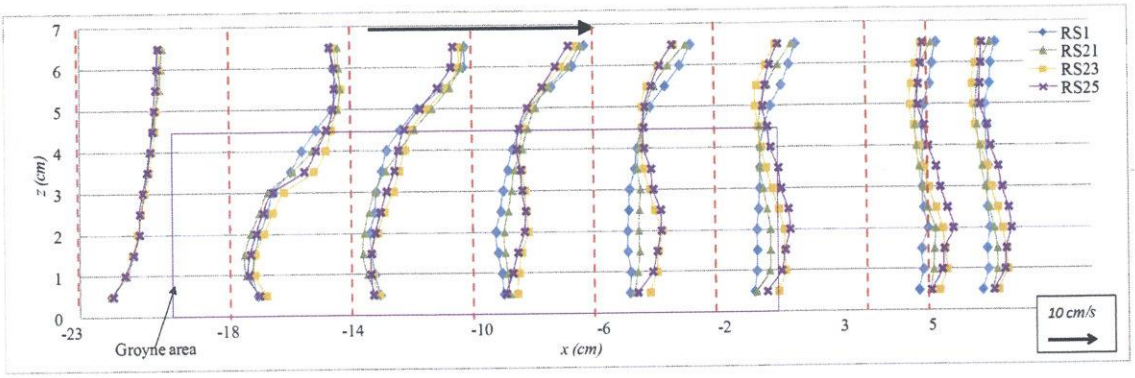

a) Longitudinal block in the upstream side of lateral entrance

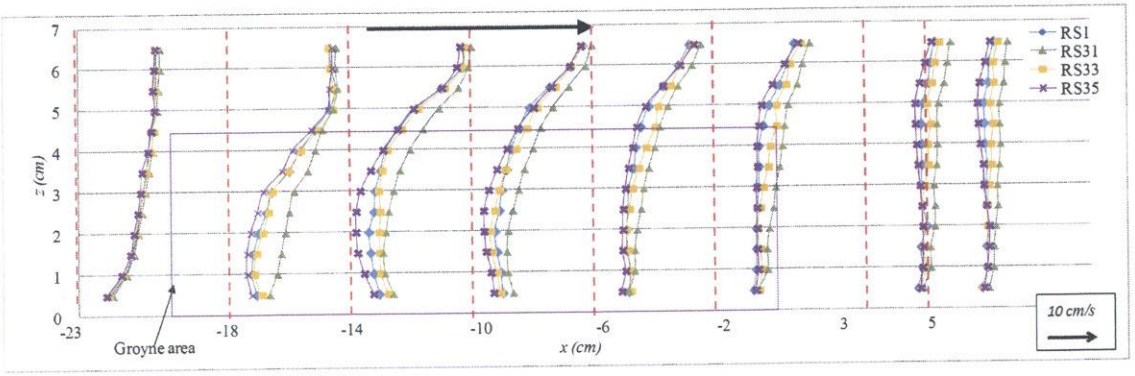

b)) Longitudinal block in the downstream side of lateral entrance

Figure 4.20: Vertical distribution of time-averaged longitudinal velocity (U) on the vertical plane of y/GL=1.17 under the submerged condition

curvature than that in emerged case. It means the more vortex structure has the opportunity to enter the inner zone of the submerged box groyne. Under the submerged condition, the distribution and value of turbulence intensity in the main stream has a great relationship with the mass exchange process in the lateral side and the distribution of downflow in the main stream. The combined action of these two factors dominates the turbulence intensity in the main stream.

When the longitudinal block is set in the upstream side, the maximum value of longitudinal turbulence on the horizontal plane is smaller than the case without the longitudinal block. It is caused by the mixing with the downflow from the top of upstream of longitudinal block (as shown in Fig. 4.17 and 4.18). But the area of high intensity expands to the downstream as the length of longitudinal block grows, induced by the less energy transport

to the inner zone of box groyne from the lateral interface. The intensity of transverse turbulence in front of the second groyne is enhanced by the upstream longitudinal block. And it keeps the high value when the lateral entrance becomes smaller, which is different with the emerged cases. There are three main reasons for this phenomenon. The first one is the smaller scale of large coherent structure makes it is possible to more enter the inner zone by the narrow entrance. The second reason is resistance to inflow at the lateral entrance is reduced because the roof entrance is a better choice for outflow. On the vertical plane of y/GL=0.5, the intensity of vertical turbulence becomes strong when the upstream longitudinal block is set. The last one is mentioned above that the closer mixing layer under the submerged condition provides more possibility to vortex structure enter the inner zone.

When the longitudinal block is set in the downstream side, the maximum value of longitudinal turbulence on the horizontal plane is smaller than the case without the longitudinal block. It is caused by the mixing with the outflow from the upstream of the lateral entrance as shown in Fig. 4.14. As a result, when the length of the downstream longitudinal block is short (CASE RS31 and RS32), the distribution of high intensity of longitudinal turbulence becomes smaller with the increasing length of longitudinal block, accompanied with the strong transverse turbulence around the entrance. But when the length of the downstream longitudinal block is long (CASE RS33, RS34 and RS35), the distribution of high intensity of longitudinal turbulence becomes larger in range and value with the increasing length of longitudinal block, accompanied with the weak transverse turbulence around the entrance. On the vertical plane of y/GL=0.5, the intensity of vertical turbulence suddenly becomes strong when the shortest downstream longitudinal block is set. And then the intensity is smaller with the increase of the downstream longitudinal block.

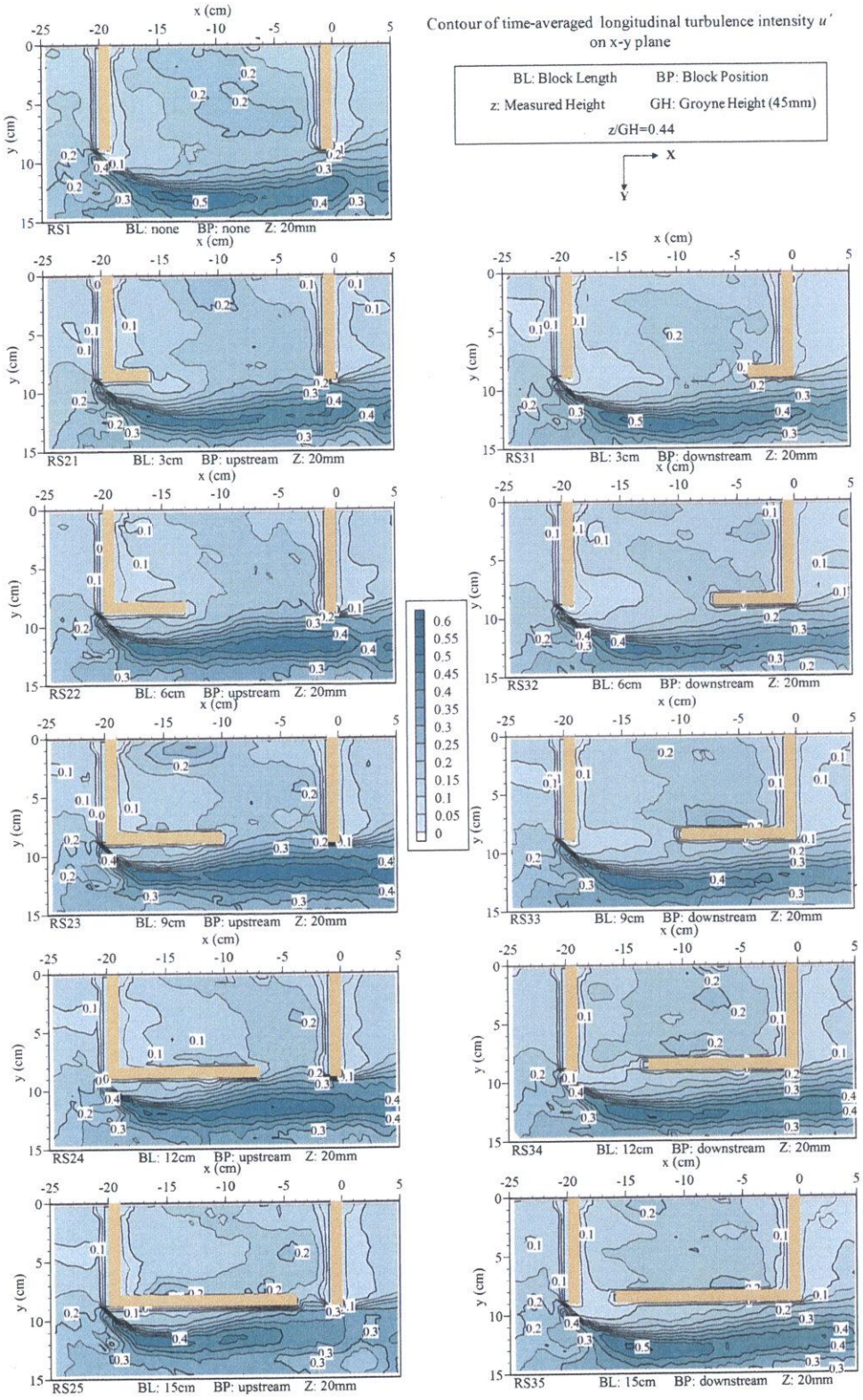

Figure 4.21: Contours of dimensionless time-averaged longitudinal turbulence u' on the horizontal plane (x-y)of z/GH=0.44 under the submerged condition

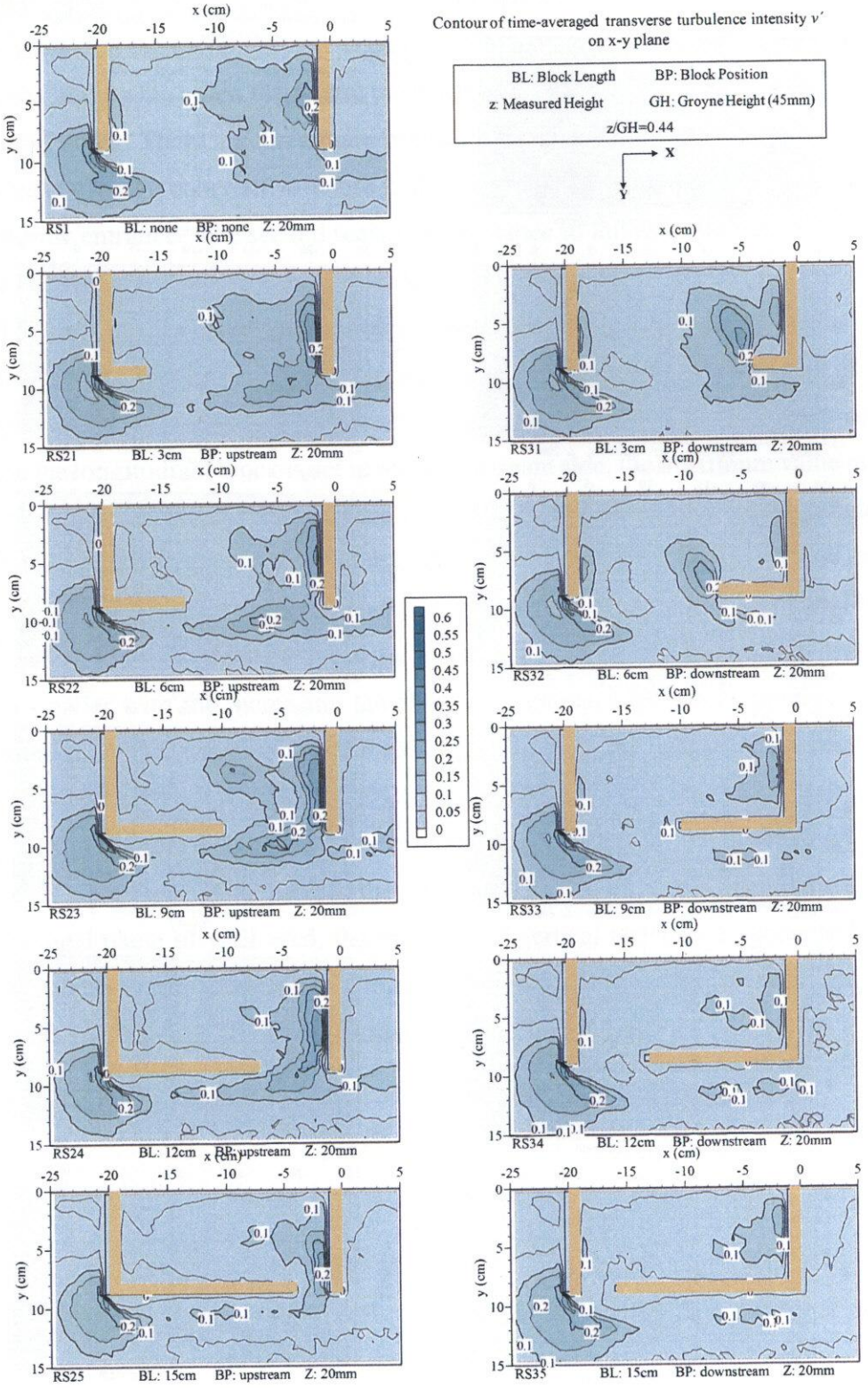

Figure 4.22: Contours of dimensionless time-averaged transverse turbulence v' on the horizontal plane (x-y)of z/GH=0.44 under the submerged condition

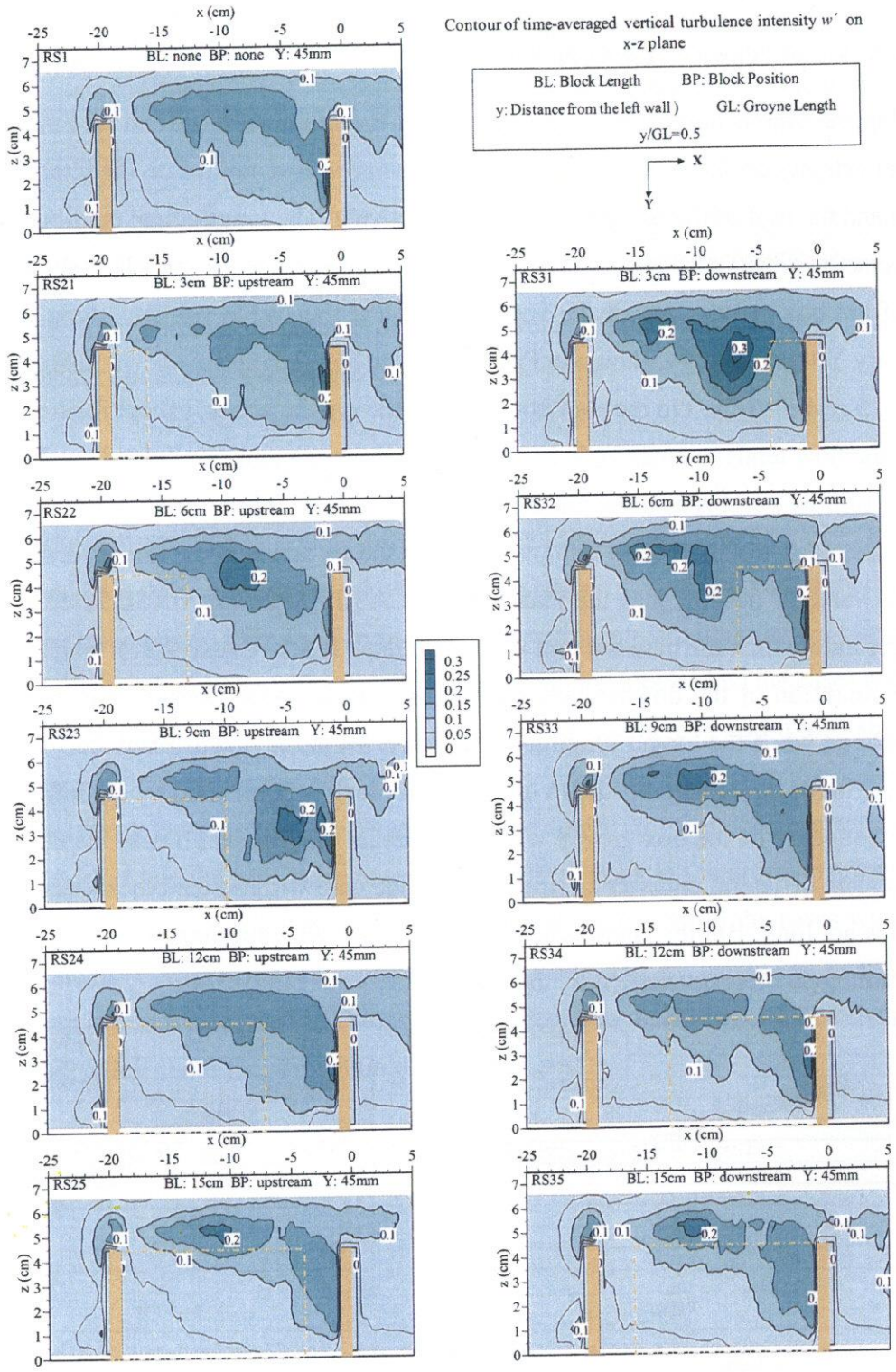

Figure 4.23: Contours of dimensionless time-averaged vertical turbulence w' on the vertical plane (x-z)of y/GL=0.5 under the submerged condition

4.2.4 Exchange processes

Distribution of velocity at the entrance

Based on the time-averaged transverse velocity on the lateral entrance and the time-averaged vertical velocity on the roof entrance, mass exchange was examined on the interface of the lateral and the roof of the box groyne zone respectively. The longitudinal distribution of the transverse-averaged vertical velocity along the roof boundary Z9 (z/GH=1, shown in Fig. 2.7) of the box groyne and of the vertical-averaged transverse velocity along the lateral boundary Y9 (y/GL=0.94, shown in Fig. 2.7) of the box groyne are shown in Fig. 4.24 and Fig. 4.25 respectively. On the roof boundary of the groyne zones, except for some special areas, the flow tends to enter in front of the second groyne and exit behind the first groyne and the turning point is near the middle of the box groyne. When the longitudinal block set in the upstream, a considerable outflow occurs in the section near the top of second groyne, and the value of outflow gets the maximum in CASE RS22. But CASE RS25 shows the stronger inflow than the case without the longitudinal block (CASE RS1), which is similar to the condition of the downstream longitudinal block. And the intensity of inflow becomes large when the longer longitudinal block is set in the downstream side. The lateral interface in the cases with upstream longitudinal block is dominated by the inflow. On the lateral boundary of the box groyne with downstream longitudinal block, the inflow in the downstream of lateral entrance is stronger than the case without the block when the block length is not long. But the lateral interface in the cases with long length of the downstream longitudinal block is dominated by the outflow.

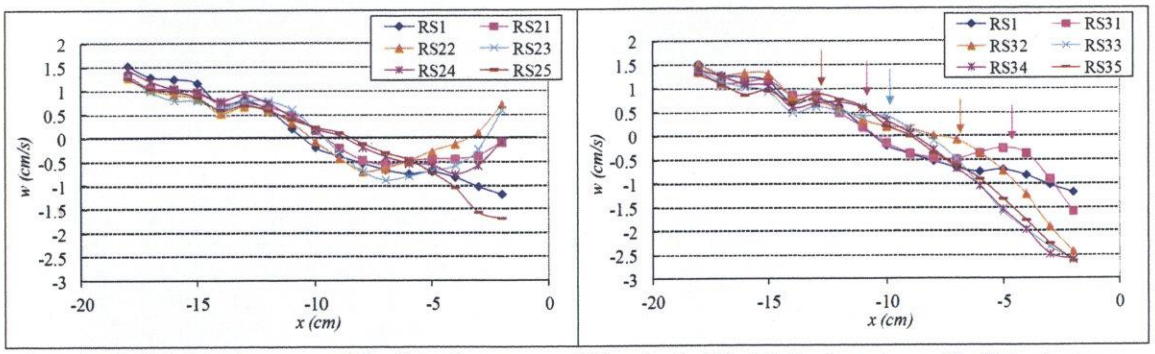

a) Longitudinal block in the upstream side of lateral entrance b) Longitudinal block in the downstream side of lateral entrance

Figure 4.24: Longitudinal distribution of transverse-averaged vertical velocity W along the roof boundary under the submerged condition

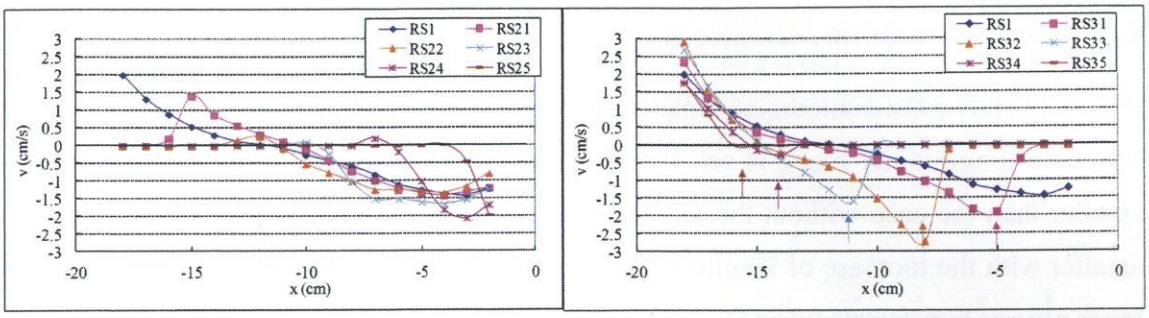

a) Longitudinal block in the upstream side of lateral entrance b) Longitudinal block in the downstream side of lateral entrance

Figure 4.25: Longitudinal distribution of vertical-averaged transverse velocity V along the lateral boundary under the submerged condition

Exchange coefficient obtained by PIV data

Fig. 4.26 shows the exchange coefficient obtained by instantaneous velocity from PIV. Due to the complicate three-dimensional flow inside the box groyne, the modified method proposed in the last chapter is not used here. The cases with upstream longitudinal block show stronger exchange ability than the case without longitudinal block. And the cases with 0.5S of block length (CASE RS23) have a highest exchange coefficient, and it also shows the high exchange ability under the emerged condition. The most cases with the downstream longitudinal block have a close or a larger exchange coefficient than the case without longitudinal block. Only the case with longest longitudinal block in the downstream side gets a lowest value of exchange coefficient. And exchange coefficient in the cases with 0.33S of block length (CASE RS32) is highest in group RS3. The exchange coefficient in the case with an upstream longitudinal block is larger than that in the case with a downstream longitudinal block under the same ratio of block length.

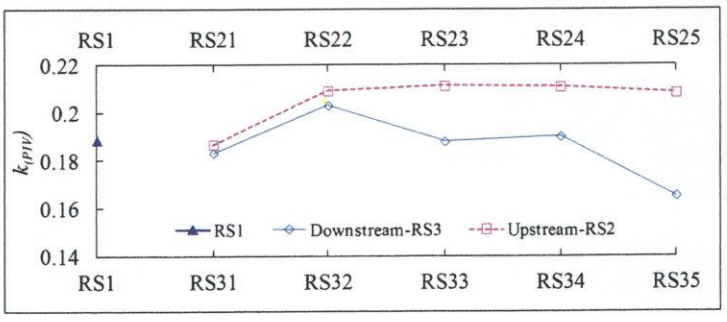

Figure 4.26: Exchange coefficient obtained by PIV data under the submerged condition

4.2.5 Bed shear stress

Fig. 4.27 shows the contours of dimensionless time-averaged bed shear stress. When the upstream longitudinal block is set, the maximum value around the tip of first groyne is smaller than the case without the longitudinal block, and the area of high value becomes smaller with the increase of longitudinal block. And the area of high value expands to the inner zone of box groyne when the length of longitudinal block is not too long, which easily causes the scour in front of the second groyne. When the downstream longitudinal block is set, there is not large different in the distribution of bed shear stress in the main stream. But the bed shear stress in the inner zone becomes larger in range and value as the length of longitudinal block increases.

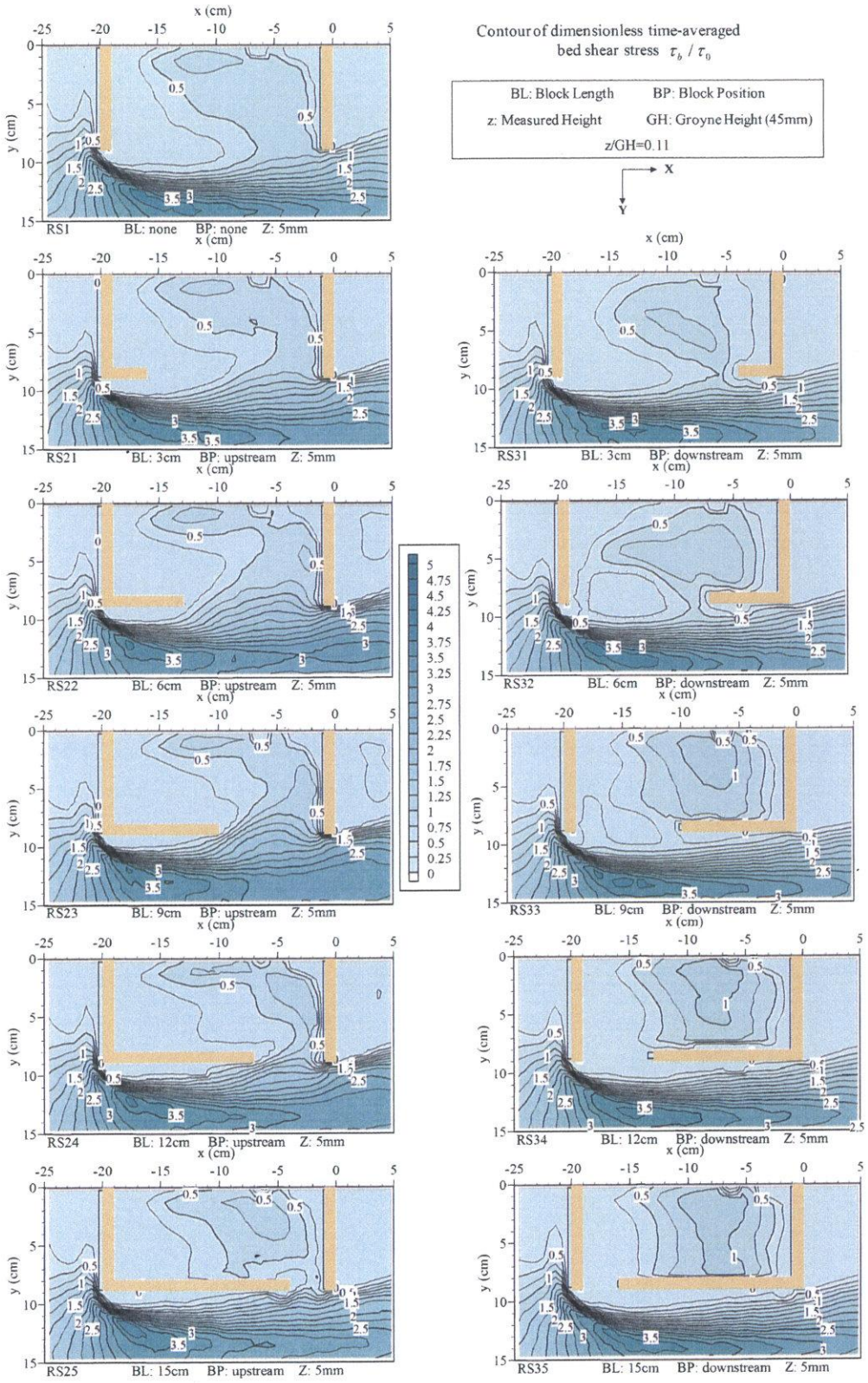

Figure 4.27: Contours of dimensionless time-averaged bed shear stress(τ_b/τ_0)under the submerged condition

4.3 Effects of the spacing of box groyne

Beside the spacing 18cm (S/GL=2), the other two kinds of spacing as 12cm (S/GL=1.33) and 24cm (S/GL=2.67) are introduced to explore the effect of different spacing of groyne on the flow field around the submerged box groyne. The length of longitudinal block taken as 0.5 ratio of spacing is 6cm and 12 cm for 12cm spacing and 24 cm spacing respectively. The case name is given in the Table. 4.1.

Table 4.1: The name of the case with other spacings under the submerged condition

Spacing (cm)	Block Position		
	none	upstream	downstream
12	RS1-12	RS23-12	RS33-12
24	RS1-24	RS23-24	RS33-24

4.3.1 Mean velocity in the inner zone of box groyne

Fig. 4.28 shows the comparisons of mean velocity in the inner zone of box groyne U_{ig} under different spacing ratio. For the cases without the longitudinal block and the cases with downstream longitudinal block, the mean velocity in the inner zone reduces as adding the spacing of box groyne. For the cases with upstream longitudinal block, the case of 18cm spacing (S/GL=2) has the highest mean velocity in the inner zone. The mean velocity of submerged box groyne presents radically different result from that of the emerged condition showing the increase of mean velocity as adding spacing. Under the 12cm spacing (S/GL=1.33), there is the close value between the case without the longitudinal block (CASE RS1-12) and the case with downstream longitudinal block (CASE RS33-12). And the mean velocity is largely reduced by the setting of the downstream longitudinal block. But the setting of longitudinal block has a slight impact to the mean velocity under the 24 cm spacing (S/GL=2.67).

The characteristics of three-dimensionality Ft shown in Fig. 4.29 present the weaker three-dimensionality appears with the increase of spacing when longitudinal block is not set or set in the downstream side. For the cases with an upstream longitudinal block, the case of 18cm spacing (S/GL=2) has the highest mean velocity in the inner zone. The arrangement of longitudinal block improves the three-dimensionality for the all cases except for the

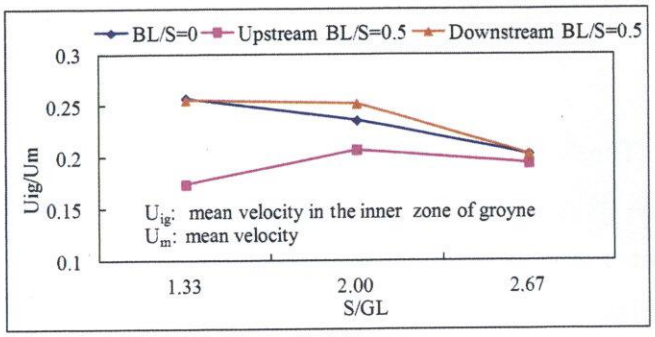

Figure 4.28: Comparisons of mean velocity in the inner zone of submerged box groyne U_{ig} under different spacing ratio

case of 12cm spacing with upstream longitudinal block (CASE RS23-12). The case of 12cm spacing with a downstream longitudinal block (CASE RS33-12) presents very strong three-dimensionality.

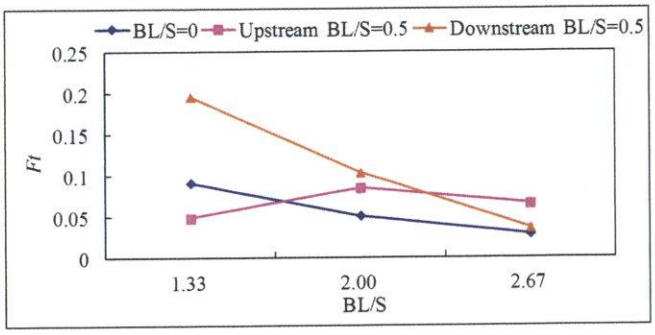

Figure 4.29: Comparison of three-dimensionality in the inner zone of submerged box groyne under the submerged condition

4.3.2 Flow structures

Flow pattern around the groyne area

Fig. 4.30~4.32 show the time-averaged velocity vectors U_{uv} and U_{uw} for the cases with 12cm spacing (S/GL=1.33) on the horizontal (x-y) and vertical (x-z) plane. Fig. 4.33~4.35 show the time-averaged velocity vectors for the cases with 24cm spacing (S/GL=2.67) on the horizontal (x-y) and vertical (x-z) plane. Fig. 4.36 shows the time-averaged velocity vectors U_{vw} on the transverse (y-z) plane. Compared with the time-averaged velocity for the case with 18cm spacing, it is clear that the gyre system in the groyne field is largely

changed by the different spacing of box groyne.

(a)Spacing=12cm The flow pattern in the case without longitudinal block (CASE RS1-12) on the horizontal plane of z=5mm (z/GH=0.11) and 20mm (z/GH=0.44) shows the gyre system in the inner zone is completely changed from the emerged cases, that the two-parallel-gyre system becomes one-gyre system like the submerged case with 18cm spacing (S/GL=2). But the transverse velocity in front of the second groyne is obviously stronger than the case with 18cm spacing. What makes this large difference happen? According to the discussion in the last section, it is known that the submergence makes the mixing layer move toward the box groyne and the curvature of its arc shape of area become larger. This change provides more possibility to vortex structure enter the inner zone of box groyne with smaller spacing. Due to the stronger inflow in the downstream of lateral entrance, much water enters the inner zone from the low level in front of the second groyne and increases the outflow near the left wall of channel, as shown in Fig. 3.30(b). Fig. 4.6 and Fig. 4.36(a) show that, in front of the second groyne, the intensity of inflow from the horizontal mixing layer (HML) is enhanced by narrowing the spacing of box groyne when there is not longitudinal block set.

When the longitudinal block is set in the upstream side, although the strong inflow also appears in the downstream of lateral entrance, there is not positive vertical velocity distribute in front of the second groyne on the vertical plane of y/GL=0.06 as the case of 18cm spacing with an upstream longitudinal block (CASE RS23). But the large distribution of positive vertical velocity moves to the upstream. It is because the large inflow from the horizontal mixing layer (HML) enters the inner zone in front of the second groyne, and it changes the direction of flow in the low level to the upstream. And the inflow in the downstream of lateral entrance is not as strong as that in CASE RS23. On the vertical plane of y/GL=0.84, there also is the upflow in front of the second groyne but weaker.

When the longitudinal block is set in the downstream side, the gyre around the lateral entrance is stronger than the case with 18cm spacing. Fig. 4.7 and Fig. 4.36(a) shows in front of the second groyne, the intensity of inflow from the horizontal mixing layer (HML) is also enhanced by smaller spacing of box groyne like the case without the longitudinal block. And this inflow in front of the second groyne is strongest under the same spacing. In general, the reduction of spacing has an effect on attracting the inflow from the downstream

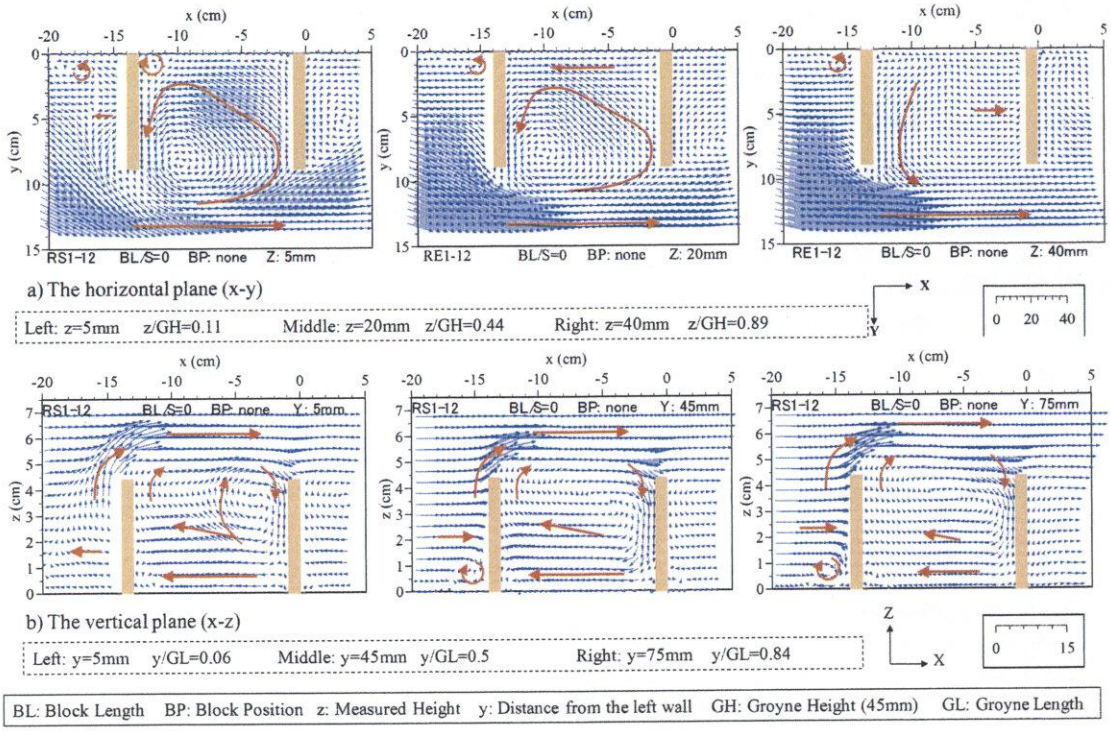

Figure 4.30: Time-averaged velocity vectors on horizontal plane and vertical plane for case of 12cm spacing without longitudinal block (CASE RS1-12)

of roof interface.

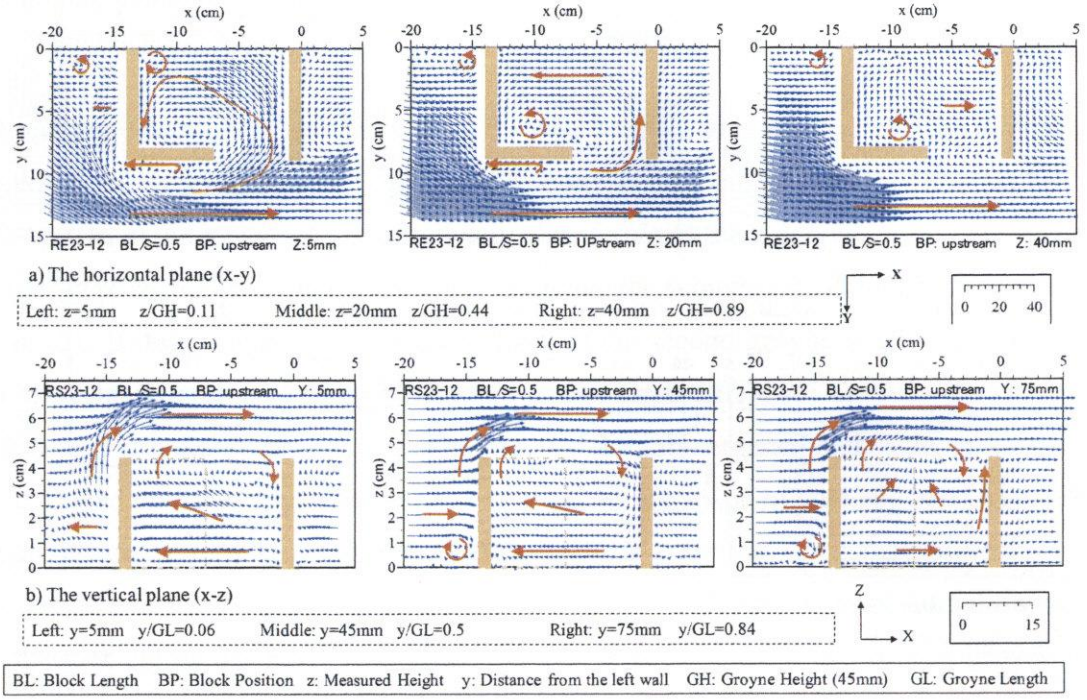

Figure 4.31: Time-averaged velocity vectors on horizontal plane and vertical plane for case of 12cm spacing with an upstream longitudinal block (CASE RS23-12)

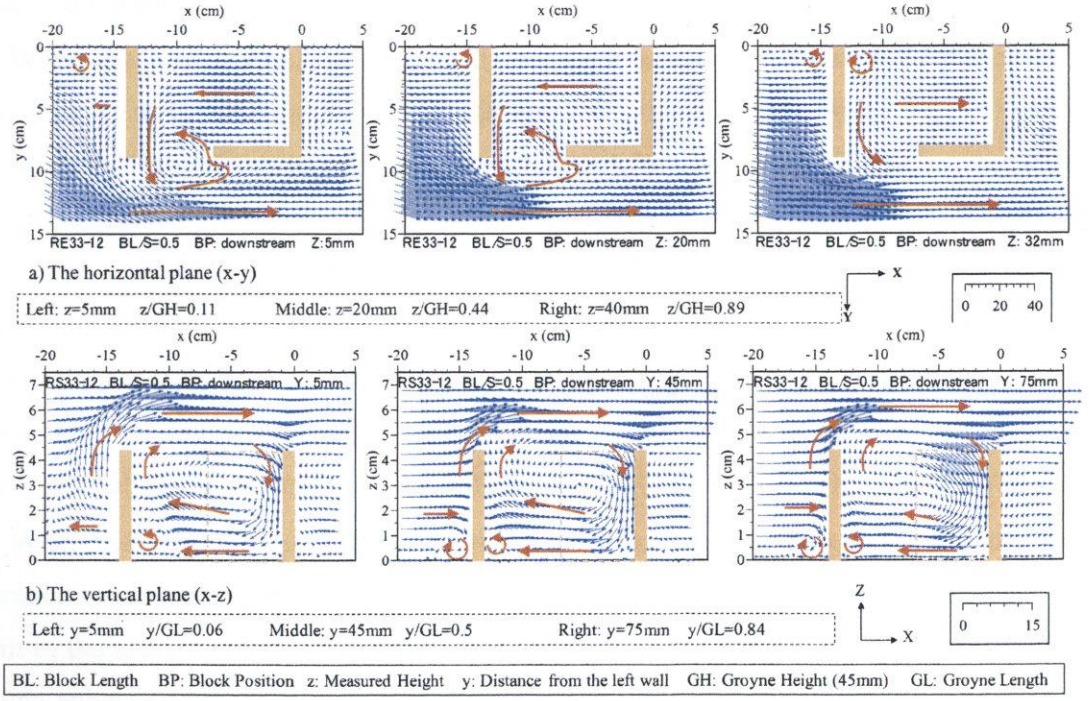

Figure 4.32: Time-averaged velocity vectors on horizontal plane and vertical plane for case of 12cm spacing with a downstream longitudinal block (CASE RS33-12)

(b)Spacing=24cm Adding the spacing of box groyne makes the flow pattern of the case without longitudinal block (CASE RS1-12) on the horizontal plane of z=5mm (z/GH=0.11) and 20mm (z/GH=0.44) become complex. On the vertical plane, the case without longitudinal block shows a similar distribution of vertical velocity in front of the second groyne with the case of 18cm spacing with an upstream longitudinal block (CASE RS23). The outflow in front of the second groyne appears near the section of the left wall and the lateral entrance.

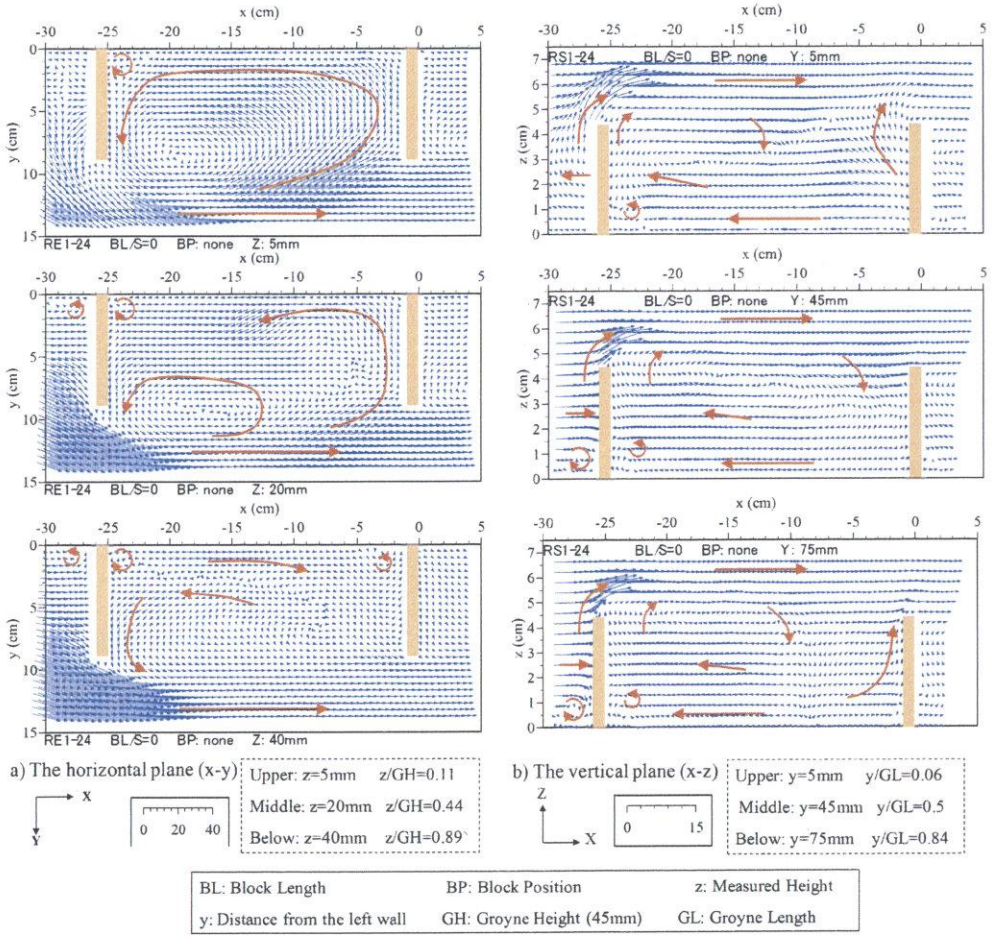

Figure 4.33: Time-averaged velocity vectors on the horizontal plane (x-y)and vertical (x-z) plane for the case of 24cm spacing without longitudinal block (CASE RS1-24)

When the longitudinal block is set in the upstream side, the secondary gyre on the horizontal plane enlarges. And the powerful inflow in the lateral entrance enters the inner zone with strong vortex structure, causing the considerable upflow flow out from the roof interface.

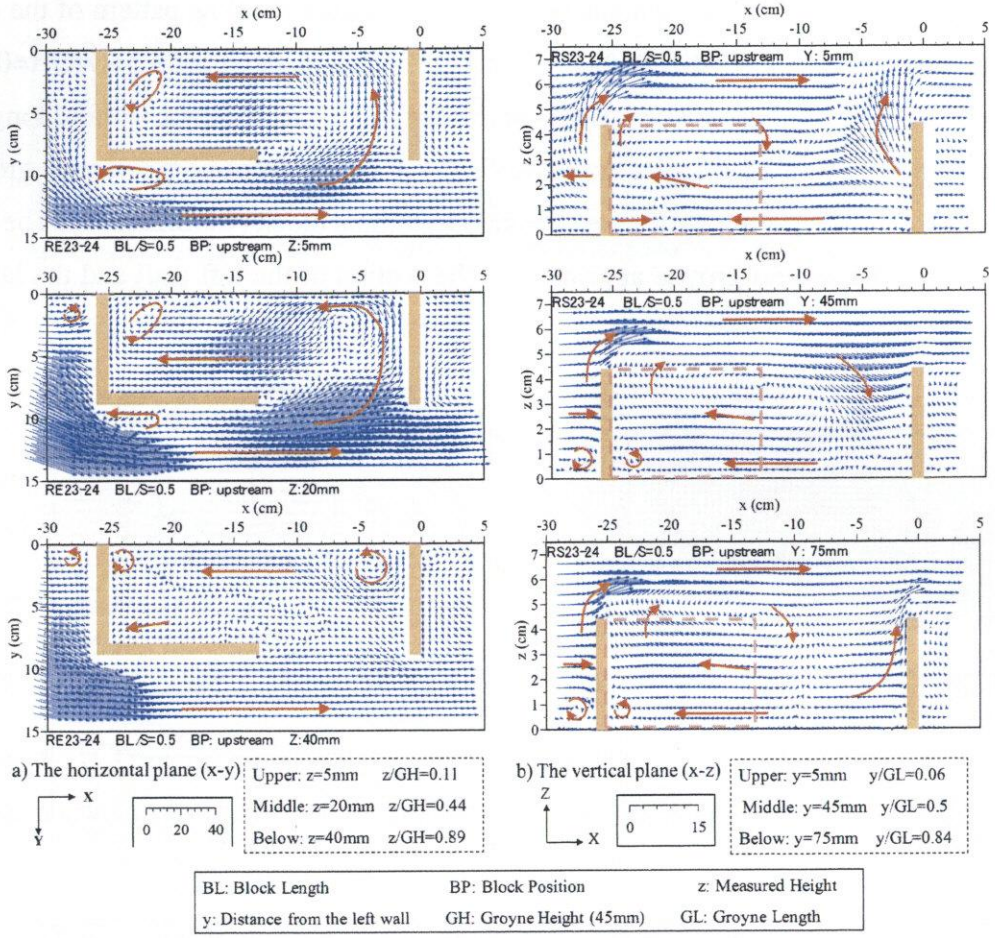

Figure 4.34: Time-averaged velocity vectors on the horizontal plane (x-y)and vertical (x-z) plane for the case of 24cm spacing with an upstream longitudinal block (CASE RS23-24)

When the longitudinal block is set in the downstream side, the high longitudinal velocity is mainly distributed in the transverse middle of box groyne on the horizontal plane compared with the case with 18cm spacing (CASE RS1). And the wider spacing causes the inflow from the horizontal mixing layer (HML) less enter the inner zone in front of the second groyne instead of in the longitudinal middle of box groyne. But the intensity of inflow in front of the second groyne is still larger than other cases under the same spacing.

Generally, the setting of longitudinal block has the similar effect on the flow pattern under different spacing. Be different with the emerged condition, the cases with the same lateral entrance are not picked to discuss. The participation of the horizontal mixing layer (HML) makes no comparison exist between them.

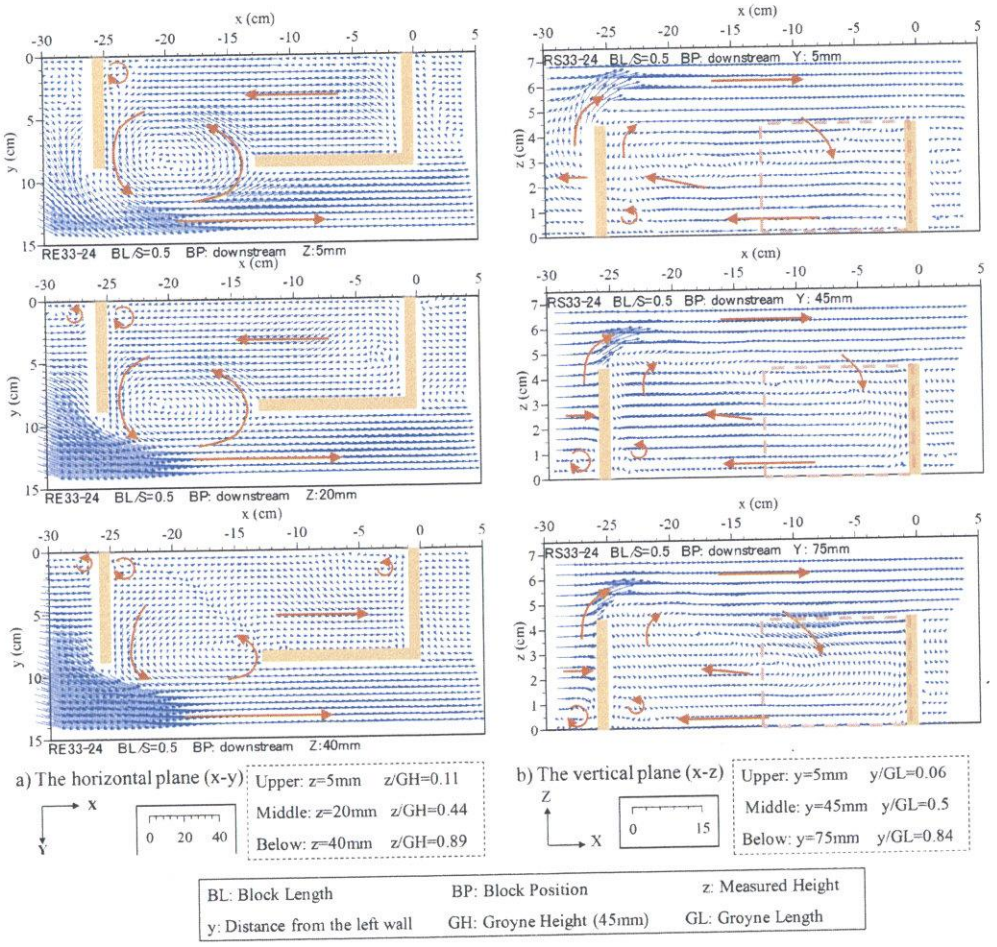

Figure 4.35: Time-averaged velocity vectors on the horizontal plane (x-y)and vertical (x-z) plane for the case of 12cm spacing with a downstream longitudinal block (CASE RS33-24)

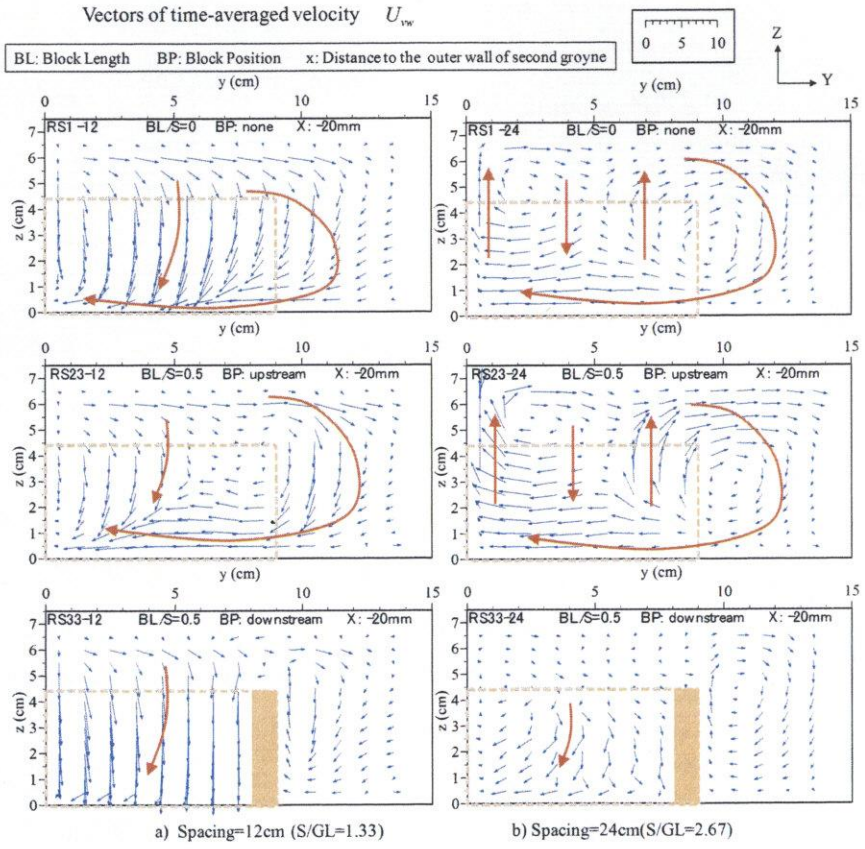

Figure 4.36: Time-averaged velocity vectors on the transverse plane (y-z)(x=-20mm) for the cases with different spacing under the submerged condition

Distribution of velocity in the main stream

The profiles of longitudinal velocity distribution (U) on the y/GL=1.17 plane in Fig. 4.37 are used to clarify the effect of the arrangement of longitudinal block on the main stream. Fig. 4.37(a) shows the wider spacing of box groyne causes the acceleration of flow in the upper level as going downstream and the reduction of velocity in the downstream section of box groyne in the main stream. As shown in Fig. 4.37(b) and (c), the arrangement of longitudinal block in the upstream side induces the acceleration moving from the groyne height level to the bottom plane as going downstream for the cases with 12cm (S/GL=1.33) and 24cm (S/GL=2.67) spacing, as same as the tendency under the case with 18cm spacing (S/GL=2). And it also causes the reduction of flow in the upper level. When the spacing is added to 24cm (S/GL=2.67), the accelerating effect of the downstream longitudinal block on the upper flow as going downstream is obvious.

4.3.3 Turbulent characteristic

The time-averaged turbulence intensity is denoted by in the longitudinal component u', the transverse component v' and the vertical component w'. The contours of dimensionless time-averaged turbulence intensity on the horizontal plane (x-y) of z/GH=0.44 and the vertical plane (x-z) of y/GL=0.5 are shown in Fig. 4.38~4.40 for cases with 12cm (S/GL=1.33) and 24cm spacing (S/GL=2.67).

(a)Spacing=12cm On the horizontal plane of z/GH=0.44, the area with high value of longitudinal turbulence in the main stream related to the mixing layer moves toward the box groyne without the longitudinal block compared with the case of 18cm spacing without longitudinal block (CASE RS1). It promotes the mass exchange in the lateral interface and induces the large distribution of transverse turbulence around the entrance. Then the high transverse turbulence in the upstream of the lateral entrance promotes the mass exchange here. It leads to the smaller maximum value of longitudinal turbulence in the mixing layer compared with other cases under 12cm spacing. The high intensity of longitudinal turbulence in the case with upstream longitudinal block means the downflow from the top of upstream of longitudinal block is not strong. Beside that, the effect of the longitudinal block on the horizontal distribution of turbulence intensity is as same as the cases with 18cm spacing. On the vertical plane of y/GL=0.5, the distribution of high intensity of

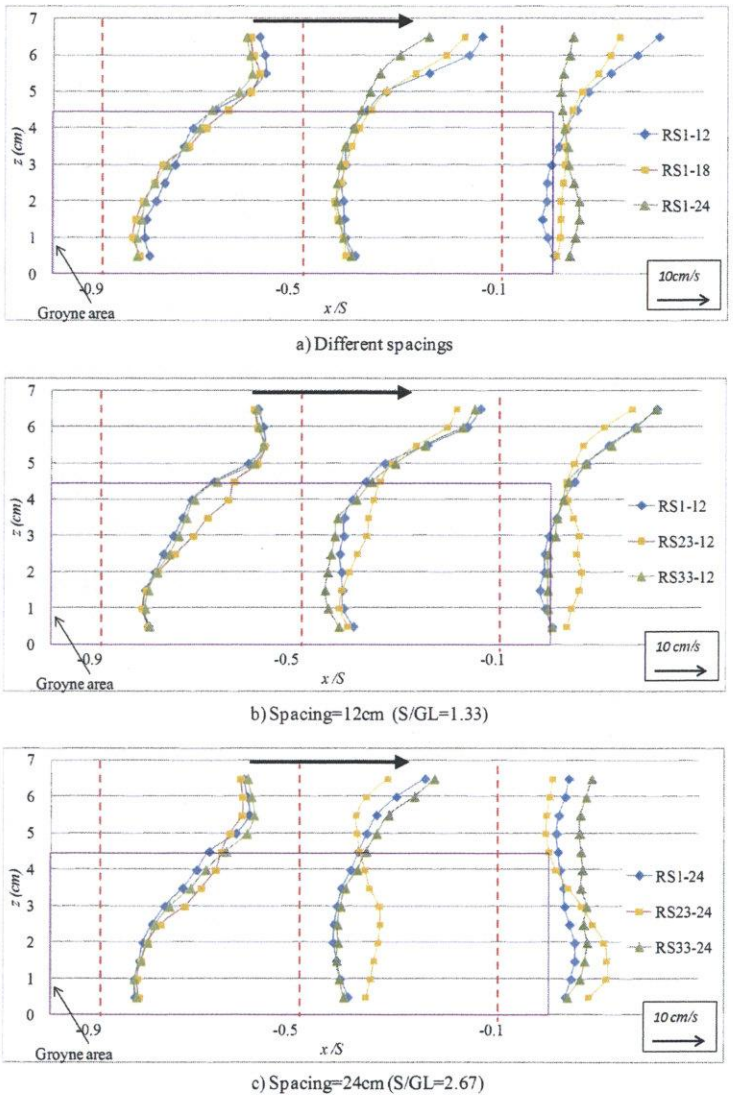

Figure 4.37: Vertical distribution of time-averaged longitudinal velocity (U) on the vertical plane of y/GL=1.17 under the submerged box groyne with different spacing

transverse turbulence is mainly in front of the first groyne, causing the amount of inflow here.

(b)Spacing=24cm On the horizontal plane of z/GH=0.44, the area with high value of longitudinal turbulence for the case without the longitudinal block is larger in range and value than the case of 18cm spacing without longitudinal block (CASE RS1). It is caused by the combined action of less mass exchange process in the lateral side and the smaller

downflow in the main stream. The effect of the longitudinal block on the horizontal distribution of intensity is as same as the cases with 18cm spacing. On the vertical plane of y/GL=0.5, the distribution of transverse turbulence is smaller and weaker than the cases with other spacing under the same ratio of longitudinal block.

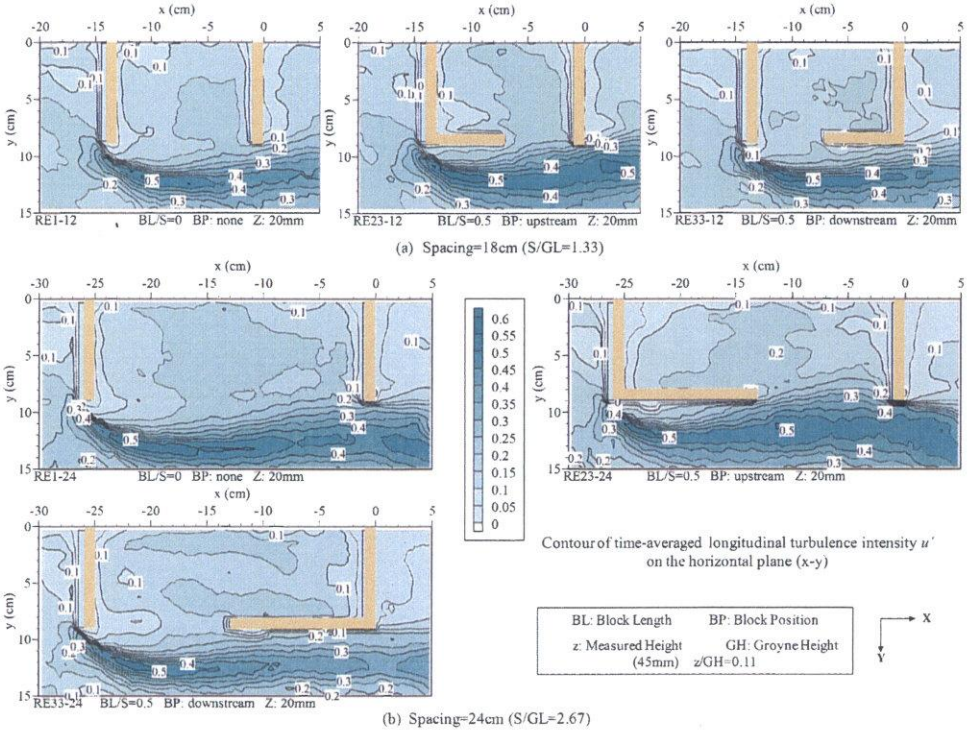

Figure 4.38: Contours of dimensionless time-averaged longitudinal turbulence u' on the horizontal plane of z/GH=0.44 under the submerged box groyne with various spacings

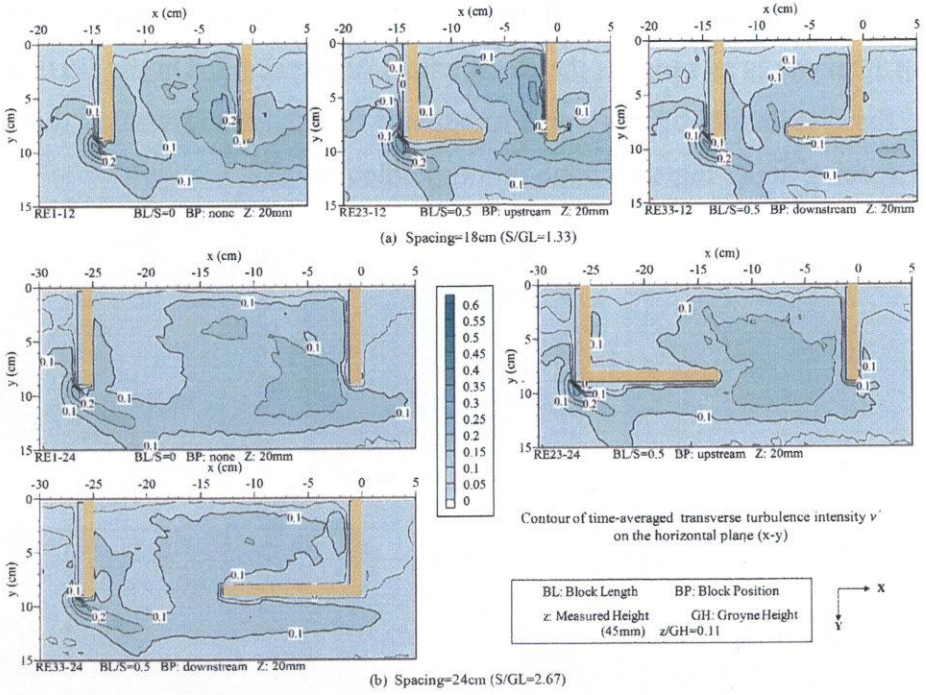

Figure 4.39: Contours of dimensionless time-averaged transverse turbulence v' on the horizontal plane of z/GH=0.44 under the submerged box groyne with various spacings

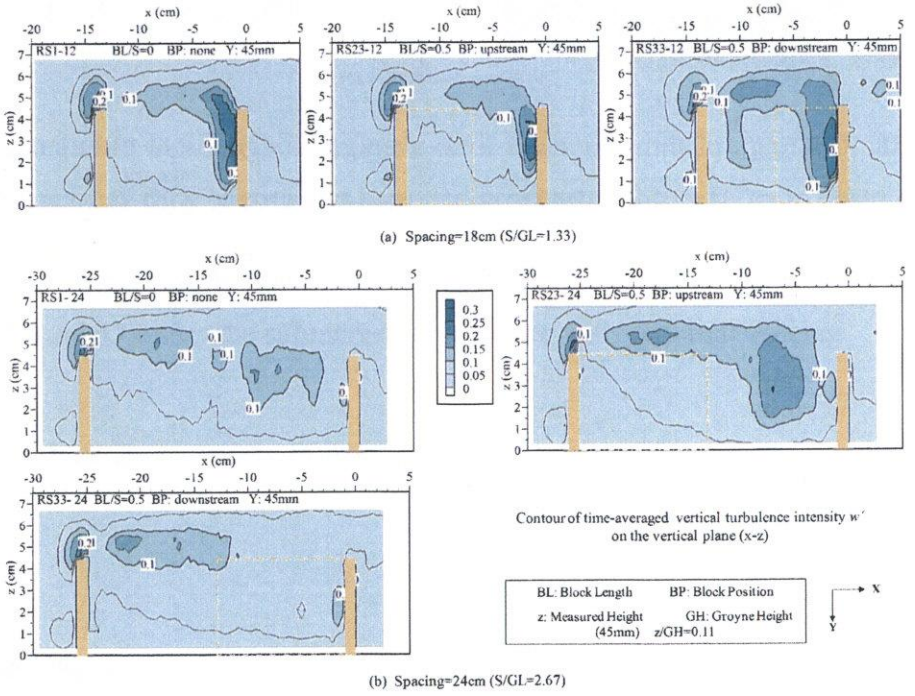

Figure 4.40: Contours of dimensionless time-averaged vertical turbulence w' on the vertical plane of y/GL=0.5 under the submerged box groyne with various spacings

4.3.4 Exchange processes

Distribution of velocity at the entrance

Based on the time-averaged vertical velocity on the roof entrance, mass exchange was examined on the roof boundary of the box groyne zone. The longitudinal distribution of the transverse-averaged vertical velocity along the roof boundary Z9 (z/GH=1, shown in Fig.2.2) of the box groyne are shown in Fig. 4.41. The distribution of vertical velocity is similar in the upstream section of roof boundary, while the large difference happens in the downstream section of roof boundary. In the case with 12cm spacing (S/GL=1.33), the curve of the longitudinal distribution presents the convex shape, generating a radical fall. In the case with 24cm spacing (S/GL=2.67), the curve of the longitudinal distribution presents the concave shape. The strongest downflow appears in far away from the second groyne. But the effect of longitudinal block is same under the different spacing. The longitudinal block in the upstream increases the resistance of entering the inner zone in front of the second groyne. And the longitudinal block in the downstream increases the resistance of entering the inner zone in front of the second groyne.

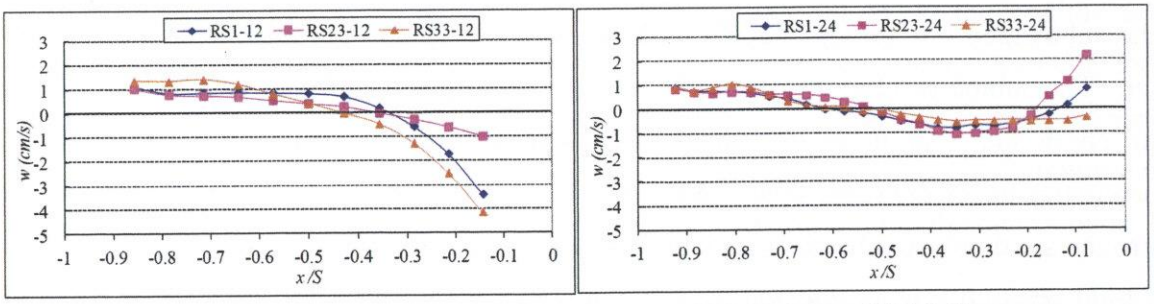

a) Spacing=12cm (S/GL=1.33) b) Spacing=24cm (S/GL=2.67)

Figure 4.41: Longitudinal distribution of transverse-averaged vertical velocity W along the roof boundary under the submerged box groyne with various spacings

Exchange coefficient obtained by PIV data

Fig. 4.42 shows the exchange coefficient obtained by instantaneous velocity from PIV. Due to the complicate three-dimensional flow inside the box groyne, the modified method proposed in the last chapter is not used here. When the spacing reduced to 12cm (S/GL=1.33), the case without the longitudinal block get the maximum value of exchange coefficient,

but the difference between three cases is small. Under the condition with 24cm spacing (S/GL=2.67), the upstream longitudinal block promotes the mass exchange process while the downstream longitudinal block weakens it.

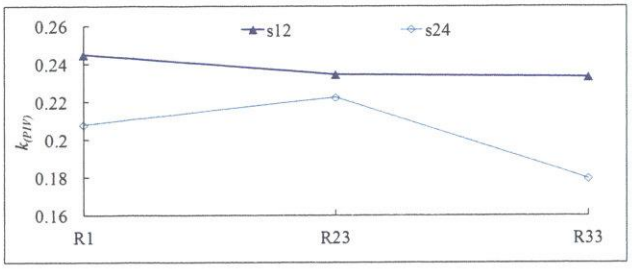

Figure 4.42: Exchange coefficient obtained by PIV data under the submerged box groyne with various spacings

4.4 Summary

The results of the characteristics of flow structure, turbulence and mass exchange around the submerged box groyne studied by laboratory experiment are presented in this chapter. The submerged box groynes with various spacing and different longitudinal blocks in length and position are compared and analyzed about their effects on the flow characteristics under the same flow condition. The flow structures inside the submerged box groyne are dominated by the combined actions of the vertical mixing layer (VML) on the lateral plane of box groyne and the horizontal mixing layer (HML) on the roof plane of box groyne. On the horizontal plane, the vertical mixing layer (VML) on the lateral side is sensitive to the longitudinal block set in the lateral entrance, which brings large change to the horizontal flow pattern in the inner zone. But the change of flow pattern inside the submerged box groyne also affects the horizontal mixing layer. So the longitudinal block also has an indirect effect on the horizontal mixing process. The abundant configuration of submerged box groyne is able to realize the application for different demanding in river restoration.

The arrangement of longitudinal block clearly improves the three-dimensionality of flow and diversifies the circulation flow in the submerged groyne zone, benefiting the demanding of various aquatic animals. The mean velocity in the groyne zone of most cases

with a downstream longitudinal block increases, while that of cases with an upstream longitudinal block decrease. And the value of mean velocity increases with the longer length of the downstream longitudinal block. The relatively low mean velocity in the groyne zone in the case with an upstream longitudinal block is able to provide a good shelter for the aquatic animal during the flood season. Under the submerged condition, the mean velocity in the cases with longitudinal block is approaching the value of the case without longitudinal block. These two phenomena reveal the fact that the horizontal mixing effect contributes more extensively to the water inputs under the submerged condition.

The upstream longitudinal block greatly increases the discharge in the low level of main stream and the increase is enhanced with the longer length of longitudinal block. And the downstream longitudinal block obviously increases the discharge in the high level of main stream under the large spacing of the submerged box groyne. The intensity of downflow around the tip of first groyne reduces with the increasing height, which is different with the distribution of emerged cases. And the distribution of downflow in the main stream is going downstream with the increasing height, because the downflow in the high level is mainly caused by the overtopping flow from the top of first groyne. The upstream longitudinal block has the ability to enhance the downflow in the main channel. While the longitudinal block set in the downstream has a reduced effect on the downflow in the main stream and becomes strong as the length of longitudinal block increases. The upflow appearing in front of the longitudinal block is beneficial for the reducing the scouring around the longitudinal block. These are important characteristics affecting the bed evolution in the main stream.

The distribution of longitudinal turbulence in the main stream is related to the mixing layer. Under the submerged condition, the vertical mixing layer moves toward the submerged box groyne, and the arc shape of area has larger curvature than that in emerged case. It means the more vortex structure has the opportunity to enter the inner zone of the submerged box groyne. Under the submerged condition, the distribution of turbulence intensity in the main stream has a great relationship with the mass exchange process in the lateral side and the distribution of downflow in the main stream. The combined action of these two factors dominates the turbulence intensity in the main stream. The energy diffusion in the vertical mixing layer is increased by the downflow from the top of first groyne under the submerged condition. When the longitudinal block is set in the upstream side, the stronger downflow is generated by the effect of upstream longitudinal block, and

it promotes the energy diffusion in the vertical mixing layer. When the longitudinal block is set in the downstream side, the stronger outflow from the inner zone also promotes the energy diffusion in the upstream of the vertical mixing layer. As for the lateral interface, the longitudinal block totally controls the water exchange between the submerged box groyne and main stream, but it also significantly affects the water exchange process in the roof interface in front of the second groyne. The exchange process is promoted by the upstream longitudinal block and downstream longitudinal block under moderate length. The longitudinal block set in the downstream has an ability of attracting inflow from the roof boundary and it is enhanced by the longer block.

Narrow or widen the spacing of submerged box groyne also lead to the change of flow structure and mass transport between the submerged box groyne and main channel. The mean velocity in the inner zone and the three-dimensionality reduces as adding the spacing of submerged box groyne under most conditions. The setting of longitudinal block has a slight impact to the mean velocity under the 24 cm spacing (S/GL=2.67). Different with the emerged case, the submerged box groyne with small spacing (S/GL=1.33) receives more energy input both from the vertical mixing layer and horizontal mixing layer. In general, the setting of longitudinal block has the similar effect on the flow pattern under different spacing. For example, the longitudinal block in the upstream increases the resistance of entering the inner zone in front of the second groyne while the longitudinal block in the downstream decreases it.

The three-dimensional flow pattern in the submerged box groyne has been described in detail in this chapter. The different arrangements of longitudinal block have largely changed the flow structure around the submerged box groyne, creating the abundant environment for the aquatic life.

Chapter 5

Bed Deformation and Flow Characteristics of Box Groyne in the Movable Bed

5.1 Introduction

The characteristics of flow structures and turbulence actions are discussed in the previous chapters. The interaction between the flow characteristics and bed evolution is conducted to seek equilibrium condition in the channel. In this chapter, the laboratory experiment in the movable bed is conducted to investigate the effect of box groyne on the transportation of bed load.

A description of the bed deformation around the traditional box groyne induced by the three-dimensional turbulent flow is presented under different hydraulic condition. The bed deformation of emerged box groyne is investigated under the similar hydraulic condition as the experiment in the fixed bed. The study of submerged box groyne is also in the process but under the lower water depth due to the restrictions of experimental conditions. The various longitudinal blocks are taken into account on different block lengths and positions in the lateral entrance. Bed evolution is a long-term process depending on the many kinds of parameters as properties of fluid, flow condition, material of bed sediment, geometry of channel and structure of groyne and so on. But the short-term deformation also is able to reveal the difference between kinds of groyne structures. In this study, the short-term deformation with two hours of water time around various box groynes are measured for exploring the effects of longitudinal block.

The interaction between flow field and bed evolution is a complex process. The different behaviors of flow field induced by the bed deformation are inevitable. In that case, the flow velocity around the groyne field in the movable bed is an important part in the discussion of this study. Only the velocity in the inner zone of box groyne and small area of main channel is measured in three hours after two hours of water time to avoid great evolution during the measurement. It is because the temporal status of bed deformation picked for investigation

in this study. The comparison of flow field between the cases under the fixed bed and movable bed is operated to investigate the effect of bed deformation on the flow pattern. And the presentation of flow structure in the fixed bed also is helpful to the understanding of the formation mechanism of bed deformation.

5.2 Bed deformations and flow characteristics around the emerged box groyne

5.2.1 The sketch of bed deformation in the case without the longitudinal block (CASE RE1)

Fig. 5.1 shows the comparison of bed deformation between the box groynes without the longitudinal block under different flow conditions (CASE RE1 and CASE RE1-h). As Fig. 5.1 (a) shows, the scour hole is distributed in a large area around the first of groyne when the tip of first groyne appears the maximum value. The horseshoe vortex and the stream with high velocity in the main stream transport the sediment to the groyne zone and the downstream, greatly affecting the sediment distribution in the streamwise direction. The sediment in the upstream section of the inner zone slips into the hole dug by the horseshoe vortex, while the high positive transverse velocity (as shown in Fig. 3.4) aggravates the falling condition. It is the reason why the larger scour hole appears behind the first groyne than the condition in the single groyne. The horseshoe vortex pushes the sediment into the inner zone along the slope of scour hole. Meanwhile, the large coherent structure brings sediment to the inner zone from the downstream of entrance. The deposition in the inner zone places in the downstream section of inner zone by the effects of these two kinds of vortex structure.

The bed geomorphology of the case with higher discharge under same water time is able to help predict the future bed evolution of normal case to some degree (as shown in Fig. 5.1(b)). But it does not mean equivalent because the comparable and parallel structure for the bed geomorphology is flow condition. Under the higher discharge, the scour hole enlarges and gets the bottom, and scour extends to far downstream with the deposition of downstream side moving toward the recirculation zone. Meanwhile, the deposition in the inner zone reduces in range and height and moves in. This tendency of bed deformation is as same as the condition of 5 hours water time under normal discharge. But the scour expanding to the main channel of opposite side is caused by the high discharge without the

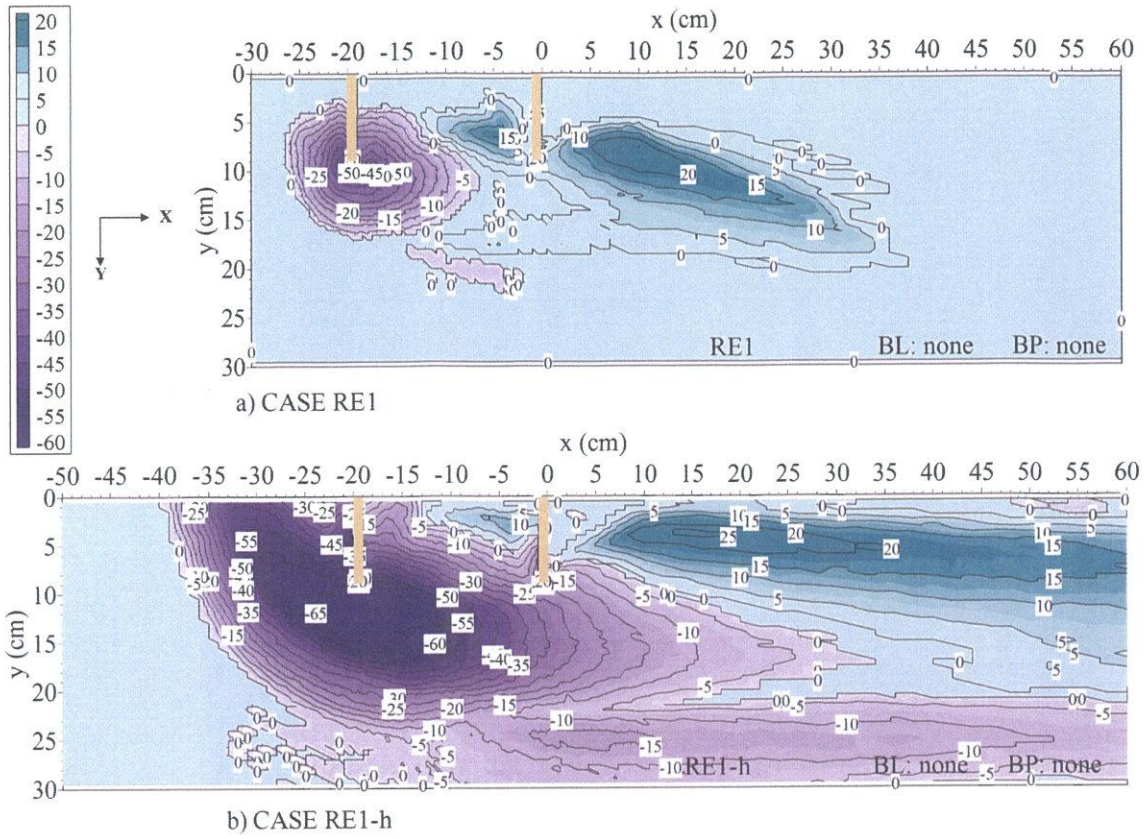

Figure 5.1: Comparison of bed deformation between the emerged box groynes without the longitudinal block under different flow conditions

Figure 5.2: The 'W' shape of scour hole int the front of first groyne

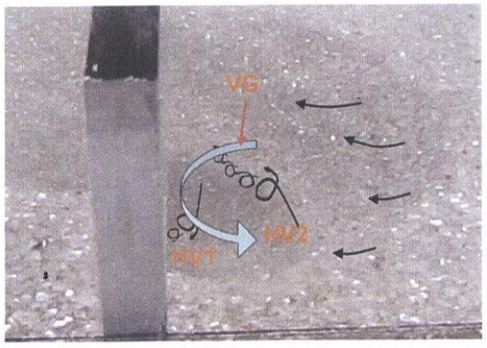

Figure 5.3: The sketch of horseshoe system in front of the first groyne

relationship to time. There is an interesting phenomenon about the scour hole in front of the second groyne that the hole with $'W'$ shape appears under higher discharge, as shown in Fig. 5.2. It is seldom observed in the previous research, which shows as $'C'$ shape or $'I'$

shape with the maximum scouring in the longitudinal distribution of x-z section locating near the wall of groyne. It is known that the horseshoe vortex it is the main reason inducing the scour hole around the first groyne. From the observation of the experiment in this study (as shown in Fig. 5.3), this effect mainly realizes by two actions. First dynamic motion occurs between the incoming flow in the upper level and the adverse pressure of the front wall of groyne, generating the horseshoe vortex scouring the tip of groyne, as the HV1 shown in Fig. 5.3. Second is that the incoming flow in the near bottom level flows down along the slope of hole, and generates the other horseshoe vortex (HV2 in Fig.5.3) by the adverse pressure of the vertical gyre (VG in Fig.5.3) in the scour hole. The main function of HV1 is hole deepening and widening while that of HV2 is widening. The combined actions of these two kinds of horseshoe vortex create the morphology of the scour hole around the first groyne. The intensity of HV2 is weak when the scour hole in front of the groyne is in small size at firstly. And then it becomes stronger with the enlarging scour hole. But the effect of HV1 is stronger than the HV2 under most conditions besides the following condition. One is the restrictions of HV1 when the scouring gets the bottom. The other is the enhancement of HV2 when the transverse velocity in front of the groyne becomes larger by the longer groyne length. The formation of $'W'$ shape above mentioned is due to the high intensity of HV2 induced by these two reasons.

5.2.2 The sketch of bed deformation in the case with an upstream longitudinal block (Group RE2)

Fig. 5.4 and 5.5 shows the contour of bed deformation for the cases with the longitudinal block set in the upstream side of entrance. It is clear that the scour hole and sediment distribution along the bed are largely affected by the arrangement of longitudinal block. The setting of the upstream longitudinal block has an efficient effect on the reduction of the scour hole, mainly caused by the restrictions on the development of horseshoe vortex. It is known that the longitudinal block in the upstream side restrains the development of horseshoe structure in the upstream section of box groyne by reducing the activity space. There is radically fall in maximum scour depth when the shortest longitudinal block is set in the upstream (CASE RE1), and this case gets the minimum value among all the cases. According to the comparison of the time-averaged velocity vectors U_{uw} on the vertical plane near the longitudinal block in the fixed bed (as shown in Fig. 3.8), it is found that the

reverse flow with positive vertical velocity in the shielding field distributes in front of the upstream longitudinal block, and its distribution on the plane near the bottom is closest to the tip of first groyne in the case with the shortest block length. In that way, the reverse flow with positive vertical velocity has a promotion effect on the reduction of horseshoe vortex or a constrained effect, which will be given the answer in the later discussion. The setting of upstream longitudinal block prevents sediment transport to the box groyne and causes the fewer depositions in the inner zone. As discussion of bed shear stress in the fixed bed in section 3.2.5, the shape of high bed shear stress in the downstream of entrance skews to the upstream side in the case without the longitudinal block (CASE RE1), while the shape of Group R2 is parallel to the wall of second groyne. It causes the different distribution shape of deposition in the inner zone between the CASE RE1 and CASE RE21. The scour hole in front of the second groyne is observed in the most cases with upstream longitudinal block, which is induced by the strong vortex structure inputting to the inner zone. As mentioned in the chapter 3, the upstream longitudinal block has an effect on promoting the vortex structure around the entrance. And then the small deposition in the inner zone mainly comes from the scour hole in front of the second groyne. Due to the less sediment transported to the downstream, the deposition largely reduces and more distributes in the section of box groyne as the length of longitudinal block grows. In particular, the amount of sediments distributes in front of the longitudinal block in the case with the longest length of longitudinal block.

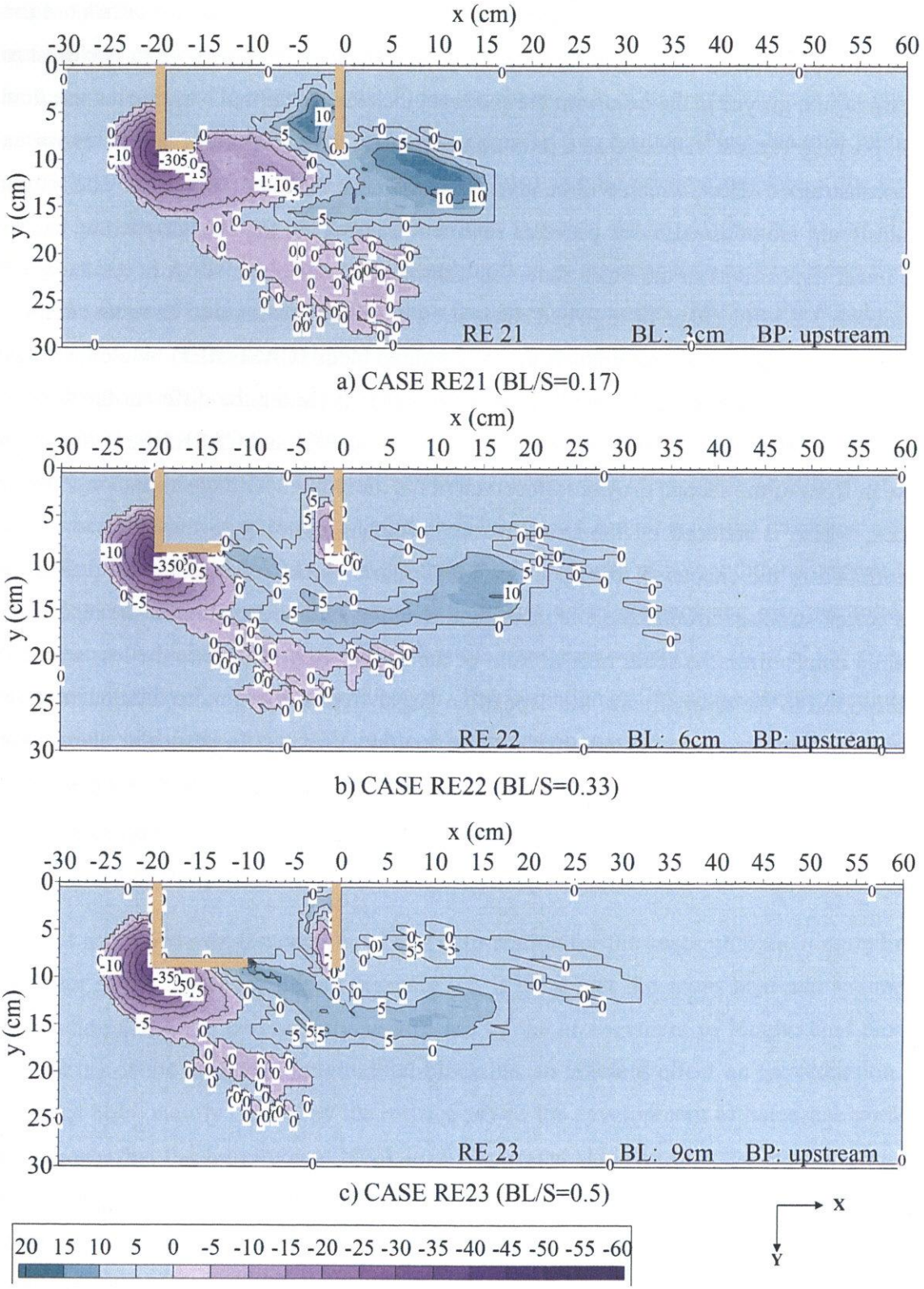

Figure 5.4: Comparison of bed deformation between the emerged box groynes with an upstream longitudinal block (Group RE2) Part 1

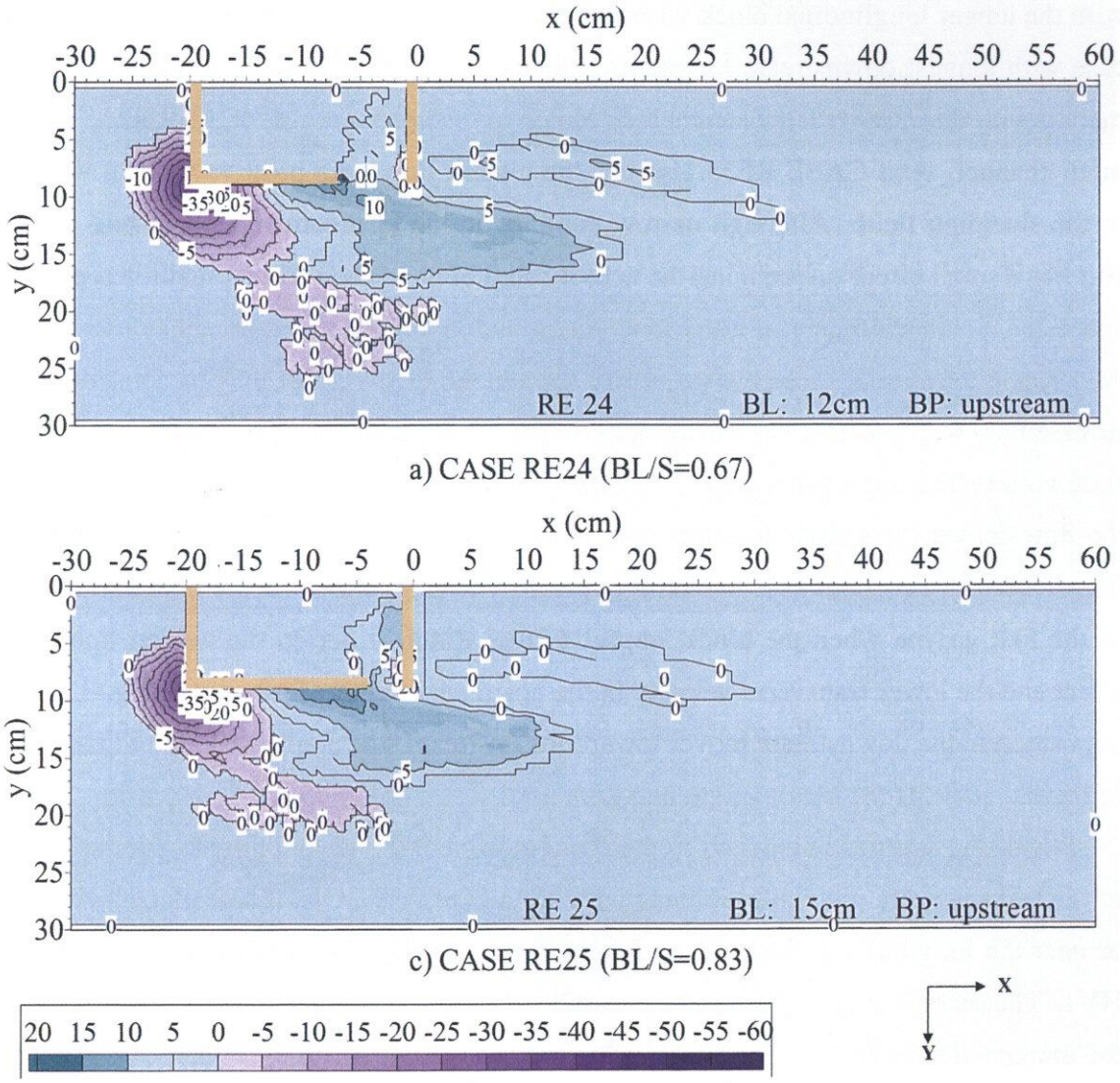

Figure 5.5: Comparison of bed deformation between the emerged box groynes with an upstream longitudinal block (Group RE2) Part 2

5.2.3 The sketch of bed deformation in the case with a downstream longitudinal block (Group RE3)

Fig. 5.6 and 5.7 show the contour of bed deformation for the cases with the longitudinal block set in the downstream side of entrance. The scale of the scour hole distinctly reduces with the longer longitudinal block when the block length beyond 6cm (BL/GL=0.33). The case with longest downstream longitudinal block (CASE RE35) has a similar bed deformation with the case with the same block length in the upstream side (CASE RE25) in the main channel. And CASE RE35 also has the reverse flow with positive vertical velocity in the shielding field. Although narrow entrance in the upstream section of box groyne still has a small effect on reducing the activity area of horseshoe vortex, it still has enough space for the development of horseshoe vortex and to supply the sediment to inner zone. As a result, the similar scour hole is able to support the theory about the promoted effect of reverse flow with positive vertical velocity in the shielding field on the reduction of horseshoe vortex. The appropriate length of the downstream longitudinal block is beneficial for the flow deliver the sediment to the inner zone when there is enough wide of entrance. It is noticed that, the scour hole behind the first groyne has a smaller scale than that in front of the first groyne when the block length is long, which is due to the weaker horseshoe effect and the lower transverse velocity in the upstream of entrance shown in Fig. 3.3. The deposition in the downstream moves toward the upstream side along the longitudinal block in smaller scale as the block length becomes long.

Beside the deposition induced by the scour in front of the second groyne, the deposition of the bed generally distributes in three parts for all the cases. One is placed the inner zone or near the longitudinal block as the emerged cases, which is mainly contributed by the HV1. The second is placed around the middle of channel, which is mainly contributed by the combined effect of HV2 and high velocity in the main stream. The third one is placed in the downstream side. It is also contributed by the combined effect of HV2 and high velocity in the main stream. And the mobile sediment induced by the HV1 is carried by the shear flow to bypass the second groyne or the tip of longitudinal block, and also has a contribution to the third part of deposition. But the third deposition part in the emerged cases is not distinct due to the small scale of the scour hole in the upstream.

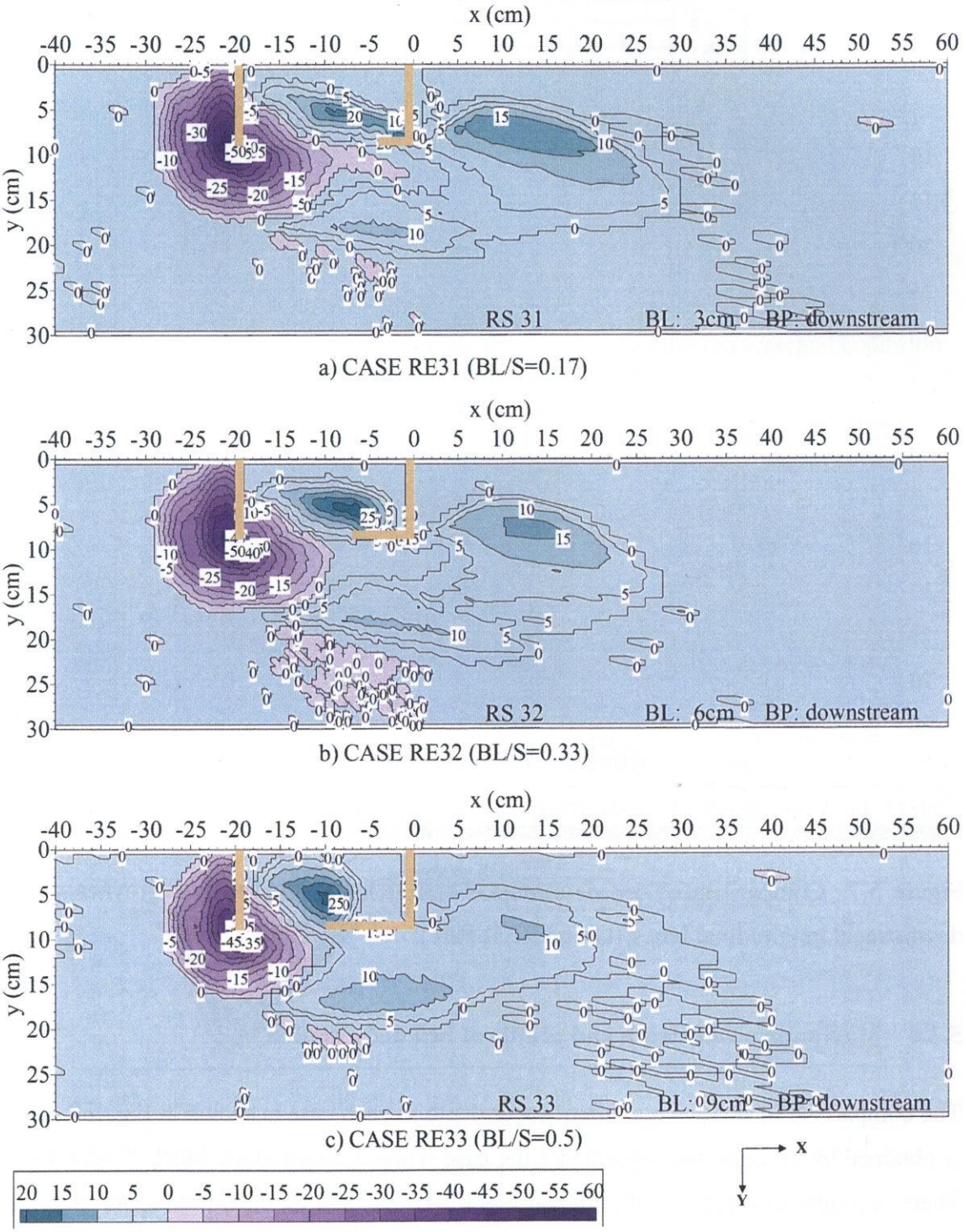

Figure 5.6: Comparison of bed deformation between the emerged box groynes with a downstream longitudinal block (Group RE3) Part 1

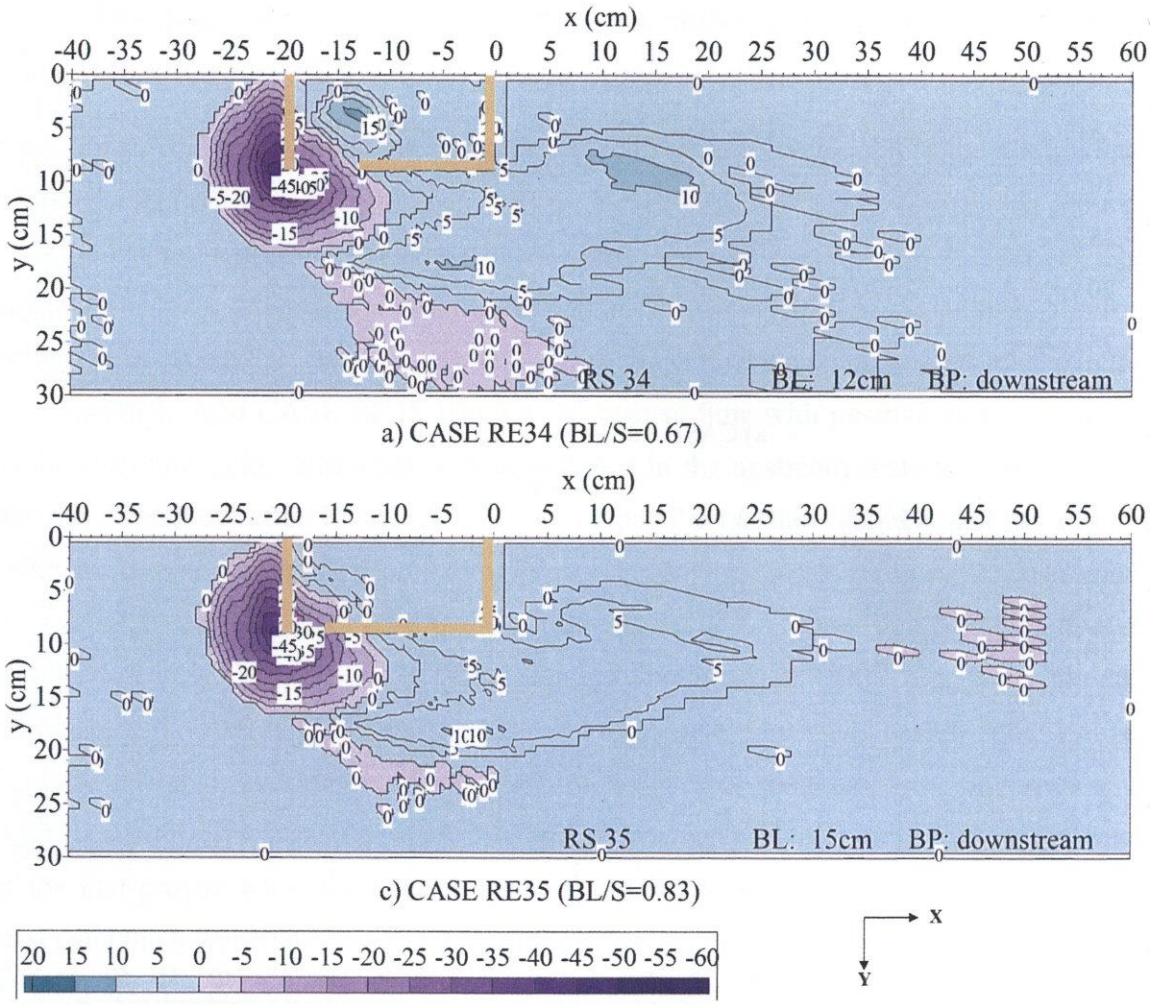

Figure 5.7: Comparison of bed deformation between the emerged box groynes with a downstream longitudinal block (Group RE3) Part 2

5.2.4 Maximum scour depth and profile of bed deformation

The comparison of relative maximum scour depth in each case is shown in Fig. 5.8, and it is obtained by dividing the value under the case without longitudinal block (CASE RE1). There is a distinct effect of longitudinal block on reduction of maximum scour depth for most cases. The value of maximum scour depth generally decreases as the length of the downstream longitudinal block increases. The longitudinal block set in the upstream has a great effect on reducing the maximum scour depth, and it is helpful for the protection of first groyne.

Fig. 5.9 shows the longitudinal profile of bed deformation on the section of y=10cm

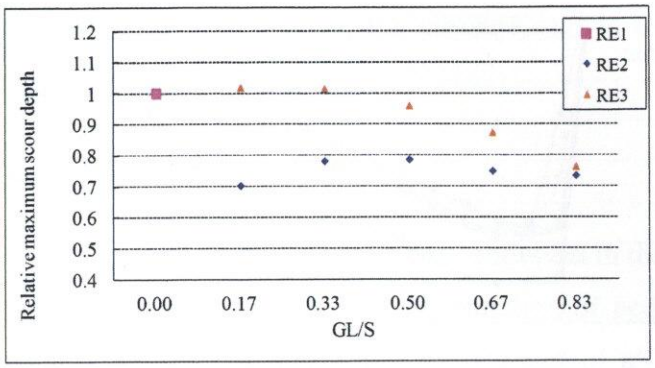

Figure 5.8: Comparison of relative maximum scour depth under the emerged condition

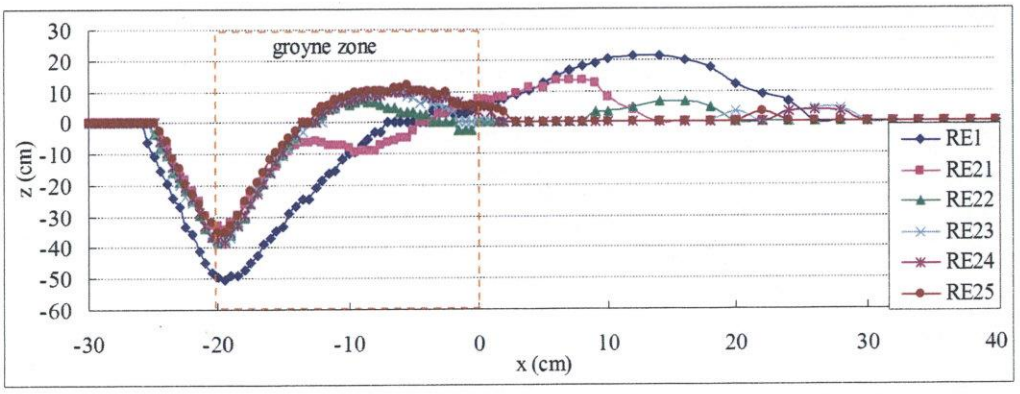

a) Longitudinal block in the up stream side of lateral entrance

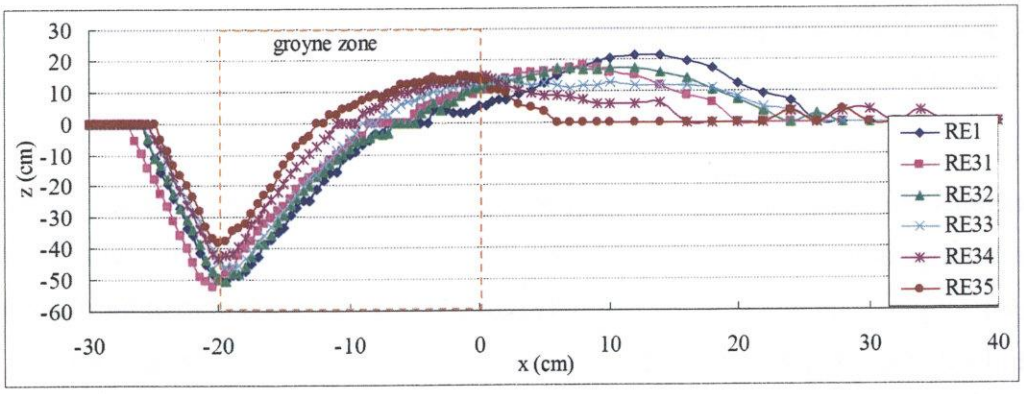

b)) Longitudinal block in the downstream side of lateral entrance

Figure 5.9: Longitudinal profile of bed deformation on the section of y=10cm (y/GL=1.11)under the emerged condition

(y/GL=1.11). Fig. 5.10 shows the transverse profile of bed deformation on the section of x=-19.5cm (x/S=-1.08). And the maximum scour depth places around the cross of these

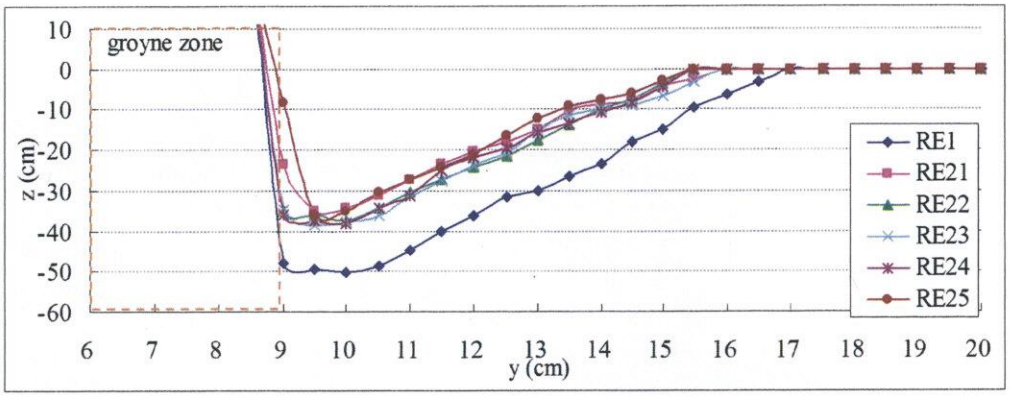

a) Longitudinal block in the upstream side of lateral entrance

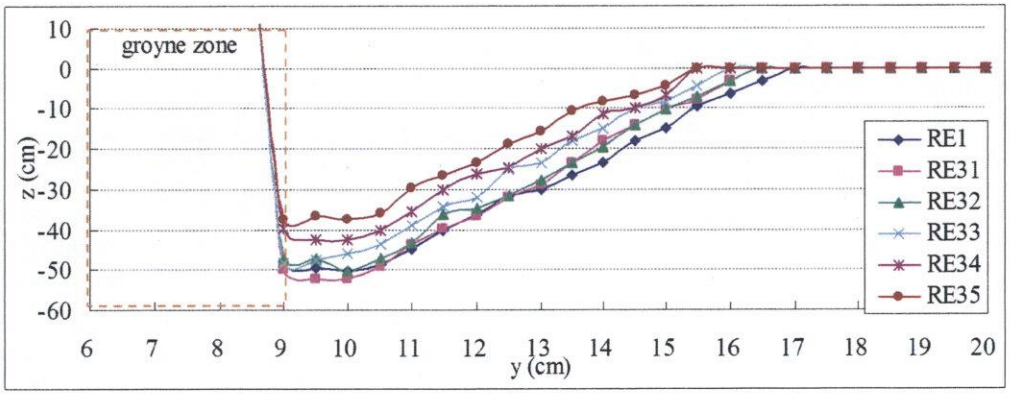

b)) Longitudinal block in the downstream side of lateral entrance

Figure 5.10: Transverse profile of bed deformation on the section of x=-19.5cm (x/S=-1.08)under the emerged condition

two sections. Not only the maximum scour depth, but also the scour volume is controlled by the arrangement of longitudinal block. The scour volume is largely reduced by the upstream longitudinal block, while is slowly reduced to the longer length of the downstream longitudinal block. On the longitudinal profile of bed deformation on the section of y=10cm (y/GL=1.11), it is found that the long block length makes the deposition mainly distribute in the section of box groyne when the longitudinal block is set in the upstream. And when the longitudinal block is set in the downstream, the sand bar moves toward the upstream as the increment of the block length. In particular, there is a small scour hole appear behind the prime scour hole in the CASE RE21.

It is noticed that, the variation trend of the distribution of turbulence intensity or bed shear stress induced by the effect of longitudinal block is not matching the scour condition

around the tip of first groyne. This is because the measurement in the fixed bed can not well perform the effect of horseshoe vortex.

5.2.5 Flow structures in the groyne field

The measurement of velocity around the box groyne is conducted in the CASE RE1, RE23 and RE33 to investigate the flow field under the deformation of bed. Fig. 5.11 shows the time-averaged velocity vectors U_{uv} on the horizontal plane of z/GH=0.56~0.67. Due to the large bed deformation in the groyne section for the case without the longitudinal block (CASE RE1), the flow pattern is greatly changed and generates the strong three-dimensional flow in the inner zone. The water in the low level largely enters the inner zone along the slope of the scour hole due to the dynamic motion of HV1. And then the circulation flow in the transverse section (y-z) is generated and shows the outflow in the upper layer as shown in Fig. 5.11(a). The inputting flow in the downstream of entrance still generates a horizontal circulation flow as the condition in the fixed bed. But it distributes differently because of the performance of transverse circulation flow.

The flow pattern also performs as strong three-dimensional flow in the inner zone when the longitudinal block is set, which shows a different gyre system with the condition in the fixed bed. At the entrance of the cases with an upstream longitudinal block, the shear flow with transverse velocity and high longitudinal velocity is fully distributed because of the deposition outside of entrance, as shown in Fig. 5.11(b).

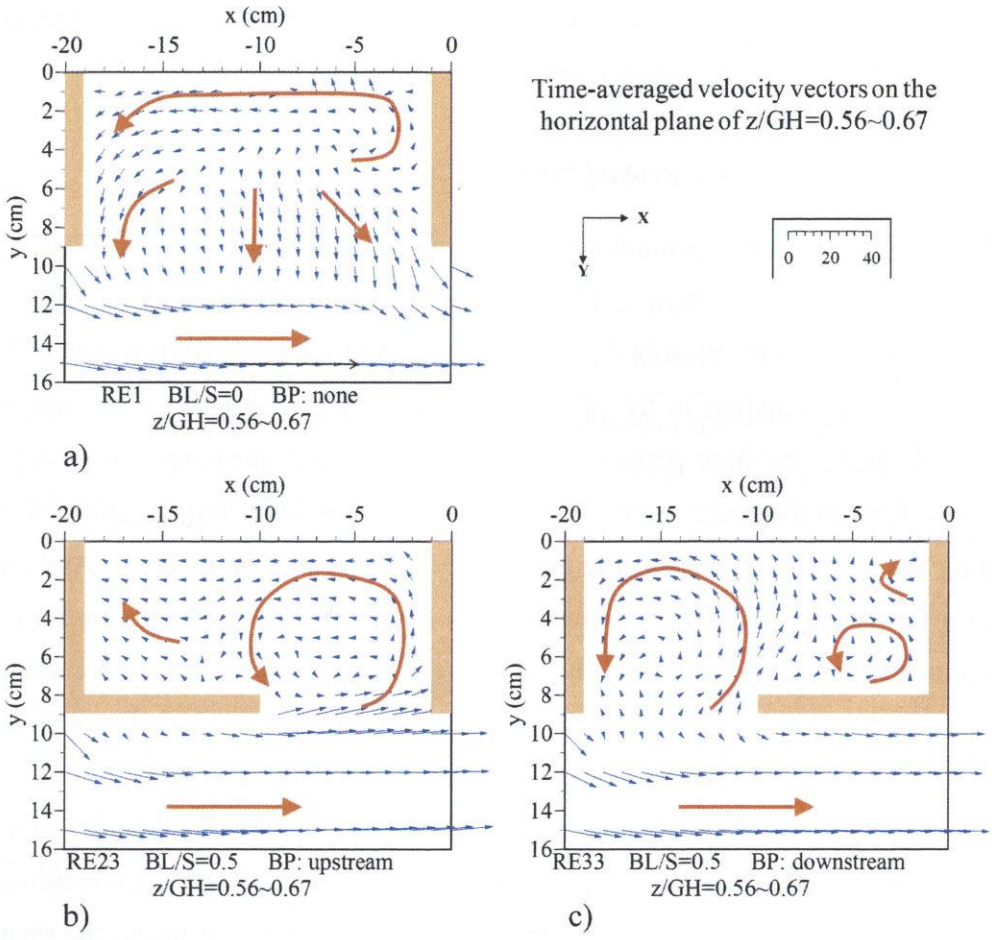

Figure 5.11: Time-averaged velocity vectors U_{uv} on the horizontal plane of z/GH=0.56~0.67 under the emerged condition

5.3 Bed deformations and flow characteristics around the submerged box groyne

5.3.1 The sketch of bed deformation in the case without the longitudinal block (CASE RS1)

The submergence is one of important factors affecting the geometry and depth of scour in the channel with groyne, as the study shown in Kuhnle et al. 1999 and Elawady et al. 2001. The figures of scour hole in the study of Kuhnle et al. (1999) showed in Fig. 5.12 present two different geometries of scour hole under low and high submergence ratio (h/GH) for single groyne. The maximum scour depth with low submergence ratio locates at the tip of groyne, whereas it with high submergence ratio has a place at about one-half the groyne from the channel wall of the upstream side of groyne. And a prominent secondary region of

scour appears near the downstream side of groyne with higher submergence ratio. Fig. 5.13 shows the bed deformation between the submerged box groynes without the longitudinal block. The maximum scour depth in this study also places around the tip of first groyne as the above experiment result with low submergence ratio. The scour hole behind the first groyne is distinctly smaller than the scour hole in front of the first groyne. And it is because the positive transverse velocity in the upstream of entrance (as shown in Fig 4.8(b)) is weak and cannot support more sediments slip to the scour hole as the emerged cases. There is another scour hole appear around the second groyne. As described in the section 4.2.2, the vertical mixing layer (VML) is closer to the box groyne under the submerged condition, and it causes that there is high longitudinal velocity distributed around the second groyne (as shown in Fig. 4.8). Beside that, the downflow over the top of first groyne (as shown in Fig. 4.17) arouses the scour around the second groyne together.

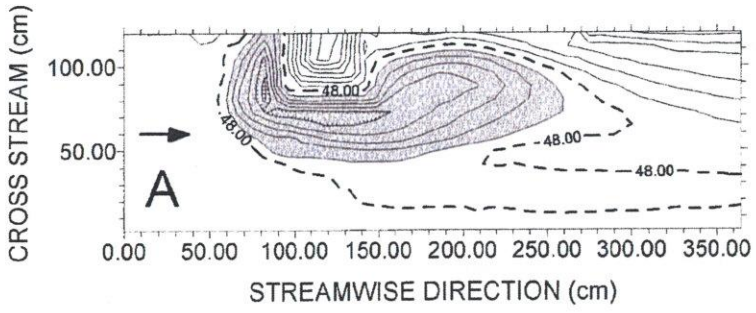

a) Submergence ratio=1.15

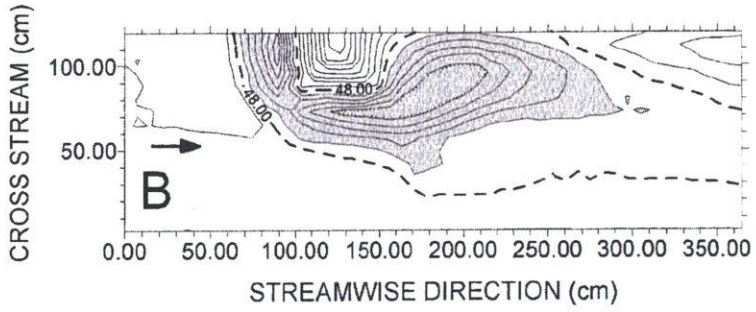

b)) Submergence ration=1.92

Figure 5.12: Contour of scour with different submergence ratio (h/GH)in the study of Kuhnle et al. 1999. (Contour interval is 2cm .Elevation of initial bed surface is 48cm. Elevations less than 46 cm are shaded)

In the inner zone of box groyne, the distribution of deposition extends to the upstream

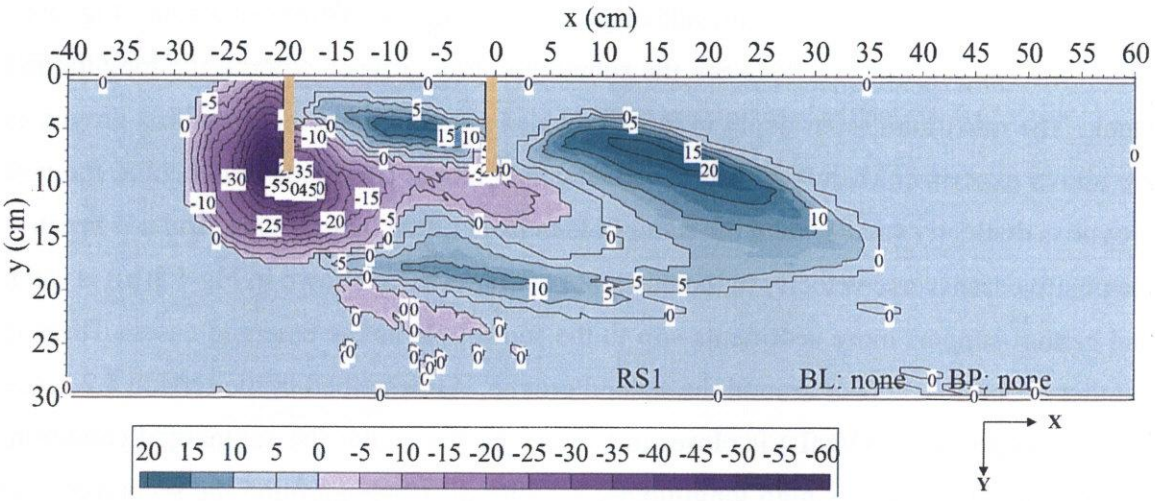

Figure 5.13: Contour of bed deformation in the submerged box groynes without the longitudinal block(CASE RS1)

section of box groyne, because of the high reverse flow near the bottom induced by the horizontal mixing layer (HML) as described in section 4.2.2. The third deposition as mentioned above performs clearly here because of the enlarged scour hole.

5.3.2 The sketch of bed deformation in the case with an upstream longitudinal block (Group RS2)

Fig. 5.14 and 5.15 show the contour of bed deformation for the submerged cases with the longitudinal block set in the upstream side of entrance. There is an obvious effect of upstream longitudinal block on the reduction of the scour hole around the first groyne under the submerged condition. When the block length is short as 0.17S (CASE RS21), the scour hole around the second groyne disappears by the covering of the mobile sediment transported from the inner zone under strong longitudinal shear flow. As the block length increases, the scour hole is generated in front of the second groyne by the inputting fluid with high intensity near the bed (as shown in Fig. 4.4). The inputting water flows toward the wall of second groyne and forms the horseshoe vortex by the adverse pressure of wall as what happens in the upstream of first groyne. The formation mechanism of these two scour holes around the two groynes is same. It is deduced that, the CASE RS22 has the strongest inputting fluid with the high longitudinal velocity around entrance from the shape and height of deposition in its inner zone. And it leads to the maximum scour hole in front

of the second groyne. As mentioned in the previous discussion, there is also a scour hole existing in front of the second groyne under the emerged cases. But it is totally different formation mechanism between these two kinds of scour hole. There is a new scour hole in the downstream side in the CASE RS22, RS23 and RS24. It is known from the discussion in the section 4.2.2 that, the upstream longitudinal block has a work of making water in the upper level beyond the box groyne transported to the low level of the main stream as going downstream. It benefits the generation of downflow in the downstream side of main stream. This strong downflow easily causes the scour in the main channel when it unites the high flow in the main stream. And the scour hole extends to the downstream side with the increasing length of longitudinal block. But this effect is radically reduced when the longest longitudinal block is set (CASE RS25).

As the length of longitudinal block is added, higher percentage of deposition distributes in the section of box groyne, and amount of it concentrates upon the tip of longitudinal block. The deposition in the inner zone is largely reduced by setting the long longitudinal block in the upstream side.

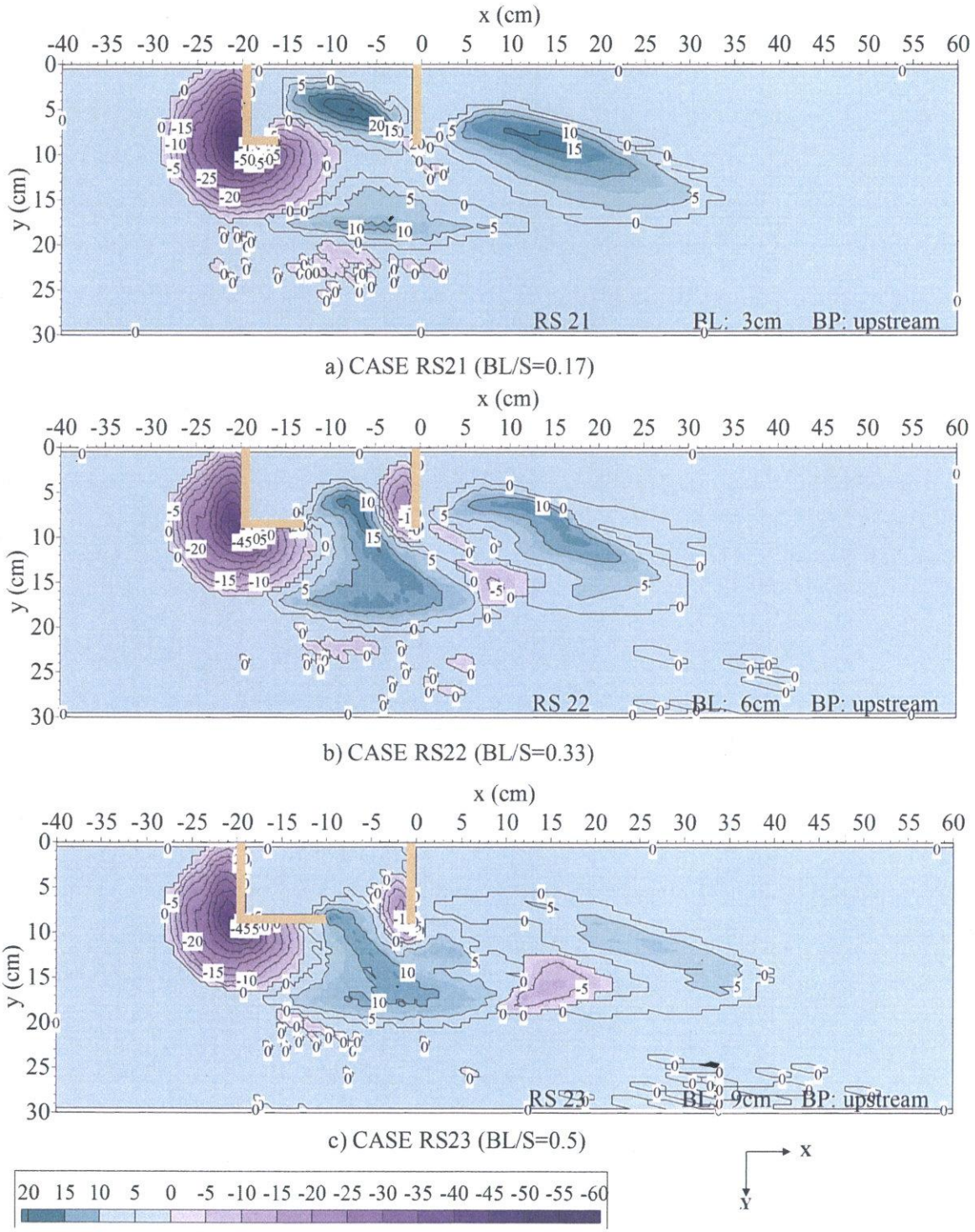

Figure 5.14: Comparison of bed deformation between the submerged box groynes with an upstream longitudinal block (Group RS2) Part 1

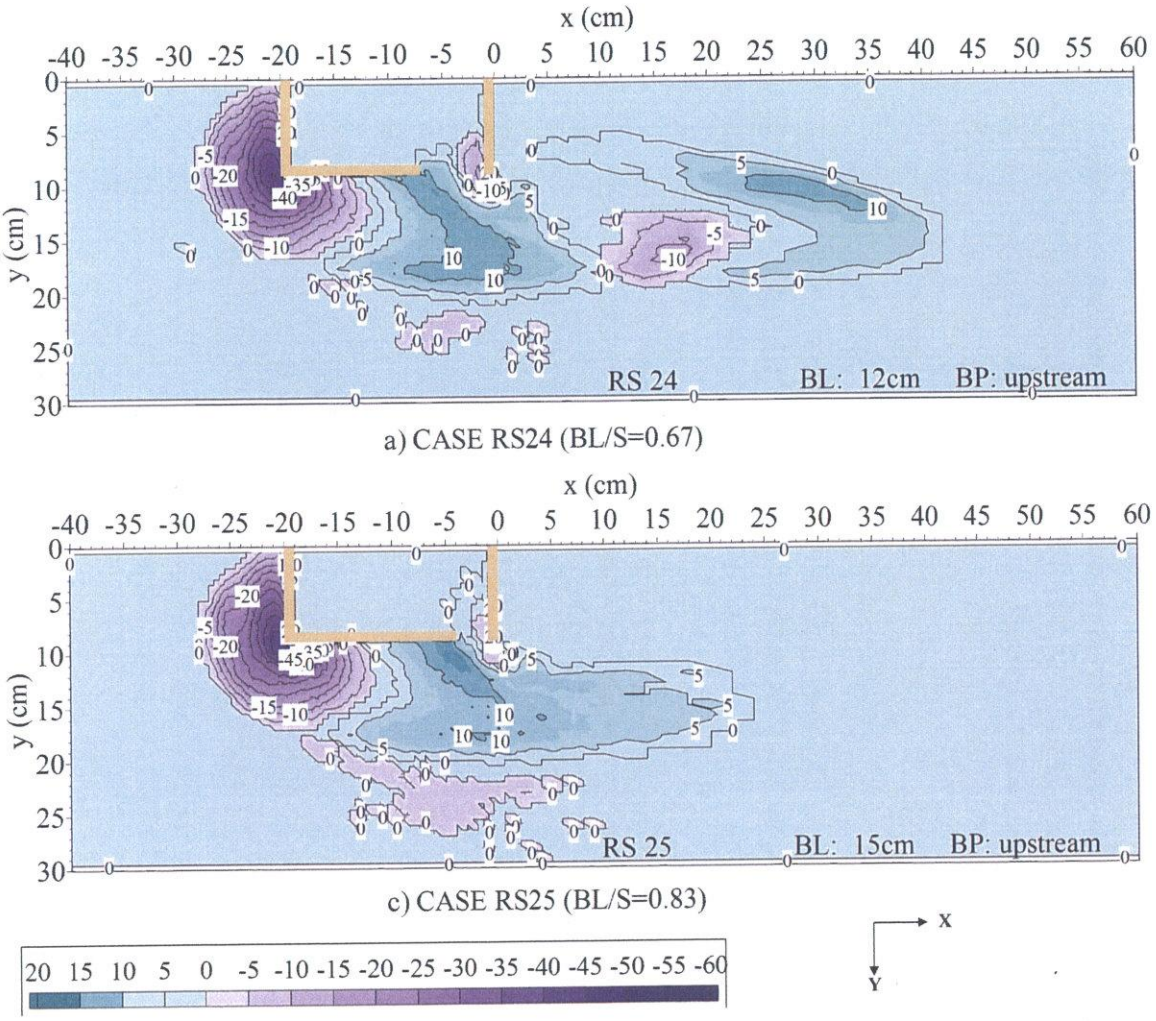

Figure 5.15: Comparison of bed deformation between the submerged box groynes with an upstream longitudinal block (Group RS2) Part 2

5.3.3 The sketch of bed deformation in the case with a downstream longitudinal block (Group RS3)

Fig. 5.16 and 5.17 show the contour of bed deformation for the submerged cases with the longitudinal block set in the downstream side of entrance. The scale of the scour hole also distinctly reduces with the longer longitudinal block when the block length beyond 6cm (BL/GL=0.33) as emerged cases. Beside the scour hole around the first groyne, there are not other holes on the channel bed. According to the comparison of the distribution of vertical velocity on the horizontal plane in the fixed bed (as shown in Fig. 4.17 and 4.18), the cases with a downstream longitudinal block show a weaker downflow around the second

groyne than the case without the longitudinal block. So the scour around the second groyne can not be generated. A mass of sediment deposits in the inner zone when the setting of the downstream longitudinal block keeps an enough space for the HV1 delivering the sediment (as CASE RS31, RS32 and RS33). Meanwhile the longitudinal block successfully reduces the sediment transport from the inner zone to the downstream; hence, their depositions in the inner zone are larger than the case without the longitudinal block.

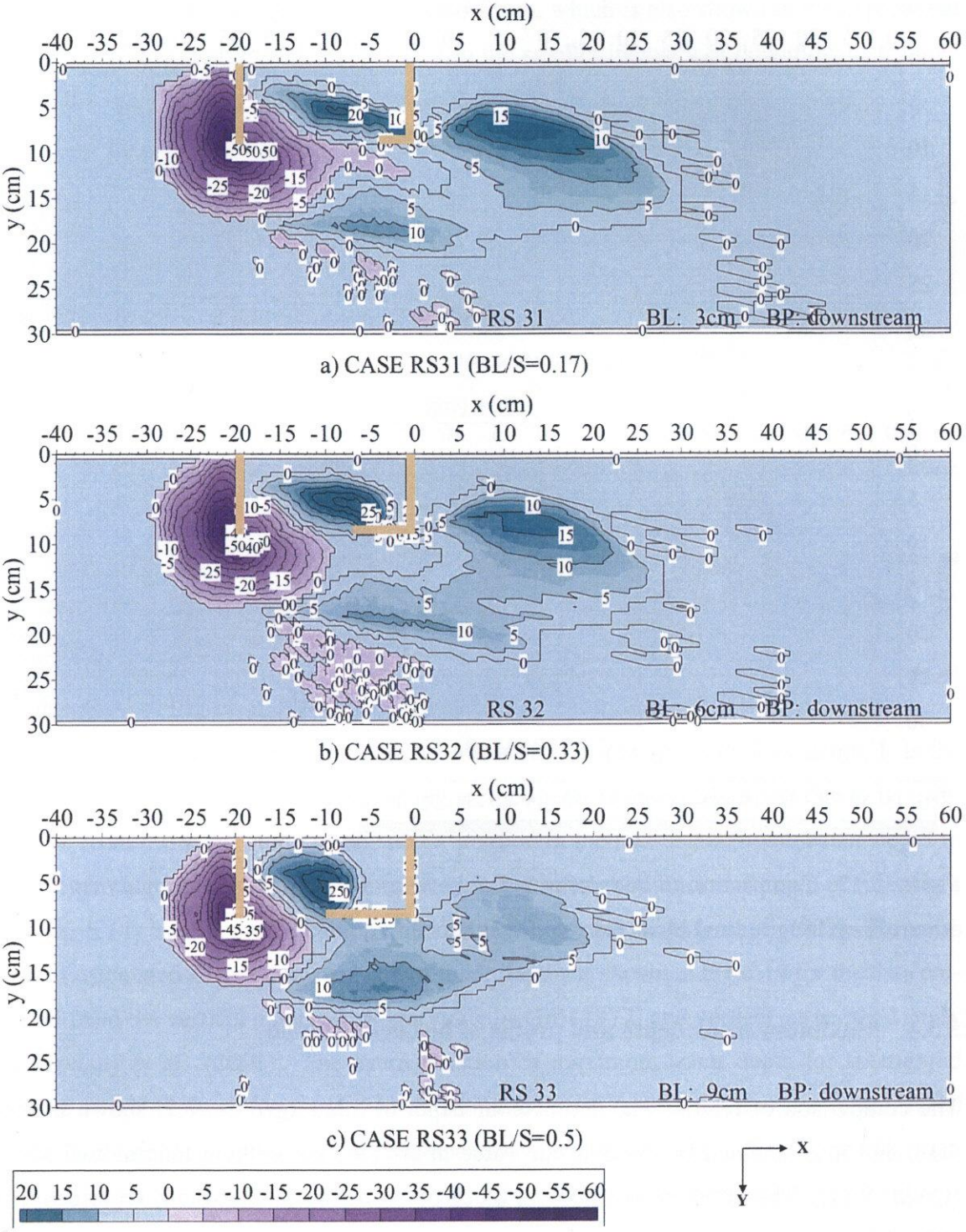

Figure 5.16: Comparison of bed deformation between the submerged box groynes with a downstream longitudinal block (Group RS3) Part 1

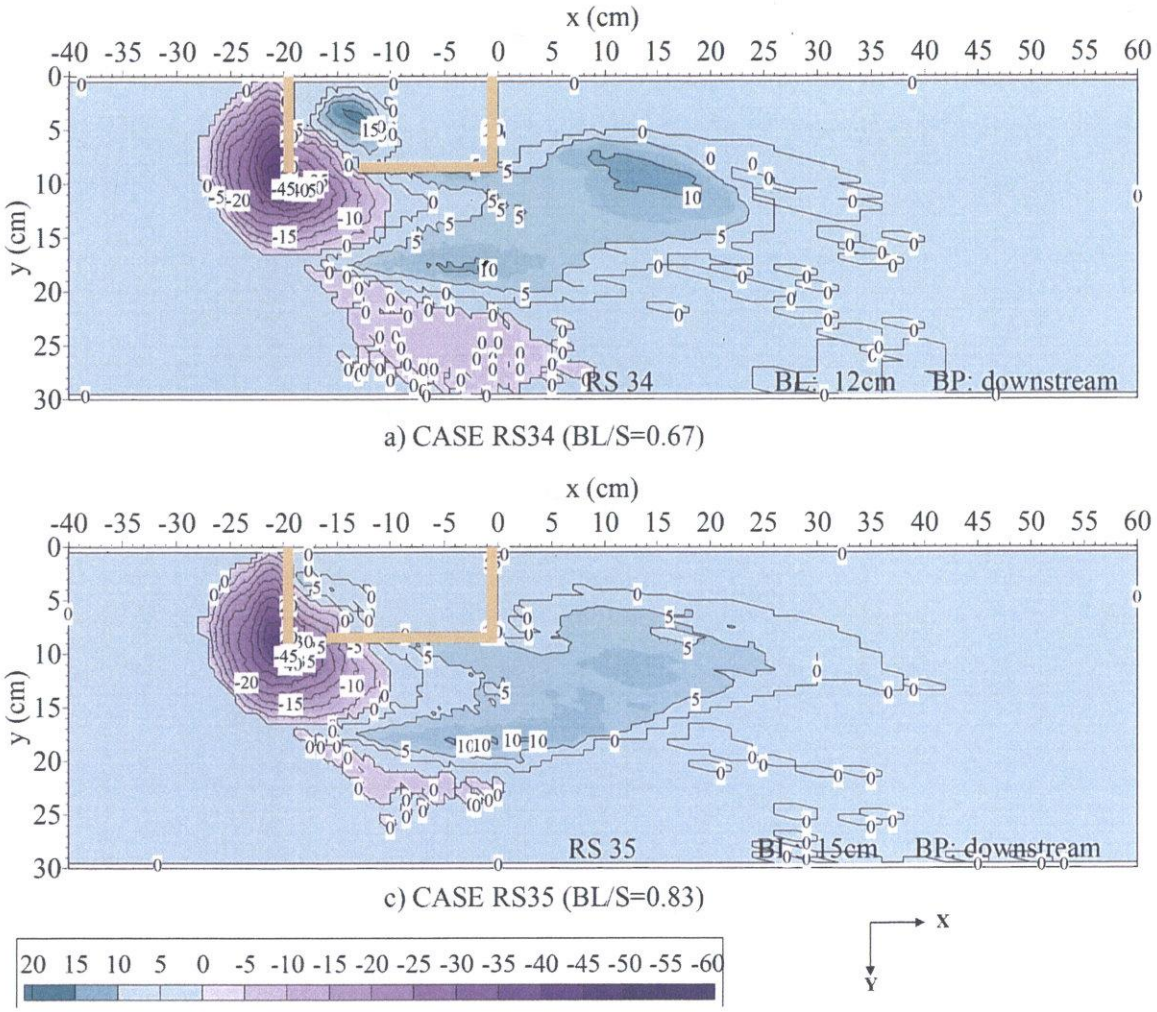

Figure 5.17: Comparison of bed deformation between the submerged box groynes with a downstream longitudinal block (Group RS3) Part 2

5.3.4 Maximum scour depth and profile of bed deformation

The comparison of relative maximum scour depth in submerged cases is shown in Fig. 5.18, and it is obtained by dividing the value under the case without longitudinal block (CASE RS1). The effect of longitudinal block on reduction of maximum scour depth is clear. The maximum reduction of scour depth is attained in CASE RS24 among the cases with an upstream longitudinal block, while it attained in CASE RS33 among the cases with a downstream longitudinal block. It means that the long longitudinal block has no superiority on the reduction of scour under the submerged condition. Compared with the maximum scour depth under the emerged condition, the effect of upstream longitudinal

block is weakened under the submerged condition, which is also shown in the experiment results in Cheng et al. (1994). It is leaded to the smaller intensity of downflow distributed along the longitudinal block.

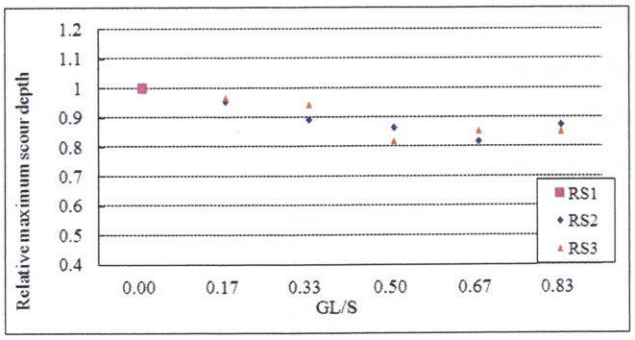

Figure 5.18: Comparison of relative maximum scour depth under the submerged condition

The calculating equation of maximum scour depth based on the abutment studies of Coleman et al. (2003), Melville (1997) and Melville and Coleman (2000) is as follows:

$$d_s = K_{yL} K_I K_d K_s K_\theta K_G K_t \tag{5.1}$$

where the factors are defined in Table 5.1. In here, y is the approach flow depth, L is the abutment length. Whereas this calculating method aims at emerged groyne due to its origination from the scour study of abutment, prediction method of maximum scour depth in submerged groyne is lacking. And overestimation of maximum scour depth occurs when the Eq. 5.1 is used in the calculation of submerged groyne (Kuhnle et al. 1999). The relation of calculated to measured maximum scour depths is shown in Fig.5.19 for the data collected from the vertical emerged groyne study of Gill (1972) and vertical submerged study of Elawady et al. (2001). The overestimation of maximum scour depth for submerged groyne is definitely shown, and the overestimated ratio (ratio of calculated to measured value) is related to groyne length and submergence as shown in Fig. 5.20. In general, more overestimate occurs as the groyne length and submergence ratio increased. Fig. 5.21 shows the relation of calculated to measured maximum scour depths for the data in this study. The emerged box groyne also has overestimation of maximum scour depth and more serious as time going. The maximum scour depth in box groyne cases generally shows smaller value compared with that in single groyne case, due to the weaker development of horseshoe vortex affected by strong positive transverse velocity in the upstream side of entrance and

the higher water level behind the first groyne induced by the second groyne. More overestimation of maximum scour depth occurs in the submerged box groyne and becomes serious as time going due to the effect of submergence and second groyne. The overestimation also induced by the existence of longitudinal block. Less study on estimation of maximum scour depth in the box groyne or groyne group, whereas it is very necessary for its widely application in river engineering practices. In this study, the factor of submerged groyne K_{sub} is introduced to improve the calculating equation, which is based on the study of Elawady et al. (2001). K_{sub} is related to the groyne length and submergence as follows:

$$d_s = K_{yL}K_I K_d K_s K_\theta K_G K_t K_{sub} \tag{5.2}$$

$$K_{sub} = exp[-1.114(\frac{GL}{B})^{0.433}|ln(\frac{GH}{h})|^{2.833(\frac{GL}{B})^{0.662}}] \tag{5.3}$$

Fig. 5.22 shows the relation of improving calculated to measured maximum scour depths for the data of the case without longitudinal block (CASE RE1 and RS1) in this study. But the factors of box groyne need more sediment experiments to determine.

Fig. 5.23 shows the longitudinal profile of bed deformation on the section of y=10cm (y/GL=1.11) under the submerged condition. Fig. 5.24 shows the transverse profile of bed deformation on the section of x=-19.5cm (x/S=-1.08) under the submerged condition. The scour volume is controlled by the arrangement of longitudinal block. As shown in Fig. 5.24 (a), the position of maximum scour depth moves to the downstream when the maximum scour depth is reduced in the cases with an upstream longitudinal block. And the setting of the upstream longitudinal block makes the downstream slope of hole become steep. The long block length makes the deposition mainly distribute in the section of box groyne when the longitudinal block is set in the upstream. And when the longitudinal block is set in the downstream, there is the amount of sediment distributed in the downstream side of box groyne, which is different with the condition in the emerged cases.

Table 5.1: Factors influencing local abutment-scour depth (obtained from Coleman et al. 2003)

Factor (1)	K (2)	Method of Estimation (3)
Flow depth-abutment size	K_{yL}	$K_{yL} = 10y$ $\frac{y}{L} \le 0.04$ $K_{yL} = 2\sqrt{yL}$ $0.04 < \frac{y}{L} \le 1$ $K_{yL} = 2L$ $\frac{y}{L} > 1$
Flow intensity	K_I	For uniform sediments: $d_{50a} \equiv d_{50}$ and $V_a \equiv V_c$ For nonuniform sediments: $d_{50a} = d_{max}/1.8 \approx d_{84}/1.8 = \sigma_g d_{50}/1.8$; and $V_a = 0.8V_{ca}$, where V_{ca} is V_c calculated for d_{50a} $K_I = \frac{V-(V_a-V_c)}{V_c}$ for $[V-(V_a-V_c)]/V_c < 1$ $K_I = 1.0$ for $[V-(V_a-V_c)]/V_c \ge 1$
Sediment size	K_d	$K_d = 1.0$ $\frac{L}{d_{50a}} > 60$
Foundation shape	K_s^*	Shape: Vertical-wall 1.0; Wing-wall 0.75; Spill-through 0.5 : 1 (H : V) 0.6; Spill-through 1 : 1 0.5; Spill-through 1.5 : 1 0.45
	K_s	$K_s = K_s^*$ $\frac{L}{y} \le 10$ $K_s = K_s^* + 0.667(1-K_s^*)\left(0.1\frac{L}{y}-1\right)$ $10 < \frac{L}{y} < 25$ $K_s = 1.0$ $\frac{L}{y} \ge 25$
Foundation alignment	K_θ^*	θ (°): 30, 45, 60, 90, 120, 135, 150 K_θ^*: 0.90, 0.95, 0.98, 1.0, 1.05, 1.07, 1.08
	K_θ	$K_\theta = K_\theta^*$ $\frac{L}{y} \ge 3$ $K_\theta = K_\theta^* + (1-K_\theta^*)\left(1.5-0.5\frac{L}{y}\right)$ $1 < \frac{L}{y} < 3$ $K_\theta = 1.0$ $\frac{L}{y} \le 1$
Approach-channel geometry	K_G	Case A (Figure 8): [Simple rectangular river channel] $K_G \equiv 1.0$ Case C (Figure 8): [Abutment well back from the flood-channel edge] Consider only the flood channel flows of y* and set $K_G = 1.0$ Case B (Figure 8): [Abutment in the main channel] $K_G = \sqrt{1-\left(\frac{L^*}{L}\right)\left[1-\left(\frac{y^*}{y}\right)^{5/3}\left(\frac{n}{n^*}\right)\right]}$ Case D (Figure 8): [Abutment near the flood channel edge] Abutment at about the flood-channel edge: Case B with $L^*/L = 1.0$. Abutment near the flood channel edge but not extending into the main channel: Estimate K_G by interpolating conservatively between estimates for longer (Case B) and shorter (Case C) abutments in the same channel.
Time	K_t	$\frac{t_e V}{L} = 10^6\left(\frac{V}{V_c}\right)^3\left(\frac{y}{L}\right)\left\{3-\left[1.2\left(\frac{y}{L}\right)\right]\right\}$ for $y/L < 1$ and $L/d_{50a} > 60$ $\frac{t_e V}{L} = 1.8\times 10^6\left(\frac{V}{V_c}\right)^3$ for $y/L \ge 1$ and $L/d_{50a} > 60$ $K_t = \exp\left[-0.07\left(\frac{V}{V_c}\right)^{-1}\left\lvert\ln\left(\frac{t}{t_e}\right)\right\rvert^{1.5}\right]$ for $V/V_c < 1$ $K_t = 1.0$ for $V/V_c \ge 1$ (d_s developing rapidly for live-bed conditions)

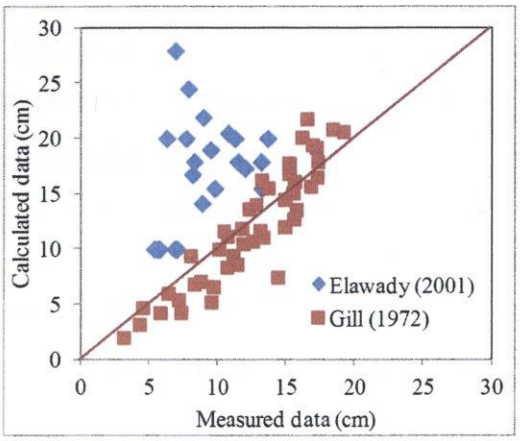

Figure 5.19: Comparison of measured and calculated maximum scour depth using Eq. 5.1 for the data collected by Gill (1972) and Elawady et al. (2001)

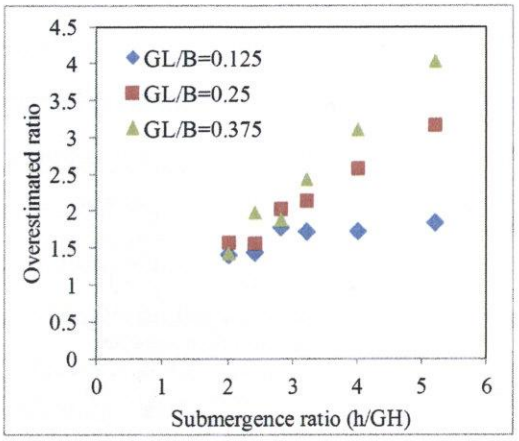

Figure 5.20: omparison of overestimated ratio with different submergence ratio and groyne length for the data collected by Elawady et al. (2001)

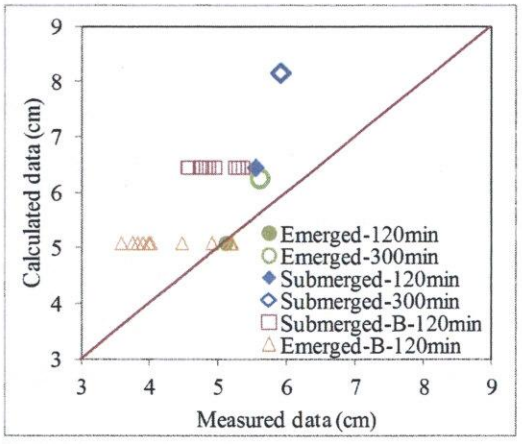

Figure 5.21: Comparison of measured and calculated maximum scour depth using Eq. 5.1 for the data in this study

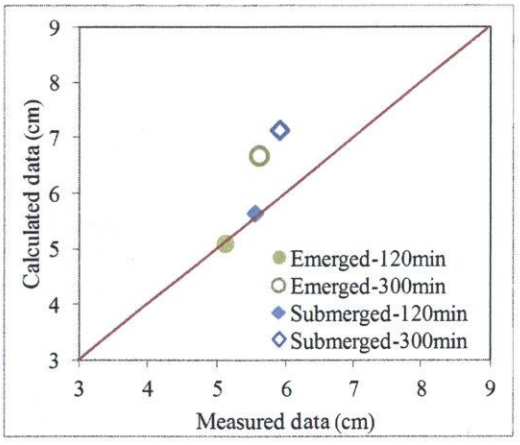

Figure 5.22: Comparison of improving measured and calculated maximum scour depth using Eq. 5.2 for the data in this study (CASE RE1 and RS1)

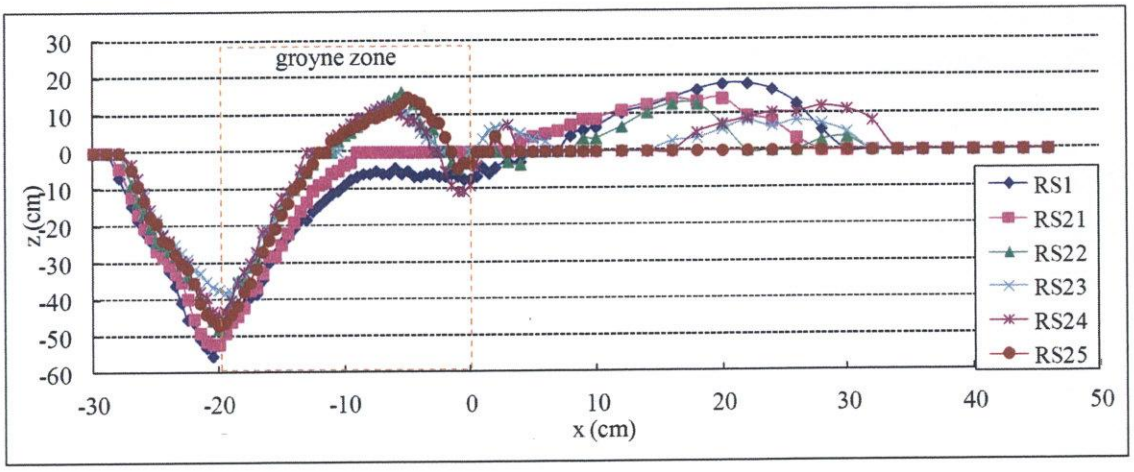

a) Longitudinal block in the upstream side of lateral entrance

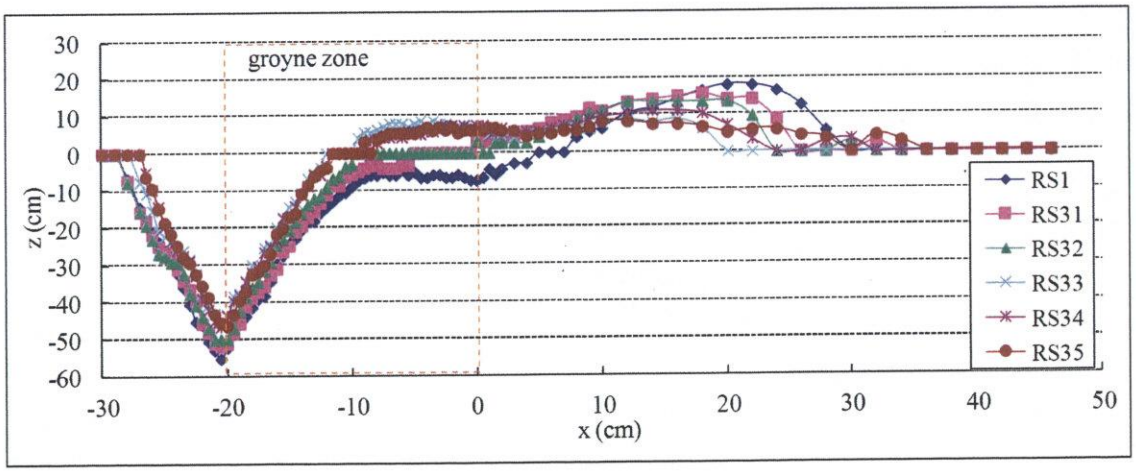

b)) Longitudinal block in the downstream side of lateral entrance

Figure 5.23: Longitudinal profile of bed deformation on the section of y=10cm (y/GL=1.11)under the submerged condition

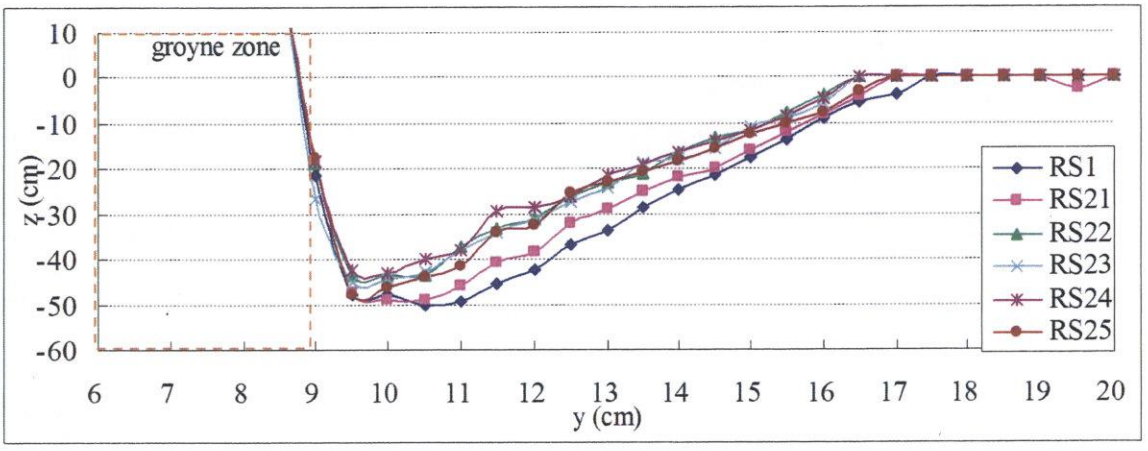

a) Longitudinal block in the upstream side of lateral entrance

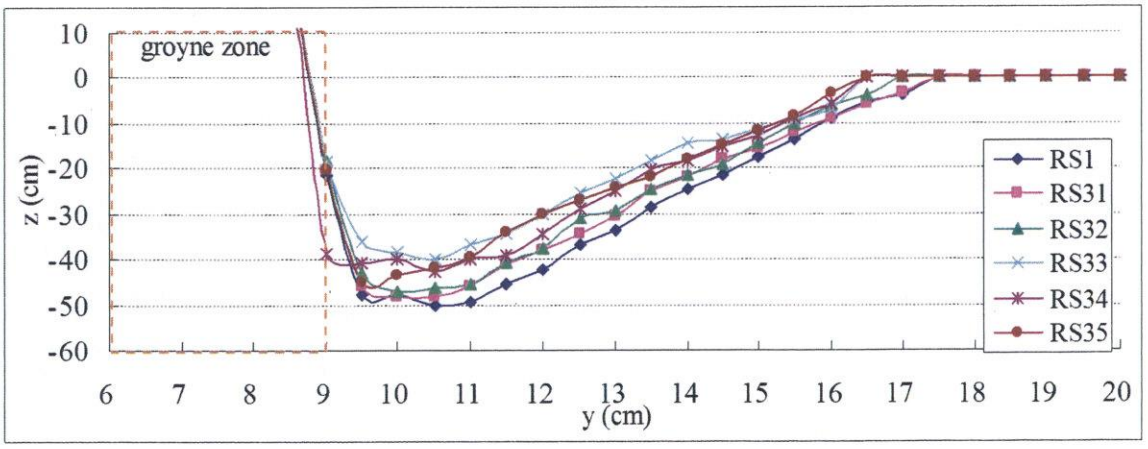

b)) Longitudinal block in the downstream side of lateral entrance

Figure 5.24: Transverse profile of bed deformation on the section of x=-19.5cm (x/S=-1.08)under the submerged condition

5.3.5 Flow structures in the groyne field

The measurement of velocity around the box groyne is conducted in the CASE RS1, RS23 and RS33 to investigate the flow field under the deformation of bed. Fig.5.25 shows the time-averaged velocity vectors U_{uv} on the horizontal plane of z/GH=0.56~0.67 under the submerged condition. Due to the large bed deformation in the groyne section, the flow pattern presents different behaviors and makes the three-dimensional flow in the inner zone become complex. Lots of water in the low level enters the inner zone along the slope of the scour hole and mound of deposition due to the dynamic motion of horseshoe vortex as emerged cases, generating a circulation flow in the transverse section (y-z). It increases the complexity of three-dimensional flow with the other two kinds of circulation flow induced by horizontal mixing layer (HML) and vertical mixing layer (VML) respectively, and makes the flow pattern be sensitive to the bed deformation inside the box groyne. In particular, the inputting flow with high longitudinal velocity around the entrance of CASE RS23 is the same as its flow pattern in the fixed bed, which generates the horseshoe vortex to scour the bed in front of the second groyne. There is a whole gyre generated inside the box groyne of CASE RS33. Although the flow field in the inner zone has different behaviors due to the bed deformation in the groyne zone, the flow pattern in the fixed bed is still able to provide some of the useful information to understanding the formation mechanism of bed deformation, especially for the main channel.

5.4 Summary

This chapter mainly presents the measurement results on the bed deformation and flow structure around the submerged box groyne with longitudinal block in the movable bed. The distribution of bed deformation aroused by the structure of box groyne is described in detail. The formation mechanisms of scour and deposition are discussed compared with the measurement of flow field in the fixed bed. The transport model of sediment to the inner zone is critical to the distribution of deposition relative to the formation of the groyne ecological system. The arrangement of longitudinal block in the lateral entrance directly affects the transportation corridor of sediment to the inner zone. Furthermore, the flow structure changed by the longitudinal block has an indirect impact to the transportation. The flow structures in the inner zone and a part of main stream are measured after bed

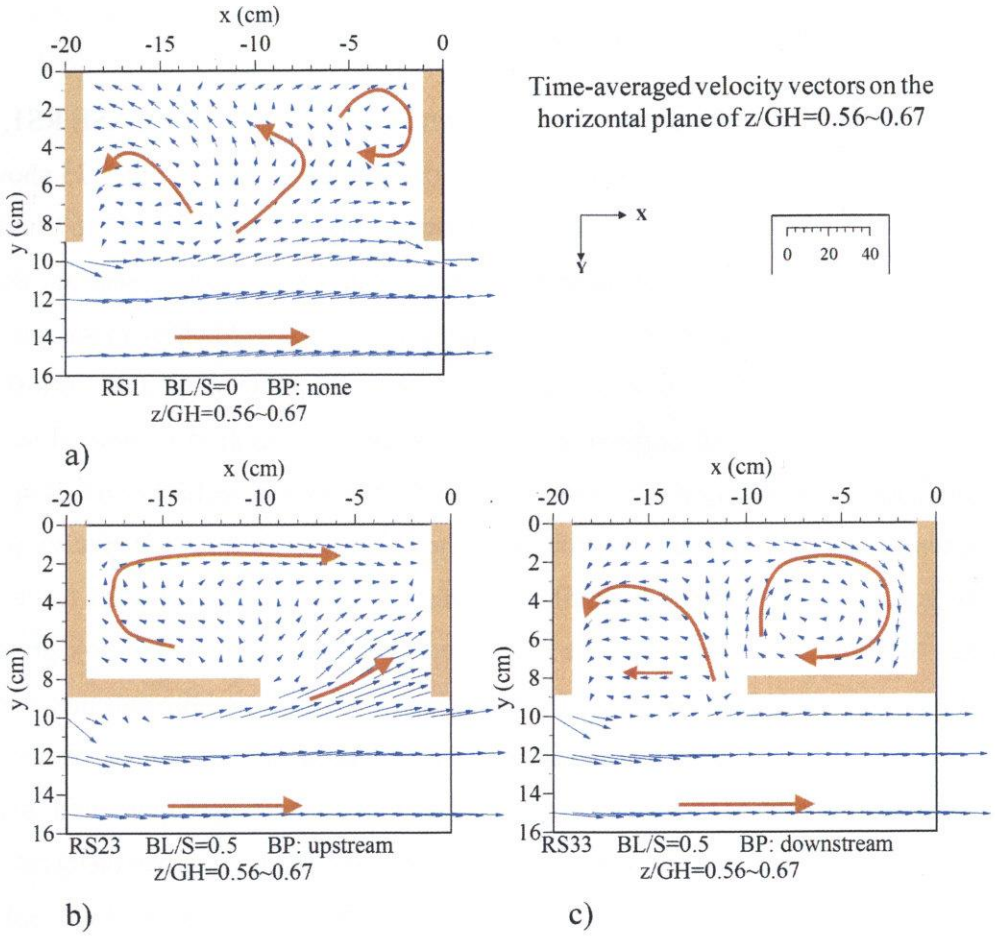

Figure 5.25: Time-averaged velocity vectors U_{uv} on the horizontal plane of z/GH=0.56~0.67 under the submerged condition

deformation. It presents the impact of bed deformation on flow field and provides more evidences to the formation mechanism of deformation in the groyne zone.

The scour hole around the first groyne is mainly induced by that the horseshoe vortex, and its effect mainly realizes by two actions. First dynamic motion occurs between the incoming flow in the upper level and the adverse pressure of the front wall of groyne, generating the horseshoe vortex (HV1) scouring the tip of groyne. Second is that the incoming flow in the near bottom level flows down along the slope of hole, and generates the other horseshoe vortex (HV2) by the adverse pressure from the vertical gyre in the scour hole. These two horseshoe vortices cause the three depositions distributed in the different placements on the bed. One is placed the inner zone or near the longitudinal block, which is mainly contributed by the HV1. The second is placed around the middle of channel, which

is mainly contributed by the combined effect of HV2 and high velocity in the main stream. The third one is placed in the downstream side. It is also contributed by the combined effect of HV2 and high velocity in the main stream. And the mobile sediment induced by the HV1 is carried from the inner zone to downstream side, and also has a contribution to the third part of deposition.

The setting of the upstream longitudinal block has an efficient effect on the reduction of the scour hole, mainly caused by the restrictions on the development of horseshoe vortex. The restriction reflects in the two aspects. The longitudinal block in the upstream side reduces the motion space of the horseshoe structure in the upstream section of box groyne, and the reverse flow with positive vertical velocity in the shielding field shown in the flow pattern in the fixed bed restrains the development of horseshoe vortex and the transportation of sediment to the downstream by horseshoe vortex. And the long longitudinal block on the downstream side also has a reduced effect on scour hole around the first groyne because of the same reasons. Under the emerged condition, the setting of the upstream longitudinal block causes the fewer depositions in the inner zone, while the appropriate length of the downstream longitudinal block is beneficial for the sediment deposit in the inner zone. The smaller scour hole behind the first groyne is due to the weaker horseshoe effect and the lower transverse velocity in the upstream of entrance for emerged cases with a downstream longitudinal block. The scour hole in front of the second groyne is observed in the most emerged cases with an upstream longitudinal block, which is induced by the strong vortex structure inputting to the inner zone. Under the submerged condition, there also has a scour hole in front of the second groyne for the cases with an upstream longitudinal block. Its formation mechanism is that, the inputting fluid flows toward the wall of second groyne and forms a horseshoe vortex by the adverse pressure of wall as what happens in the upstream of first groyne. For submerged cases with an upstream longitudinal block, the strong downflow in the main stream causes a new scour in the main channel when it unites the high flow in the main stream. And the scour hole extends to the downstream side with the increasing length of longitudinal block. The sediment deposited in the inner zone is largely reduced by setting the long longitudinal block in the upstream side, while it increases when the length of the downstream longitudinal block is equal or less than 0.5S under the submerged condition. The maximum scour depth generally decreases as the length of the downstream longitudinal block adds when the box groyne is emerged. And the longitudinal block set

in the upstream has a great effect on reducing the maximum scour depth. But when box groyne becomes submerged, the long longitudinal block has no superiority on the reduction of scour and the effect of upstream longitudinal block is weakened. The flow field in the inner zone has different behaviors due to the bed deformation around the groyne section. But the flow pattern in the fixed bed is still able to provide some of the useful information to the understanding of bed deformation.

The calculation method of maximum scour depth based on the scour study of abutment is introduced to estimate maximum scour depth and compare with measured value for box groyne. The emerged box groyne has overestimation of maximum scour depth and more serious as time going due to the existence of second groyne. More overestimation of maximum scour depth occurs in the submerged box groyne and becomes serious as time going due to the effect of submergence and second groyne.

In general, the arrangement of longitudinal block has a great impact on the distribution of bed deformation. The different distribution of scour and deposition in the inner zone of box groyne induced by the longitudinal block is able to provide flexible habitats for aquatic life.

Chapter 6

Conclusions and Recommendations

6.1 Conclusions

The effect of longitudinal block set in the lateral entrance on the box groyne is concerned in this study from the investigations on flow characteristics and bed deformation. The laboratory experiments are both conducted in the fixed bed and movable bed, to explore realization of a miniature aquatic system by the adequate configuration of longitudinal block. Although there are many different types of box groyne, the object of this study mainly is focused on the box groyne with lateral longitudinal block composed by straight and L-shape groyne, which is used in many engineering practices. The flow characteristics and bed deformation with three-dimensional characteristics around box groyne is investigated both under the emerged and submerged condition.

The main work during this study is summarized as follows:

(1) Under the same spacing of box groyne, the effects of different configurations of longitudinal block are discussed by measurement of flow field in the fixed bed under the emerged condition. The longitudinal block is configured in the upstream side and downstream side of the lateral entrance with different block length. The measurement technology of Particle Image Velocimetry (PIV) is used to explore the flow field and mass exchange process by analyzing its instantaneous velocity vectors. The Dye Concentration Measurement (DCM) provides a distinct and visual method to present the development of vortex structure in the mixing layer and its effects on the mass exchange between the inner zone of the emerged box groyne and the main stream.

(2) The calculation methods of exchange coefficient obtained by the PIV and DCM experiment are both modified to adapt the emerged box groyne cases in this study and work well.

(3) Under the submerged condition in the fixed bed, the three-dimensional flow around the box groyne is described in detail from the flow field measured by Particle Image Velocimetry (PIV). The effect of longitudinal block with different length and position as the emerged condition are also discussed.

(4) This thesis also studies on the box groyne with different spacing from the measured data of Particle Image Velocimetry (PIV) in the fixed bed. Both emerged and submerged conditions are taken into account. The longitudinal block with the same ratio of block length also is an important aspect in discussion when it's set in the different side of lateral entrance.

(5) The sediment experiment and velocity measurement in the movable are conducted in the box groyne. The block length and position are the main factors in the comparison between the configurations of longitudinal block. The flow characteristics obtained by the experiment of fixed bed is helping to reveal the formation mechanism of bed deformation with the measured flow field after bed deformation in the movable bed.

The conclusions of this study are summarized as follows:

(1) Flow characteristics change greatly when varying the placement and length of the longitudinal block in the emerged box groyne with fixed bed. The setting of the longitudinal block makes the area of high longitudinal velocity in the main stream to move closer to the groyne zone comparing with that in the case without the longitudinal block. It also reduces the area of vertical velocity around the tip of first groyne, which benefits the reduction of scouring. The longitudinal block placed in the upstream side of entrance causes weaker driving gyre, smaller mean velocity in the inner zone and stronger velocity fluctuation with longer length and enhances the turbulence motion. As the length of longitudinal block is added from 3cm (CACE RE21) to 6cm (CASE RE22), the area with high turbulence in main stream enlargers, but turbulent motion inside the box groyne weakens. When the length keeps increasing, the area with high turbulence in main stream reduces but is still larger than the area in the case without the longitudinal block. Setting the longitudinal block in the downstream side of entrance promotes the development of secondary gyre greatly, meanwhile, the driving gyre moves toward the outside with reduced dominated area when the block turns longer, and it reduces mean velocity and turbulence inside the box

groyne. Generally, the setting of longitudinal block has the effect of enhancing the velocity intensity at the entrance by narrowing the entrance. The upstream setting of longitudinal block essentially promotes the development of vortex by reducing the energy diffusion with the fluid from the inner zone of box groyne in the upstream of mixing layer, so as to benefit the mass and momentum exchange around the entrance by increasing the turbulent flow in the downstream side of entrance. Meanwhile, the existence of the longitudinal block reduces the size of the interface between the box groyne and the main stream to weak the exchange process at the entrance.

(2) The different configurations of longitudinal block in length and position also largely affects the flow structure around the submerged box groyne in the fixed bed, creating the abundant environment for the aquatic life. The vertical mixing layer (VML) on the lateral side is sensitive to the longitudinal block set in the lateral entrance, which brings large change to the horizontal flow pattern in the inner zone. But the change of flow pattern inside the submerged box groyne also affects the horizontal mixing layer. So the longitudinal block also has an indirect effect on the horizontal mixing process. The setting of longitudinal block clearly improves the three-dimensionality of flow and diversifies the circulation flow in the submerged groyne zone, benefiting the demanding of various aquatic animals. The mean velocity in the groyne zone of most cases with a downstream longitudinal block increases, while it of cases with an upstream longitudinal block decreases. And the value of mean velocity is increased with the longer length of the downstream longitudinal block. The relatively low mean velocity in the groyne zone in the case with an upstream block can provide a good shelter for the aquatic animal during the flood season. Under the submerged condition, the mean velocity in the cases with longitudinal block is approaching the value of the case without longitudinal block. These two phenomena reveal the fact that the horizontal mixing effect contributes more extensively to the water inputs under the submerged condition. The distribution of longitudinal turbulence in the main stream is related to the mixing layer. Under the submerged condition, the vertical mixing layer moves toward the submerged box groyne, and the arc shape of area has larger curvature than that in emerged case. It means more vortex structures have the opportunity to enter the inner zone of the submerged box groyne. Under the submerged condition, the distribution of turbulence intensity in the main stream has a great relationship with the mass exchange process in the

lateral side and the distribution of downflow in the main stream. The combined action of these two factors dominates the turbulence intensity in the main stream. The energy diffusion in the vertical mixing layer is increased by the downflow from the top of first groyne under the submerged condition. When the longitudinal block is set in the upstream side, the stronger downflow is generated by the effect of upstream longitudinal block, and it promotes the energy diffusion in the vertical mixing layer. When the longitudinal block is set in the downstream side, the stronger outflow from the inner zone also promotes the energy diffusion in the upstream of the vertical mixing layer. As for the lateral interface, the longitudinal block totally controls the water exchange between the submerged box groyne and main stream, but it also significantly affects the water exchange process in the roof interface in front of the second groyne. The exchange process is promoted by the upstream longitudinal block and downstream longitudinal block under moderate length. The longitudinal block set in the downstream has an ability of attracting inflow from the roof boundary and it is enhanced by the longer block.

(3) Narrow or widen the spacing of box groyne also lead to the change of flow structure and mass exchange between the box groyne and main channel both under the emerged and submerged condition. When the box groyne is emerged, the mean velocity in the inner zone increases with decreasing slope as adding the spacing of box groyne whether there is longitudinal block or not. With the spacing increasing, the velocity reduction becomes larger when the longitudinal block is set in the upstream side of entrance, while it becomes smaller when the longitudinal block is set in the downstream side of entrance. The case without the longitudinal block has the strongest exchange ability, while the case with the downstream longitudinal block has the weakest. And the he exchange coefficient in the case with 18cm spacing (S/GL=2) is highest. In particular, for the case without the longitudinal block under 12cm spacing (S/GL=1.33) (CASE RE1-12), two-parallel-gyre system is generated like the driving gyre locates the entrance area along with the parallel secondary gyre. Lowering the spacing of box groyne makes the vortex structure develop insufficiently when it gets the downstream of entrance. Hence, the less vortex structure enters into the inner zone when the second groyne places around the top of the arc curve of mixing layer. When the spacing is long, although sufficiently developed large coherent structure delivers the amount of water to the inner zone from the downstream side of entrance, the intensity of vortex structure

is reduced by the energy diffusion in the long mixing layer. In general, the theory about the effect of different lengths and positions of the longitudinal block on the flow characteristics works when the spacing of box groyne is equal to or larger than 2 times of groyne length without oversize. When the box groyne becomes submerged, the combined effects of the vertical mixing layer (VML) and horizontal mixing layer (HML) on the groyne system brings some brand-new features to the flow characteristics around the box groyne. The mean velocity in the inner zone and the three-dimensionality reduces as adding the spacing of submerged box groyne under most conditions. The setting of longitudinal block has a slight impact to the mean velocity under the 24 cm spacing (S/GL=2.67). Different with the emerged case, the submerged box groyne with small spacing (S/GL=1.33) receives more energy input both from the vertical mixing layer and horizontal mixing layer. The setting of longitudinal block generally has the similar effect on the flow pattern in the cases with different spacing, especially in the cases with 2GL and 2.67GL spacing. For example, the longitudinal block in the upstream increases the resistance of entering the inner zone in front of the second groyne while the longitudinal block in the downstream decreases it.

(4) There are two useful methods evaluating the exchange ability of the emerged box groyne, which are based on PIV and DCM respectively. But they still have some weaknesses to make an overall evaluation for the box groyne in this study. Hence the estimation equations of water exchange coefficient obtained by PIV and DCM methods are modified to suitable for the box groyne with a several gyres system and arc shape of mixing layer respectively, and has fairly good applicability. According to the results obtained by modified method, it can get some findings about the exchange ability of the whole box groyne. Generally, with block length increasing, the exchange process becomes slower. Under the same longitudinal block length condition, the cases with downstream longitudinal block display lower the exchange ability. The cases with the short longitudinal block (RE21, RE22) in the upstream present a higher exchange ability than the case without longitudinal block, to further clarify the effect of the short block placed in the upstream side on the enhancement of interchange mechanism.

(5) The scour hole around the first groyne is concerned in this study due to its threat to the safety of groyne structure. The setting of the upstream longitudinal block has an efficient effect on the reduction of the scour hole, mainly caused by the restrictions of

the development of horseshoe vortex. The restrictions reflect on the two aspects. The longitudinal block in the upstream side reduces the motion space of the horseshoe structure in the upstream section of box groyne, and the reverse flow with positive vertical velocity in the shielding field restrains the development of horseshoe vortex and the transportation of sediment to the downstream by horseshoe vortex. And the long longitudinal block in the downstream side also has a reduction effect on scour hole around the first groyne because of the same reasons. The maximum scour depth generally decreases as the length of the downstream longitudinal block adds when the box groyne is emerged. And the longitudinal block set in the upstream has a great effect on reducing the maximum scour depth. But when box groyne becomes submerged, the long longitudinal block has no superiority on the reduction of scour and the effect of upstream longitudinal block is weakened.

(6) Beside the reduction effect of longitudinal block on scour hole around the first groyne, there also are many other interesting characteristics carried by different configurations of longitudinal block. Under the emerged condition, the setting of the upstream longitudinal block causes the fewer depositions in the inner zone, while the appropriate length of the downstream longitudinal block is beneficial for the sediment deposit in the inner zone. The smaller scour hole behind the first groyne is due to the weaker horseshoe effect and the lower transverse velocity in the upstream of entrance for emerged cases with a downstream longitudinal block. The scour hole in front of the second groyne is observed in the most emerged cases with an upstream longitudinal block, which is induced by the strong vortex structure inputting to the inner zone. Under the submerged condition, there also has a scour hole in front of the second groyne for the cases with an upstream longitudinal block. Its formation mechanism is that, the inputting fluid flows toward the wall of second groyne and forms the horseshoe vortex by the adverse pressure of wall as what happens in the upstream of first groyne. For submerged cases with an upstream longitudinal block, the strong downflow in the main stream causes a new scour in the main channel when it unites the high flow in the main stream. And the scour hole extends to the downstream side with the increasing length of longitudinal block. The sediment deposited in the inner zone is largely reduced by setting the long longitudinal block in the upstream side, while it increases when the length of the downstream longitudinal block is equal or less than 0.5S under the submerged condition. The flow field in the inner zone has different behaviors due

to the bed deformation around the groyne section. But the flow pattern in the fixed bed is still able to provide some of the useful information to the understanding of bed deformation.

6.2 Recommendations

The investigation of the flow characteristics and local scour around the kinds of box groyne in this study is mainly for the realization of ecological box groyne by the adequate configuration of longitudinal block. According to the discussion in this study, some recommendations are raised as follows:

(1) The traditional box groyne has a monotony flow pattern and high velocity inside the groyne zone, and thus it can not provide a good ecological environment for the aquatic life. The setting of the longitudinal block in the lateral side of box groyne creates a rich environment with a diversified gyre system and strong three-dimensional flow, and the dead water zone behind the longitudinal block is a good shelter area for aquatic animal and a deposition placement for growth of aquatic plant. And its restrictive effect on scour process around the first groyne is also an important advantage for groyne protection. In general, the setting of the longitudinal block in the lateral side of box groyne is able to provide a suitable habitat for aquatic life.

(2) Both under the emerged and submerged condition, the mean velocity in the inner zone of box groyne with the longitudinal block set in the upstream of lateral entrance is smaller than the case without the longitudinal block. And its strong exchange ability and turbulence motion around the entrance is able to keep supplying the fresh water to the inner zone. Its effect on the reduction of the scour hole also presents well, especially under the emerged condition. When the block length is between 0.33~0.67S, the box groyne work efficiently. In particular, the case with 0.5S block length presents outstanding due to its highest exchange ability, rich circulation flow, enough dead water zone behind the longitudinal block, and it is very suitable habitat and shelter during flood season for aquatic animal.

(3) The longitudinal block set in the downstream side of the lateral entrance has some same function as the condition with upstream longitudinal block. It also benefits the deposition in the inner zone. In particular, when the block length is between 0.33~0.67S, the amount of sediment deposits in the large area of the inner zone behind the longitudinal block, and their dead water zones distribute very small velocity. These characteristics mean that they are able to provide aquatic plant a good growth environment. And the large scour hole in the inner zone water satisfies the water depth condition for some aquatic animals.

(4) The spacing of box groyne is an important design parameter. The spacing ratio S/GL picked in the study is 1.33 to 2.67. Although smaller spacing also is able to create a diversified environment with low mean velocity under the emerged condition, the low exchange ability and small groyne field is not suitable. The configurations of longitudinal block play roughly the same effect between the box groyne with 2GL and 2.67GL spacing. Although the box groynes with different spacing are able to create a diversified environment for the ecological purpose by the configurations of longitudinal block, the box groyne with S/GL=2 spacing still is the best choice. Because it has the high exchange ability to maintain a healthy ecological environment, and it can keep moderate velocity in the inner zone both under the emerged and submerged condition.

(5) Due to the variation in discharge of river, the box groyne in some river can not keep one flow condition all the time. It is emerged under normal condition, and then become submerged when the flooding season comes. The flow structure of the submerged box groyne with longitudinal block is largely different with that of emerged case. And the difference between the effects of longitudinal block on the emerged box groyne and submerged box groyne still exists. The selection of longitudinal block with overall consideration about these two flow conditions is necessary.

References

[1] Gill M. A. Erosion of sand beds around spur dikes. *Journal of Hydraulics Division, ASCE*, 98(9):1587–1602, 1972.

[2] Kadota A. et al. Instantaneous-advective structures of large scale coherent vortices around a single groyne. In *Advances in Water Resources and Hydraulic Engineering*, pages 1137–1142, 2009.

[3] Kadota A. and Suzuki K. Flow visualization of mean and coherent flow structures around T-type and L-type groynes. In *River Flow 2010*, pages 203–210, 2010.

[4] Kadota A. and Suzuki K. Local sour and development of sand wave around T-type and L-type groynes. In *International Conference on Scour and Erosion 2010*, pages 707–714, 2010.

[5] Mccoy A., Constantinescu S.G., and Weber L. Coherent structures and mass exchange processes in channel flow with spanwise obstructions. In *ERCOFTAC International Symposium on Enginnering Turbulence Modeling and Measurement, Sardinia, Italy*, 2005.

[6] Mccoy A., Constantinescu S.G., and Weber L. Exchange processes in a channel with two emerged groynes. *Flow Turbulence Combustion*, 77:97–126, 2006.

[7] Tominaga A. and Matsumoto D. Diverse riverbed figuration by using skew spur-dike groups. In *River Flow 2006, Lisbon, Portugal*, pages 421–427, 2006.

[8] Tominaga A., Ijima K., and Nakano Y. Flow structures around submerged spur dikes with various relative height. In *Pro. of 29th IAHR Congress, Beijing, China*, pages 421–427, 2001.

[9] Mansoori A.R. et al. Three-dimensional features of the turbulent flow around series of groynes with different shapes of head. *Journal of Japan Society of Civil Engineers B1(hydraulic Enigeering)*, 68(4):61–66, 2012.

[10] Mccoy A.W. *Numerical investigations using LES: exploring flow physis and mass exchange processes near groyne*. PhD thesis, University of Iowa, USA, 2006.

[11] Melville B.W. Pier and abutment scour:integrated approach. *Journal of Hydraulic Engineering, ASCE*, 123(2):125–136, 1997.

[12] Melville B.W. and Coleman S.E. *Bridge scour*. Water Resources Publications, LLC, 2000.

[13] Melville B.W. and Chiew Y.M. Time scale for local scour at bridge piers. *Journal of Hydraulic Engineering, ASCE*, 125(1):59–56, 1999.

[14] Inglis C.C. *The behaviour and control of rivers and canals.* C.W.I.N.R.S. poona, Res. Pub., 1994.

[15] Cheng C.H., Liu J.X., and Xu G.X. Characteristics of flow exerted by hooked groin. *Journal of Chongqing Jiaotong Institute*, 13(1):58–69, 1994.

[16] Liu J.X. Cheng C.H. Characteristics of scour-deposition around hooked spur-dike. *Journal of Chongqing Jiaotong Institute*, 13(3):75–82, 1994.

[17] Shields F. D., Knight S. S., and Cooper C. M. Rehabilitation of aquatic habitats in warmwater streams damaged by channel incision. In *in Mississippi. Hydrobiologia*, 1998.

[18] Ahmad D.A. et al. Temporal evolution of scouring around a series of L-head groynes. In *Proc. of 33rd IAHR Congress*, pages 2207–221, 2009.

[19] Elawady E., Michiue M., and Hinokidani O. Experimental study of flow behavior around submerged spur-dike on rigid bed. *Annual Journal of Hydraulic Engineering,JSCE*, 44:539–544, 2000.

[20] Elawady E., Michiue M., and Hinokidani O. Movable bed scour around submerged spur-dikes. *Annual Journal of Hydraulic Engineering,JSCE*, 45:373–378, 2001.

[21] Chen F. and Ikeda S. Experimental study on horizontal separetion eddies in open-channel flow with groins. *Annual Journal of Hydraulic Engineering, JSCE*, 40:787–792 (in Japanese), 1996.

[22] Duan J. G. Mean flow and turbulence around a laboratory spur dike. *Journal of Hydraulic Engineering, ASCE*, 135(10):803–811, 2009.

[23] Zhang H. *Study on flow and bed evolution in channels with spur dikes.* PhD thesis, Kyoto University, 2005.

[24] Zhang H. and Nakagawa H. Scour around spur dike: Reccent advances and future researches. *Annuals of Disaster Prevention Research Institute, Kyoto University*, 51(B):663–652, 2008.

[25] Schlosser I.J. Aconceptual framework for fish communities in small warmwater streams.community and evolutionary ecology of North American stream fishes. W.J. Matthews and D.C. Heins, eds. pages 17–24. University of Oklahoma Press, Norman , Okla., 1987.

[26] Liu J., Tominaga A., and Nagao M. Numerical simulation of the flow around the spur dikes with certain configuration and angles with bank. *Joural of Hydroscience and Hydraulic Engineering*, 12(2):85–100, 1994.

[27] Tominaga A.and Jong J. Effects of conjunction channel on water exchange in riverside embayment. *Journal of Hydro-environment Research*, 4:163–173, 2008.

[28] Weiss J. The dynamics of enstrophy transfer in two-dimensional hydrodynamics. *Physica*, D48:273–294, 1991.

[29] Weiss J.B. Vortex statistics from eulerian and lagrangian time series. *Physical Review Letters*, 89:284501, 2002.

[30] Shields F. D. JR., Cooper C.M., and Knight S.S. Experiment in stream restoration. *Journal of Hydraulic Engineering, ASCE*, 121(6):494–502, 1995.

[31] Kern K. *Chapter 20:rehabilitation of stream in south west germany. River Conservation and Management.* John Wiley and Sons, 1992.

[32] Thiemann K., Yossef F.M.M, and Barkdoll B. A laboratory study of the effects of groyne height on sediment behavior in rivers. In *Conference Proceeding Of World Water and Environmental Resources Congress 2005, ASCE*, pages 590–601, 2005.

[33] Ghodsian M.and Vaghefi M. Experimental study on scour and flow field in a scour hole around a T-shape spur dike in a 90^o bend. *International Journal of Sediment Research*, 24(2):145–158, 2009.

[34] Kurzke M., Weitbrecht V., and Jirka H.G. Laboratory concentration measurements for determination of mass exchange between groyne fields and main stream. In *River Flow 2002, Balkema*, pages 369–376, 2002.

[35] Raffel M. et al. *Particle Image Velocimetry: A Practical Guide, publisher = Springer, year = 2007.*

[36] Vaghefi M., Ghodsian M., and Neyshabouri A.A.A.S. Experimental study on scour around a T-Shaped spur dike in a channel bend. *Journal of Hydraulic Engineering, ASCE*, 138(5):471–474, 2012.

[37] Yaeger M. and Duan J.G. Mean flow and turbulence around two series of experimental dike. In *Proc. of World Environmental and Water Resources Congresss 2010*, pages 1114–1121, 2010.

[38] Yossef M.F.M. and Vriend H.J. Flow details near river groynes: experimental investigation. *Journal of Hydraulic Engineering, ASCE*, 137(5):504–516, 2011.

[39] Walter M.L., Howard E.C., and Warren J.M. Missouri river design study-Report on laboratory investigation of (l-head) river control structures. U. S. ARMY ENGINEER DISTRICT, 1964.

[40] Rajaratnam N. and Nwachukwu B.A. Flow near groin-like structures. *Journal of Hydraulic Engineering, ASCE*, 109(3):463–480, 1983.

[41] Rajaratnum N. and Nwachukwu B.A. Flow near groin-like structures. *Journal of Hydraulic Engineering, ASCE*, 109(3):463–480, 1983.

[42] Klingeman p.C., Kehe s.M., and Owusu Y.A. Missouri river design study-Report on laboratory investigation of (l-head) river control structures. Oregon State University, Water Resources Research Institute, Corvallis, Oregon, USA, 1984.

[43] Ying Q. and Jiao Z.B. *Groin Hydraulics*. China Ocean Press, 2004.

[44] Ettema R. and Muste M. Scale effects in flume experiments on flow around a spur dike in flatbed channel. *Journal of Hydraulic Engineering, ASCE*, 130(7):635–646, 2004.

[45] Kuhnle R.A., Alonso C., and Shields F. Geometry of scour holes associated with 90^o spur dikes. *Journal of Hydraulic Engineering,ASCE*, 125(9):972–978, 1999.

[46] Kuhnle R.A., Alonso C., and Shields F. Local scour associated with angled spur dikes. *Journal of Hydraulic Engineering,ASCE*, 128(12):1087–1093, 2002.

[47] Kuhnle R.A. and Alonso C.and Shields F. Geometry of scour holes around spur dikes, an experimental study. In *Proceedings of the Conference on Management of Landscapes Disturbed by Channel Incision*, pages 283–287, 1997.

[48] Kuhnle R.A., Jia Y.F., and Alonso C.V. Measured and simulated flow near a submerged spur dike. *Journal of Hydraulic Engineering, ASCE*, 1348(7):916–924, 2008.

[49] Copeland R.R. Bank protection techniques using spur dikes. Hydrulics Laboratory, U.S. Army Engineers Waterways Experiment Station;Vicksburg, Mississippl, 1983.

[50] Shields F. D. JR.and Milhous R.T. Sedimentation and aquatic habitat in river system, asce task committee on sediment transport and aquatic habitat. *Journal of Hydraulic Engineering, ASCE*, 118(5):669–687, 1992.

[51] Ouillon S. and Dartus D. Three-dimensional computation of flow around a groyne. *Journal of Hydraulic Engineering, ASCE*, 123(11):962–970, 1997.

[52] Sobhan S.A. and Das S.K. Spacing of straight spurs in series. *Journal of Civil Engineering*, 27(2):175–181, 1999.

[53] Coleman S.E., Lauchlan C.S., and Melville B.W. Clear-water scour development at bridge abutments. *Journal of Hydraulic Research, IAHR*, 41(5):521–531, 2003.

[54] Molls T., Chaudhry M.H., and KHAN k.W. Numerical simulation of two-dimensional flwo near a spur dike. *Advances in Water Resources*, 18(4):227–236, 1995.

[55] Ohmoto T., Hirakawa R., and Koreeda N. Effects of water surface oscillation on turbulent flow in an open channel with a series of spur dikes. In *Pro. of Hydraulic Measurements and Experimental Methods 2002*, pages 108–117, 2002.

[56] Weitbrecht V., Kuhn G., and Jirka G.H. Large scale piv-measurements at the surface of shallow water flows. *Flow Measurement and Instrumentation*, 13:237–245, 2002.

[57] Weitbrecht V. and Socofsky S.A.and Jirka G.H. Experiments on mass exchange between groin fields and main stream in rivers. *Journal of Hydraulic Engineering, ASCE*, 134(2):173 183, 2008.

[58] Babarutsi S.and Chu V.H. Dye-concentration distribution in shallow recirculating flows. *Journal of Hydraulic Engineering, ASCE*, 117(5):643–659, 1991.

[59] V. Weitbrecht, Uijttewaal W., and Jirka G.H. 2d particle tracking to determine transport characteristics in rivers with dead zones. In *Proceedings Int. Symp. Shallow Flows, Delft, The Netherlands.*, volume 2, pages 103–110, 2003.

[60] Uijttewaal W.S.J. Effect of groyne layout on the flow in groyne fields: laboratory experiments. *Journal of Hydraulic Engineering, ASCE*, 131(9):782–791, 2005.

[61] Uijttewaal W.S.J., Lehmann D., and Mazijk A. Exchange processes between a river and its groyne fields: model experiments. *Journal of Hydraulic Engineering, ASCE*, 127(11):928–936, 2001.

[62] Iwagaki Y. Fundamental study on critical tractive force. *Tans.JSCE*, 41:1–21, 1956.

[63] Mayerle Y., Toro F.M., and Wang S.S.Y. Verification of a three-dimensional numerical model simulation of the flow in the vicinity of spur dikes. *Journal of Hydraulic Research*, 33(2):2150–2156, 1983.

[64] Tominaga A.and Nakano Y. and Fujita T. Visualization analysis of flow structures in submerged spur dikes. *Annual Journal of Hydraulic Engineering, JSCE*, 4:1041–1046 (in Japanese), 2000.

List of Tables

1.1 Reported effects on fish biomass of adding groynes or extending groynes in Eroded, Warmwater Streams. (Obtained from Kuhnle et al. 1999) 3

2.1 The model parameters of different groyne spacing 17

2.2 The model parameters of groyne with 18cm spacing 17

2.3 The flow conditions in the fixed bed 24

2.4 The flow conditions in the movable bed 24

3.1 The name of the case with other spacings under emerged condition . 55

4.1 The name of the case with other spacings under the submerged condition 102

5.1 Factors influencing local abutment-scour depth (obtained from Coleman et al. 2003) 143

List of Figures

1.1 Sketch of single and box groyne 2

1.2 The box groyne in upper Upper Mississippi River 2

1.3 Effect of groyne spacing on flow pattern in the box groyne(obtained from Copeland 1983) 5

1.4 Gyre system with different aspect ratio W/L (W:groyen length, L:Spacing) (obtained from Weitbrecht et al. 2008) 6

1.5 Flow and scour pattern at a circular pier (obtained from Melville and Coleman 2000) 7

1.6 Magnitude of the mean velocity field around several types of groynes under the emerged and submerged conditions(obtained from Kadota 2010) 9

1.7 Temporal bed deformation of a series of L-shape groyne (obtained from Ahmad et al. 2009) 10

1.8 Sketch of adopted model 11

1.9 Schematic research subject of this study 11

2.1 Sketch of the flume with fixed bed 13

2.2 Sketch of the triangular weir (V-notch weir) 14

2.3 Photo of the flume with movable bed 15

2.4 The flume with movable bed 16

2.5 Arrangement of box groyne model 16

2.6 The photo of model 16

2.7 Typical setup for PIV technique in a wind tunnel 18

2.8 Arrangement of PIV on the horizontal plane $(x - y)$ 19

2.9 Arrangement of PIV on the vertical plane $(x - z)$ 20

2.10 Projection of the laser sheet 20

2.11 The procedure of dye concentration measurement (DCM) 21

2.12 Cumulative semi-logarithmic probability size-frequency graph . . . 22

2.13 Arrangement of devices measuring bed deformation 22

2.14 Arrangement sketch of Electromagnetic Current Meter (EMV) . . . 23

2.15 Apparatus of Electromagnetic Current Meter (EMV) 23

3.1 Comparison of mean velocity in the inner zone of emerged box groyne for all layers 27

3.2 Time-averaged velocity vectors on the horizontal plane (x-y) near the middle of water depth (z/GH=0.44)under emerged condition . . 31

3.3 Contours of dimensionless time-averaged velocity in the longitudinal direction (U) on the horizontal plane (x-y) near the middle of water depth (z/GH=0.44)under emerged condition 32

3.4 Contours of dimensionless time-averaged velocity in the transverse direction (V) on the horizontal plane (x-y) near the middle of water depth (z/GH=0.44)under emerged condition 33

3.5 The distance from the start point of reverse flow to the outer wall of the second groyne X_c under emerged condition 34

3.6 Contours of dimensionless time-averaged velocity in the vertical direction (W) on the horizontal plane (x-y) in different measured layers for case without the longitudinal block (CASE RE1) 35

3.7 Contours of dimensionless time-averaged velocity in the vertical direction (W) on the horizontal plane (x-y) near the bottom of the channel (z/GH=0.18)under emerged condition 36

3.8 Time-averaged velocity vectors on the vertical plane (x-z) y=95mm (y/GL=1.06) under emerged condition 37

3.9 Autocorrelation results for velocity fluctuation in the transverse direction at the upstream of entrance on the horizontal plane (x-y) near the middle of the channel (z/GH=0.44)under emerged condition . . . 38

3.10 Vertical distribution of longitudinal velocity (U) on the vertical plane (x-z)under emerged condition 39

3.11 Contours of dimensionless time-averaged turbulence intensity in the longitudinal direction (u') on the horizontal plane (x-y) near the middle of water depth (z/GH=0.44)under emerged condition 42

3.12 Contours of dimensionless time-averaged turbulence intensity in the transverse direction (v') on the horizontal plane (x-y) near the middle of water depth (z/GH=0.44)under emerged condition 43

3.13 Contours of instantaneous Okubo-weiss parameter on the horizontal plane (x-y) near the middle of water depth (z/GH=0.44)under emerged condition 45

3.14 Images of dye distribution at various times (CASE RE1) 46

3.15 Images of dye distribution for some examples under emerged condition 46

3.16 Longitudinal distributions of time-averaged transverse velocity along the interface under emerged condition 47

3.17 Exchange coefficient obtained by PIV data under emerged condition 48

3.18 Exchange coefficient obtained by DCM and PIV method under emerged condition(a: effects of the length of upstream longitudinal block; b: effects of the length of longitudinal downstream block) 50

3.19 Exchange coefficient obtained by modified DCM and PIV method under emerged condition(a: effects of the length of upstream longitudinal block; b: effects of the length of longitudinal downstream block) 51

3.20 Exchange coefficient obtained by modified DCM and modified PIV method under emerged condition(a: effects of the length of upstream longitudinal block; b: effects of the length of longitudinal downstream block) 51

3.21 Temporal variation of dye concentration under emerged condition(a: effects of the length of upstream longitudinal block; b: effects of the length of longitudinal downstream block) 51

3.22 Contours of dimensionless time-averaged bed shear stress(τ_b/τ_0)under emerged condition 54

3.23 Comparisons of mean velocity in the inner zone of emerged box groyne U_{ig} under different spacing ratio 56

3.24 Time-averaged velocity vectors on the horizontal plane (x-y) near the middle of water depth (z/GH=0.44) for the cases with different spacings under emerged condition 57

3.25 Contours of dimensionless time-averaged velocity in the longitudinal direction (U) on the horizontal plane (x-y)(z/GH=0.09) for the cases with different spacings under emerged condition 58

3.26 Contours of dimensionless time-averaged velocity in the transverse direction (V) on the horizontal plane (x-y)(z/GH=0.09) for the cases with different spacings under emerged condition 59

3.27 Images of dye distribution at various times (CASE RE32-18) 60

3.28 Transverse distribution of longitudinal velocity (U) on the horizontal plane (x-y) of z/GH=0.09 for the cases with different spacings under emerged condition 61

3.29 Contours of dimensionless time-averaged turbulence intensity in the longitudinal direction (u') on the horizontal plane (x-y)(z/GH=0.09) for the cases with different spacings under emerged condition 62

3.30 Contours of dimensionless time-averaged turbulence intensity in the transverse direction (v') on the horizontal plane (x-y)(z/GH=0.09) for the cases with different spacings under emerged condition 63

3.31 Modified exchange coefficient obtained by PIV data for emerged boxgroyne under different spacings 65

3.32 Arrangement of pile group in front of first groyne 66

3.33 Time-averaged velocity on the horizontal plane (x-y) near the middle of water depth (z/GH=0.44) for the case with piles group in front of the first groyne under emerged condition 67

3.34 Time-averaged turbulence intensity on the horizontal plane (x-y) near the middle of water depth (z/GH=0.44) for the case with piles group in front of the first groyne under emerged condition 67

4.1 Comparison of mean velocity in the inner zone of box groyne for all layers 72

4.2 Comparison of three-dimensionality in the inner zone of submerged box groyne 74

4.3 Three-dimensional streamlines and time-averaged velocity vectors on the horizontal plane (x-y and vertical (x-z) plane for the case without longitudinal block (CASE RS1) 77

4.4 Three-dimensional streamlines and time-averaged velocity vectors on the horizontal plane (x-y) and vertical (x-z) plane for the case with an upstream longitudinal block (BL/S=0.5 CASE RS23) 78

4.5 Three-dimensional streamlines and time-averaged velocity vectors on the horizontal plane (x-y) and vertical (x-z) plane for the case with a downstream longitudinal block (BL/S=0.5 CASE RS33) . . . 79

4.6 Time-averaged velocity vectors on the various transverse plane (y-z) for the case without longitudinal block (CASE RS1) 80

4.7 Time-averaged velocity vectors on the transverse plane (y-z)(x=-20mm) for the case with longitudinal block (CASE RS23 and RS33) 80

4.8 Contours of dimensionless time-averaged velocity on the horizontal plane (x-y)of z/GH=0.44 and vertical plane (x-z)of y/GL=0.5 for the case without longitudinal block (CASE RS1) 82

4.9 Contours of dimensionless time-averaged longitudinal velocity U on the horizontal plane(x-y)of z/GH=0.44 for the group with upstream longitudinal block (Group RS2) 83

4.10 Contours of dimensionless time-averaged transverse velocity V on the horizontal plane (x-y)of z/GH=0.44 for the group with upstream longitudinal block (Group RS2) 83

4.11 Contours of dimensionless time-averaged longitudinal velocity U on the vertical plane (x-z)of y/GL=0.5 for the group with upstream longitudinal block (Group RS2) 84

4.12 Contours of dimensionless time-averaged vertical velocity W on the vertical plane (x-z)of y/GL=0.5 for the group with upstream longitudinal block (Group RS2) 84

4.13 Contours of dimensionless time-averaged longitudinal velocity U on the horizontal plane (x-y)of z/GH=0.44 for the group with downstream longitudinal block (Group RS3) 85

4.14 Contours of dimensionless time-averaged transverse velocity V on the horizontal plane (x-y)of z/GH=0.44 for the group with downstream longitudinal block (Group RS3) 86

4.15 Contours of dimensionless time-averaged longitudinal velocity U on the vertical plane (x-z)of y/GL=0.5 for the group with downstream longitudinal block (Group RS3) 87

4.16 Contours of dimensionless time-averaged vertical velocity W on the vertical plane (x-z)of y/GL=0.5 for the group with downstream longitudinal block (Group RS3) 87

4.17 Contours of dimensionless time-averaged vertical velocity W on the various horizontal plane (x-y) for the case without longitudinal block (CASE RS1) 88

4.18 Contours of dimensionless time-averaged vertical velocity W on the horizontal plane (x-y) of z/GH=0.5 for the cases with longitudinal block (Group RS2 and Group RS3) 90

4.19 Transverse distribution of time-averaged longitudinal velocity (U) on the horizontal plane of z/GH=1.22 under the submerged condition 92

4.20 Vertical distribution of time-averaged longitudinal velocity (U) on the vertical plane of y/GL=1.17 under the submerged condition . . . 93

4.21 Contours of dimensionless time-averaged longitudinal turbulence u' on the horizontal plane (x-y)of z/GH=0.44 under the submerged condition 95

4.22 Contours of dimensionless time-averaged transverse turbulence v' on the horizontal plane (x-y)of z/GH=0.44 under the submerged condition 96

4.23 Contours of dimensionless time-averaged vertical turbulence w' on the vertical plane (x-z)of y/GL=0.5 under the submerged condition . 97

4.24 Longitudinal distribution of transverse-averaged vertical velocity W along the roof boundary under the submerged condition 98

4.25 Longitudinal distribution of vertical-averaged transverse velocity V along the lateral boundary under the submerged condition 99

4.26 Exchange coefficient obtained by PIV data under the submerged condition 99

4.27 Contours of dimensionless time-averaged bed shear stress(τ_b/τ_0)under the submerged condition 101

4.28 Comparisons of mean velocity in the inner zone of submerged box groyne U_{ig} under different spacing ratio 103

4.29 Comparison of three-dimensionality in the inner zone of submerged box groyne under the submerged condition 103

4.30 Time-averaged velocity vectors on horizontal plane and vertical plane for case of 12cm spacing without longitudinal block (CASE RS1-12) 105

4.31 Time-averaged velocity vectors on horizontal plane and vertical plane for case of 12cm spacing with an upstream longitudinal block (CASE RS23-12) 106

4.32 Time-averaged velocity vectors on horizontal plane and vertical plane for case of 12cm spacing with a downstream longitudinal block (CASE RS33-12) 106

4.33 Time-averaged velocity vectors on the horizontal plane (x-y)and vertical (x-z) plane for the case of 24cm spacing without longitudinal block (CASE RS1-24) 107

4.34 Time-averaged velocity vectors on the horizontal plane (x-y)and vertical (x-z) plane for the case of 24cm spacing with an upstream longitudinal block (CASE RS23-24) 108

4.35 Time-averaged velocity vectors on the horizontal plane (x-y)and vertical (x-z) plane for the case of 12cm spacing with a downstream longitudinal block (CASE RS33-24) 109

4.36 Time-averaged velocity vectors on the transverse plane (y-z)(x=-20mm) for the cases with different spacing under the submerged condition 110

4.37 Vertical distribution of time-averaged longitudinal velocity (U) on the vertical plane of y/GL=1.17 under the submerged box groyne with different spacing 112

4.38 Contours of dimensionless time-averaged longitudinal turbulence u' on the horizontal plane of z/GH=0.44 under the submerged box groyne with various spacings 113

4.39 Contours of dimensionless time-averaged transverse turbulence v' on the horizontal plane of z/GH=0.44 under the submerged box groyne with various spacings 114

4.40 Contours of dimensionless time-averaged vertical turbulence w' on the vertical plane of y/GL=0.5 under the submerged box groyne with various spacings 114

4.41 Longitudinal distribution of transverse-averaged vertical velocity W along the roof boundary under the submerged box groyne with various spacings 115

4.42 Exchange coefficient obtained by PIV data under the submerged box groyne with various spacings 116

5.1 Comparison of bed deformation between the emerged box groynes without the longitudinal block under different flow conditions 121

5.2 The 'W' shape of scour hole int the front of first groyne 121

5.3 The sketch of horseshoe system in front of the first groyne 121

5.4 Comparison of bed deformation between the emerged box groynes with an upstream longitudinal block (Group RE2) Part 1 124

5.5 Comparison of bed deformation between the emerged box groynes with an upstream longitudinal block (Group RE2) Part 2 125

5.6 Comparison of bed deformation between the emerged box groynes with a downstream longitudinal block (Group RE3) Part 1 127

5.7 Comparison of bed deformation between the emerged box groynes with a downstream longitudinal block (Group RE3) Part 2 128

5.8 Comparison of relative maximum scour depth under the emerged condition 129

5.9 Longitudinal profile of bed deformation on the section of y=10cm (y/GL=1.11)under the emerged condition 129

5.10 Transverse profile of bed deformation on the section of x=-19.5cm (x/S=-1.08)under the emerged condition 130

5.11 Time-averaged velocity vectors U_{uv} on the horizontal plane of z/GH=0.56~0 under the emerged condition 132

5.12 Contour of scour with different submergence ratio (h/GH)in the study of Kuhnle et al. 1999. (Contour interval is 2cm .Elevation of initial bed surface is 48cm. Elevations less than 46 cm are shaded) 133

5.13 Contour of bed deformation in the submerged box groynes without the longitudinal block(CASE RS1) 134

5.14 Comparison of bed deformation between the submerged box groynes with an upstream longitudinal block (Group RS2) Part 1 136

5.15 Comparison of bed deformation between the submerged box groynes with an upstream longitudinal block (Group RS2) Part 2 137

5.16 Comparison of bed deformation between the submerged box groynes with a downstream longitudinal block (Group RS3) Part 1 139

5.17 Comparison of bed deformation between the submerged box groynes with a downstream longitudinal block (Group RS3) Part 2 140

5.18 Comparison of relative maximum scour depth under the submerged condition 141

5.19 Comparison of measured and calculated maximum scour depth using Eq. 5.1 for the data collected by Gill (1972) and Elawady et al. (2001) 144

5.20 omparison of overestimated ratio with different submergence ratio and groyne length for the data collected by Elawady et al. (2001) . . 144

5.21 Comparison of measured and calculated maximum scour depth using Eq. 5.1 for the data in this study 144

5.22 Comparison of improving measured and calculated maximum scour depth using Eq. 5.2 for the data in this study (CASE RE1 and RS1) . 144

5.23 Longitudinal profile of bed deformation on the section of y=10cm (y/GL=1.11)under the submerged condition 145

5.24 Transverse profile of bed deformation on the section of x=-19.5cm (x/S=-1.08)under the submerged condition 146

5.25 Time-averaged velocity vectors U_{uv} on the horizontal plane of z/GH=0.56~0.67 under the submerged condition 148

Acknowledgement

I would like to acknowledge the following people who supported me with sincere gratitude. First and foremost, I would like to express my heartfelt gratitude to my supervisor, Prof. Akihiro TOMINAGA, who has provided me with valuable guidance in my study during this doctorate. His supervision, encouragement and support bring me a meaningful and pleasurable experience in my academic work of Nagoya Institute of Technology (NIT). My sincere thankfulness is sent to his wife for her enthusiasm and delicious Japanese food. I would like to express my deep gratitude to Prof. Yonglai ZHENG, my supervisor at Tongji University, who led me to hydraulic and geotechnical engineering, and extended my academic view during undergraduate and graduate study. I owe my debt of gratitude to Prof. Feng ZHANG and Prof. Yu HUANG (Tongji University), who gave me the opportunity to study and enrich my life in NIT. Special thanks go to the family of Prof. Feng ZHANG, whose kindness and enthusiasm empower me warm.

I would like to express deeply thankful to Dr. Kenjirou SHOU, Mr. Toshiyuki OZAWA, Dr. Joefung JONG, Dr. Oktariyanto Nugroho EKA, Mr. Sayed Hashmat SADAT, Mahmoud MONA. I benefited a great deal from their advices and guidance throughout this study, and enjoyed diversified foreign culture from the communication with them. My sincere thanks also go to all members of Tominaga's Laboratory who always make me feel welcome and warmth. Special thanks go to Miss. Ayano SASAI, who provided me lots of helps when I was new in Japan.

I feel much indebted to Human Development Office of NIT International Center for their efforts on welcome and assistance to international students. I would like to express my sincere gratitude to the Ministry of Education, Culture, Sports, Science and Technology (MEXT) for providing my financial support.

Last but not least, I would like to extend my deep gratitude to all my friends from China and other countries. They were the strong power supporting my work and made my life colorful. The friendships engaged with them are always my treasured memory. This thesis

is especially dedicated to my parents, who always give me their patience and love unreservedly. Great appreciation goes to Nagoya, and the period of my life in this city will be my precious wealth of life supporting me in the future.